Evaluation of the pharmacokinetic properties of new taxane derivatives

Thesis

EVALUATION OF THE PHARMACOKINETIC PROPERTIES OF NEW TAXANE DERIVATIVES

Elena Marangon

Laboratory of Cancer Pharmacology
Department of Oncology
Mario Negri Institute

Director of Studies: Maurizio D'Incalci, M.D.
Supervisor: Prof. Peter B. Farmer

Thesis submitted for the degree of
Doctor of Philosophy
The Open University, London

Milan, Italy

September 2009

I would like to express my gratitude to my director of studies, Maurizio D'Incalci, M.D. and my supervisor, Prof. Peter B. Farmer for having given me the possibility to do my PhD and for their helpful comments and suggestions.

I would like to thank Indena S.p.A. for having supported me and for having provided all the taxanes for my PhD studies.

Many thanks to my colleagues of the Clinical Pharmacology Unit.

My sincere thanks also go to Stefania for her precious help with the references of this thesis.

I am really grateful to my sister Lisa for her priceless English support.

Finally, I cannot stop thanking Federica, Massimo and Renzo for their help, support and encouragement, they were more helpful than they may think.

Taxanes represent a very important class of anticancer agents available for clinical use since 1990s. Currently, two taxanes, paclitaxel and docetaxel, are included in multidrug regimens for the therapy of several solid tumours, such as ovary, breast, head and neck, prostate and non-small cell lung cancers.

Taxanes act by inhibiting microtubule dynamics, thereby blocking cell cycle and activating cell death. Despite the relevant contribution of taxanes in improving the overall survival and the quality of life of cancer patients, there are some limitations in the therapeutic use of these drugs that have driven research for new analogues having an enlarged antitumour activity profile, with more favourable chemical-physical properties and pharmacological profile in terms of selectivity and tolerability. Because of its molecular complexity, paclitaxel is an ideal candidate for systematic modification to develop an understanding of its structure-activity relationships.

Among all the investigated structural changes, two of them - the C-ring opening and the introduction of a functional group in position 14 - led to the compounds studied in this thesis: IDN 5390, IDN 5614, IDN 5738, IDN 5839 and IDN 6140. The opening of C-ring led to C-seco paclitaxel analogues, IDN 5390 and IDN 5614, while IDN 5738, IDN 5839 and IDN 6140 have an introduction of a functional group in position 14.

The main feature of C-seco taxanes is related to their antiangiogenic properties against a scanty cytotoxicity which renders these taxanes cytostatic compounds rather than cytotoxic ones. Whereas the main characteristic of 14-functionalized taxanes is to be poor substrates for P-gp system, showing as a consequence good oral bioavailability, distribution in central nervous system and activity on paclitaxel-resistant tumours.

The aim of this project was to characterize the preclinical pharmacokinetics of the aforementioned new taxane derivatives.

To describe the pharmacokinetic/metabolic profile of these compounds, as first step, it was necessary to develop and validate the assays to determine the concentration of the

new derivatives in biological specimens. Consequently, the validated assays were applied to characterize the pharmacokinetics and the bioavailability of the new derivatives in mice after oral and intravenous administration. The methods were based on high-performance liquid chromatography coupled with tandem mass spectrometry (LC-MS/MS) technique, because of its success in pharmacokinetic studies with small molecules and due to its high sensitivity and specificity.

IDN 5390 and IDN 5614 showed a very high metabolic clearance that limits their systemic disposition and renders advisable a careful characterization of their main metabolites in terms of *in vitro* biological activity and toxicity, in case of further clinical development.

As regards the 14-functionalized derivatives, IDN 5738 and IDN 5839 showed an interesting pharmacokinetic profile, nevertheless superimposable with that of ortataxel - their parent compound under clinical evaluation - against a halved half-life and a comparable cytotoxic activity on two sensitive and resistant human breast tumour cell lines (LCC6/LCC6-MDR and MCF-7/MCF-7-R), rendering them little interesting for further development.

The last studied analogue, IDN 6140, seemed to be the most interesting one due to its peculiar pharmacokinetic properties: good bioavailability, very long half-life and high distribution both in normal and tumour brain tissue. It showed considerable reduction in tumour volume in CD1 xenografted nude mice obtained inoculating orthotopically two human glioma cell lines, U-87 MG and GBM. These results suggest a potential efficacy of this compound for the therapy of central nervous system tumours and brain metastasis.

To my parents, Emanuela and Gianni

and to my sister Lisa

CONTENTS

List of figures

List of tables

CHAPTER 1

INTRODUCTION

1.1. History and discovery of taxanes

Paclitaxel (Taxol®) and docetaxel (Taxotere®) (figure 1, panel A and B, respectively) are the most important members of the taxane family.

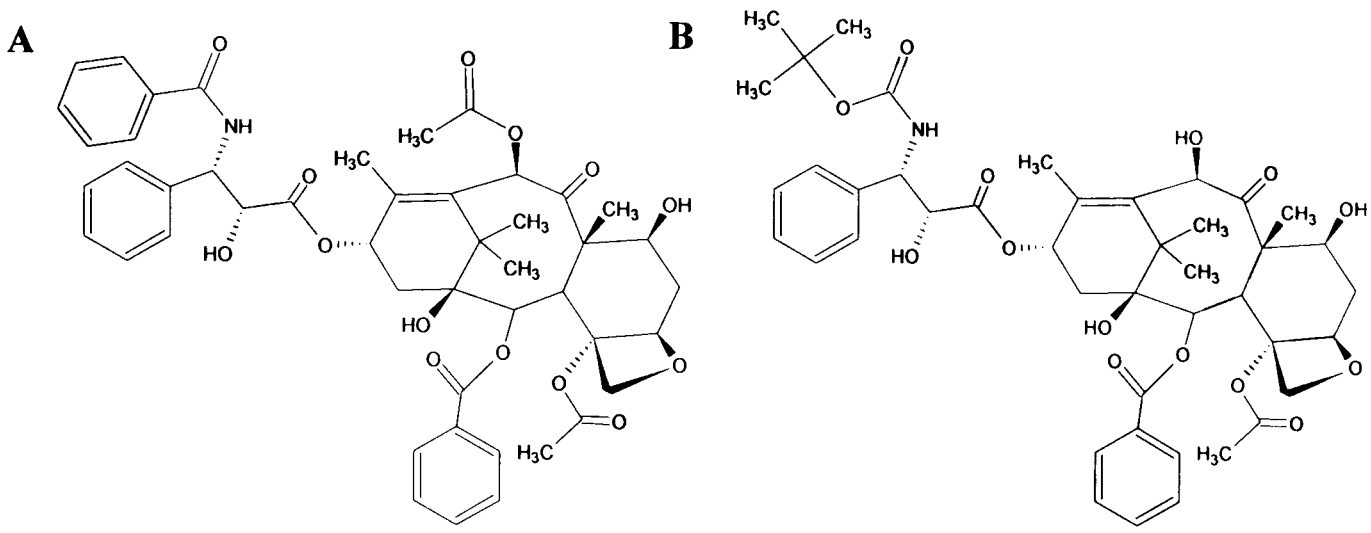

Figure 1. Chemical structure of paclitaxel (panel A) and docetaxel (panel B)

Paclitaxel is a natural product first isolated from the bark of the Pacific Yew (*Taxus brevifolia*) while docetaxel, a semi-synthetic taxane analogue derived from the European Yew (*Taxus baccata*), was identified in the 1980s. Paclitaxel can also be derived from the leaves of European Yew, which is a more renewable source than the bark of the Pacific Yew. This ended a point of conflict in the early 1990s: many environmentalists, including Al Gore, had opposed the harvesting of paclitaxel for cancer treatments.

The yews (members of the genus Taxus of the family Taxaceae) are non-resinous evergreen gymnosperms that are widely distributed throughout the moderate zone of the northern hemisphere. They grow primarily in the understory of moist, forested habitats in cool, temperate to subtropical climates [1]. The growth form may be a tree or a shrub. Crowns of these shrubby forms may attain as much as 24 m in diameter [2]. The main stem of the yew tree can become quite stout in proportion to its height. Often the large diameter is attained by multiple stems that have fused over time.

English (or European) yew has reached great age (1000 years) and girth, especially those planted in country churchyards [3].

Taxus plants were known and cultivated for centuries: in 1021, Avicenna, a persian doctor, introduced the medicinal use of Taxus baccata for phytotherapy in the "Canon of Medicine". He named this herbal drug as "Zarnab" and used it as a cardiac remedy. The leaves of *Taxus baccata* contain an alkaloid mixture (taxines). It was recently demonstrated that this drug possessed calcium channel blocking activity [4]. The first report about anticancer activity dates back to the beginning of 1900's, when a British official, in the Indian subcontinent, noted that parts of *Taxus baccata* were used to treat cancer: in the Central Himalayas, the plant was used in fact to cure breast and ovary cancer.

The research on the anticancer properties of the plants started in the late 1950s when the U.S. National Cancer Institute (NCI) initiated a program to screen 35000 plant species for anti-cancer activity. As part of this program the U.S. Forest Service collected bark from the Pacific yew, *Taxus brevifolia*, and shipped it to NCI. Extracts from the bark were found to have anti-tumor activity and, in 1971, the active ingredient was identified as paclitaxel [5].

As narrated by Wall and Wani, the isolation procedure, finally adopted after several unsuccessful trials, was carried out by ethanol extraction followed by a concentration procedure. The obtained ethanolic residue was partitioned between water and chloroform. At the end, the choloroformic residue was countercurrent extracted many times using a Craig apparatus (designed to obtain multiple liquid-liquid extractions permitting the separation of substances with different distribution coefficients). In this manner, approximately 0.5 g of taxol were isolated, for the first time in 1964, starting with 12 kg of air-dried stem and bark. The yield was about 0.004% [6]. All the various steps were monitored by an *in vivo* bioassay which involved the inhibition of the

Walker Carcinosarcoma solid tumor. The isolation hence was carried out laboriously, but - thanks to the mild countercurrent distribution methodology - with no losses by the treatment or no changes in the unknown chemical constitution of the eventual product occurred. Much simpler procedures have been subsequently developed.

The name "taxol" was assigned before knowing the complete structure of the compound, but it was evident that it contained some hydroxyl groups, and the name sounded interesting.

In 1979, Susan Horowitz identified the unique mechanism of action of paclitaxel and when the NCI screening program was closed in 1981, paclitaxel was the only compound left to be tested in humans [7].

1.2. Taxane mechanism of action

Taxanes are microtubule-interfering agents. Microtubules are part of cytoskeleton - within the cell's cytoplasm - and are involved in numerous cellular functions, including the maintenance of cell shape, intracellular transport, secretion and neurotransmission.

Microtubules are made up of polymers of tubulin and tubulin molecules, in their turn, are made up of a heterodimer consisting of α- and β-tubulin subunits. There are at least 6 α- and β-tubulin isotypes, differing in their intracellular localization. The tubulin subunits are arranged head to tail as are the molecules when they join together to form protofilaments. Each microtubule consists of 12 or 13 protofilaments aligned in parallel with the same polarity.

Microtubules are highly dynamic and unstable structures that are constantly incorporating free dimers and releasing dimers into the soluble tubulin pool (figure 2).

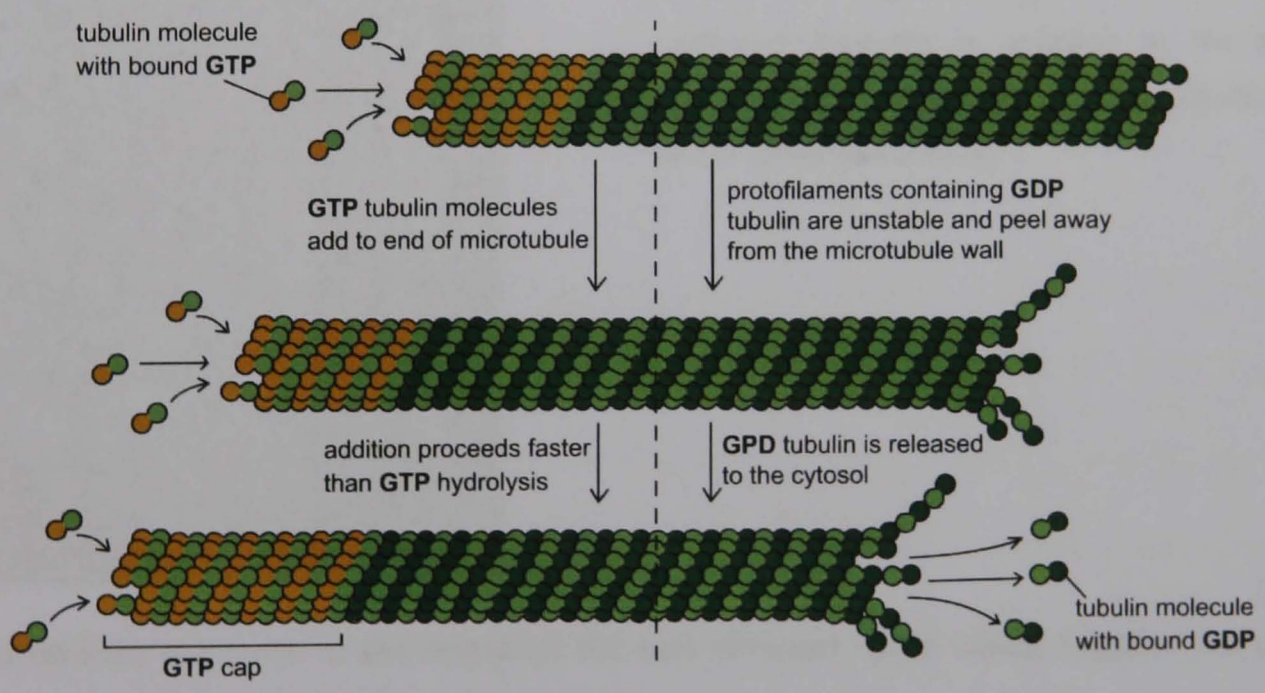

Figure 2. Microtubule ends in growing and shrinking states [from web source]

Actually, they have a plus (+) end where there tends to be rapid tubulin assembly and a minus (-) end with slow assembly or even disassembly [8]. The minus end is often anchored at the microtubule-organising centres with the plus end free in the cytoplasm.

Both ends having the ability to switch spontaneously from a growing to a shortening state, dependent on a cycle of GTP hydrolysis and exchange. GTP and magnesium are required for assembly. The combination of growth, shrinkage and rapid transitions between the two states of microtubules is known as "dynamic instability".

Concentration of Ca^{2+} is another factor that influences the degree of tubulin polymerization promoting the inhibition of assembly [9]. The modulation of the dynamics at the end of the microtubules is carried out by the microtubule associated proteins.

Taxanes bind to the β-tubulin subunit of the tubulin heterodimer (figure 3), accelerate the polymerization of tubulin and stabilize the resultant microtubules inhibiting their depolymerization.

Figure 3. Molecular structure of a tubulin dimer. The α-tubulin subunit is on top, indicating a microtubule polarity with the (-) end towards the top of the page. The two GTP subunits are drawn as space filling models, and the paclitaxel molecule is attached to the β-tubulin subunit and drawn as a ball and stick model [from web source]

This inhibition results in the arrest of the cell division cycle which triggers the cell-signaling cascade, leading to apoptosis of cancer cells [10, 11].

Docetaxel and paclitaxel share a mutual binding site on the β-tubulin subunit and docetaxel has a higher affinity for this site resulting in more potent tubulin assembly promoter and tubulin stabilizer than paclitaxel [12].

1.3. Role of taxanes in cancer therapy

Both paclitaxel and docetaxel are indicated as preferred agents for recurrent and metastatic breast cancer by The National Comprehensive Cancer Network (NCCN) clinical practice guidelines for breast cancer [13]. They are also widely used in the treatment of ovarian carcinomas and are being adopted as standard therapies for lung, digestive and prostate cancers. Other solid tumours that these drugs have been effective in treating include carcinomas of the head and neck and bladder.

Though preclinical and toxicology studies of paclitaxel were well characterized in the late 1970s, it was not tested on humans till the mid-1980s and the results of the phase I trial were reported in 1987 [14]. The reasons for this delay in the clinical development of paclitaxel must be sought in its poor acqueous solubility and in acute hypersensitivity reactions (HSRs) later attributed to the solvent Cremophor EL (a polyoxyethylated castor oil vehicle) and reduced by the use of corticosteroid premedication. In 1991, NCI started collaborating with Bristol Myers Squibb for the development of the drug, marketed as Taxol® [7]. In 1996, a phase III study showed that survival time for women with advanced ovarian cancer treated with the first line paclitaxel-cisplatin combination was increased by 50% over the standard cisplatin-cyclophosphamide treatment [15]. Shortly thereafter paclitaxel in combination with carboplatin (showing a better toxicity profile than paclitaxel-cisplatin) was introduced as the primary treatment of carcinoma of the ovary in patients with advanced disease or residual disease after initial surgery [16]. Nowadays, paclitaxel has a wide clinical spectrum of activity being used for the treatment of breast, lung, head and neck and ovarian cancers [17-20]. Less common cancers, such as endometrial, unknown primary, testes, esophageal and Kaposi's sarcoma, also have meaningful response rates to paclitaxel either alone or in combination with other agents [21-23].

Docetaxel entered phase I trials in 1990 and, of the several regimens studied, a 1-hour infusion every 3 weeks given at a dose of 100 mg/m^2 was selected for phase II evaluation [24]. Thanks to the less toxic effects of docetaxel vehicle (polysorbate 80) in comparison to paclitaxel one, the phase I trials drew to a close without the use of premedication and with only infrequently documented reactions. However, in a phase II trial, in patients with metastatic breast cancer, HSRs were noted more often and the protocol of the study was amended twice to include the use of a premedication regimen [25]. Docetaxel is now given with premedication to ameliorate their severity.

This taxane demonstrated evidence of antitumour activity in the course of phase I evaluation: responses were seen in breast, ovarian cancer and non-small cell lung cancer (NSCLC) [24-26]. Much of the phase II development focused on these same tumour types. Docetaxel has shown activity against numerous cancers, including breast, lung, head and neck, ovarian, and prostate. At present, it is approved for use as a single agent for the treatment of patients with locally advanced or metastatic breast cancer after failure of prior chemotherapy, and in combination with doxorubicin and cyclophosphamide for the adjuvant treatment of operable node-positive breast cancer [26]. It is also approved as a single agent for the treatment of patients with unresectable locally advanced or metastatic NSCLC after failure of prior platinum-based chemotherapy, in combination with cisplatin for patients with unresectable locally advanced or metastatic NSCLC who have not received prior chemotherapy, and in combination with prednisone for patients with androgen-independent (hormone-refractory) metastatic prostate cancer [24-26].

1.4. Pharmacology of taxanes (paclitaxel vs docetaxel)

Most studies on the clinical activity of taxanes were performed on paclitaxel or docetaxel that are the two taxanes used in clinical practice. Only in the recent years, comparative data have been available thanks to direct clinical comparisons of the two taxanes in metastatic breast, ovarian, and lung cancer. These results suggest a more favourable benefit-to-risk ratio for docetaxel compared to paclitaxel when these drugs are used as single agents or in combination with other chemotherapeutic agents in an every-3-week dosing regimen. Paclitaxel and docetaxel are structurally similar but pharmacological data support the difference between the taxanes.

Gligorov and Lotz [27] summarized the major differences between the two taxanes in terms of molecular pharmacology.

Docetaxel exhibits greater affinity to β-tubulin, targeting centrosome organization and acting on cells in three phases of the cell cycle (S, G_2 and M), whereas paclitaxel causes cell damage by affecting the mitotic spindle in only two phases of the cell cycle, G_2 and M. As regards the cell cycle phases, it is important to note that docetaxel is almost totally lethal against S-phase cells, while the maximum resistance to paclitaxel is early in the S phase.

Bcl-2 (B-cell leukemia 2) is an anti-apoptotic protein over-expressed in several solid tumours: breast, lung, prostate and nasopharyngeal cancers. Both taxanes cause Bcl-2 phosphorylation leading to apoptosis, but the concentration of docetaxel needed to cause apoptosis through Bcl-2 is 100 times less than paclitaxel [28].

Moreover, in comparison to paclitaxel, docetaxel exhibits greater uptake into and slower efflux from P388 murine leukemia cell line [29]. There is no definitive explanation for the greater uptake of docetaxel in P388 cells, but its slower efflux could be associated with its greater affinity for β-tubulin.

As already mentioned, taxanes arrest cell cycle in the G_2/M phase, which is the most sensitive stage to radiation. An *in vitro* study on human head and neck cancer cells (ZMK-I), and in cervical carcinoma cells (CaSki) clearly demonstrated that docetaxel is a better radiosensitizer than paclitaxel [30].

On the basis of the advantages of docetaxel in respect to paclitaxel listed in the first part of this paragraph, it would be assumed that docetaxel anti-cancer activity is better than that of paclitaxel.

A phase III study comparing paclitaxel with docetaxel, in patients with advanced breast cancer, proved that docetaxel was superior to paclitaxel in terms of median overall survival (15.4 vs 12.7 months), median time to progression (5.7 months vs 3.6 months) and overall response rate (32% vs 25%) [31]. Although the incidence of treatment-related hematologic and non-hematologic toxicities was greater for docetaxel than for paclitaxel, the quality of life scores were not statistically different between treatment groups over time [31].

In the following pages, I summarized:

1- the pharmacokinetic principles useful to describe a drug behaviour inside the body and

2- the available pharmacokinetic/pharmacodynamic data that explain the different clinical development strategies for the two molecules as well as the different clinical results.

1.5. Pharmacokinetic principles

The pharmacokinetics describes temporal patterns of response to drug administration following acute and chronic dosing. The pharmacokinetics is necessary to provide a rational basis for drug design, drug selection and dosage regimen design. Poor pharmacokinetic properties of a drug may limit its clinical application. In particular, the pharmacokinetics studies how the body handles drug and that means how drug is absorbed, distributed, metabolized and eliminated. All these processes are influenced by genetics, body size, age, disease, other drugs and the pharmacokinetic behaviour is a function of route of administration, dosage form, physicochemical properties of drug and physiology of the body.

When a drug is administered intravascularly, no absorption step is required, but when a drug is administered extravascularly, it must be absorbed. The absorption is the process by which unchanged drug proceeds, within the body, from site of administration to site of measurement. Monitoring intact drug in blood or plasma offers an useful means of assessing the entry of drug into the systemic circulation. This fraction of an administered dose of a drug is available at the site of action and it is defined as drug bioavailability. By definition, when a drug is administered intravenously, its bioavailability is 100%, because all of the dose enters the general circulation. With no other route of administration, blood concentration can be promptly and better controlled: following an intravenous bolus dose, elevated concentrations of drug in the blood can be reached and following an infusion at a controlled rate, constant concentration can be maintained.

When a drug is administered via other routes, its bioavailability decreases because of several possible sites of loss during absorption phase, especially for a drug given orally. A drug decomposition may occur in the gastrointestinal lumen and there could be a low

intestinal permeability or metabolism by enzymes in the gut lumen or gut wall. Even though the drug leaves the gastrointestinal tract, it is not absorbed systemically, because firstly it passes in liver through the portal vein. The liver is a site of elimination and every drug loss during absorption phase is known as the *first-pass effect*. Moreover, absorption is not restricted to oral administration. It occurs as well following intramuscular, subcutaneous and other extravascular routes of administration.

Once absorbed, a drug is distributed by blood to the various organs of the body. Distribution is a reversible transfer and is influenced by how much each organ is perfused, by organ size, by binding of drug within blood (plasma proteins) and in tissues, and by permeability of tissue membranes. A drug is distributed to all sites including the elimination organs and the elimination is the irreversible loss of a drug by all processes from site of measurement. Distinguishing between distribution and elimination as a cause for a decline in concentration in blood or plasma is often difficult. Disposition is the term used to indicate both processes. Disposition may be defined as all the events that occur subsequent to the absorption of a drug.

Drug elimination occurs by two processes, excretion and metabolism; excretion is the irreversible loss of chemically unchanged drug in urine and in faeces, and metabolism is the conversion of one chemical species to another. The two principal organs of elimination are the kidneys and the liver. The kidneys are the main site for excretion of the unchanged drug and, through the nephron, the basic unit of the kidney, act by three different mechanisms: glomerular filtration, tubular secretion and tubular reabsorption. The liver is the usual organ for drug metabolism, where hepatic enzymes catalyze various biochemical reactions. Metabolites are products more polar and less lipid-soluble than the original drug thanks to chemical modifications that ultimately promote the drug excretion from the body. Drug metabolism is obtained by two types of enzymatic reactions: phase I (biotransformation) characterized by reactions of

oxidation, hydroxylation, reduction and hydrolysis and phase II (conjugation) characterized by reactions of addition of a new functional group such as glucuronide, sulfate, methyl and acetyl groups, glutathione and amino acids.

The phase I detoxification system is composed mainly of the cytochrome P450 supergene family of enzymes which are a large group of monooxygenase enzymes responsible for the oxidative metabolism of toxic hydrocarbons.

Over 60 key forms are known, with hundreds of possible genetic variations, and the main ones are: CYP1A, CYP2B, CYP2C and CYP3A; the last one metabolizes about 50-60% of drugs.

All these pharmacokinetic processes are defined by the variations of drug plasma (or blood) concentrations, because, in pharmacology, the concentration in plasma (or blood) is the only directly accessible parameter. Blood or plasma, besides being a practical and convenient site of measurement, is the most logical one for determining drug in the body. Blood receives drugs from the site of administration and carries them to all organs, including those in which the drugs act. So, drug plasma concentrations are correlated to those at sites of action.

Measuring drug plasma concentration in samples collected at specific time points, it is possible to obtain plasma concentration-time profiles after different routes of administration. The shape and the mathematical elaboration of these profiles provide the main pharmacokinetic parameters during the different phases of absorption, distribution and elimination.

When there is an absorption, the drug plasma concentration increases with time up to a maximum value, indicated as C_{max}, maximal concentration, the highest drug concentration observed in plasma following administration of an extravascular dose. This parameter is important because therapeutic failure results both when the concentration is too low, giving ineffective therapy, and also when it is too high,

producing unacceptable toxicity. Between these limits of concentrations there is a region, known as "therapeutic window", associated with possible therapeutic success.

The time at which the highest drug concentration occurs is called the time of maximum concentration, T_{max}. C_{max} and T_{max} are correlated and both depend on how quickly the drug enters into and is eliminated from the body.

Another fundamental parameter obtained by plasma concentration-time profile, useful to define the bioavailability of a drug, is the area under the curve (AUC), because it is a measure of the total systemic exposure to the drug. To calculate the AUC value, the concentration must be integrated with respect to time. The AUC value represents the amount of unchanged drug that has reached the general circulation. To determine the bioavailability of a drug is necessary to compare the AUC after intravenous administration with the AUC after extravascular administration. In particular, the bioavailability is the dose-corrected area under curve (AUC) non-intravenous divided by AUC intravenous. Bioavailability must be considered when calculating dosages for non-intravenous routes of administration.

The drug distribution phase, that has already begun during the absorption phase or soon after an intravenous bolus, is characterized by the volume of distribution. The volume of distribution is the apparent volume into which the drug is dissolved. The term "apparent" is used because this pharmacokinetic parameter has not a real physiological meaning, but it is the fictitious dilution space into which the drug distributes and it is useful to correlate the drug concentration in plasma with its amount in the body. The volume of distribution depends on binding to both plasma proteins and tissues constituents, and can vary widely, with values ranging from 3 L to 40000 L. When it has a consistent value, it is possible to assume that the drug is not in systemic circulation, but in tissues. Knowing plasma volume and volume of distribution, the fraction of drug in body, in and outside plasma, can be estimated.

Once distribution equilibrium has been achieved, the time taken for the plasma concentration to fall by one half is called the elimination half-life ($t_{1/2}$) of the drug. The knowledge of the half-life is useful for the determination of the frequency of administration of a drug (the number of intakes per day) for obtaining the desired plasma concentration. The elimination half-life is independent of the amount of drug in the body and less drug is eliminated in each succeeding half-life.

The rate of drug elimination by all routes normalized to the concentration of the drug in some biological fluid is defined as clearance. The clearance is the most useful parameter for the evaluation of an elimination mechanism. It is the apparent volume of plasma (or blood or plasma water) completely cleared of drug per unit of time. The clearance is an additive parameter and total clearance is the sum of all organs clearance, especially hepatic and renal clearance, the two major organs of elimination. Liver blood clearance is the product of liver blood flow and extraction ratio (E); the extraction ratio is the rate of drug extraction related to the rate at which it is presented to the organ and the value of E varies from 0 (no elimination) to 1 (complete elimination). The rate of drug extraction is the difference between the rate of presentation of a drug to an organ of elimination and the rate at which drug leaves this organ. Renal clearance is the ratio of the rate of urinary excretion to plasma drug concentration and it is the net effect of drug filtration, secretion and tubular reabsorption.

1.6. Pharmacokinetics of taxanes

1.6.1. Paclitaxel

1.6.1.1. Preclinical pharmacokinetics of paclitaxel

The pharmacokinetics of paclitaxel after i.v., i.p., p.o., and s.c. administration of 22.5 mg/kg were studied in mice by Eiseman et al. [32]. Additional studies in mice were made after i.v. bolus dosing at 11.25 mg/kg or 3 h continuous i.v. infusions delivered at the infusion rate of 43.24 μg/kg/min. After i.v. administration to male mice, paclitaxel clearance resulted to be 3.25 mL/min/kg and the terminal half-life was 69 min. Paclitaxel disappeared more quickly after i.v. administration to female mice, with clearance and half-life of 4.54 mL/min/kg and 43 min, respectively. The bioavailability of paclitaxel was <10%, 0%, and 0% after i.p., p.o., and s.c. administration, respectively. Pharmacokinetic parameters resulted similar after i.v. delivery of paclitaxel at 22.5 and 11.25 mg/kg; however, the clearance calculated in these studies was much lower than that found with 3-h continuous i.v. infusions, suggesting non-linear pharmacokinetics. After i.v. administration, paclitaxel was distributed extensively to all tissues (Vd = 250-325 mL/kg), particularly in liver, lung and kidney but not in brain and testicle. Other studies conducted in rats, to determine the distribution and the excretion of paclitaxel, showed similar results, with high distribution in the main organs, no evidence of distribution in brain and testis, extensive metabolism and >50% of dose recovered in bile after 24 h of collection [33-35]. Higher elimination was found in mice, in fact, Bardelmeijer et al. in a more recent study with [^{3}H]paclitaxel, recovered about 70% of the radioactivity including those of metabolites in faeces [36].

1.6.1.2. Clinical pharmacokinetics of paclitaxel

Paclitaxel is insoluble in aqueous solution and it is therefore formulated in 50% ethanol and 50% cremophor-EL (a polyoxyethylated castor oil derivative) to improve its solubility [37].

Paclitaxel is given only intravenously because of its poor oral bioavailability (5-8%).

According to the initial clinical pharmacology data, elimination of paclitaxel from plasma appeared biphasic with linear pharmacokinetic behaviour. These early studies, however, used variable infusion schedules of the drug with 1, 6, and 24 hours infusions, and were hampered by suboptimal analytical techniques. Hamel et al. found the alpha (α) and beta (β) half-lives to be 0.045 and 0.75 h, respectively, with paclitaxel bolus intravenous administration [38]. Further early phase studies in which the drug was administered with 6 or 24 hours infusions consistently showed a biexponential elimination [14, 39-42]. Linear kinetics was assumed, as clearance seemed independent of dose, especially with 24 hours infusion schedules [43, 44].

With refinement of measurement techniques, elimination of paclitaxel has been found to have a three-phase elimination curve and non-linear pharmacokinetic behaviour, particularly with shorter infusions. Typical values reported for the α, β, and gamma (γ) half-lives are 0.19 h (range 0.01–0.40 h), 1.90 h (range 0.50–2.8 h), and 20.7 h (range 4.0–65.0 h), respectively [45].

Studies in mice and humans determined that paclitaxel exhibited nonlinear pharmacokinetics, a characteristic further augmented by the addition of cremophor-EL, as vehicle in the clinical formulation to improve its water solubility [46]. Paclitaxel showed a disproportionate increase in plasma C_{max} and AUC as the dose increased, suggesting saturation of elimination at higher concentrations of paclitaxel [47, 48]. Several studies with paclitaxel given as a 6 h infusion documented non-linear pharmacokinetics with doses higher than 250 mg/m^2 [14, 39, 40], while others reported that a lower dose of

135 mg/m^2 is the critical threshold for non-linear kinetics [49, 50]. Similar findings were noted with 3 h infusion schedules in patients who received doses of 135 and 175 mg/m^2 (> dose of 30%), where an over-proportion increase of 70% and 80% of C_{max} and AUC was observed [49, 51, 52] and in pharmacokinetic studies in children showing non-linear disappearance of paclitaxel with saturation of elimination pathways and tissue distribution [53].

As expected the non-linear pharmacokinetic behaviour of paclitaxel with shorter administration schedules was accompanied to both saturable tissue distribution and drug elimination processes [47, 48]. As paclitaxel C_{max} and AUC disproportionately increase with the dose of drug administered, saturation must occur during drug elimination, though saturable tissue distribution cannot be ruled out [51, 54]. Implications of a saturable non-linear model include relative saturation of paclitaxel binding sites at lower C_{max} and more effective binding of paclitaxel with shorter infusion schedules compared with longer infusion schedules [55]. Such implications have likely addressed to the adoption of shorter infusion schedules and lower drug dosages administered weekly rather than every three weeks [56].

Paclitaxel is bound to proteins in plasma, tissues, and tubulins. In plasma, protein binding is 95-98% as determined with equilibrium dialysis and ultracentrifugation methods [14, 41]. Paclitaxel is bounded mainly to α1- acid glycoprotein and to a minor extent to albumin and lipoproteins [57]. Supporting extensive drug binding *in vivo*, total volumes of distribution have been reported as significantly variable, dependent from the dose/schedule and larger than that of total body water, ranging from 50 L/m^2 to over 650 L/m^2 [14, 39, 43, 44]. In addition, paclitaxel shows high distribution in specific tissue of organs as kidney, lung, spleen, and in third space fluids, including ascitic and pleural fluid [14, 58]. As reported by Fujita et al, the most impressive high distribution was found in liver and tumour tissues [59]. Paclitaxel does not penetrate in tumour sanctuary tissues,

including testicles and brain, in which it is undetectable, and it is not present in cerebral spinal fluid [58, 60].

Despite the fact that paclitaxel is highly bound to plasma proteins and in tissues (tubulin), it is readily cleared from plasma. The major route of elimination is biliary excretion. Walle et al. and Monsarrat et al. demonstrated in rats and humans that one-fifth of the dose of paclitaxel is recovered from bile within 24 hours after administration [33, 61]. Paclitaxel metabolites are also measurable in bile, they account for the majority of drug elimination from the body via faecal excretion. Metabolite concentrations are higher than paclitaxel parent compound concentrations in bile if measured *in vivo*.

In humans, renal excretion and other extrahepatic excretion mechanisms account for less than 10% of elimination [14, 41, 54]. The literature suggests that there is a modest suppression of cytochrome P450 activity in patients with chronic renal failure; unfortunately no clinical studies have examined the impact of renal failure on paclitaxel pharmacokinetics [62-64]. For patients with liver dysfunction there are few clinical studies that provide guidance with respect to dosing. Fennelly et al. showed that patients with either elevated liver enzymes or elevated total bilirubin are more likely to develop myelosuppression with paclitaxel treatment than those patients who have neither abnormality [65, 66]. As such, it is prudent that dose reductions be considered for those individuals with hyperbilirubinemia and/or increased liver transaminases [67, 68].

1.6.1.3. Metabolism of paclitaxel

Paclitaxel undergoes hepatic oxidative metabolism by the cytochrome P450 family. The majority of the metabolites are excreted in the bile with only 5-10% in the urine.

Monsarrat et al. were one of the first groups to examine hepatic metabolism and biliary excretion of paclitaxel, first in rats and then in humans [33, 34]. They identified nine metabolites (see table 1) in rats and five in a patient who had external biliary drainage. Subsequently, among the known metabolites, five were also identified in mice [36].

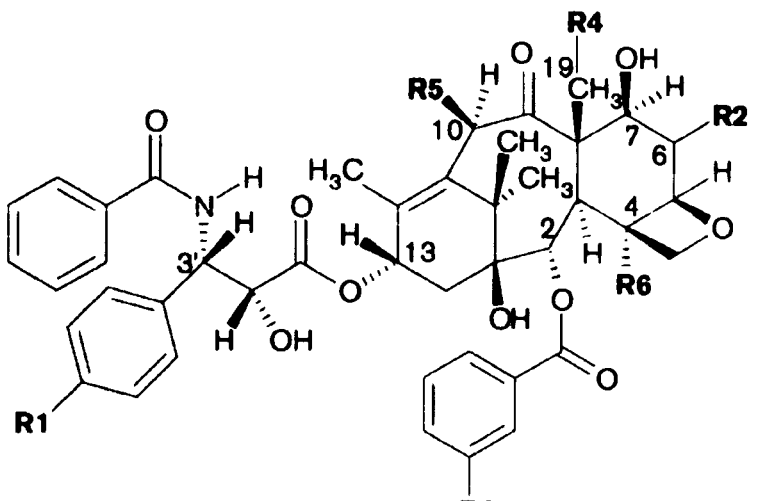

R3

Structure	R1	R2	R3	R4	R5	R6	Species
Paclitaxel	H	H	H	H	$OCOCH_3$	$OCOCH_3$	-
7-epipaclitaxel	H	H	H	H	$OCOCH_3$	$OCOCH_3$	Human
3'*p*-hydroxypaclitaxel	OH	H	H	H	$OCOCH_3$	$OCOCH_3$	Human, rat, mouse
6 α-hydroxypaclitaxel	H	OH	H	H	$OCOCH_3$	$OCOCH_3$	Human, mouse
6 α,3'p-dihydroxypaclitaxel	OH	OH	H	H	$OCOCH_3$	$OCOCH_3$	Human, mouse
10-deacetylpaclitaxel	H	H	H	H	OH	$OCOCH_3$	Cell culture, human
Baccatin III	13-OH	H	H	H	$OCOCH_3$	$OCOCH_3$	Human, rat
10-deacetyl baccatin III	13-OH	H	H	H	OH	$OCOCH_3$	Cell culture, human
2-*m*-hydroxypaclitaxel	H	H	OH	H	$OCOCH_3$	$OCOCH_3$	Rat, mouse
19-hydroxypaclitaxel	H	H	H	OH	$OCOCH_3$	$OCOCH_3$	Rat, mouse
4-deacetylpaclitaxel	H	H	H	H	$OCOCH_3$	H	Rat
2*m*-hydroxy-4-deacetyl paclitaxel	H	H	OH	H	$OCOCH_3$	H	Rat

Table 1. Structure formulas of paclitaxel and its known metabolites [Bardelmeijer et al.] [36]

Interestingly, most of the metabolites were hydroxylated though obvious significant differences exist in the site of hydroxylation and metabolite proportions found in bile. The major human metabolite discovered was 6α-hydroxypaclitaxel. This metabolite was not formed in rats and is modified from paclitaxel via stereospecific hydroxylation at the 6-position on the taxane scaffold as determined by nuclear magnetic resonance [69]. Two other major metabolites are 3′-*p*-hydroxypaclitaxel and 6α,3′-*p*-dihydroxypaclitaxel. All the metabolites were commonly detected when paclitaxel was administered with 3 hours infusions [70].

The main metabolite was not active when tested against ovarian and colorectal cancer cell lines; in fact, 6α-hydroxypaclitaxel is approximately 30 times less cytotoxic than paclitaxel and thus the 6α-hydroxylation reaction is felt to be a detoxification reaction [69, 71]. Activity of 3′-*p*-hydroxypaclitaxel was, in contrast, reduced but not absent in ovarian cancer cell lines. All the three metabolites cited before retained bone marrow toxicity when tested on human bone marrow cells [71].

Studying paclitaxel metabolism by liver microsomes, Cresteil et al. demonstrated that diazepam inhibits the formation of the major metabolite, 6α-hydroxypaclitaxel, suggesting that a cytochrome P450 2C family member was responsible for 6α-hydroxypaclitaxel formation [72]. Subsequently, Rahman et al. and more recently Henningsson et al. showed the role of cytochrome P450 2C8 (CYP2C8) in metabolism of paclitaxel to 6α-hydroxypaclitaxel [73, 74]. Cresteil et al. also showed that cytochrome P450 3A4 (CYP3A4) was responsible for the metabolism of paclitaxel to 3′-*p*-hydroxypaclitaxel [72] and Harris et al. successively confirmed it [75].

1.6.1.4. Pharmacodynamics of paclitaxel

The main purpose of investigating and understanding pharmacokinetics of a drug is to determine whether there is a relationship between pharmacokinetic parameters and drug efficacy and toxicities. In the case of paclitaxel, multiple studies have established relationships between paclitaxel pharmacokinetics and pharmacological effects [39, 45, 47, 53, 54, 76]. The best model to predict the relationship between paclitaxel's plasma concentration and effects is the threshold model, in which the length of time that paclitaxel concentration exceeds a threshold concentration is predictive of toxicity. According to some studies, the duration of paclitaxel concentrations above a threshold value correlates with not only the toxicity, but also the antitumor activity [45, 51, 53, 55].

The most concerning side effects of paclitaxel are neutropenia and neuropathy. Gianni et al. studied paclitaxel in 30 patients with varying doses and infusion schedules. A comparison between a 135 or 175 mg/m^2 dose given by a 3- or 24-h infusion versus a 225 mg/m^2 dose by 3-h infusion was made [51]. Neutropenia was the most significant toxicity and was correlated with paclitaxel concentration above 0.05 μmol/L; no relationship was noted with paclitaxel AUC or C_{max} concentrations. Similarly, Huizing et al. studied paclitaxel in 18 heavily platinum pre-treated ovarian cancer patients [70]. Women were treated with paclitaxel 135 or 175 mg/m^2 on a 3 or 24 hours infusion schedule. A relationship was again found between neutropenia and the duration that paclitaxel exceeding a certain concentration threshold; in this study the concentration threshold was 0.1 μmol/L. Again there was no relationship between AUC or C_{max} and toxicity. Further studies confirmed the threshold model, Henningsson et al. treated 26 patients with paclitaxel doses ranging from 135 to 225 mg/m^2 [47]. Total and free (fraction unbound to protein) paclitaxel plasma concentrations were measured and again, duration of total paclitaxel above a threshold concentration, 0.2 μmol/L, predicted for neutropenia. A subsequent study on a larger group of 45 patients found that free

paclitaxel concentrations were a slightly better predictor than total paclitaxel concentrations for toxicity but did not improve the goodness of fits of their pharmacodynamic model [76].

Two studies suggested a trend for increased neurotoxicity with increased paclitaxel AUC [53]. In the first study, conducted in children with solid tumours, using paclitaxel in a dose range of 200–420 mg/m^2, Sonnichsen et al. observed a trend for higher paclitaxel AUCs in children with neurologic toxicity compared to children without toxicity [53]. In children with neurotoxicity, paclitaxel AUC was 54 μmol/L h compared to 30 μmol/L h in those without neurotoxicity ($p = 0.062$). In the second study, breast cancer patients were treated with paclitaxel and it was observed that patients developing neurotoxicity had higher AUCs than the others. In contrast, a study performed in non-small cell lung cancer patients by Rowinsky et al. failed to show an association of paclitaxel plasma levels and neurotoxicity [77].

1.6.2. Docetaxel

1.6.2.1. Preclinical pharmacokinetics of docetaxel

The pharmacokinetics of docetaxel was evaluated in a number of animal species prior to clinical testing during 1990-1998 period [78-80]. In normal and tumour-bearing mice, the plasma pharmacokinetics of docetaxel were biphasic with α and β half-lives of 7 min and 1.2 h [78, 80]. Both the C_{max} and the AUC increased proportionally with dose over the range from 13 to 62 mg/kg [81]. The total body clearance was 2.2 L/h/kg at the dose of 37 mg/kg, whereas the corresponding volume of distribution at steady state was 2.2 L/kg, indicating appreciable tissue uptake and binding. The AUC at the maximum tolerated dose in mice was found to be 17 mg/L h, which is approximately 3-fold higher than the one observed in clinical studies (approximately 5 mg/L h at 100 mg/m^2 - see clinical pharmacokinetics -).

The kinetics of docetaxel in rats has also been described as being linear over the clinically relevant range of doses, although there was a trend towards a decreased clearance at the highest dose (20 mg/kg) [80, 81]. This is consistent with the nonlinear elimination of docetaxel by the isolated perfused rat liver over the concentration range from 5 to 50 mmol/L [82].

In dogs, administration of docetaxel 30 mg/m^2 over 10 minutes yielded biphasic pharmacokinetics with plasma half-lives of 4 minutes and 6.6 hours. Averaged AUC and clearance were 1.7 mg/L h and 17.6 L/h/m^2, respectively [78]. The dose of 30 mg/m^2 corresponds to the "toxic-dose" generating the highest concentration in this species [83], and the relatively low AUC observed (1.7 mg/L h) is in support of the higher sensitivity of the dog to docetaxel compared with rodents (AUC at MTD in mice = 17 mg/L h). The binding of docetaxel to plasma proteins ranges from 70 to 95% in mice, rats and dogs [78, 84]. The kinetics and biodistribution of [^{14}C]-labelled docetaxel have been studied

in mice (111 mg/m^2) and dogs (15 mg/m^2) [84]. The elimination of radiolabelled docetaxel from normal tissues in mice was biphasic with terminal half-lives of 2 to 4.5 h. In contrast, the elimination from colon adenocarcinoma xenografts was appreciably slower, with half-life of approximately 22 h. As a result, the AUC of docetaxel in tumour tissue significantly exceeded that in plasma at all doses despite the fact that the Cmax in tumour was less than 10% of those in plasma [81].

In mice and dogs, the uptake of radiolabelled docetaxel has been shown to be wide in a range of tissues including liver, gastrointestinal tract, biliary tree, pancreas, muscle and haemopoietic tissues [78, 79]. Immediately after administration, the highest concentrations of radioactivity were found in liver, bile and intestine, consistent with hepatobiliary excretion. There was no detectable uptake of radiolabelled docetaxel into the central nervous system.

1.6.2.2. Clinical pharmacokinetics of docetaxel

Unfortunately, as reported for paclitaxel, docetaxel has low (<10%) and highly variable oral bioavailability [85]. There is a number of important mechanisms that explains the low oral absorption of taxanes, including high affinity for drug transporters in the gastrointestinal tract, such as P-gp (ABCB1), which limits absorption, and high extraction of the drug by extensive metabolism in the intestine and/or liver (first-pass effect) by CYP3A [86]. Evidence of this, is that the AUC of oral docetaxel increased 9-fold when coadministered with ciclosporin, a competitive inhibitor of ABCB1 and substrate of CYP3A4 [87].

In general, the pharmacokinetic profile of intravenous docetaxel is characterized by substantial inter-patient variability [88-90]. In a population pharmacokinetic study of more than 600 patients receiving docetaxel 75–100 mg/m^2, the median clearance was 36 L/h (5^{th}-95^{th} percentile: 17–59 L/h), representing approximately a variation of 3.5-fold in

this population [89]. In a more recent study in which patients received docetaxel 75 mg/m^2 approximately 10-fold variation in drug clearance was observed [91].

The docetaxel dosage used for treating cancer patients ranges from 35 to 100 mg/m^2 as a 1 hour intravenous infusion administered once every 3 weeks or once a week for three consecutive weeks (3-weeks). The comparative pharmacokinetic parameters of docetaxel administered weekly at a dose of 35 mg/m^2 and 3-weekly schedules were summarized by Baker et al. [92]. Mean ± SD docetaxel clearance values were similar for both weekly and 3-weekly schedules (overall means 25.2 ± 7.7 and 23.7± 7.9 L/h/m^2, respectively; p = 0.5467). Values for terminal elimination half-life were also similar with both schedules of administration (overall means 16.5 ± 11.2 and 17.6 ± 7.4 hours, respectively; p =0.6990). On average, C_{max} values with weekly docetaxel 35 mg/m^2 over 30 minutes were comparable with those achieved with 3-weekly docetaxel 75 mg/m^2 over 1 hour, but less than those achieved with 3-weekly docetaxel 100 mg/m^2 over 1 hour. On the other hand, estimated cumulative AUC_∞ during 3 weeks of treatment was larger following docetaxel 35 mg/m^2 weekly (4.44 ± 1.24 μg/mL*h) than with docetaxel 60 mg/m^2 (2.85 ± 1.40 μg/mL*h) and 75 mg/m^2 (3.05 ± 0.85 μg/mL*h) administered 3-weekly, but in the range of that achieved with 100 mg/m^2 (5.62 ± 2.12 μg/mL*h) administered 3-weekly.

Considering the differences in the incidence of severe myelosuppression between the two schedules of administration and the exposure-toxicity relationships for 3-weekly regimens (see pharmacodynamics of docetaxel), pharmacokinetic data showing similar exposure (AUC_∞) over a 3-week period for both weekly and 3-weekly regimens suggest that the exposure-toxicity relationships for 3-weekly administration do not apply to weekly regimens.

In vitro studies have demonstrated that docetaxel is extensively bound to albumin and α1-acid glycoprotein and that the latter is the main determinant of variability in

docetaxel serum binding [93]. From a population pharmacokinetic model involving 547 patients, α1-acid glycoprotein was identified as a significant predictor of docetaxel total clearance. In patients with high plasma levels of protein (>2.6 mg/mL) total clearance of docetaxel decreased by 19% [94].

The pharmacokinetic profile of docetaxel has been evaluated in patients with variable degrees of hepatic impairment achieving the conclusion that docetaxel dose reductions of 20-40% are required in patients with moderate or severe liver function impairment [95]. Previously, Bruno et al. in their population pharmacokinetic analysis of patients, receiving docetaxel 75–100 mg/m^2 3-weekly, identified a subset of patients with mild hepatic impairment defined as total bilirubin <1.5 times the normal level (ULN), elevated transaminases (≥ 1.5 to ≤ 3.5 times the ULN) concurrent with increased alkaline phosphatase (≥ 2.5 to ≤ 5 times the ULN) [89]. These patients showed a 27% reduction in docetaxel total clearance, whereas in studies conducted in patients with moderate (total bilirubin ≥ 1.5 to ≤ 3.0 times the ULN) and severe (total bilirubin ≥ 3.0 times the ULN) impairment the reduction of clearance was found to be 50% [92].

1.6.2.3. Metabolism of docetaxel

Pharmacokinetic studies in mice, rats and dogs have demonstrated that docetaxel is extensively metabolized [82, 84, 96]. The major docetaxel metabolites and less than 10% of the parent drug are excreted into the faeces, whereas the total urinary excretion is <10% [79]. The metabolites amounted to 75% of the dose injected and similar data were obtained in clinical studies. This suggests that sequential metabolism and biliary excretion are the principal pathways of excretion of docetaxel. Therefore, the mechanisms of elimination appear to be very similar to those of paclitaxel [33].

CYP3A4 and CYP3A5 are the most important enzymes among the four members of the CYP3A subfamily (CYP3A4, CYP3A5, CYP3A7, CYP3A43) involved in docetaxel metabolism and elimination [97, 98]. The metabolites demonstrate substantially reduced cytotoxic activity against cancer cells and bone marrow compared with the parent drug, making biotransformation a major route of inactivation [96, 99]. Table 2 reports the 4 major docetaxel metabolites which were identified in animals and humans and synthesized [82, 90, 100, 101].

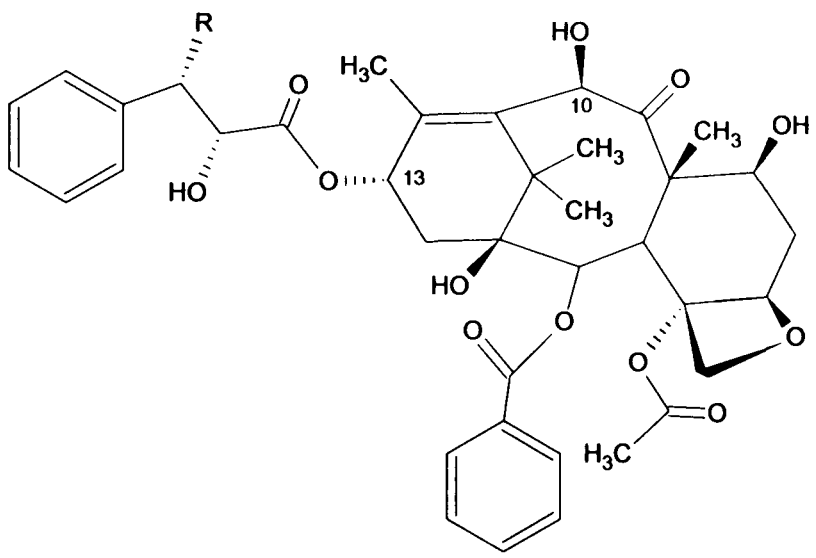

Structure	R
Docetaxel	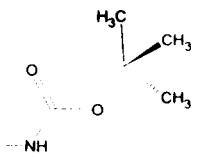
Metabolite M1 and M3	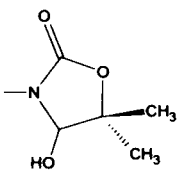
Metabolite M2	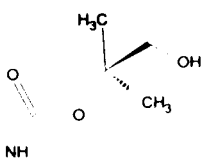
Metabolite M4	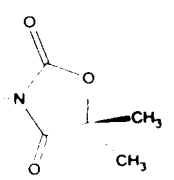

Table 2. Chemical structure of docetaxel and its principal known metabolites

The principal site of metabolism is the tert-butylpropionate side chain (R_2 of docetaxel structure) which undergoes a series of oxidation reactions beginning with the oxidation of one of the methyl groups leading to M2. This is probably followed by cyclisation of putative unstable aldehyde and acid metabolites of the alcohol to 2 diastereoisomers (M1 and M3) and a ketone metabolite (M4). The last one was determined as the most abundant metabolite present in plasma of cancer patients treated with 100 mg/m^2 of docetaxel with C_{max} between 0.022 and 0.23 mg/L [90]. There was no evidence of the formation of glucuronide or other conjugates for docetaxel and its metabolites.

Unlike for paclitaxel, oxidation of the taxane nucleus and the C-3' phenyl of the C-13 side chain does not take place to any significant extent [102]. There is also little interspecies difference in the spectrum of metabolites produced. Correlations between the production of the tertbutyl alcohol and N-erythromycin demethylation and 6 β-testosterone hydroxylation in human liver microsomes, implicate cytochrome P450 (CYP3A) in the metabolism of docetaxel in humans [99, 102, 103]. This is supported by inhibition studies carried out with ketoconazole, troleandomycin and antibodies directed to CYP3A.

1.6.2.4. Pharmacodynamics of docetaxel

The observed large pharmacokinetic variability for docetaxel has important clinical consequences. In the above mentioned population pharmacokinetic studies (dose administered: 75-100 mg/m^2 and 75 mg/m^2, respectively, see 1.6.2.2.), decrease of docetaxel clearance (Cl) was accompanied by an increase frequency of grade 4 neutropenia and fever. For a 50% decrease of Cl, neutropenia increase of 450% [88] and even a 25% decrease of Cl comported a 150% increase of cases with febrile neutropenia. Another study, with docetaxel administered as a 3-weekly regimens,

demonstrated that AUC was the only significant predictor of toxicity, as grade 3/4 mucositis, grade 3/4 diarrhoea, severe asthenia and febrile neutropenia [94].

Docetaxel exposure has also been related to the efficacy of treatment, in particular AUC was a significant predictor of time to tumour progression in NSCLC [88]. Low docetaxel AUC (because of increased clearance) was associated with a shorter time to progression and time to death [104]. The use of growth factors has the potential benefit of maintaining docetaxel AUC while reducing the incidence of febrile neutropenia.

More recently, the association between exposure to unbound docetaxel and neutropenia in cancer patients was studied [105]. Docetaxel was administered 3-weekly at a dose of 75 mg/m^2 to 104 patients. From this analysis, unbound docetaxel AUC was better correlated than total AUC, with both percentage of decrements in absolute neutrophil count ($p = 0.002$ vs $p = 0.029$) and worst grade of neutropenia ($p = 0.013$ vs $p = 0.220$), in the way that higher exposure was associated with worse haematological toxicity. The conclusion was that unbound docetaxel is more closely related to the induced myelosuppression than the total drug. Finally, a paper by Charles et al. reported the first description of factors predictive of toxicity and survival. Patients with reduced docetaxel clearance and elevated α1-acid glycoprotein levels evidenced bad adverse effects and worse survival [106].

1.7. New taxanes

Despite the relevant contribution of taxanes in modern chemotherapy, in improving the overall survival and the quality of life of cancer patients, there are some limitations in the therapeutic use of these drugs because of the following reasons:

- the water solubility of both paclitaxel and docetaxel is very low. For this reason, paclitaxel is formulated in the nonionic surfactant cremophor-EL and dehydrated ethanol (1:1 by volume) to enhance its solubility [37]. Docetaxel is slightly less hydrophobic and it is formulated in tween 80 (polysorbate 80). Both cremophor-EL and tween 80 are biologically and pharmacologically active compounds with clinically important adverse effects, including hypersensitivity reactions and peripheral neuropathy [107, 108];
- the limiting toxicities for these drugs are neutropenia, mucositis and neuropathy;
- the drug resistance to these compounds. Many patients, even those responding initially to therapy, fail to respond further when disease relapses (acquired resistance), and a minor number does not even respond at the first cycle of therapy (intrinsic resistance);
- poor bioavailability;
- lack of penetration of the blood brain barrier (BBB).

To get round these problems, two different strategies were chosen:

1- To improve the efficacy of the existing members of taxane family getting their formulations better;

2- To synthesize new analogues having an enlarged antitumor activity profile, in particular on taxanes-resistant tumours, with more favourable chemical-physical properties and pharmacological profile in terms of selectivity and tolerability.

1.7.1. New formulations

As regards new formulations of paclitaxel and docetaxel, they are under development to improve delivery, pharmacokinetic properties and to reduce drug resistance. As I described before, paclitaxel exhibits nonlinear pharmacokinetics with saturable metabolism and distribution to tissues [51, 53]. The nonlinear behaviour of paclitaxel has been in part attributed to the formulating reagent, cremophor-EL. Cremophor-EL also contributes to decrease the oral bioavailability of paclitaxel [109, 110], thereby limiting the usefulness of this formulation for oral use. Cremophor-EL systemic exposure is higher when this formulation is given over 1 h than longer infusions [111]. This result explains the higher incidences of hypersensitivity reactions and peripheral neurotoxicity observed with infusions of 1 h rather than with 3 and 24 hours infusions [112, 113].

Docetaxel formulated with tween 80 shows linear pharmacokinetics and has lower incidence of neurotoxicity and hypersensitivity reactions in comparison with paclitaxel [114].

All the above mentioned limitations of formulating paclitaxel with cremophor-EL prompted the development of novel formulations, but only three, Abraxane, Genexol-PM and MBT-0206 achieved clinical relevance.

Abraxane (ABI007) seems to be the most interesting one [115-117]. It is paclitaxel formulated as an albumin-bound nanoparticle (diameter of 130-nm) free from any kind of solvent. In a phase III study performed in metastatic breast cancer patients, the formulation showed greater efficacy and a favourable safety profile compared to standard paclitaxel formulated in cremophor-EL [118, 119]. Abraxane showed linear pharmacokinetics and improved therapeutic index, also avoiding the use of corticosteroid premedication required for solvent-based taxanes [119, 120]. FDA approved

abraxane for the treatment of breast cancer after failure of combination chemotherapy for metastatic disease or relapse [115, 116].

The second formulation is Genexol-PM, a sterile, lyophilized polymeric micellar formulation of paclitaxel solubilized in methoxy polyethylene glycol-poly (D,L-lactide) [121]. It has better tissue distribution in mouse models than Taxol® with good antitumour efficacy [121]. In a first phase I study of Genexol-PM on a 3-weekly schedule, dose-limiting toxic effects of neuropathy and neutropenia were observed at 390 mg/m^2 [122]. In contrast, in a recent phase I study conducted on a weekly basis for 3 weeks, doses of 80-200 mg/m^2 given as 1-h infusion were well tolerated [123]. Genexol-PM showed linear pharmacokinetics, and responses were observed in patients with refractory tumours, including patients who had previously failed taxane-based chemotherapy [123].

The last formulation, MBT-0206, is cationic lipid complexes of paclitaxel and is now under clinical phase II investigation. It has been shown to be bound and internalized selectively by angiogenic tumour endothelial cells after intravenous injection providing a vascular targeting agent [124]. In a phase Ib study, conducted in patients with metastatic breast cancer and tumour progression after anthracycline based chemotherapy, MBT-0206 showed a favourable safety profile together with promising efficacy data. Good tolerability as well as the different mechanism of action of MBT-0206 offer the possibility of prolonged treatment or combination therapy [125].

1.7.2. New analogues

1.7.2.1. New analogues under clinical evaluation

As mentioned before, in addition to the drawback of the low solubility of taxanes - responsible for the formulation in cremophor-EL and tween 80 - the main disadvantages of both paclitaxel and docetaxel are drug resistance, poor bioavailability and no penetration in the blood-brain barrier.

A well characterized mechanism of resistance is over-expression of the MDR-1 gene encoding for P-glycoprotein (P-gp) which is involved in pumping out the drug from cells that express this protein in different tissues.

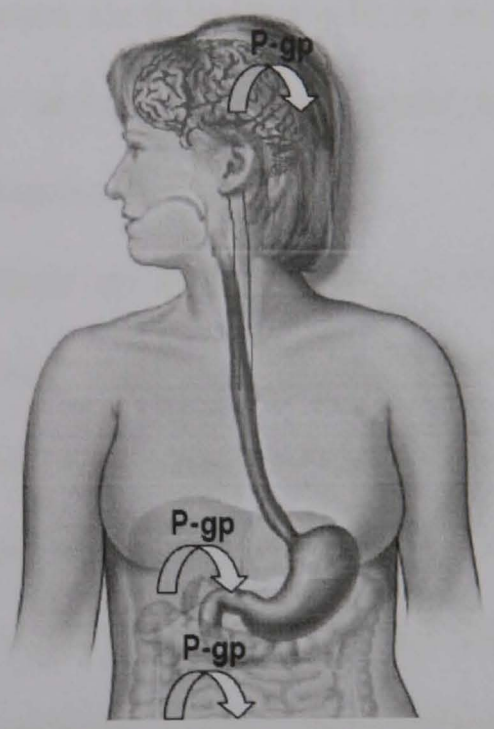

Figure 4. Schematic representation of the transport of paclitaxel by P-glycoprotein. Elimination of paclitaxel from the liver to the bile, from the central nervous system as well as the reduced absorbtion of paclitaxel in the gastro-intestinal tract is believed to be associated with P-gp transport [from web source].

Paclitaxel and docetaxel are substrates of P-gp having 3 important effects:

1- They are inactive against P-gp over-expressing tumours [126, 127].

2- Being P-gp expressed in the luminal side of plasma membrane of gut epithelial cells [128, 129], the absorption in the gut of paclitaxel and docetaxel is prevented [130],

explaining their low bioavailability. In fact, the use of inhibitors of P-gp blocks the efflux of taxanes from intestinal cells, thus increasing the absorption of these compounds [87, 131].

3- P-gp is also present in brain endothelial cells which are a constituent of the blood brain barrier (BBB) [132]. As a result of complex tight junctions that cause severe restriction of the paracellular pathway, BBB is much tighter than peripheral microvessels. Therefore, penetration across BBB is confined to transcellular mechanisms [133]. But, due to P-gp on the luminal side of plasma membrane in brain endothelial cells [132, 134], paclitaxel and docetaxel hardly penetrate into the brain parenchyma through brain endothelial cells. For this reason, paclitaxel cannot reach tumour cells in the brain parenchyma - unless combined with P-gp inhibitors [135] - and cannot make its effect even though tumour cells do not express P-gp [136, 137].

Other mechanisms of resistance are directly related to the taxane binding site on β-tubulin, identified both as point mutations in tubulin [138] and as differential expression of β-tubulin isotypes, discovered for paclitaxel-resistant ovarian cancer cells [139].

These considerations explain why it is potentially of great interest to identify and develop new taxanes with a low binding affinity for P-gp and/or different affinity toward tubulin isotypes. In particular, taxanes characterized by the low binding affinity for P-gp should be not cross resistant to paclitaxel and docetaxel and possess good oral bioavailability as well as crossing the BBB. The oral route for a taxane is of clinical interest, not only because of practical convenience for patients as well as reduced costs, but also because prolonged administration of low doses of taxanes may be clinically very effective and may possibly involve mechanisms other than anti-mitotic, e.g. anti-angiogenesis [140-142].

Numerous novel taxane derivatives with improved biological activity, synthesized in the last ten years, were available for pharmacological evaluation and reached the phase of clinical development.

In this part of the introduction, I summarize the derivatives possessing the most interesting pharmacological profile and, at the end, I described those that I studied in my thesis.

Table 3 reports a list of analogues that either entered clinical trials or are currently under clinical investigation as ortataxel [143, 144], BMS-275183 [145, 146], BMS-188797 [147, 148], larotaxel [149], carbazitaxel [150], milataxel [151], tesetaxel [152] and TL-310 [153]. The table summarizes the status of the clinical development and their main pharmacokinetic properties. Some of them are characterized by high oral bioavailability.

DRUG	STRUCTURE	STATUS	PROPERTIES
ORTATAXEL (IDN 5109)	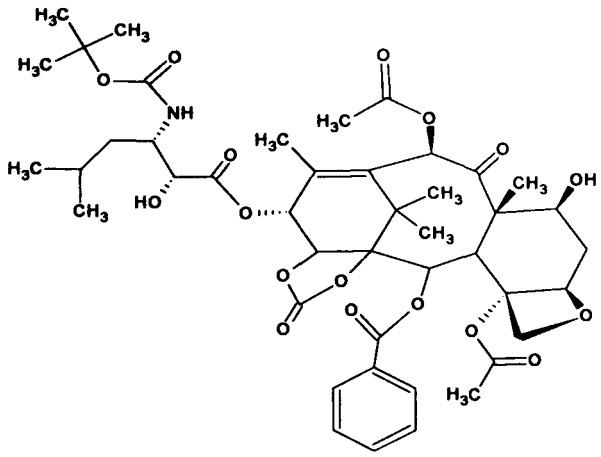	Phase II (i.v.) Phase I (oral) Formulation: Polysorbate 80/Ethanol/Citric acid	Oral bioavailable Linear pharmacokinetics Half-life: 25 h (range 22-35 h) Blood Brain Barrier crossing
BMS -275183	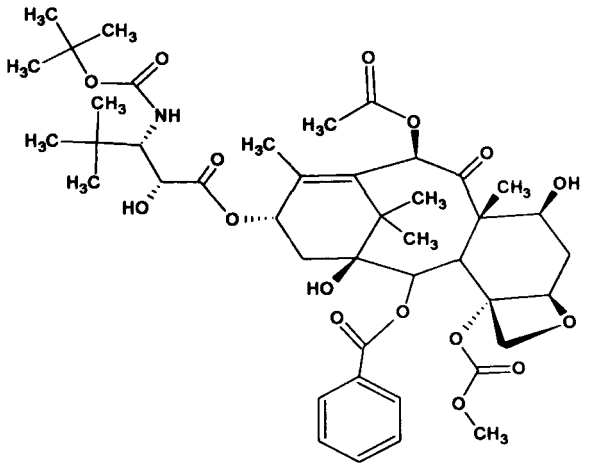	Phase II (oral) Formulation: Lipophilic solvent (i.e. Peceol)	Oral bioavailable Non linear pharmacokinetics Half-life: 22 h (range 19-73 h)
BMS-188797	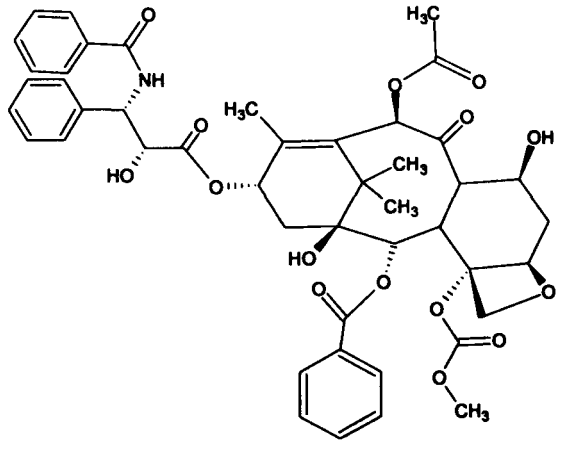	Phase I (i.v.) Formulation: Cremophor EL/Ethanol (1:1) in reduced conc. (-35%) compared to paclitaxel	Linear pharmacokinetics Half-life: 25 h (range 14-37 h)
LAROTAXEL (XRP 9881)	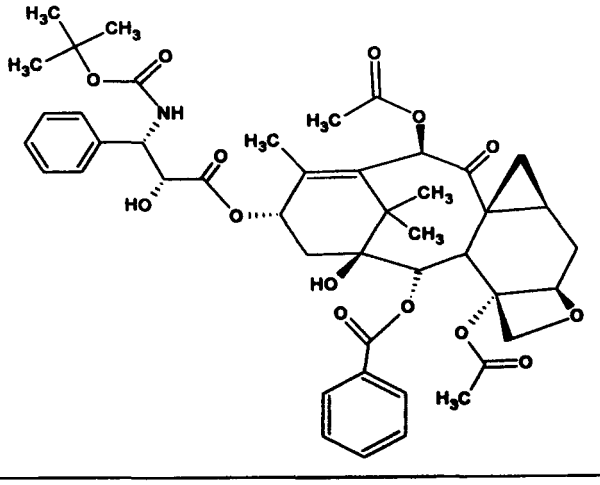	Phase III (i.v.) Formulation: Polysorbate 80/Ethanol/Water	Non linear pharmacokinetics Half-life: 19 h (range 13-36 h) Blood Brain Barrier crossing

Table 3. Taxanes analogues approved or under clinical development for cancer treatment (1/2)

DRUG	STRUCTURE	STATUS	PROPERTIES
CARBAZITAXEL (XRP 6258)	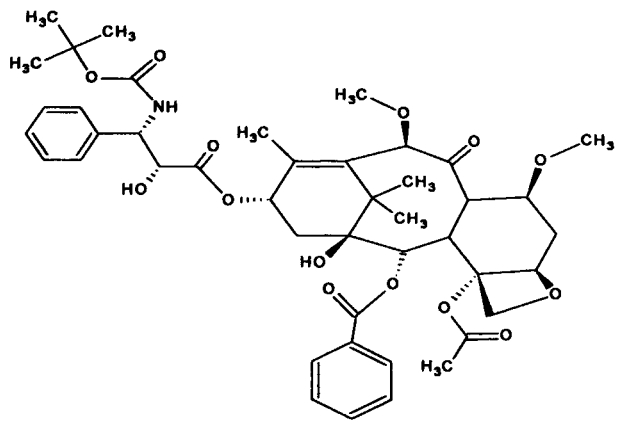	Phase II (i.v.) Formulation: Polysorbate 80/ Ethanol/water	Linear pharmacokinetics Half-life: 77 h (range 51-96 h) Blood Brain Barrier crossing
MILATAXEL (MAC 321)	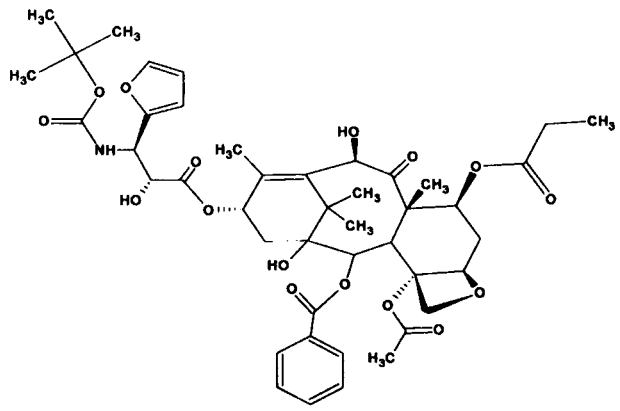	Phase II (i.v.) Phase I (oral) Formulation: Cremophor-EL/Ethanol/ water (in reduced conc. compared to paclitaxel)	Oral bioavailable Non linear pharmacokinetics Half-life: 45 h (range 20-228)
TESETAXEL (DJ 927)	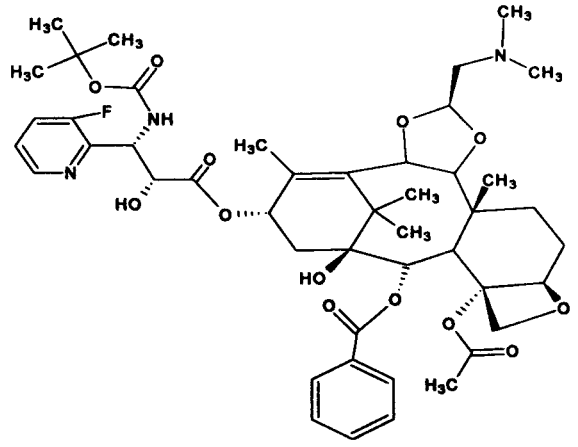	Phase I/II (oral) Formulation: not specified (compound highly soluble)	Oral bioavailable Non linear pharmacokinetics Half-life: 167±77 h
TL-310	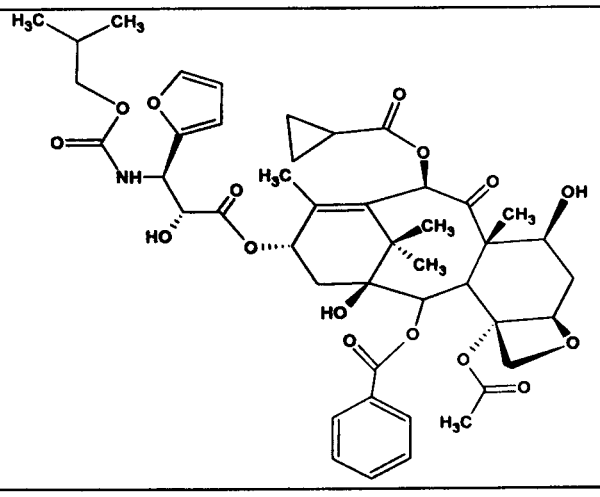	Phase I (oral) Formulation: not specified (compound highly soluble)	Oral bioavailable Half-life: 80 h

Table 3. Taxanes analogues approved or under clinical development for cancer treatment (2/2)

Many of these taxanes were obtained by modifying substituents at C3' of the C13 side chain (figure 5), where one or both the phenyl groups in paclitaxel structure were replaced by other functional groups [146, 151, 153, 154].

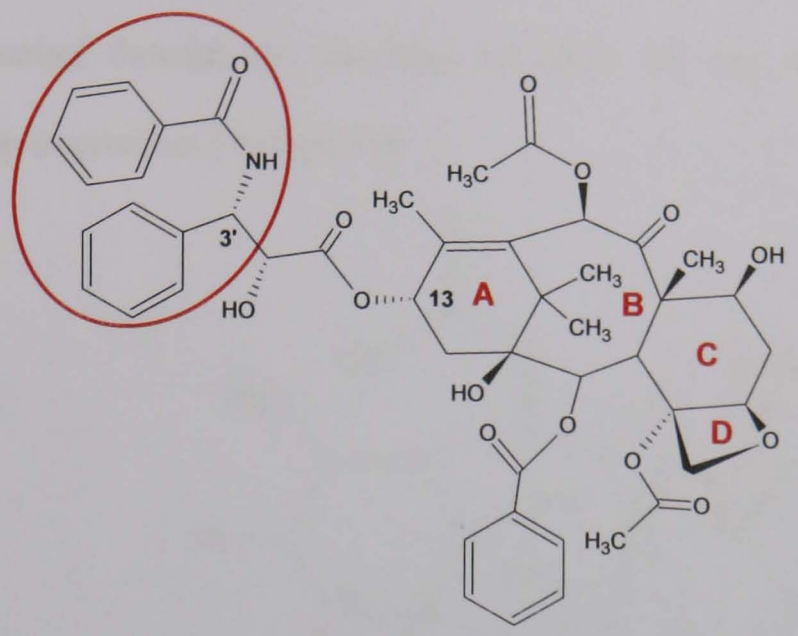

Figure 5. Paclitaxel chemical structure

These structural modifications made the novel taxanes more soluble, more potent and effective against paclitaxel-resistant tumour cells. It is still not clear how these structural changes at C3' affect the metabolism of taxanes, which is crucial to efficacy, toxicity, route of administration, pharmacokinetics and pharmacodynamics [155, 156].

Paclitaxel, because of its molecular complexity, is an ideal candidate for systematic modification to develop an understanding of its structure-activity relationships. For this reason, besides the modification of the side chain in position 13, many other structural changes were introduced on taxane structure such as the modification of the C-7 position with hydrophobic arenecarbonylcinnamoyl groups [157], the replacing of the 2-benzoyl group with substituted 2-aroyl groups, the synthesis of D-secotaxanes [158] and so on.

1.7.2.2. New analogues studied in this thesis

The derivatives considered in this thesis - IDN 5390, IDN 5614, IDN 5738, IDN 5839 and IDN 6140 - were obtained by two different main modifications on taxane structure: the C-ring opening through the cleavage of bond 7-8 and the introduction of a functional group in position 14 (figure 6) .

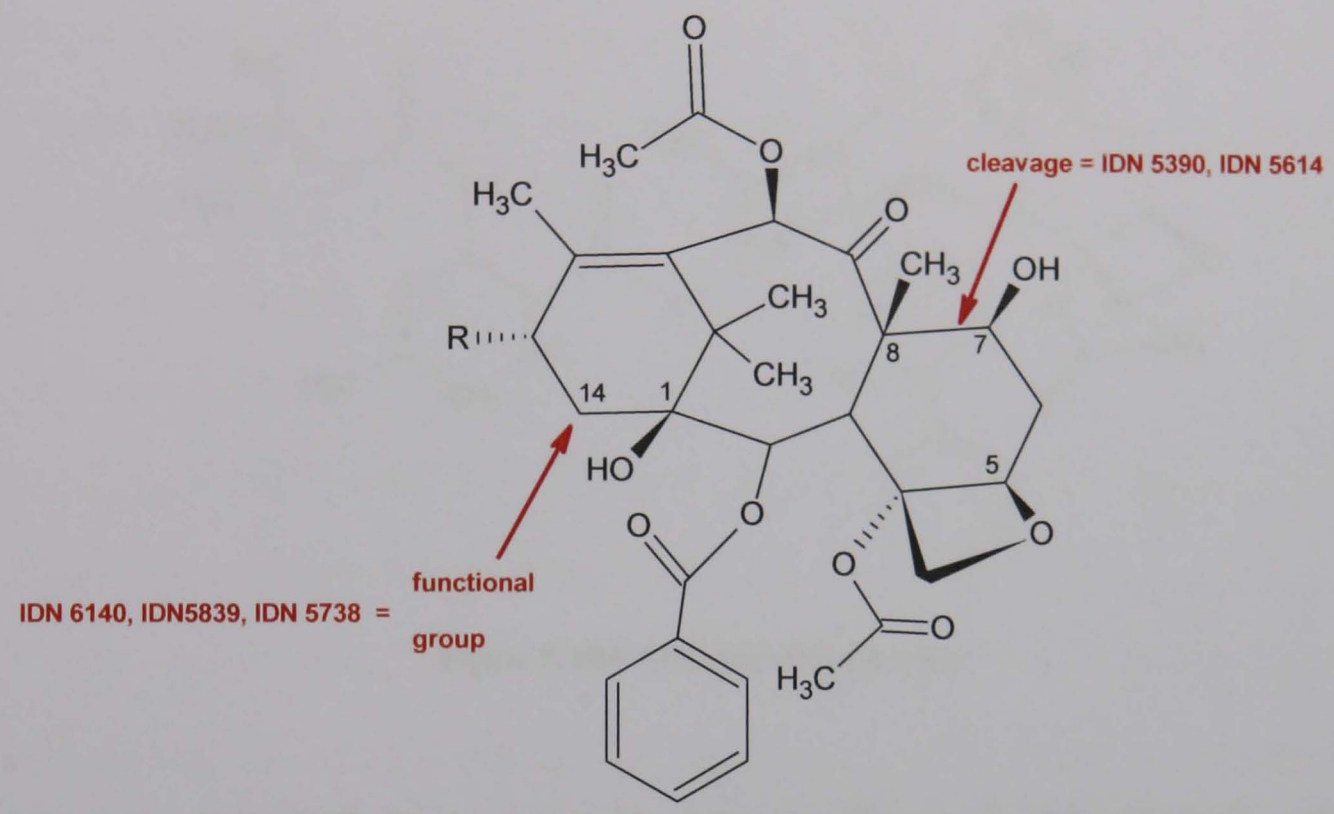

Figure 6. Main structural modifications introduced on taxane scaffold to obtain the studied derivatives

1.7.2.2.1. C-seco derivatives

The opening of C-ring led to C-seco paclitaxel analogues [159] and among them, IDN 5390, [13-(N-Boc-3-*i*-butylisoserinoyl)-C-7,8-*seco*-10-deacetylbaccatin III, figure 7], was initially selected for its ability to inhibit endothelial cell motility [160]. This antiangiogenic effect was confirmed in a paclitaxel-resistant tumor model [161].

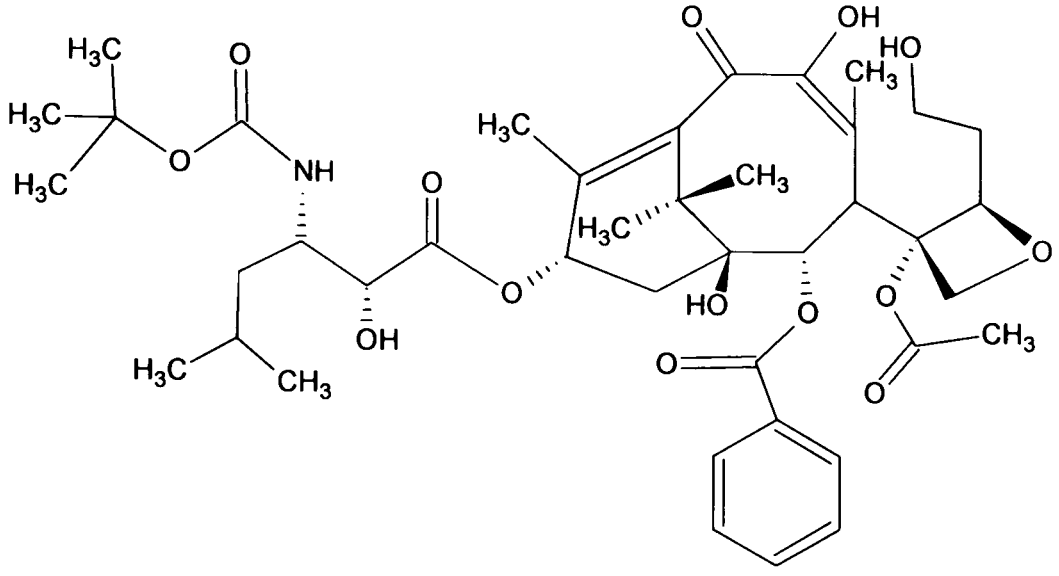

Figure 7. IDN 5390 chemical structure

Moreover, IDN 5390 has a favourable bioavailability, it is well tolerated without causing any apparent toxicity (i.e. no body weight loss at therapeutically active dose), even upon repeated oral treatment, and showed a significant antineoplastic activity on a panel of different tumour models, including some paclitaxel-resistant tumours [161, 162]. A variety of mechanisms have been proposed to explain taxane resistance, but one of the most prominent mechanism of drug resistance seems to be the overexpression of specific tubulin isotypes: class III ß-tubulin [139]. The expression of class III β-tubulin confers intrinsic resistance to paclitaxel, but IDN 5390 is not conditioned by this class of tubulin. This finding might explain why the combination IDN 5390/paclitaxel yields a strong synergism in tubulin polymerization experiments as well as in whole cells [163], providing the rational for the combined use of two taxanes with different affinity toward tubulin isotypes as a novel approach to overcome paclitaxel resistance.

On the basis of my pharmacokinetic results, in particular about the metabolism of IDN 5390, Indena S.p.A. synthesized and provided me a new derivative, IDN 5614, structurally related to IDN 5390.

1.7.2.2.2. 14-functionalized derivatives

The other mentioned modification is concerned the "southern hemisphere" of taxanes structure comprising the C14 and C1 to C5 positions. From extensive studies performed by many research groups on the structure-activity relationship of paclitaxel, docetaxel and their analogues, it has emerged that structural changes in this region of the molecules exert a major role on taxane biological activity [164].

In particular, the introduction of a hydroxyl group in position 14 of 10-deacetylbaccatin III confers to that a better water solubility [165].

For this reason, several derivatives of 14-β-hydroxyl-10-deacetylbaccatin III have been screened and the research conducted to the identification of ortataxel (see table 3), characterized by the presence of a carbonate group between positions 1 and 14 [(3a*S*,4*R*,7*R*,8a*S*,9*S*,10a*R*,12a*S*,13*S*,13a*S*)-7,12a-bis(acetyloxy)-4-({(2*R*,3*S*)-3-[*tert*-butoxycarbonyl)amino]-2-hydroxy-5-methylhexanoyl}oxy)-9-hydroxy-5,8a,14,14-tetramethyl-2,8-dioxo-3a,4,7,8,8a,9,10,10a,12,12a,12b,13-dodecahydro-6,13amethano [1,3]dioxolo[8,9]cyclodeca[1,2-*d*][1]benzoxet-13-yl benzoate] [166, 167].

Ortataxel was selected in pre-clinical studies because it did not show any appreciable neurotoxicity or cardiotoxicity and exhibited much less general toxicity while maintaining excellent cytotoxicity, which provides a wider therapeutic window [154].

Ortataxel is a poor substrate of P-gp system, having 3 important effects:

1- this taxane is active against paclitaxel-resistant tumours overexpressing P-gp;
2- ortataxel shows a good bioavailability and it was found to be highly active when given orally [168-170];

3- ortataxel can reach the brain tissue passing through the BBB [154]. Taking into account also that paclitaxel is active on human glioblastomas [171] and on human glioma cells *in vitro* [172] and on melanoma brain metastasis animal model and glioblastoma animal model - when administered with a P-gp inhibitor [173] - it is easy to explain the observed ability of ortataxel to affect the growth of intracranial tumours [174].

For these reasons, ortataxel was selected for further developments and entered phase I-II clinical trials. It showed encouraging activity and clinical benefit in heavily pre-treated metastatic breast and non-small cell lung cancer patients [143, 144, 175].

With the aim of further improving the pharmacological properties of ortataxel, a new family of 1,14 substituted taxanes was synthesized by Indena S.p.A. by quenching the potassium enolate of the 13-oxo-7-protected-baccatin with different electrophile substituents (figure 8), generating a wide number of C-14 modified derivatives, which were further developed to the corresponding taxoids [176, 177].

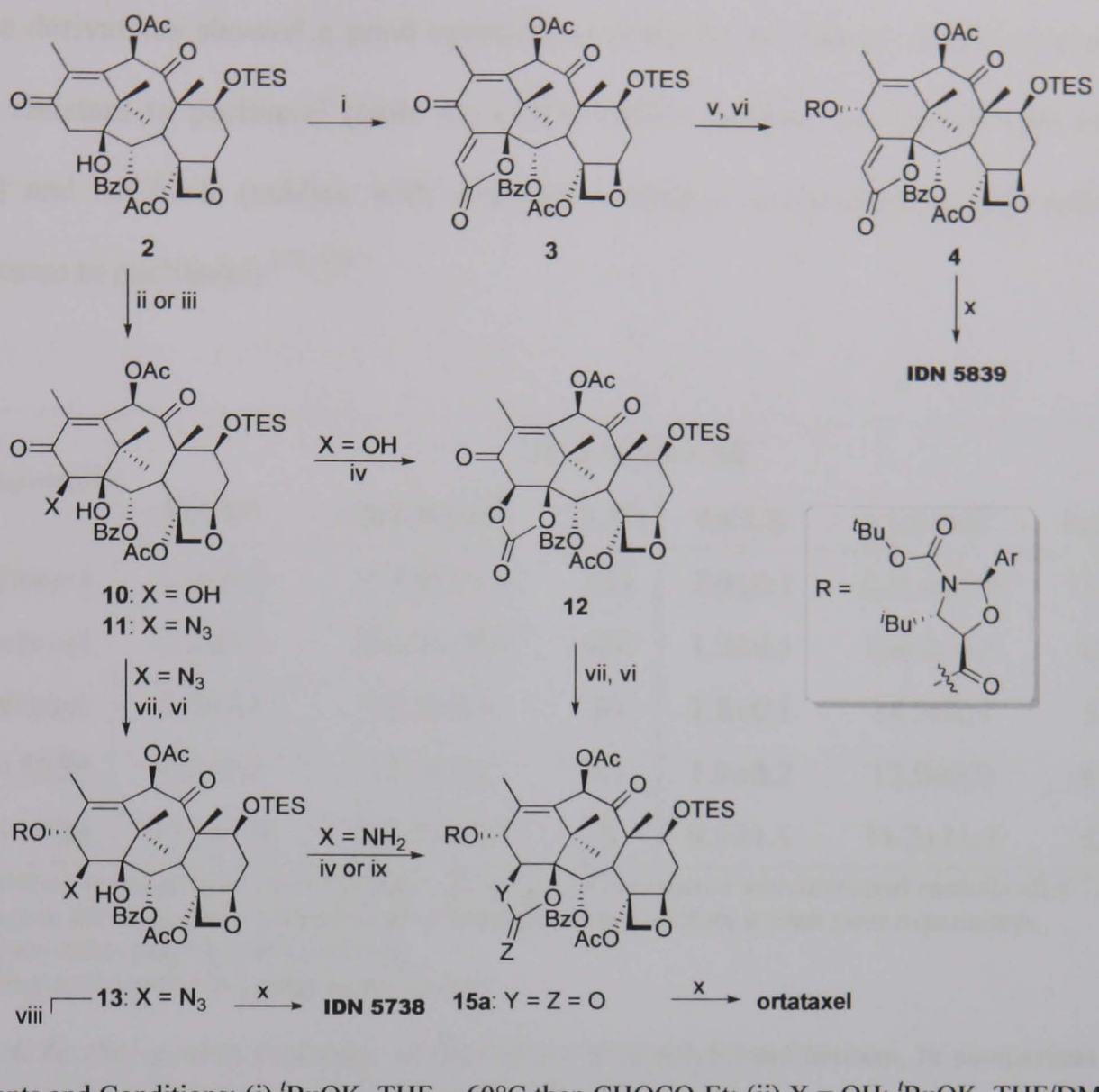

[a]Reagents and Conditions: (i) ^{t}BuOK, THF , -60°C then $CHOCO_2Et$; (ii) X = OH: ^{t}BuOK, THF/DMPU, -70°C then oxaziridine; (iii) X = N_3: ^{t}BuOK, THF/DMPU, -70°C then TsN_3 then NH_4Cl; (iv) $COCl_2$, Py; (v) H_2, Pd/C, AcOEt; (vi) *N*-Boc-norstatinic acid, DCC/DMAP, CH_2Cl_2; (vii) $NaBH_4$, EtOH; (viii) H_2, Pd/C, (ix) Z = S $(2\text{-Py})_2CS$, (x) Py/HF then MeCOCl, MeOH.

Figure 8. Synthetic procedures for the preparation of IDN 5738 and IDN 5839

Two derivatives, IDN 5738 and IDN 5839 (figure 9, panel A and B, respectively) were selected for preclinical evaluation.

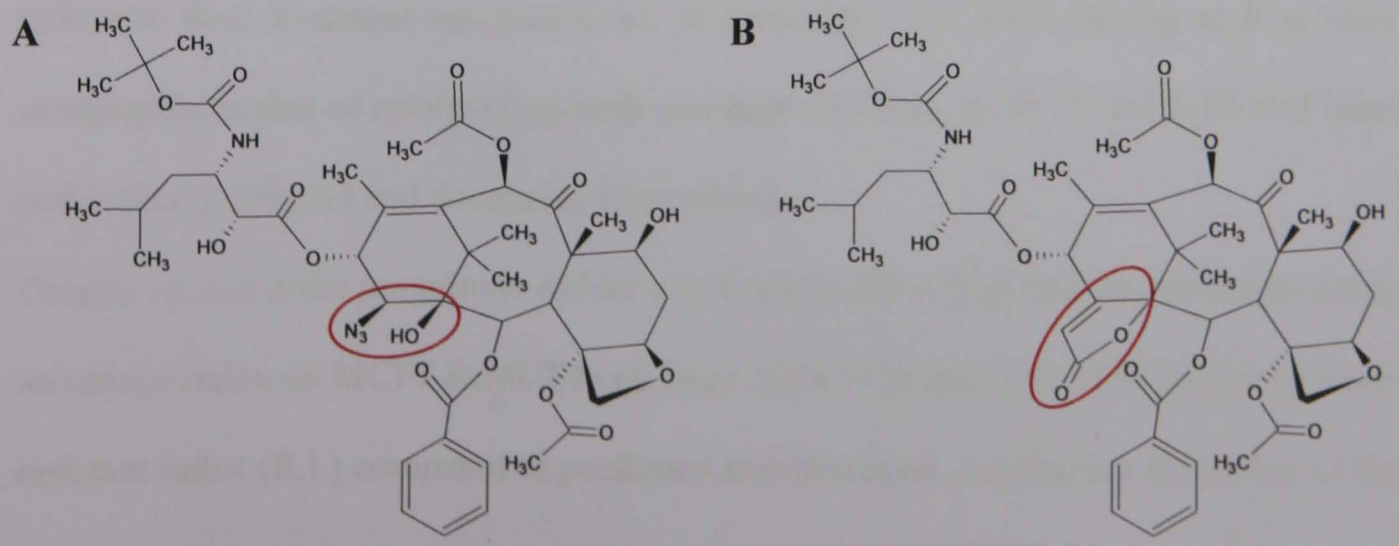

Figure 9. Chemical structures of IDN 5738 and IDN 5839

These derivatives showed a good cytotoxic activity on two human breast tumour cell lines resistant to paclitaxel (table 4), LCC6-MDR1 (subline transfected with MDR1 gene) and MCF7-R (subline with acquired resistance to doxorubicin and collateral resistance to paclitaxel) [178, 179].

Compound	[a]IC_{50} (nM) ± SE					
	MCF7	MCF7-R[b]	R.I.[c]	LCC6	LCC6-R[b]	R.I.[c]
paclitaxel	1.4±0.3	354.0±35.0	253	2.0±0.1	221.0±6.6	111
docetaxel	0.5±0.1	230.0±16.0	460	1.2±0.1	110.2±4.6	92
ortataxel	1.6±0.1	32.0±2.4	20	2.8±0.1	14.3±0.4	5
IDN 5839	0.4±0.1	17.0±1.4	43	1.9±0.2	12.0±0.9	6
IDN 5738	22.3±1.8	188.0±12.0	8	9.3±1.1	74.2±11.1	8

[a]Concentration required for 50% reduction of cell growth compared with untreated controls after 72 h of exposure to the drug. Mean ± standard error values are reported from at least three experiments.
[b]Cell lines expressing high levels of P-gp.
[c]IC_{50} drug-resistant line/IC_{50} drug sensitive line.

Table 4. *In vitro* growth inhibitory activity (IC_{50}) of 14-substituted taxanes, in comparison with paclitaxel and docetaxel, on human breast cancer cell lines.

The collected data showed that on sensitive cell lines, IDN 5738 and IDN 5839, were cytotoxic at nanomolar concentrations and, in particular, IDN 5839 was characterized by an IC_{50} value comparable to that of paclitaxel, docetaxel and ortataxel.

On multidrug resistant MCF7-R and LCC6-MDR cell lines, both of them resulted more cytotoxic than docetaxel and paclitaxel. In particular, IDN 5839, having an IC_{50} value comparable to that of ortataxel on both resistant cell lines, is 18-21 and 9-14 fold more active than paclitaxel and docetaxel, respectively.

Despite its one order magnitude milder cytotoxicity, IDN 5738 had the most interesting resistance index on MCF7-R/MCF7 cell lines. IDN 5738 and IDN 5839 showed a lower resistant index (R.I.) compared to paclitaxel and docetaxel, confirming the ability of the

14 modified taxanes to overcome multi drug resistance effect (MDR), as it was demonstrated for ortataxel [180].

In order to better characterize these compounds, the tubulin interaction was investigated evaluating the ability of IDN 5738 and IDN 5839 to stabilize tubulin and promote its polymerization. Experiments were carried out using bovine brain purified tubulin and densitometry testing the two compounds at the same concentration (10 μM). IDN 5738 and IDN 5839 were effective in inducing tubulin polymerization. Moreover, the results obtained with IDN 5839 were very close to those obtained with docetaxel and ortataxel (Indena S.p.A. internal report).

Afterwards, on the basis of pharmacokinetic data produced about IDN 5738 and IDN 5839, I obtained and studied a third derivative, IDN 6140 (figure 10) synthesized by Indena S.p.A.

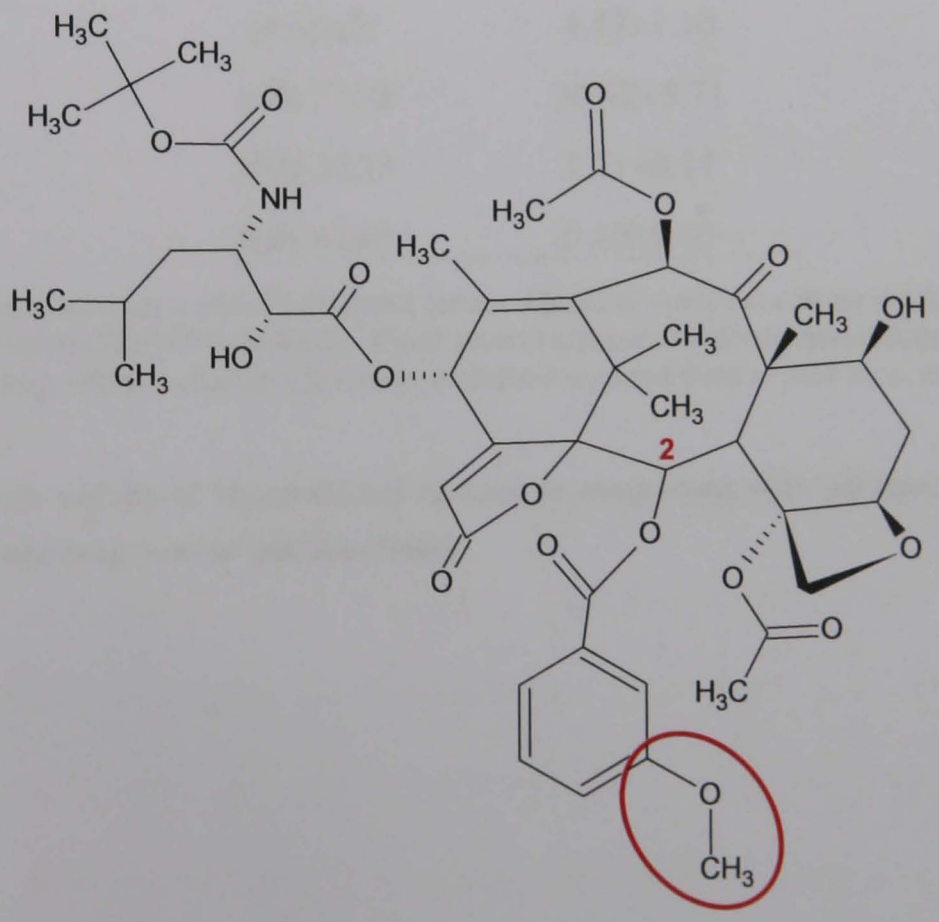

Figure 10. IDN 6140 chemical structure

The interest for IDN 6140 was based on a well known and reported characteristic of paclitaxel chemistry. The meta derivatives, and in particular methoxy derivatives, were much more cytotoxic than paclitaxel, thanks to the "*meta*-effect" that it is the enhanced interaction between the C-2 ring and asp224 in the β-tubulin binding pocket [181, 182]. IDN 6140 was in fact obtained by the introduction of a methoxy meta-substituent on the 2-benzoate of taxane scaffold of IDN 5839 structure.

Even IDN 6140 was selected for the subsequent preclinical evaluation on the basis of its cytotoxic activity. On a human lung cancer cell line (H460), it showed a potent cytotoxic activity, superior not only respect to paclitaxel (40-fold), but even to ortataxel (9-fold) [183] (table 5).

[a]compound	[b]IC_{50} (nM) ± SD
paclitaxel	21.0±3.2
ortataxel	4.47±1.10
IDN 5738	26.42±5.71
IDN 5839	1.31±0.11
IDN 6140	0.49±0.03

[a]Compounds were dissolved in 10% DMSO and further diluted in complete culture medium.
[b]Concentration required for 50% reduction of cell growth compared with untreated controls after 72 h of exposure to the drug. Mean ± standard deviation values are reported from at least three experiments

Table 5. Cytotoxic activity of 14-substituted taxanes, in comparison with paclitaxel and docetaxel, on human lung tumour cell line (H460)

The general aim of my thesis is the characterization of the preclinical pharmacokinetic profile of the aforementioned new taxane derivatives. To do that, firstly I developed and validated the assays to determine the concentration of the new compounds in biological specimens, and then I have applied them to study the pharmacokinetics in mice. The methods were based on high-performance liquid chromatography coupled with tandem mass spectrometry (LC-MS/MS) technique. The following pages will summarize the principles of mass spectrometry.

1.8. Mass spectrometry

The application of pharmacokinetics is very important to evaluate the drug disposition and, consequently, to optimize the therapy.

In order to define the pharmacokinetic profile of a compound, the method and the analytical technique used are fundamental. The higher the sensitivity of the method is, the better the description of the drug kinetics will be, in terms of a much longer monitoring of drug concentration, which also means a better description of the terminal elimination phase thanks to an appropriate limit of quantitation.

In the last 30 years, there has been significant improvements in analytical technologies applied in cancer pharmacology to measure drug concentration and to study drug metabolism. At the beginning, the concentration data from plasma or other biological matrix were usually obtained by HPLC-UV/VIS methods; the next step was to prefer, when it was possible, the use of a fluorescence detector, but the real change in bioanalysis was the development of bench-top mass spectrometry as a method of detection, combined with liquid chromatography (LC-MS). Within a few years, LC-MS has become the method of choice for quantitative drug analysis to support

pharmacokinetics and drug metabolism studies. Besides the possibility to reduce time of analysis, coupling the mass spectrometer with LC provides significant improvements in assay sensitivity and specificity, in fact this technique makes possible the determination of picomolar drug concentrations in body fluids. The increase in sensitivity and specificity caused 3 important effects:

1- the possibility to detect species at very low concentration;

2- the possibility to use very small amount of sample, that is particularly important in pediatric studies or in preclinical studies conducted in small animals. In small animal studies, this is relevant for the analysis of fluids produced in small amount such as bile, or in blood microsampling. The use of serial bleeding is increasingly employed because of the following advantages: it leads to a reduction in animal usage - associated with a reduction in compound required for such experiments -, in differences due to dosing error and in animal to animal variation. According to these advantages, the euthanasia of animals is not required or greatly reduced, as they may be reused after several weeks recovery and washout;

3- the drug and its metabolites can be detected from complex matrices such as tissues or whole blood.

Mass spectrometry is a powerful analytical tool both for drug quantitative and qualitative analysis. The quantitative information is obtained by using a mass spectrometer capable of MS/MS fragmentation. MS/MS is necessary because many compounds have the same intact mass, while the fragmentation pattern is compound specific. The combination of parent mass and its fragment ions is used to monitor selectively the compound that has to be quantified.

MS/MS fragmentation is also fundamental for qualitative information, because the mass spectrum of every compound is unique and it can be used like a chemical fingerprint to

characterize the sample, even in case where only picogram amounts of analyte are available.

In my thesis, I performed the quantitative bioanalysis by using a triple quadrupole mass spectrometer, while I studied the metabolic profile by using an ion trap mass spectrometer.

In LC-MS the sample is introduced into the mass spectrometer after its separation in an HPLC column. Charged ions of the analytes are then produced into the ion source of the mass spectrometer. These ions are separated by the MS analyser on the basis of their mass to charge (*m/z*) ratio. There are different types of MS ion sources, but the most commonly used in pharmacokinetic studies is Electrospray Ionization (ESI), an atmospheric pressure ionization (figure 11).

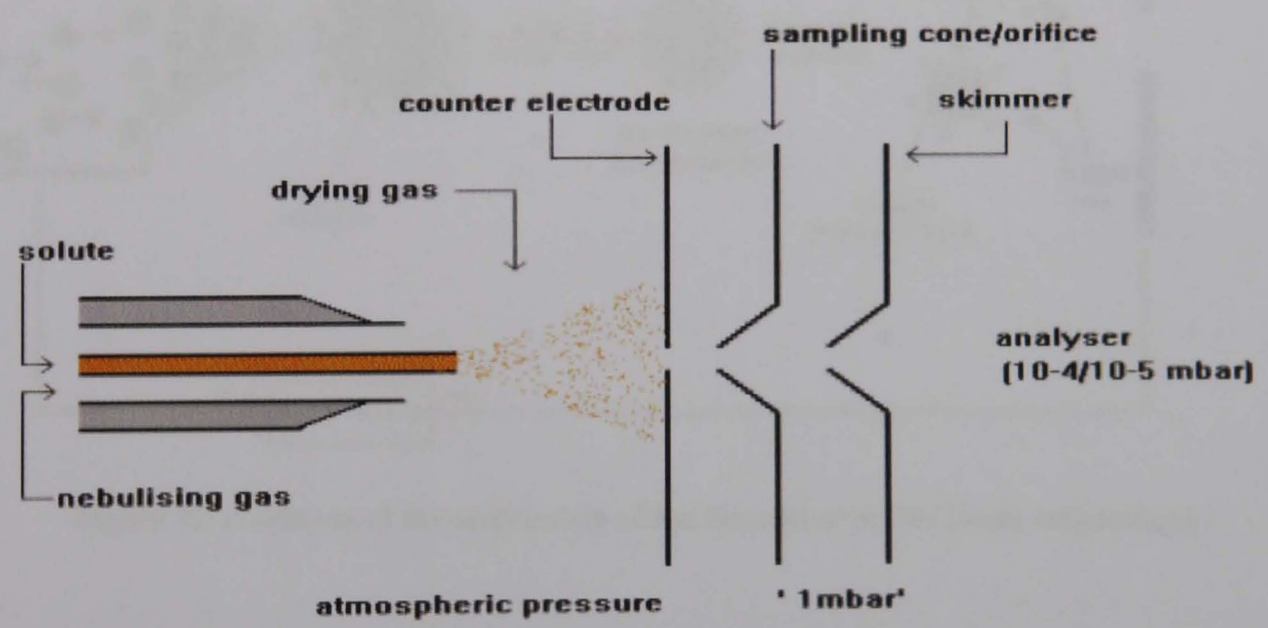

Figure 11. A scheme of an Electrospray Ionization source [from web source]

Electrospray spectra are produced by passing a liquid stream through a metal capillary maintained at high voltage (2000-5000 V). This forces the spraying of charged droplets from the needle with a surface charge of the same polarity of the charge on the needle. The droplets are repelled from the needle towards the source sampling orifice on the counter electrode. As the droplets traverse the space between the needle tip and the

orifice, solvent evaporation occurs thanks to the presence of a nebulizer and a heated desolvation gas. This causes the reduction of the droplet size to a point in which the repulsive forces between charges, on the surface of the droplets, are sufficient to overcome the cohesive forces of surface tension, leading to the "coulombic" explosion and, consequently, the droplet is ripped apart. This produces smaller droplets that can repeat the process as well as naked charged analyte molecules. These analyte ions can be singly or multiply charged and are emitted into the gas phase where they are focused and introduced into the MS analyser, kept under high vacuum (figure 12).

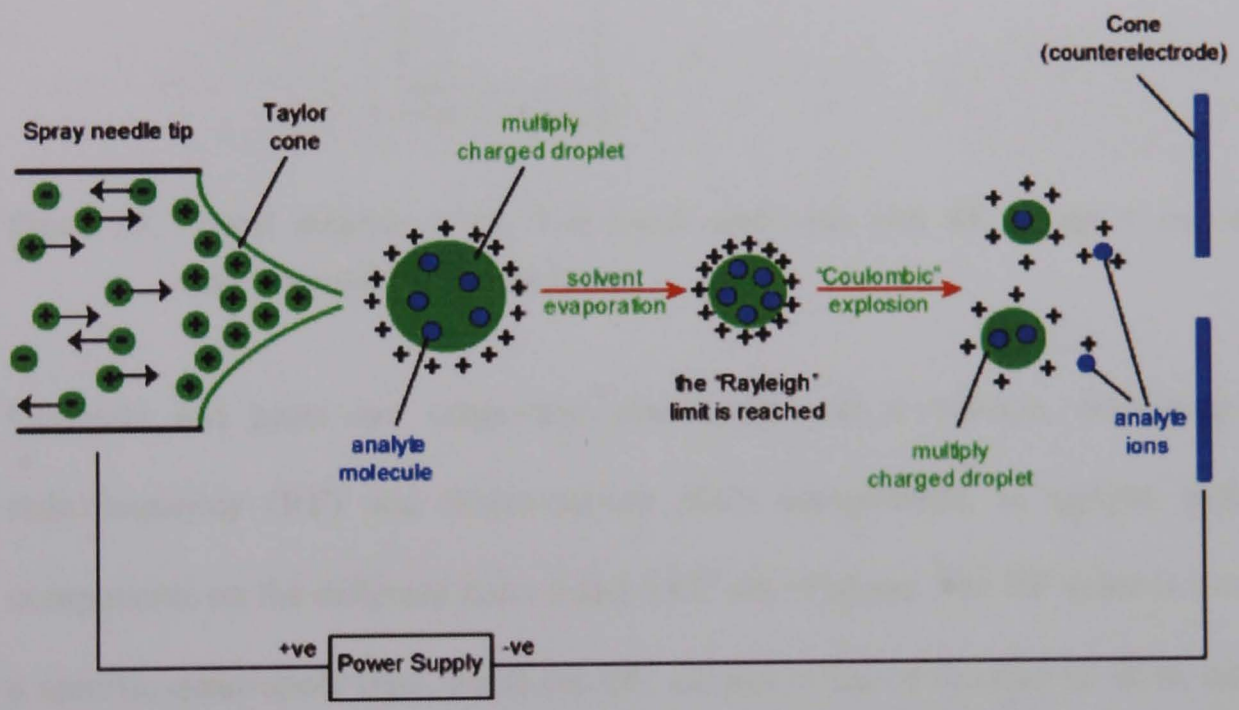

Figure 12. A scheme of the mechanism of ion formation in ESI [from web source]

The production of smaller droplets is enhanced by lower mobile phase flow rate and use of volatile mobile phases. ESI is a soft ionization technique - as very little residual energy is retained by the analyte after ionization - and does not cause decomposition of labile compounds. It is characterized by an efficient ion production and it can operate in either positive or negative ion mode.

From the ion source, ions are transferred to the mass spectrometer, where they are analysed.

A triple quadrupole mass spectrometer is characterized by three consecutive quadrupole analysers: the first and the third ones work as mass filters, while the second as a collision cell. A quadrupole consists of four parallel rods arranged symmetrically around a central axis (figure 13).

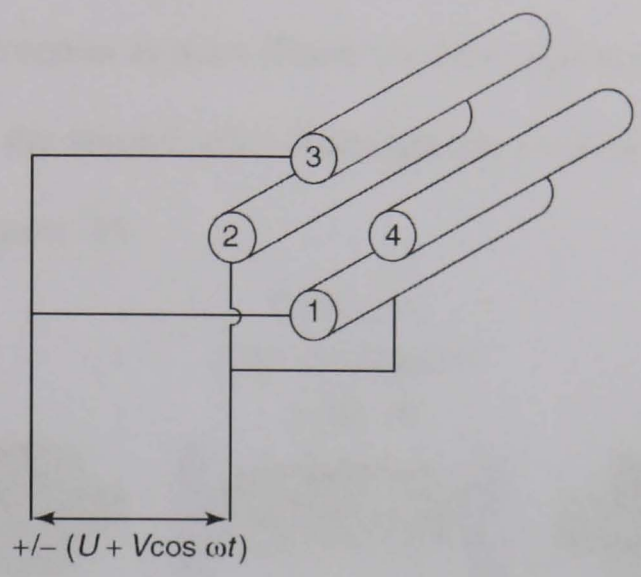

Figure 13. Circuit diagram of the four quadrupole rods with RF voltage *V cos ωt* and the superimposed DC voltage *U*

Opposite rod pairs are connected electrically and a voltage, consisting of both radiofrequency (RF) and direct-current (DC) components, is applied with the RF components on the different pairs being 180° out of phase. The RF value is a constant of a specific quadrupole type, while the DC voltage is varied in order to allow only ions of a particular *m/z* to follow a stable trajectory through the rods and reach the detector, while all other ions hit the quadrupoles because of their unstable path (figure 14).

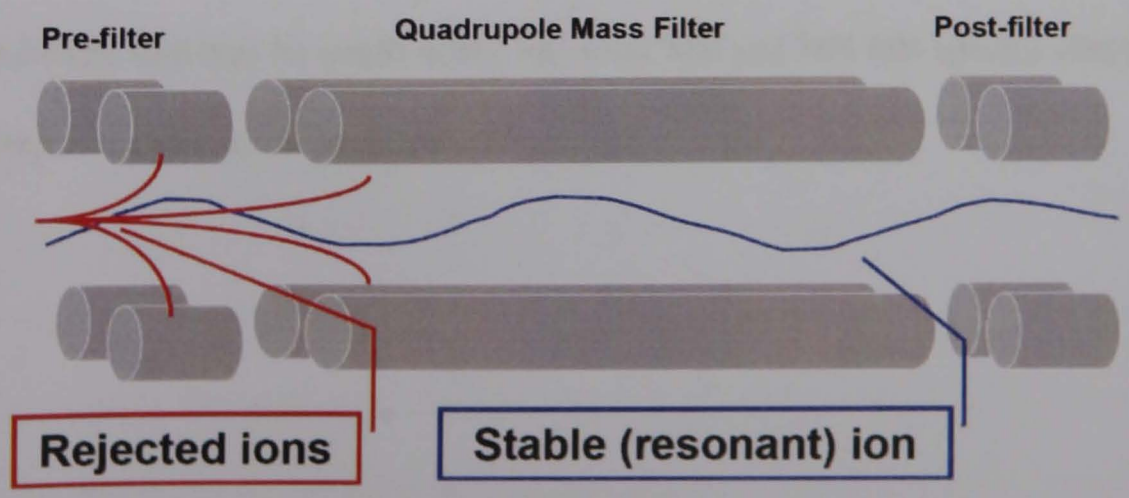

Figure 14. Scheme of a quadrupole filter

According to the aims of the analysis, the first and the third quadrupole can be used in different scan modes to acquire and visualize data. Each quadrupole can be set to filter only one *m/z* ratio or to scan over a wide *m/z* range. The most common scan mode for a quantitative analysis is defined as Selected Reaction Monitoring (SRM), characterized by the use of two quadrupoles as mass filters: the first quadrupole selects the precursor ion of the analyte and the second, after fragmentation in the collision cell, selects the specific product ion (figure 15).

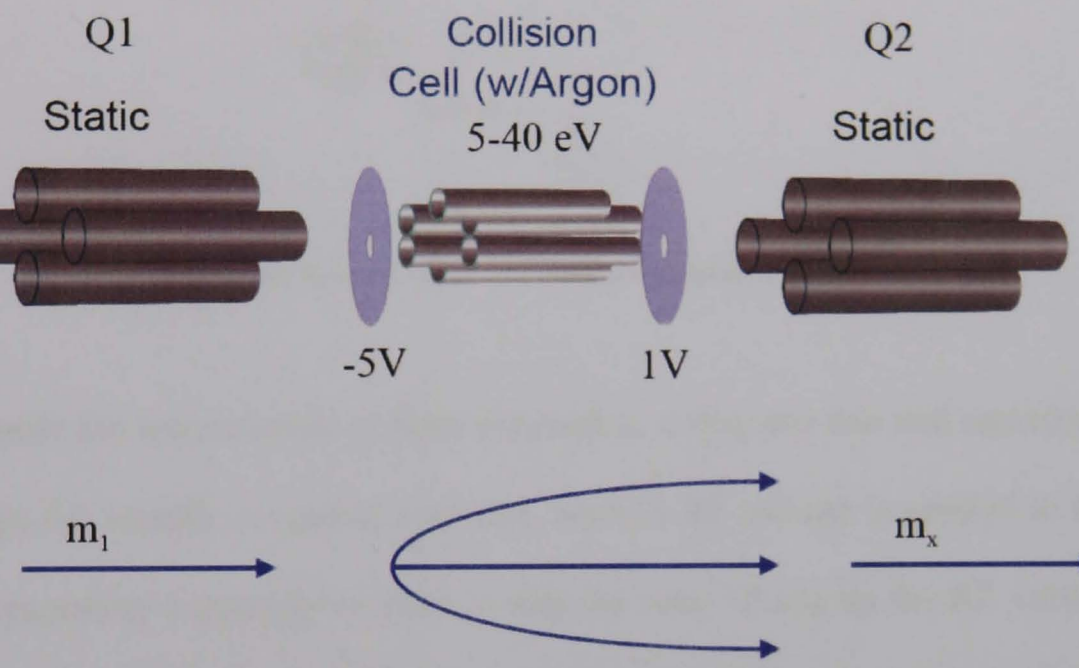

Figure 15. Selected Reaction Monitoring in a triple quadrupole

This acquisition mode maximizes the signal/noise ratio of the compound and it is highly specific.

The study of the metabolic profile of a drug needs qualitative analyses for structural identifications, that can be made using full scan MS and MS/MS spectra obtained with an ion trap mass spectrometer (figure 16).

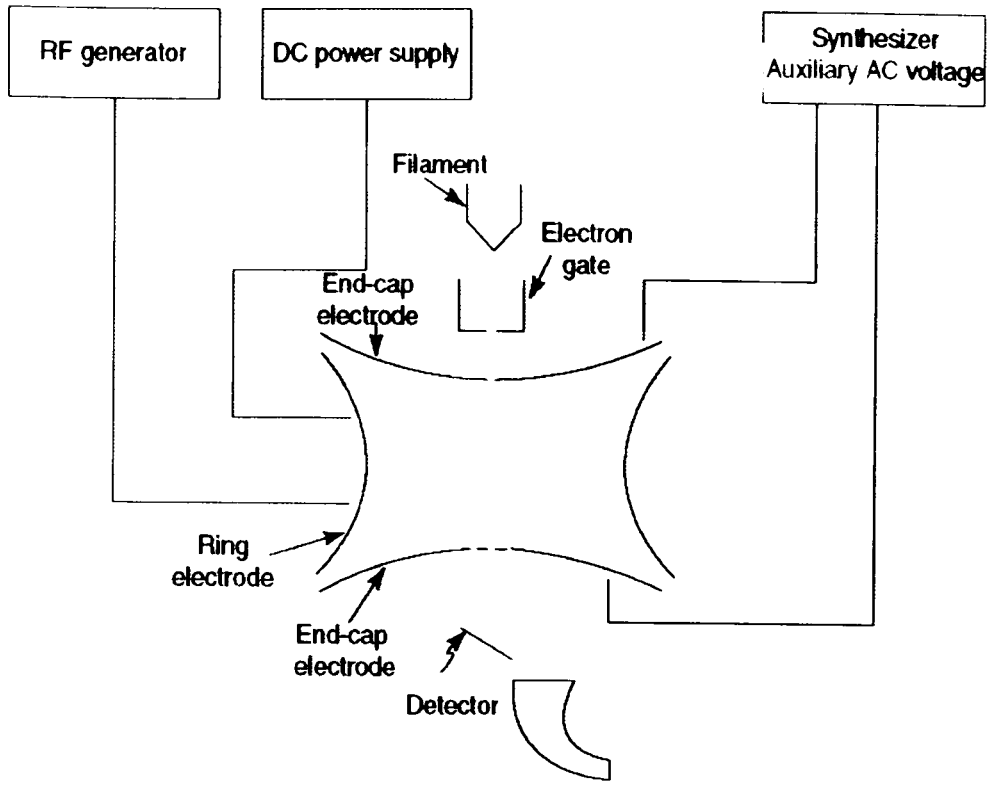

Figure 16. Scheme of an ion trap mass spectrometer

The quadrupole ion trap consists of three electrodes: a ring and two end cap electrodes. The end caps are usually at ground potential, while a RF voltage is applied to the ring electrode, generating a quadrupole field to trap the ions. Changing the RF voltage in a systematic way, a complete mass spectrum may be obtained: all ions, created during a given time period, are trapped until an RF voltage is applied to the ring electrode and then, on the basis of their *m/z* ratio, sequentially ejected from the analyser and directed towards the detector. Helium gas in the trap favours the trapping efficiency by contracting the ions trajectories to the centre of the trap and reducing the kinetic energy of the ions. This allows ions of a given *m/z* to form a packet. The ion packet is ejected more quickly and efficiently than a diffuse cloud of ions, thus improving resolution.

During the analysis, all ions (in gas phase) generated from the sample, are acquired in a wide and fixed mass range and it is possible to observe the MS and MS/MS spectra corresponding to the peaks appeared in the LC-MS trace. The obtained fragmentation profile is useful to have structural information and allows the study of possible metabolites. With an ion trap spectrometer, it is possible to work in MS/MS mode, but,

since the ion trap consists of a single element, it is usually indicated as MS/MS "in time". As well, even sequential MS/MS analysis (MS^n) can be undertaken by the ion trap. By using appropriate scanning modes, the ion trap excludes all non-interesting ions and selects the wanted precursor ion; then, by applying an appropriate RF voltage, causes its fragmentation and the ejection of fragments to the detector. The ability of the ion trap technique to perform multiple stages of mass spectrometry increases greatly the amount of structural information that can be obtained for a given molecule.

CHAPTER 2

AIMS

The general aim of my thesis is the characterization of the preclinical pharmacokinetic profile of new taxane derivatives, C-seco and 14-β-functionalized analogues, synthesized by Indena S.p.A.

At the beginning of this thesis work, only three new compounds were available: IDN 5390 - obtained by the opening of C-ring -, IDN 5738 and IDN 5839, both of them derived from the introduction of a functional group in position 14 of taxane scaffold.

Successively, on the basis of pharmacokinetic data collected about these three analogues, two more compounds were synthesized by Indena S.p.A.: IDN 5614 and IDN 6140, the former structurally related to IDN 5390 and the latter to IDN 5839.

To describe the pharmacokinetic profile of a drug within an organism, it is necessary to define its absorption, distribution, metabolism and excretion. All these steps influence the drug plasma levels and the kinetics of drug exposure to the tissues and hence influence the pharmacodynamics of the compound. To elucidate the metabolic pathway of the new taxane derivatives, whenever necessary, metabolic studies are performed both *in vitro,* using mouse and human liver microsomes or S9 fraction, and *in vivo* in rodent models.

To describe the pharmacokinetic/metabolic profile of a compound, as first step, it is necessary to develop and validate the assay to determine the concentration of the new derivative in biological specimens. Consequently, the validated assay is applied to characterize the pharmacokinetics and the bioavailability of the compound in mice after oral and intravenous administration. The methods currently applied are generally based on high-performance liquid chromatography coupled with tandem mass spectrometry (LC-MS/MS) technique, because of its high sensitivity and specificity that is required for pharmacokinetic studies with potent small molecules that are used at relatively low doses.

CHAPTER 3
MATERIALS AND METHODS

3.1. Materials and animals

3.1.1. Standards and reagents, chemicals, control mouse plasma, mice, materials and supplies and instrumentation

3.1.1.1. Standards and reagents

IDN 5390 (lot no. 553/16), paclitaxel (lot no. 27759/K3, used as internal standard, IS, in the quantitation method of IDN 5390), IDN 5614 (lot # PGB646), IDN 5738 (lot # 624/12, ba 02/957/LR), IDN 5839 (lot # 638/41), IDN 5127 (ba 186/18-CoA n.91/061/LR, used as IS in the quantitation method of IDN 5738 and IDN 5839) and IDN 6140 (708/30 – ba. 06/0335 LR3) were obtained from Indena S.p.A., Settala, Milan, Italy.

7-ethoxycoumarin (lot # 054K3687), NADPH generating system: ßNADP, uridine diphosphate glucuronic acid (UDPGA), glucose-6-phosphate dehydrogenase, glucose-6-phosphate, magnesium chloride and D-saccharic acid 1,4 lactone, PAPS and Bovine Serum Albumin (BSA) were obtained from Sigma Aldrich, St Louis, MI, USA.

7-hydroxycoumarin (lot. # 1123370) was obtained from Fluka Chemie, Sigma Aldrich, St Louis, MI, USA.

Metabolic profiles of IDN 5390 and IDN 5614 were determined in hepatic microsomes (batch 0410046) of CD1 female mice obtained from Xenotech, LLC (KS, USA). Metabolic profile of IDN 5390 was determined also in human hepatic microsomes (batch 0212063) from Xenotech, LLC (KS, USA). Metabolic profile of IDN 6140 was determined in pooled CD-1 mouse liver S9 fraction (M1500.S9 Lot. No. 0310217) obtained from Xenotech, LLC (KS, USA).

3.1.1.2. Chemicals

Methanol and acetonitrile of HPLC grade, glacial acetic acid and formic acid for analysis were obtained from Carlo Erba (Milan, Italy).

Water of HPLC grade was obtained from a Milli Ro 60 Water System, Millipore (Milford, MA, USA).

0.9% NaCl solution was obtained from SALF S.p.A. (Bergamo, Italy).

3.1.1.3. Control mouse plasma

Female CDF1 control mouse plasma was obtained from IFFA (Credo, France) for experiments with IDN 5390. For evaluating the pharmacokinetics of IDN 5738, IDN 5839 and IDN 6140 female CD1 control mice plasma was used and it was obtained from Charles River Laboratories Italia (Calco, Italy). Three different batches of plasma were used: lot. 09-02/03/05, lot. 12-21/03/05 and lot. 49-04/12/06 for IDN 5738, IDN 5839 and IDN 6140, respectively.

3.1.1.4. Mice

Female CDF1 mice (body weight 20±2 g) were obtained from IFFA (Credo, France). CD1 female mice (body weight 25±2 g) were obtained from Charles River Laboratories Italia (Calco, Italy). They were housed and handled according to the institutional guidelines (Legislative Decree 116 of Jan 27, 1992. Authorisation n.169/94-A issued Dec. 19, 1994 by Ministry of Health) and international laws and policies (EEC Council Directive 86/609, OJ L 358. 1, Dec. 12, 1987; Standards for the Care and Use of Laboratory Animals, United States National Research Council, Statement of Compliance A5023-01, Nov. 6, 1998).

3.1.1.5. Materials and supplies

Pipets, models P20, P100, P200 and P1000 Pipetman, were obtained from Gilson Medical Electronics S.A. (Villiers-le-Bel, France).

Disposable Pipets Tips, for P20, P100, P200 and P1000 Pipetman, were obtained from Rainin Instruments (Woburn, MA, USA).

Vials (for Alliance autosampler), were obtained from Waters (Milford, MA, USA).

Disposable borosilicate glass tubes, 16 x 100 mm, were obtained from Corning Inc. (Corning, NY, USA).

Vials and limited volume inserts for WISP 717 autosampler were obtained from Waters.

3.1.1.6. Instrumentation

The HPLC-UV system, consisting of a Model 717 WISP autosampler, a Model 510 pump, a detector Model W2487 at variable wavelength UV-VIS and an acquisition system Empower Software Chromatography Manager, came from Waters Associates (Milford, MA, USA).

Three different HPLC-MS/MS systems were used:

1- A system consisting of a Surveyor autosampler and Surveyor MS pump combined with an LCQ Deca XP Plus ion trap mass spectrometer was obtained from Thermo Electron (Waltham, MA, USA);

2- A system consisting of an Alliance series 2695 HPLC coupled with a Micromass Quattro Ultima Pt triple quadrupole mass spectrometer was obtained from Waters (Milford, MA, USA);

3- A system consisting of an HPLC Series 200 autosampler and micropump (Perkin Elmer), coupled with an API 4000 triple quadrupole mass spectrometer, was obtained from Applied Biosystems (Foster City, CA, USA). The instrument was equipped with a Turbo V ESI source.

3.2. IDN 5390 and IDN 5614

3.2.1. Stock solutions

IDN 5390 stock solution was prepared in methanol at a concentration of 1 mg/mL. The stock solution was diluted with methanol to obtain working solutions at concentrations of 100, 10 and 1 μg/mL. Paclitaxel stock solution was prepared in ethanol at the concentration of 100 μg/mL. It was diluted with ethanol to obtain a working solution at the concentration of 20 μg/mL. IDN 5614 solution was prepared in methanol at the concentration of 4 mM.

3.2.2. Treatment formulation

Vials of IDN 5390 formulated in polysorbate 80 (Montanox 80 VG DF) at the concentration of 80 mg/mL were provided by Indena S.p.A. (Settala, Milan, Italy). The stock solution was diluted with 0.9% NaCl just before use and administered in a volume of 10 mL/kg body weight.

3.2.3. Mouse treatment

The animals used for IDN 5390 experiments were female CDF1 mice (body weight 20±2 g). To determine the faecal and urinary excretion of IDN 5390, six groups of five mice were given 60, 90 and 120 mg/kg of the compound intravenously or orally.

To determine whether liver metabolic induction was responsible for the decrease in IDN 5390 AUC after repeated oral treatment, two groups of female mice were treated on day 7 with an i.v. dose of 90 mg/kg. The two groups had been previously treated once a day for 7 consecutive days with 90 mg/kg of oral IDN 5390 or with vehicle diluted in 0.9% NaCl solution.

3.2.4. Sampling

Faeces and urine were collected from mice housed in metabolic cages, before dosing and after 24 and 48 hours. The fractions were immediately measured and frozen stored at -20°C until HPLC-MS/MS analysis.

The pharmacokinetic study was done on day 7 after one week of daily oral treatment with saline or IDN 5390 at the dose of 90 mg/kg. Blood samples were collected at 5, 15, 30 min and 1, 1.5, 2, 4 and 24 hours after i.v. injection of IDN 5390. Four mice were used per time point. Blood was obtained from the retro-orbital plexus under diethylether anesthesia and collected in heparinized tubes. The animals were sacrificed by cervical dislocation. The plasma fraction was immediately separated by centrifugation (2500 rpm, 10 min, 4°C) and stored at -20°C until analysis.

3.2.5. Analysis

3.2.5.1. Faeces and urine

IDN 5390 was assayed in faeces and urine by LC-MS/MS. Briefly, urine samples (100 µL) were spiked with 200 ng of paclitaxel as IS. After dilution (1:1) with CH_3CN/H_2O 10:90 containing 0.1% HCOOH, 5 µL were injected into the HPLC system.

Weighed faeces were homogenized 1:4 (w/v) with 4% bovine serum albumin (BSA) solution and diluted (1:4) in water, then 1 mL was added with 400 ng of paclitaxel as IS. Finally, for extraction, 3 mL of acetonitrile were added and then the samples were vortexed and centrifuged at 4°C for 10 min at 4000 rpm. The obtained supernatant was dried under nitrogen and reconstituted with 200 µL of mobile phase. Five µL were injected into the HPLC system consisting of an Alliance series 2695 coupled with a Micromass Quattro Ultima Pt triple quadrupole mass spectrometer operating in positive ion mode. This mass spectrometer was used to obtain both the mass spectra (MS^1) and the product ion spectra (MS^2). The instrument was equipped with an electrospray

ionization interface. The biological samples were analysed with the ion-spray needle operating at +3500 V and the cone voltage at 60 V. The mass spectrometer was programmed to allow the $[M+H]^+$ ions of IDN 5390 and paclitaxel at *m/z* 788.4 and 854.6 to pass through the first quadrupole into the collision cell. The characteristic product ions of these two compounds were monitored in the third quadrupole at *m/z* 309.0, 327.0 for IDN 5390 and 286.4 and 509.5 for paclitaxel. The chromatographic separation was carried out on an Omnispher 3 C_{18} column (100 x 2.00 mm x ¼'') Varian (Palo Alto, CA, USA) using a mobile phase gradient of 0.1% HCOOH in water (MPA) and 0.1% HCOOH in acetonitrile (MPB). The gradient conditions were from 10% to 100% of MPB in 27 min at the flow rate of 0.2 mL/min.

Extracts of urine and faeces were also analysed by HPLC coupled with an LCQ Deca XP Plus ion trap mass spectrometer for the search of IDN 5390 metabolites.

3.2.5.2. Plasma samples

On plasma samples of mice given 90 mg/kg were performed the quantitation of IDN 5390 concentrations and the identification of the circulating metabolites both by LC-MS/MS analysis. Each plasma sample was analysed for the pharmacokinetic study, whereas pooled plasma obtained from four mice at each time point was analysed for the metabolic study. Plasma samples were extracted with $HCOOH/CH_3CN$ (1:1000) in proportion 1:4 (v/v), centrifuged at 13000 rpm for 10 min and the collected supernatant was dried under nitrogen. The residue was dissolved in 30 µL of initial mobile phase and injected into the HPLC coupled with a Quattro Ultima Pt mass spectrometer (for the quantitation) or with an LCQ Deca XP Plus ion trap mass spectrometer (for the identification of circulating metabolites).

For quantitation analysis, a chromatographic separation was carried out on a column SunFire C18 (3.5 µm, 2.1 x150 mm), Waters (Milford, MA, USA) using a mobile phase

gradient of 0.1% HCOOH in water (MPA) and 0.1% HCOOH in acetonitrile (MPB). The gradient conditions were from 40% to 100% of MPB in 12 min, maintenance for 2 min, changing from 100% of MPB to 40% in 1 min and re-equilibrium of the column for 6 min at the flow rate of 0.2 mL/min.

To detect the circulating metabolites, the chromatographic separation was carried out on an Omnispher 3 C_{18} column (100 x 2.00 mm x ¼'') using a mobile phase consisting of MPA and MPB. The gradient conditions were from 10% to 100% of MPB in 27 min at a flow rate of 0.2 mL/min.

3.2.5.2.1. Pharmacokinetic analysis

The concentration data at each time point obtained for pharmacokinetic elaborations were the means ± standard deviation calculated from four animals. Plasma samples with a concentration above the highest standard point of the calibration curve were diluted with control plasma and re-assayed.

Pharmacokinetic parameters were calculated using WinNonlin Pro Node 4.1 pharmacokinetic software Pharsight Co. (Mountain View, Ca., USA).

3.2.6. *In vitro* metabolism of IDN 5390 and IDN 5614 after incubation with mouse and/or human liver microsomes

3.2.6.1. Sample preparation

IDN 5390 and IDN 5614 solutions were prepared in methanol at the concentration of 4 mM to study the metabolism *in vitro* with human and/or mouse liver microsomes.

Six groups of samples were prepared according to the following scheme:

SAMPLES INCUBATED WITH IDN 5390 or IDN 5614				
Group	**n° of samples**	**Incubation time**	**Incubated with microsomes**	**Added UDPGA**
A	3	0 minutes	YES	NO
B	3	0 minutes	NO	NO
C	3	240 minutes	YES	NO
D	3	240 minutes	NO	NO
E	3	240 minutes	YES	YES

SAMPLES INCUBATED WITHOUT IDN 5390 or IDN 5614				
Group	**n° of samples**	**Incubation time**	**Incubated with microsomes**	**Added UDPGA**
F	1	0 minutes	YES	YES

The same scheme was used for incubation of 7-ethoxycoumarin to evaluate the metabolic activity of the microsomes: 7-hydroxycoumarin was identified on the basis of the retention time in comparison with the standard and used as a marker of oxidative metabolism.

Two mg of 7-ethoxycoumarin were dissolved in 1 mL of methanol and diluted to 2 mL with 0.1 M pH 7.4 KH_2PO_4 buffer. 1 mL of such solution was further diluted to 10 mL with 0.1 M pH 7.4 KH_2PO_4 buffer.

Both the compounds under study and 7-ethoxycoumarin were incubated at 37 °C up to 240 minutes.

IDN 5390 or IDN 5614 and 7-ethoxycoumarin, microsomes and reagents nominal concentrations used in the samples are reported in the following table:

Substance	Concentration	Used in group
IDN 5614 or IDN 5390	40 μM	A to E
7-ethoxycoumarin	1 μg/mL	A, C and E
Microsomes	0.5 mg/mL	A, C, E and F
$MgCl_2$	4 mM	All groups
β-D-glucose-6-phosphate	10 mM	All groups
βNADP	1 mM	All groups
Glucose-6-phosphate dehydrogenase	1.5 units/mL	All groups
UDPGA	5 mM	E and F
Saccharic acid 1,4 lactone	5 mM	E and F

Table 6. Concentrations of the test compounds and reagents used in the incubation reaction with microsomes

$MgCl_2$, β-D-glucose-6-phosphate, βNADP and glucose-6-phosphate dehydrogenase were used to prepare the NADPH regenerating solution (NRS). UDPGA and saccharic acid 1,4 lactone were added to a portion of NRS, obtaining the NRS for groups E and F.

Samples were prepared by adding 250 μL of 0.1 M pH 7.4 KH_2PO_4 buffer, 100 μL of NRS (with or without UDPGA and saccharic acid 1,4 lactone), 45 μL of deionized water and 5 μL of IDN 5614 or IDN 5390 and 7-ethoxycoumarin standard solution. In the samples, incubated either without microsomes or drugs, an equal volume of 0.1 M pH 7.4 KH_2PO_4 buffer was added.

The reaction was started by adding 100 μL of the microsomal suspension to the samples. The reaction was stopped at selected times by adding 500 μL of methanol. Samples were shaken, centrifuged at 13000 rpm for 10 minutes (4°C) and the supernatants used for HPLC-MS/MS analysis.

3.2.6.2. Sample analysis

7-ethoxycoumarin and 7-hydroxycoumarin were analysed according to the HPLC-UV/VIS method described in Appendix 1. IDN 5390 was analysed, as reported above, with the same method used to determine the metabolites in faeces and urine. IDN 5614 was analysed by HPLC-MS/MS method as described in Appendix 2.

3.2.6.3. Results evaluation

The chromatograms obtained were compared among the groups with reference to the generated metabolites.

Furthermore, a quantitative evaluation according to the following formulas was carried out. For each group, the average values were used.

$$\%\ of\ \ 7-hydroxycoumarin\ lost\ adding\ UDPGA = \frac{(peak\ area\ of\ sample\ C - peak\ area\ of\ sample\ E)}{peak\ area\ of\ sample\ C} \times 100$$

$$\%\ of\ \text{IDN 5390 or IDN 5614}\ metabolized\ without\ UDPGA = \frac{(peak\ area\ of\ sample\ A - peak\ area\ of\ sample\ C)}{peak\ area\ of\ sample\ A} \times 100$$

$$\%\ of\ \text{IDN 5390 or}\ IDN\ \text{5614}\ metabolized\ with\ UDPGA = \frac{(peak\ area\ of\ sample\ A - peak\ area\ of\ sample\ E)}{peak\ area\ of\ sample\ A} \times 100$$

$$\text{IDN5390 or IDN5614}\ stability\ (\%)\ during\ the\ incubation = \frac{peak\ area\ of\ sample\ D}{peak\ area\ of\ sample\ B} \times 100$$

$$\text{IDN 5390 or IDN 5614}\ recovery\ (\%)\ from\ microsomes = \frac{peak\ area\ of\ sample\ A}{peak\ area\ of\ sample\ B} \times 100$$

IDN 5738, IDN 5839 and IDN 6140

The following section is relative to the pharmacokinetic study of IDN 5738, IDN 5839 and IDN 6140. In order to define the pharmacokinetics of a new compound, the first step is to set up and validate a method for its quantitation.

The most important thing to verify and define when developing a quantitation method using a mass spectrometer, is the effect of the matrix - in which the compound of interest is contained - on the response of the instrument. For this reason, I summarized in the following paragraph the description of this phenomenon and the ways to overcome this problem.

3.3. Matrix effect

The HPLC-MS/MS technique offers the possibility to measure small amounts of drug in complex biological matrix, thanks to its high sensitivity and selectivity. These characteristics allow the analysts to develop methods based on an easy sample preparation and a simple chromatographic separation, even with these problematic matrices, because endogenous components of biofluids are not detected and the signal in a SRM trace is only due to the analyte of interest. However, to be further confident about the analyte quantitative determination, it is necessary to consider that these undetected matrix components could coelute with the analyte and interfere with the ionization, causing suppression or enhancement of the signal.

Current FDA requirements underline the importance to assess this phenomenon, known as "matrix effect" in mass spectrometry, because it may compromise the precision, the accuracy, the sensitivity and the selectivity of the developed method and, consequently, the reliability of analytical data produced.

A common method to evaluate qualitatively the matrix effect is the post-column infusion, that permits to identify the chromatographic region where the matrix effect manifests itself. A constant concentration of the analyte is introduced in the ion source of the mass spectrometer by using an infusion pump connected with a T junction after the HPLC column, while a blank extracted sample is injected onto the chromatographic system. The signal of the infused drug, followed in a SRM scan mode, is steady, unless endogenous components eluting from the column cause a reduction or a gain of the response. To assure the reliability of the results, it is important that these ion suppression or enhancement effects do not happen near the analyte's retention time.

A quantitative evaluation of matrix effect is achieved by comparing the response of the analyte in solvent to the response obtained by spiking the analyte into blank matrix sample after the entire procedure of extraction [184].

It is not fully clear how the matrix effect occurs, but endogenous matrix components, such as salts, fatty acid, triglycerides, amines or metabolites, and exogenous components, such as polymers from analitycal material, vehicles as tween 80 or anticoagulants, could compete with the analyte of interest in the ionization process. In particular, there is an analyte ion suppression if the interferences are preferentially ionized and there is an analyte ion enhancement if the interferences favour the ionization of the analyte. Anyway, the analyte's response in matrix could change in comparison to the response of the same analyte in solvent, because of the different conditions at which the ionization occurs. The presence of matrix material influences the droplets' properties in the ESI source: it could increase the surface tension in droplets, reduce the solvent evaporation, change the viscosity or react with analyte ions. If the matrix effect is present and not negligible, it may be eliminated or reduced to guarantee the quality of the analytical data produced. There is not a unique solution to resolve the suppression or the enhancement of the signal, because the matrix effect is compound dependent and the biological matrices are always different. One of the easiest ways consists of a sample dilution, but it is possible only if there are not problems of sensitivity. Other approaches to overcome the matrix effect are based on the attempt to obtain cleaner samples through different preparation procedures. Different solvents or different mixtures of solvents in various proportions could be used to favour the precipitation of interfering substances, on the basis of solvents properties - viscosity, density, volatility, polarity -. Moreover, it could be also useful to consider the role of additives and buffers in mobile phases [185]:

- trifluoroacetic acid is not recommended, because it causes ion suppression at any concentration level, both in negative and positive acquisition modes;
- formic acid and acetic acid at high concentrations (0.50% - 1.00%) cause a signal reduction of the analyte, while their effect (suppression or enhancement) is variable at lower concentrations (0.05% - 0.10%);
- ammonium hydroxide has the same role of formic and acetic acid in negative ion mode, but in positive ion mode, generally, it favours an increase of signal;
- ammonium formate, biphosphate, bicarbonate and nonafluoropentadecanoic acid diminish the signal both in negative and positive ion acquisition mode, and both at high and low concentrations (5 – 50 mM).

Other possibilities to reduce the matrix effect are based on the changes in mass spectrometric and chromatographic conditions. As regards mass spectrometry, an attempt could be the use of a different ion source to modify the mechanism of ion formation, while the aim of changes in chromatography would be to separate interfering substances from the analyte. If the analyte elutes in a region of the chromatogram where the signal undergoes a suppression or an enhancement, it is possible to shift the retention time of the analyte by changing the chromatographic column or gradient conditions. However, they are often time-consuming experimentations and the risk is that the suppression or the enhancement region could also shift.

As regards the validation of the quantitation methods of IDN 5738, IDN 5839 and IDN 6140, as the study of these new taxane derivatives was in a preliminary phase of the preclinical study, I chose to follow the FDA guidelines, issued in 2001, for the method validation - in order to guarantee a good reliability and precision of the calculated data - but using a simplified protocol. For this reason, the method validation was set up on three days.

In the following two paragraphs, I summed up the parameters considered during the validation study of the three new taxane derivatives and the pharmacokinetic parameters calculated after the quantitation of their concentrations.

3.4. Validation parameters

The main parameters considered for the validation of the quantitation methods were: recovery, linearity of the calibration curve, precision and accuracy, limit of detection, limit of quantitation and stability.

The recovery of an analyte is obtained from the comparison of the peak area of the analyte of interest obtained from extracted samples with that obtained from external standards prepared in solvent. The recovery of IS is evaluated in the same way. The recovery experiments were performed at two or three different concentrations. It is important that the extent of recovery is consistent, precise and reproducible.

The linearity of the calibration curves was validated over three days. Each day, a calibration curve was prepared by spiking the biological matrix with known concentrations of the analyte to define the relationship between concentration and instrument response. It consisted of six or seven standard points in a range chosen on the base of expected concentrations in the samples and was obtained using the same

biological matrix of samples to measure. The linearity of the standard curves was calculated by the HPLC-MS/MS peak areas ratio for the analyte/IS to the nominal total amount of the analyte in the standard sample. In particular, the linearity for each calibration curve was assessed by weighted least squares method, using 1/x as weighting factor.

The y axis intercept (q) and the slope (m) of the equation $y = mx + q$ were calculated elaborating the y_j and x_i values obtained from the calibration points, where:

$$y_j = \frac{A_j}{A_{is}}$$ in which A_j = peak area of j-eme analyte

A_{IS} = peak area of the Internal Standard

x_i = actual concentration of the analyte in the curve point sample.

The goodness of the fitting was evaluated by the Pearson's determination coefficient R^2. The reproducibility of each calibration curve was assessed by the mean, standard deviation (SD) and coefficient of variation (CV%) of the estimated m and R^2. The back-calculated values of individual calibrants had to be within $\leq$ 15% of their theoretical concentration ($\leq$ 20% at the limit of quantitation).

Precision and accuracy of the method were evaluated on three different days by determining the analyte in three replicates of three quality control (QC) samples at different nominal concentrations. Three different standard calibration curves were prepared and processed each day to analyse the QCs. The precision of the method at each QC concentration was reported as a CV%, expressing the standard deviation as a percentage of the mean calculated concentration and it must not exceed 15% of CV. The accuracy of the measure was determined by expressing the mean calculated QC concentration as percentage of the nominal concentration. The mean value must be within 15%.

The limit of detection (LOD) was defined as the concentration at which the signal-to-noise ratio was 3. The limit of quantitation (LOQ) was defined as the smallest amount

of the analyte that could be measured in a sample with sufficient precision and accuracy (within 20% for both parameters) and as the concentration at which the signal-to-noise ratio was at least 10. The LOQ was chosen as the lowest concentration on the calibration curve.

The stability of the analyte of interest was evaluated by analyzing the QC matrix samples in triplicate at each QC concentration level, immediately after preparation and after approximately one month of storage nominally at -20 °C. For the assessment of the stability, the analyte was quantified in the stored samples using a freshly prepared calibration curve and a set of freshly prepared QC samples. The stability was also evaluated after three freeze and thaw cycles, at one concentration and in triplicate.

The three derivatives were considered stable at each concentration when the differences between the freshly prepared samples and the stability testing samples were found to be not exceeding 15% of the nominal concentration.

3.5. Pharmacokinetic analysis

Concentration-time data of taxane derivative analogues obtained from CD1 female mice after i.v. and p.o. administration were collected and were evaluated for pharmacokinetic analysis. For each time point, the found concentration was a mean of three concentrations gathered from three animals. A non-compartmental analysis was applied and the pharmacokinetic data were elaborated by using the specific software WinNonLin Pro Node 4.1 (Pharsight Co, Mountain View, Ca, USA).

The considered parameters were:

C_{max} maximum plasma concentration

T_{max} time until C_{max} is reached

AUC	area under the concentration-time curve from time 0 to the last detectable sample
AUC_{inf}	area under the concentration-time curve extrapolated to infinite
$T_{1/2}$	plasma half-life in the terminal phase
Cl	plasma clearance
V_{bd}	volume of distribution
F	bioavailability
Ratio AUC	accumulation factor for AUC values determined in different compartments
Ratio C_{max}	accumulation factor for C_{max} values determined in different compartments

In detail, C_{max} and T_{max} were directly determined from the experimental data. AUC was determined by the trapezoidal rule. The trapezoidal rule is a numerical method to approximate the area under a curve first involves dividing the area into a number of strips of equal width. Then, approximating the area of each strip by the area of the trapezium formed when the upper end is replaced by a chord. The sum of these approximations gives the final numerical result of the area under the curve.

$T_{1/2}$ was calculated by the formula: $T_{1/2}= 0.693/k_e$, where the elimination rate constant, k_e, is the slope of the terminal phase of the plasma-concentration time curve. Its calculation was based on at least three data points. Cl is calculated as dose/AUC and F is expressed as AUCp.o./AUCi.v. corrected for the administered dose. Ratio AUC and Ratio C_{max} were estimated as the ratio tissues/plasma for AUC and C_{max} values, respectively.

3.6. IDN 5738 and IDN 5839

3.6.1. Standard and QC solutions

For standards, a stock solution for each analyte was prepared at the concentration of 101.2 µg/mL for IDN 5738 and 102.4 µg/mL for IDN 5839. For QCs, a stock solution of each analyte was prepared at 100.0 µg/mL. The stock solution of the IS was prepared at 116.2 µg/mL. All stock solutions were prepared in methanol and stored at -20°C for six months before preparing fresh ones.

Working solutions to obtain the standard points (G-B for IDN 5738 and G-A for IDN 5839) of the calibration curve and the working solutions to prepare the plasma QC samples, for both the analytes, were obtained by combining different amounts of the stock solutions and further dilution with methanol to obtain IDN 5738 and IDN 5839 at the final concentrations reported here below:

Standard	IDN 5738 concentration (µg/mL)	IDN 5839 concentration (µg/mL)
G	0.25	0.25
F	0.50	0.50
E	1.00	1.00
D	5.00	5.00
C	10.00	10.00
B	15.00	20.00
A		50.00
Quality control solution	**IDN 5738 concentration (µg/mL)**	**IDN 5839 concentration (µg/mL)**
sL	0.75	0.75
sM	6.00	15.00
sH	15.00	40.00

The IS working solution was prepared at 10 µg/mL by diluting the stock solution with methanol.

3.6.2. Preparation of standard and QC samples

Control mouse plasma aliquots (90 µL) were spiked with 10 µL of each working solution to obtain a final dilution of 1:10, giving six calibration standards in the range 0.025-1.500 µg/mL for IDN 5738 and seven in the range 0.025-5.000 µg/mL for IDN 5839.

To prepare QC samples, three fractions of mouse plasma were added with an appropriate amount of QC solutions (sL, sM and sH), obtaining QC plasma samples at the final concentrations of 0.075, 0.600 and 1.500 µg/mL for IDN 5738 and 0.075, 1.500 and 4.000 µg/mL for IDN 5839.

Several aliquots of the three fractions were stored at -20°C as controls for future assays and to check the short term stability under storage conditions.

3.6.3. Processing standards and samples

Mouse plasma samples (100 µL) were mixed with 10 µL of IS working solution (100 ng of IS) and 200 µL of 0.1% HCOOH in CH_3CN kept at 4°C. After vortexing for 10 s, the mixture was centrifuged at 4°C for 10 min at 13000 rpm. The supernatant was recovered and 5 µL were injected into the LC-MS/MS system.

3.6.4. Chromatographic conditions

The HPLC system consisted of an Alliance separation module 2695 (Waters, Milford, MA, USA).

For both methods, the samples were separated on a SunFire C18 column (3.5 µm, 150 x 2.1 mm) coupled with a C18 precolumn (4 x 3 mm) Waters (Milford, MA, USA), held at 30°C. The mobile phases for the chromatographic separation were composed of 0.1% HCOOH in water (MPA) and 0.1% HCOOH in acetonitrile (MPB). The HPLC system was set up to operate at a flow rate of 0.2 mL/min at the following gradient conditions:

step 1- from the initial condition of 50% MPB to 95% over 4 min; step 2- maintenance of 95% MPB over 2 min; step 3- from 95% MPB to 100% over 4 min; step 4- maintenance of 100% MPB over 1 min; step 5- from 100% MPB to the initial condition over 2 min; the initial condition was held for 7 min. The total run time was 20 min. Peaks were detected by SRM mode.

At the end of the daily analyses, the HPLC column was washed with CH_3OH/H_2O (1:1) for 30 min at the flow rate of 0.2 mL/min.

The temperature of the autosampler was 4°C.

3.6.5. Mass spectrometric conditions

The HPLC system was coupled with a Micromass Quattro Ultima Pt triple-quadrupole mass spectrometer (Waters, Milford, MA, USA).

The mass spectrometer operated in negative ion mode and was used to obtain both the mass spectra (MS^1) and the product ion spectra (MS^2). The instrument was equipped with an electrospray ionization interface and used argon as the collision gas. The biological samples were analysed with the ion spray needle operating at -2500 V and the cone voltage at -70 V. The mass spectrometer was programmed to allow the $[M+HCOO]^-$ of IDN 5738, IDN 5839 and IDN 5127 at *m/z* 915, 912 and 932 respectively, to pass through the first quadrupole into the collision cell. The characteristic product ions of these three compounds were monitored in the third quadrupole at *m/z* 583, 523 and 260 for IDN 5738; 806, 623 and 563 for IDN 5839 and at 826 and 583 for IDN 5127 (IS).

All mass parameters related to the two methods are schematized in the following paragraphs:

3.6.5.1. IDN 5738

Source: ElectroSpray in negative ion mode and with heater gas at 300°C

Capillary voltage (kV): -2.50

Cone voltage (V): -70

Collision cell gas: argon at a pressure of 3.54 e^{-3}

Collision energies (eV): 19.0 - 21.0

Qualitative analyses, for the acquisition of MS and MS/MS spectra, were done by direct infusion of standard solutions (1 µg/mL) of IDN 5738 and IDN 5127.

Quantitative analysis of the same substances in plasma was done by Selected Reaction Monitoring (SRM) mode, measuring the following fragmentation products of the $[M+HCOO]^-$:

Compound	$[M+HCOO]^-$ (*m/z*)	product ion (*m/z*)	collision energy (eV)
IDN 5738	915.3	583	19.0
IDN 5738	915.3	523	21.0
IDN 5738	915.3	260	19.0
IDN 5127	932.0	583	20.0
IDN 5127	932.0	826	19.0

3.6.5.2. IDN 5839

Source: ElectroSpray in negative ion mode and with heater gas at 300°C

Capillary voltage (kV): -2.50

Cone voltage (V): -70

Collision cell gas: argon at a pressure of 3.74 e^{-3}

Collision energies (eV): 16.0 - 30.0

Qualitative analyses, for the acquisition of MS and MS/MS spectra, were done by direct infusion of standard solutions (1 µg/mL) of IDN 5839 and IDN 5127.

Quantitative analysis of the same substances in plasma was done by SRM, measuring the following fragmentation products of the $[M+HCOO]^-$:

Compound	$[M+HCOO]^-$ (*m/z*)	product ion (*m/z*)	collision energy (eV)
IDN 5839	912.4	563	30.0
IDN 5839	912.4	623	17.0
IDN 5839	912.4	806.4	16.0
IDN 5127	932.0	583	20.0
IDN 5127	932.0	826	19.0

The MS and MS/MS mass spectra of IDN 5738 and IDN 5839, with chemical structures and identification of the main fragment ions are reported in figure 17.

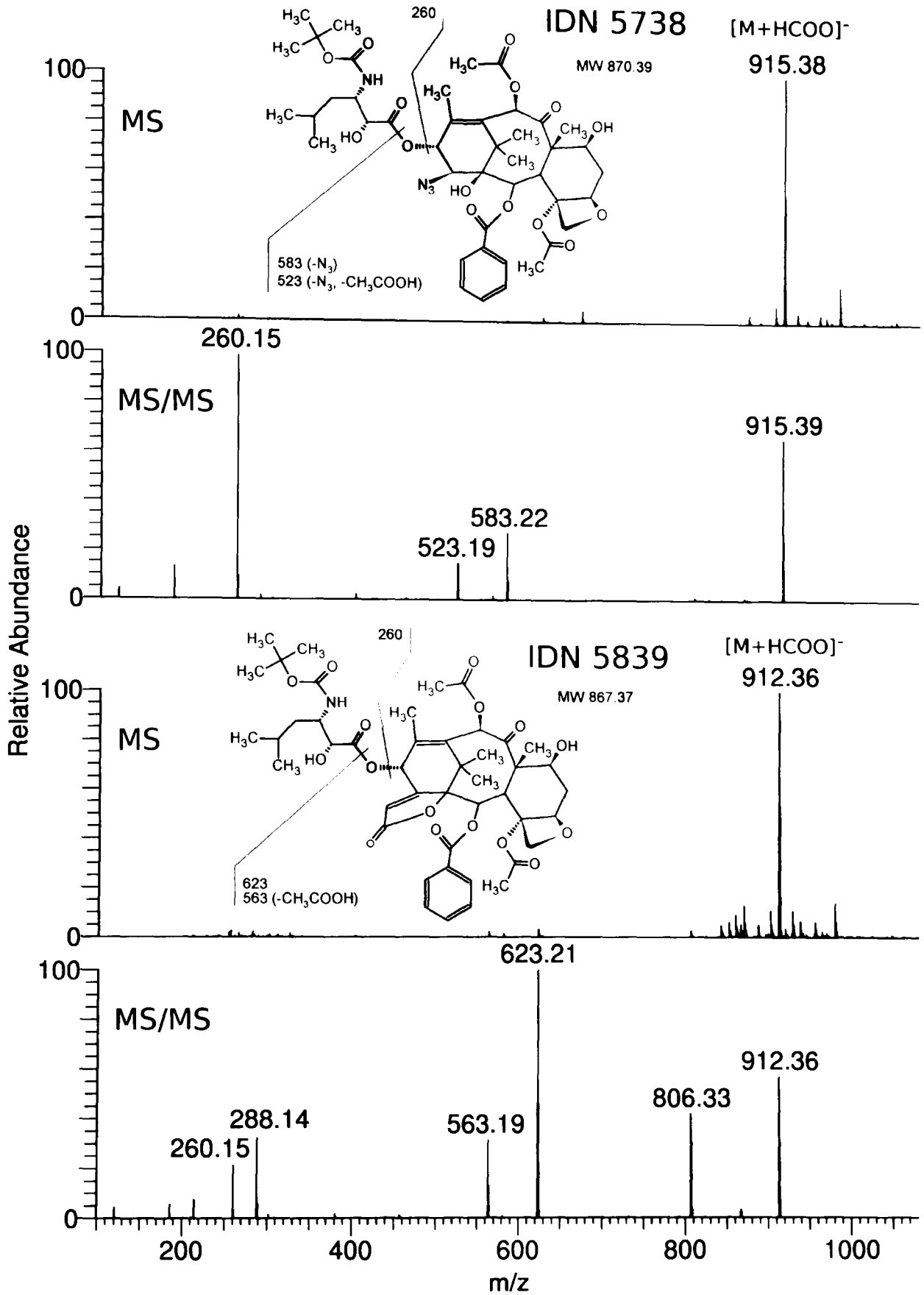

Figure 17. MS and MS/MS mass spectra of IDN 5738 and IDN 5839, with chemical structures and identification of the main fragment ions [instrument used: LCQ Deca XP Plus ion trap mass spectrometer]

3.6.6. Validation study

Two different validation studies were performed, one for each compound. The linearity of the calibration curves was validated over three days and calculated. as described in section 3.4, by the ratio of the HPLC-MS/MS peak areas for IDN 5738/IS and IDN 5839/IS to the nominal concentration of IDN 5738 and IDN 5839 in the standard sample.

Precision and accuracy of the method were evaluated on three different days by determining the analytes in three replicates of three QC samples at the nominal concentrations of 0.075, 0.600 and 1.500 μg/mL for IDN 5738 and 0.075, 1.500 and 4.000 μg/mL for IDN 5839. A standard calibration curve was prepared and processed each day to analyse the QC samples.

To establish the LOQ an aliquot of 450 μL of control plasma was spiked with 50 μL of a 0.25 μg/mL solution of IDN 5738 or IDN 5839 to produce a nominal plasma concentration of 25 ng/mL of the analyte. Five replicates of the obtained LOQ samples were processed and analysed by HPLC-MS/MS according to the previously described procedure together with a freshly prepared standard curve with a blank control and a blank control added with IS.

The percentage extraction recovery of the two analytes was calculated in triplicate at two plasma concentrations (0.100 and 1.000 μg/mL) for IDN 5738 and at three plasma concentrations (0.100, 1.000 and 5.000 μg/mL) for IDN 5839. Peak-area ratios of both analytes from extracted samples were compared to those from external standards prepared in methanol. The absence of the matrix effect that could influence the ionization of IDN 5738 and IDN 5839 was also assessed. The matrix effect, at each concentration level, was determined by comparing the mean area of the analytes prepared in solvent with the same quantity of the two taxane derivatives added to

biological matrix after the entire procedure of extraction. The absence of significant variations (< 15%) for the areas of both the analytes was verified, so it was possible to exclude any matrix effect causing ion suppression or enhancement.

The stability in the matrix of the two taxanes was evaluated analysing QC samples in triplicate at each QC concentration level, immediately after preparation and after approximately one month of storage at nominally -20°C.

3.6.7. Application of the method: pharmacokinetics of IDN 5738 and IDN 5839 in CD1mice

Both compounds were dissolved in a vehicle containing tween 80 and absolute ethanol in the proportion 1:1 and diluted (1:5) with saline to the final concentration of 6 mg/mL. Each taxane derivative was administered orally by gavage or injected in the tail vein of the mice. The experiments were carried out in 8-10 weeks old female CD1 mice (body weight 25±2 g).

To determine the pharmacokinetic profile and the bioavailability of IDN 5738 and IDN 5839 after single administration, mice were treated p.o. or i.v. with single dose of 60 mg/kg. For IDN 5738 study, blood samples were taken at the following time points: 5, 15, 30 minutes and 1, 2, 4, 8, 16 and 24 hours after i.v. administration and at 15, 30, 45 minutes and 1, 1.5, 2, 4, 8, 16 and 24 hours after oral treatment, while for IDN 5839, the sampling was conducted at 5, 15, 30 minutes and 1, 2, 4, 8 and 10 hours after i.v. administration and at 15, 30, 45 minutes and 1, 1.5, 2, 4 and 10 hours after oral treatment. Blood was obtained from the retro-orbital plexus under isoflorane anesthesia and collected in heparinized tubes. After centrifugation at 2500 rpm at 4°C for 10

minutes, plasma was separated and frozen stored at -20°C until analysis. Three mice were used for time point and animals were sacrificed by cervical dislocation.

3.6.8. Identification of circulating metabolites

Qualitative analyses of plasma samples, from mice treated with IDN 5738 and IDN 5839, have been done with the following instruments and conditions for the identification of metabolites. The HPLC-MS system consisted of a Surveyor autosampler and Surveyor MS pump, combined with a LCQ Deca XP Plus ion trap mass spectrometer Thermo Electron (Waltham, MA, USA). Separation was performed using an Omnispher 3 C_{18} column, 100 x 2.00 mm x ¼'' at a flow rate of 0.2 mL/min. The elution solvents were: water with 0.1% of formic acid (MPA) and acetonitrile (MPB); the elution gradient was from 20 to 100% of MPB in 32 min, with a 6 min hold of 100% MPB and a final re-equilibrating step to 20% of MPB for 8 min.

The LCQ ion trap was used in positive ion mode, with a standard electrospray source (ESI) directly coupled to the HPLC column. The spray capillary was kept at 5.0 kV, while the ion transfer capillary was kept at 10V, at a temperature of 225°C. Instrument data were recorded using data dependent acquisition (DDA), by programming the ion trap to perform an acquisition loop consisting of an initial full scan MS (600-1200 amu) and then by choosing, in real time, the 3 most abundant ions, to perform their MS/MS spectra (normalized collision energy of 30%).

3.7. IDN 6140

3.7.1. Pharmacokinetic study in plasma samples

3.7.1.1. Standard and QC solutions

For standards, a stock solution of the analyte was prepared at the concentration of 100.6 µg/mL. For QCs, a stock solution was prepared at 100.2 µg/mL. The stock solution of the IS, IDN 5738, was prepared at 101.2 µg/mL. All stock solutions were prepared in methanol, stored at -20°C and brought to room temperature before use.

Working solutions to obtain the plasma standard points (G-A) of the calibration curve and working solutions to prepare the plasma QC samples were obtained by combining different amounts of the stock solutions and further diluted with methanol to obtain IDN 6140 at the final concentrations reported below:

Standard	IDN 6140 concentration (µg/mL)
G	0.10
F	0.25
E	0.50
D	1.00
C	5.00
B	10.00
A	20.00
Quality control solution	**IDN 6140 concentration (µg/mL)**
sL	0.15
sM	0.75
sH	15.00

The IS working solution was prepared at 5.06 µg/mL by diluting the stock solution with methanol.

3.7.1.2. Preparation of standard and QC samples

Control mouse plasma aliquots (90 µL) were added with 10 µL of each IDN 6140 working solution to produce a final dilution of 1:10, giving seven calibration standard points in the range 0.010-2.000 µg/mL.

To prepare QC samples, three fractions of control mouse plasma were spiked with an appropriate amount of QC solutions (sL, sM and sH), obtaining a final plasma concentration of 0.015 µg/mL, 0.075 µg/mL and 1.500 µg/mL, respectively.

Several aliquots of 100 µL of the three fractions were stored at -20°C, as controls for future assays and to check the stability under storage conditions.

3.7.1.3. Processing standards and samples

Plasma samples (100 µL) were spiked with 10 µL of IDN 5738 (5.06 µg/mL in methanol) as IS and with 200 µL of 0.1% HCOOH in CH_3CN kept at 4°C. After vortex mixing for 10 s, the samples were centrifuged at 4°C for 10 min at 13000 rpm.

The supernatant was recovered and a volume of 10 µL was injected into the HPLC-MS/MS system for quantitative analysis.

3.7.1.4. Chromatographic conditions

The HPLC system consisted of a Series 200 autosampler and micropump (Perkin Elmer). The samples were separated using a SunFire C18 (3.5 µm, 150 x 2.1 mm) column coupled with a C18 precolumn (4 x 3 mm) and with the following gradient conditions:

Time (minutes)	0.1% HCOOH in H_2O (%)	0.1% HCOOH in CH_3CN (%)
0	50	50
4	5	95
6	5	95
10	0	100
13	0	100
14	50	50
20	50	50

The flow-rate was 0.2 mL/min and peaks were detected by SRM mode. At the end of the daily analyses, the HPLC column was washed with CH_3OH/H_2O (1:1) for 30 min at the flow rate of 0.2 mL/min.

The temperature of the autosampler and the column was 4°C and 30°C, respectively.

3.7.1.5. Mass spectrometric conditions

The HPLC system was coupled with an API 4000 triple quadrupole mass-spectrometer (Applied Biosystems, Foster City, CA, USA).

The mass spectrometer operated in negative ion mode and was used to obtain both the mass spectra (MS^1) and the product ion spectra (MS^2). The instrument was equipped with a Turbo V source. The biological samples were analysed with the ion spray needle operating at -4200 V. The mass spectrometer was programmed to allow the $[M+HCOO]^-$ of IDN 6140 and IDN 5738 at *m/z* 942.4 and 915.5 respectively, to pass through the first quadrupole into the collision cell. The characteristic product ions of these two compounds were monitored in the third quadrupole at *m/z* 151.1, 593.2 and 653.4 for IDN 6140 and at 260.2 and 583.4 for IDN 5738 (IS).

All the mass parameters related to the method are here schematized:

Source: Turbo V in negative ion mode and with heater gas at 350°C

Capillary voltage (kV): -4.2

CAD: 4.00

Curtain gas: 20.00

Gas 1: 35.00

Gas 2: 52.00

Collision energies (eV): -21.0 ÷ -62.0

Qualitative analyses, for the acquisition of MS and MS/MS spectra, were done by direct infusion and FIA (Flow Injection Analysis) of standard solutions (50 ng/mL) of IDN 6140 and IDN 5738.

Quantitative analysis of the same substances in plasma was done by SRM mode, measuring the following fragmentation products of the $[M+HCOO]^-$:

Compound	Q1 mass (amu)	Q3 mass (amu)	CE (V)	CXP (V)	EP (V)	DP (V)
IDN 6140	942.4	151.1	-62.0	-14.0	-11.0	-57.0
IDN 6140	942.4	593.2	-31.0	-18.0	-11.0	-57.0
IDN 6140	942.4	653.4	-21.0	-22.0	-11.0	-57.0

Compound	Q1 mass (amu)	Q3 mass (amu)	CE (V)	CXP (V)	EP (V)	DP(V)
IDN 5738	915.5	260.2	-29.0	-13.0	-11.0	-72.0
IDN 5738	915.5	583.4	-24.0	-21.0	-11.0	-72.0

The MS and MS/MS mass spectra of IDN 6140, with chemical structure and identification of the main fragment ions are reported in figure 18.

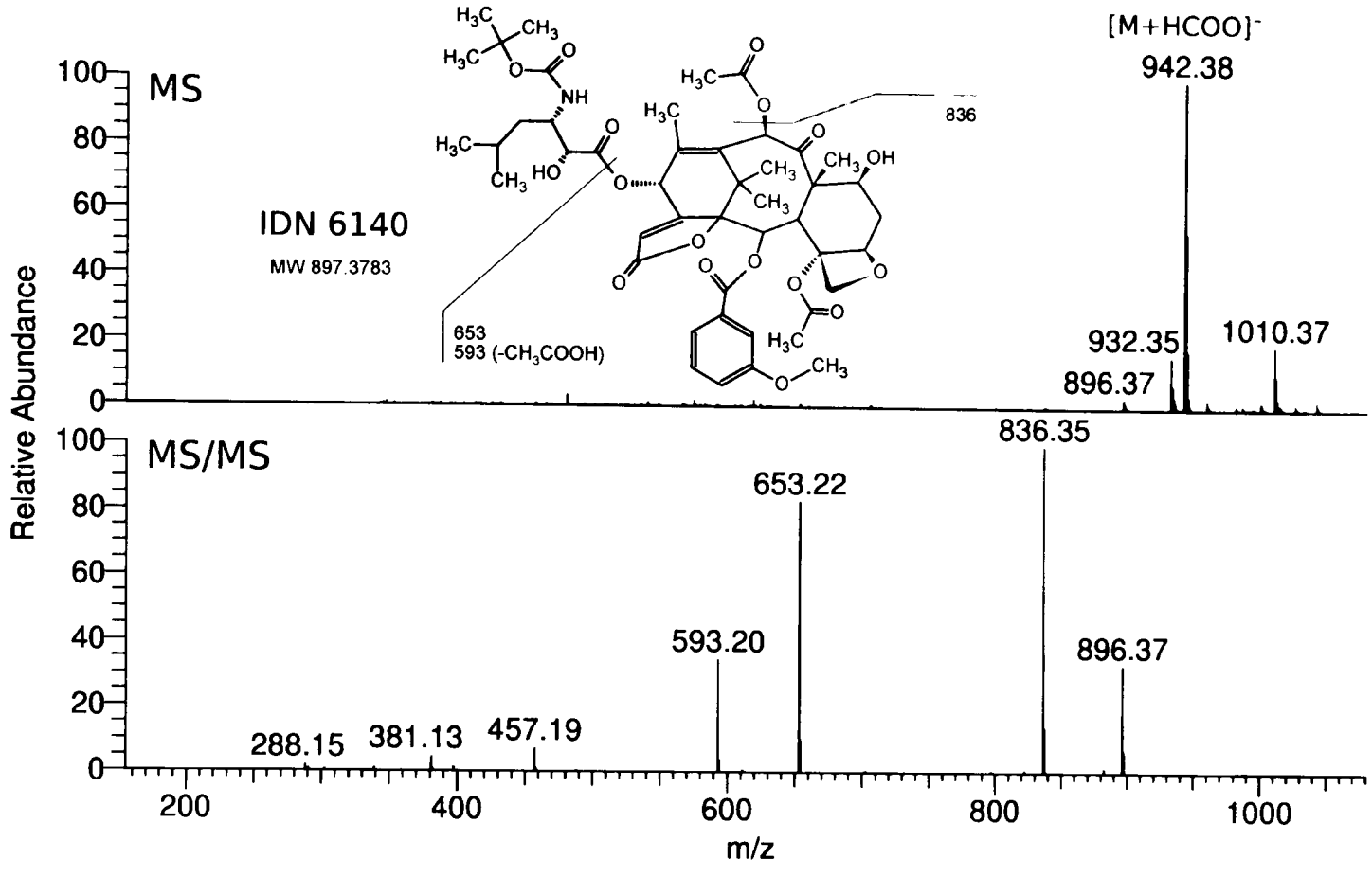

Figure 18. MS and MS/MS mass spectra of IDN 6140, with chemical structure and identification of the main fragment ions [instrument used: LCQ Deca XP Plus ion trap mass spectrometer]

3.7.1.6. Validation study

A validation study in plasma matrix was performed for IDN 6140. The linearity of the calibration curves was validated over three days and calculated, as described in section 3.4, by the ratio of the LC-MS/MS peak areas for IDN 6140/IS to the nominal concentration of IDN 6140 in the standard sample.

Precision and accuracy of the method were evaluated on three different days by determining the analyte in three replicates of three QC samples at the nominal concentrations of 0.015, 0.075 and 1.500 μg/mL. A standard calibration curve was prepared and processed each day to analyse the QC samples.

To establish the LOQ, an aliquot of 90 µL of control plasma was spiked with 10 µL of a 0.10 µg/mL solution of IDN 6140 to produce a nominal plasma concentration of 10 ng/mL of the analyte. Five replicates of the obtained LOQ samples were processed and analysed by LC-MS/MS according to the previously described procedure, together with a freshly prepared standard curve with a blank control and a blank control spiked with IS.

The percentage extraction recovery of IDN 6140 was calculated in triplicate at three plasma concentrations (0.025, 0.100 and 2.000 µg/mL). Peak-area ratios of the analyte/IS from extracted samples were compared to those from external standards prepared in 0.1% HCOOH in acetonitrile. It was also ensured the absence of the matrix effect that could influence the ionization of IDN 6140. The matrix effect, at each concentration level, was assessed by comparing the mean areas of the analyte obtained from samples prepared in solvent with those prepared adding the same quantity of IDN 6140 to biological matrix after the entire procedure of extraction. It was verified the absence of significant variations (< 15%) for the area of the analyte and IS, so it was possible to exclude any matrix effect of ion suppression or enhancement.

The stability of IDN 6140 in the matrix was evaluated analysing QC samples in triplicate at each QC concentration level, immediately after preparation and after approximately one month of storage at nominally -20°C.

3.7.1.7. Application of the method

3.7.1.7.1. Pharmacokinetics of IDN 6140 in CD1 mice

IDN 6140 was dissolved in a vehicle containing tween 80 and absolute ethanol in the proportion 1:1 and diluted (1:5) with saline to the final concentration of 0.54 mg/mL. The new taxane derivative was administered orally by gavage or injected in the tail vein of the mice. The experiments were carried out in 8-10 weeks old female CD1 mice (body weight 25±2 g).

To determine the pharmacokinetic profile and the bioavailability of IDN 6140 after single administration, mice were treated p.o. or i.v. with a single dose of 5.4 mg/kg.

At the following time points after i.v. (5, 15, 30, minutes and 1, 2, 4, 8, 16, 24, 48 hours) or p.o. treatment (15, 30, 45 minutes and 1, 1.5, 2, 4, 8, 16, 24, 48 hours), blood samples were obtained from the retro-orbital plexus under isoflurane anaesthesia and collected in heparinized tubes. Four mice were used for each time point and the animals were sacrificed by cervical dislocation. After centrifugation at 2500 rpm at 4°C for 10 minutes, plasma was separated and frozen stored at -20°C until analysis.

The tissue distribution of IDN 6140 was studied in brain and liver. These organs were removed at several time points after i.v. and p.o. treatment (15 minutes and 1, 2, 4, 8 and 24 hours), immediately frozen in dry ice and stored at -20°C until analysis.

Faeces and urine were collected from mice housed in metabolic cages, before dosing and 24 and 48 hours after the treatment. The fractions were immediately measured and frozen stored (-20°C) until the determination of IDN 6140 excretion.

3.7.1.7.2. Pharmacokinetics after oral repeated treatment

To determine whether repeated oral treatments with IDN 6140 could cause liver metabolic induction, two groups of female mice were treated on day 10 with an oral dose of 5.4 mg/kg. The two groups had been previously treated p.o. once a day for 9 consecutive days with 5.4 mg/kg of IDN 6140 or with vehicle dissolved in 0.9% NaCl solution.

Blood samples were collected at 30 and 45 min and 1, 2, 6 and 24 hours after the administration of IDN 6140. Three mice were used per time point. Blood was obtained from the retro-orbital plexus under isoflurane anesthesia and collected in heparinized tubes. The animals were sacrificed by cervical dislocation. The plasma fraction was immediately separated by centrifugation (2500 rpm, 10 min, 4°C) and stored at -20°C until analysis.

3.7.2. Distribution study in brain tissue

For the quantitation method of IDN 6140 - extracted from brain tissue - a validation study was not performed, but the matrix effect, the recovery and the intra-day precision and accuracy of the method were evaluated.

3.7.2.1. Standard and QC solutions

For standards, a stock solution of the analyte was prepared at the concentration of 99.8 µg/mL. For QCs, a stock solution was prepared at 102.8 µg/mL. The stock solution of the IS, IDN 5738, was prepared at 100.5 µg/mL. All stock solutions were prepared in methanol, stored at -20°C and brought to room temperature before use.

Working solutions to obtain the standard points (G-A) of the calibration curve and working solutions to prepare the brain QC samples were obtained by combining different amounts of the stock solutions and further diluted with methanol to obtain IDN 6140 at the final concentrations previously described for its quantitation in plasma samples. The IS working solution was prepared at 5.06 µg/mL by diluting the stock solution with methanol.

3.7.2.2. Preparation of brain standard and QC samples

Brain tissue was homogenized in 6.8 parts (w/v) of CH_3CN/CH_3OH 3:1. Homogenate was then added with 10 µL of appropriate IDN 6140 working solutions to produce a final dilution 1:10, giving seven calibration standards (0.010, 0.025, 0.050, 0.100, 0.500, 1.000, 2.000 µg/mL).

To prepare QC samples, control brain tissue - homogenized in 6.8 parts (w/v) of CH_3CN/CH_3OH 3:1 - was added with an appropriate amount of QC solutions (sL, sM

and sH), obtaining a final brain concentration of 0.015 µg/mL. 0.075 µg/mL and 1.500 µg/mL, respectively.

3.7.2.3. Processing standards and samples

Samples of brain tissue were homogenized in 6.8 parts (w/v) of CH_3CN/CH_3OH 3:1. Standard, QC and unknown samples were added with 50.6 ng of IDN 5738 as IS, shaken for 30 minutes, centrifuged at 4000 rpm for 10 minutes and the obtained supernatant dried under nitrogen. The residue was then dissolved in 1 mL of MPA/MPB 1:1, vortexed and centrifuged at 13000 rpm for 10 minutes at 4°C. A volume of 10 µL of the collected supernatant was injected into the HPLC system for quantitative analysis.

3.7.2.4. Chromatographic and mass spectrometric conditions

The chromatographic and MS conditions used, were the same reported for quantitation of IDN 6140 in plasma samples.

3.7.2.5. Matrix effect and recovery

The absence of a matrix effect that could influence the ionization of IDN 6140, was verified by injecting an extracted control brain sample into the LC-MS/MS system, during the post-column infusion of an IDN 6140 solution at a concentration of 50 ng/mL in 0.1% HCOOH in H_2O/CH_3CN 1:1.

In addition, the mean area of the analyte prepared in solvent was compared with the one obtained for the same quantity of IDN 6140 added to biological matrix after the entire procedure of extraction.

Percentage extraction recovery of IDN 6140 at the concentration of 0.100 µg/mL in triplicate was determined by comparing peak-area ratios of analyte/IS for extracted samples with those obtained from external standards prepared in MPA/MPB 1:1.

3.7.2.6. Application of the method: pharmacokinetics of IDN 6140 in normal and tumour brain tissue

To define IDN 6140 distribution in normal brain tissue, brains removed from the mice employed to assess the plasma pharmacokinetic profile were used, whereas to collect brain tumour sample, a new experiment was performed. For this purpose, U-87 MG human glioma cell line ($5x10^5$) was stereotactically injected into the brain of anesthetized CD1 nude mice. A dose of 7 mg/kg of IDN 6140 was administered to two mice as i.v. bolus four weeks after the tumour implant. Two hours after the treatment, the brain was removed, separated from the tumour and both of them immediately frozen in dry ice and stored at -20°C to be assayed for compound content.

3.7.3. Distribution study in liver tissue

Even for this tissue, a validation study was not performed, but the matrix effect, the recovery and the intra-day precision and accuracy of the method were evaluated. The development of the extraction method from liver samples was particularly difficult because of a very important matrix effect. Control liver tissue was homogenized in water in proportion 1:1 (w/v). Then a volume of different organic solvents was added in proportion 1:4 with the volume of the homogenized tissue in order to obtain the extraction procedure from the tissue. CH_3CN, CH_3OH, EtOH, CH_3OCH_3, isopropanol, a solution of CH_3OH/EtOH in proportion 1:1 and CH_3OH/CH_3CN/isopropanol 1:1:1 were tested. Each of the obtained solvent mixtures was then vortexed for 10 s and centrifuged at 4°C for 10 min at 4000 rpm. The supernatant was recovered and 20 µL were injected into the LC-MS/MS system during the post-column infusion of an IDN 6140 solution at the concentration of 50 ng/mL in 0.1% HCOOH in H_2O/CH_3CN 1:1. No one of the tested extraction solvents or mixture was appropriate to be used. As an example, figure 19 reports the chromatographic trace obtained with CH_3CN.

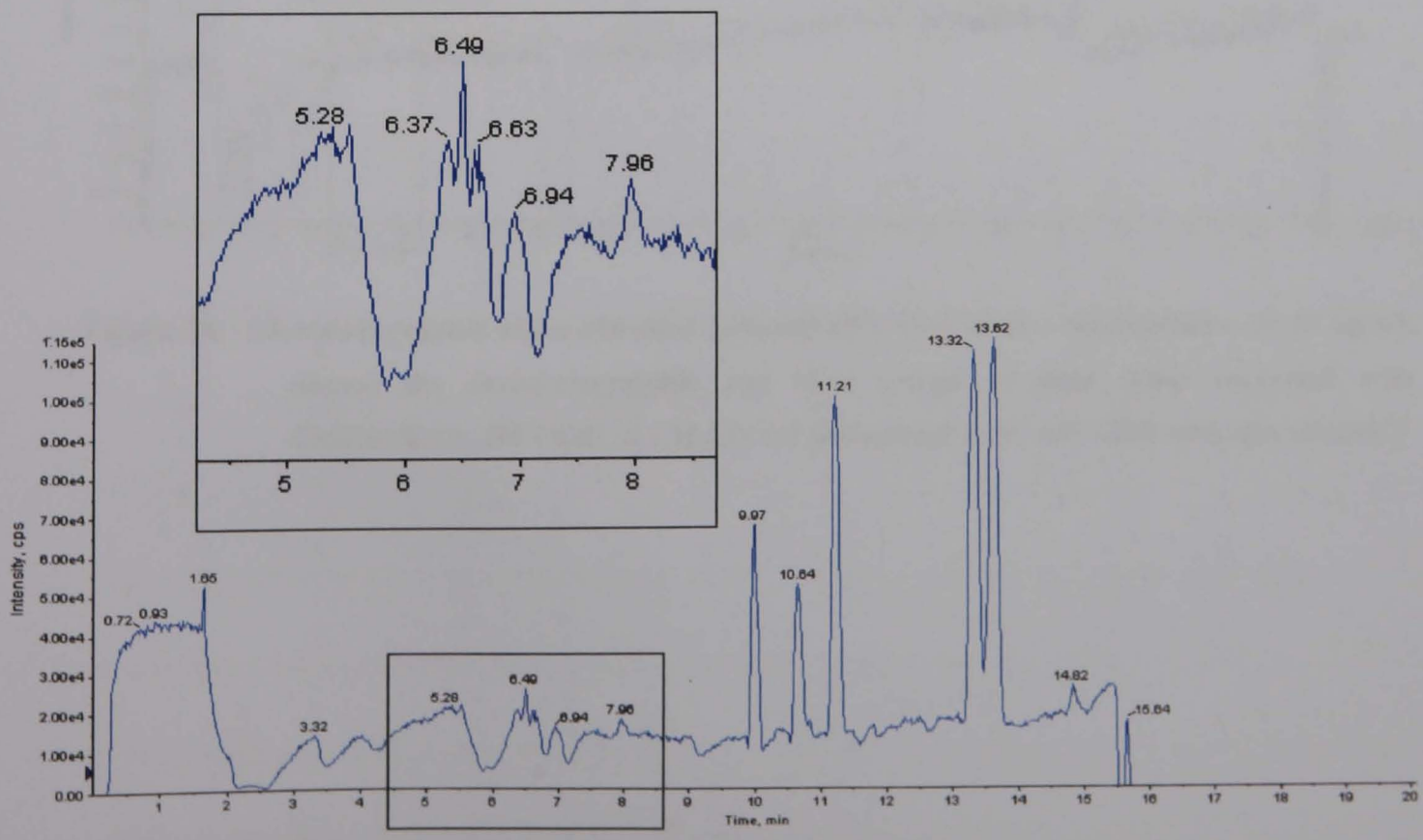

Figure 19. Chromatographic trace obtained infusing IDN 6140 at the concentration of 50 ng/mL during the chromatographic run of a sample of liver tissue extracted with CH_3CN

As it is possible to observe, close to IDN 6140 retention time (6.7 min), the trace was not steady. Many different strategies were tried to avoid the matrix effect of liver tissue: changing of chromatographic conditions, changing of ion source (APCI) and sample dilution. Taking the tested method modifications separately, the matrix effect was still very important and preventing any sort of quantitation. Finally, it was set up a method diluting the sample, changing the chromatographic conditions and the extraction solvent mixture obtaining almost the total reduction of the matrix effect during the post-column infusion (figure 20). The method is described in the following paragraphs.

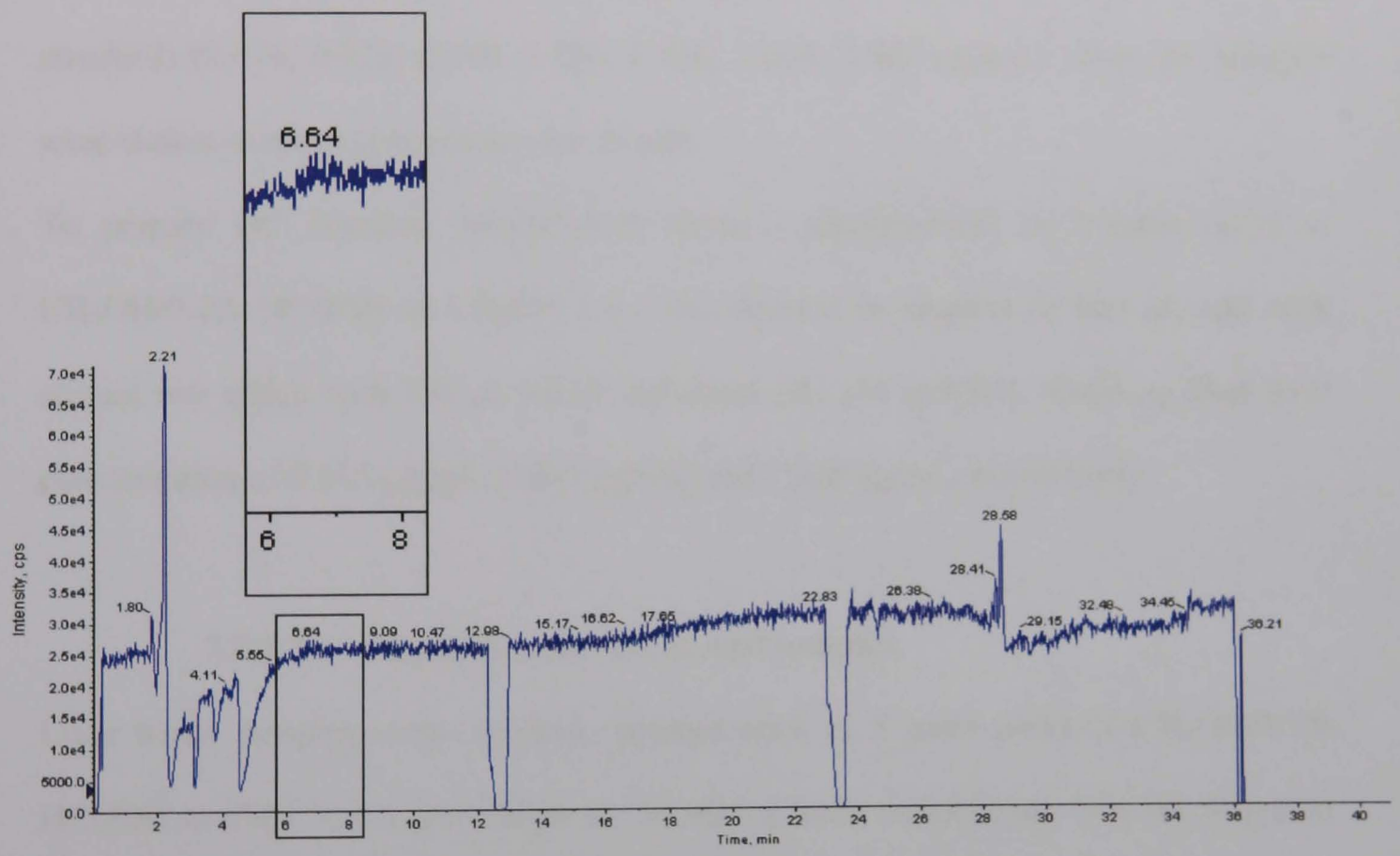

Figure 20. Chromatographic trace obtained infusing IDN 6140 at the concentration of 50 ng/mL during the chromatographic run of a sample of liver tissue extracted with CH_3OH/0.1% HCOOH in CH_3CN 1:1 [instrument used: API 4000 mass spectrometer]

3.7.3.1. Standard and QC solutions

The IDN 6140 stock and working solutions for the preparation of standard and QC samples were the same used to assay the analyte from brain tissue.

3.7.3.2. Preparation of liver standard and QC samples

Liver tissue was homogenized in 5 parts (w/v) of CH_3OH/0.1% HCOOH in CH_3CN 1:1. Homogenate was then divided in aliquots of 900 µL and each aliquot was spiked with 100 µL of appropriate IDN 6140 working solutions to produce seven calibration standards (0.010, 0.025, 0.050, 0.100, 0.500, 1.000, 2.000 µg/mL). Then the aliquots were shaken at room temperature for 30 min.

To prepare QC samples, control liver tissue - homogenized in 5 parts (w/v) of CH_3OH/0.1% HCOOH in CH_3CN 1:1 - was divided in aliquots of 900 µL and each aliquot was added with 100 µL of QC solutions (sL, sM and sH), obtaining final liver concentration of 0.015 µg/mL, 0.075 µg/mL and 1.500 µg/mL, respectively.

3.7.3.3. Processing standards and samples

Liver tissue samples were weighed, homogenized in 5 parts (w/v) of CH_3OH/0.1% HCOOH in CH_3CN 1:1 and shaken for 30 min at room temperature. One mL was then collected from each sample and used for the quantitation of IDN 6140.

Standard, QC and unknown samples were added with 506 ng of IDN 5738 as IS, vortexed, centrifuged at 4000 rpm for 10 minutes at 4°C and the obtained supernatant was transferred and centrifuged again in the same conditions. The second supernatant was dried under nitrogen. The residue was then dissolved in a volume of 0.1% HCOOH in H_2O (MPA)/0.1% HCOOH in CH_3CN (MPB) 9:1, to obtain about a 16-fold dilution (w/v) of the tissue sample analysed. After prolonged shaking - necessary to assure the complete solubilization of the residue - samples and standards were centrifuged at 4000

rpm for 10 minutes at 4°C, and 200 µL of the supernatant were transferred into vials for HPLC analysis.

A volume of 10 µL of the supernatant was injected into the HPLC system for quantitative analysis.

3.7.3.4. Chromatographic conditions

The HPLC system consisted of a Series 200 autosampler and micropump (Perkin Elmer). The samples were separated using a SunFire C18 (3.5 µm 150 x 2.1 mm) column coupled with a C18 precolumn (4 x 3 mm) and with the following gradient:

Time (minutes)	0.1% HCOOH in H_2O (%)	0.1% HCOOH in CH_3CN (%)	Flow rate (µL/min)
0	90	10	300
12	90	10	300
26	15	85	200
32	15	85	200
34	90	10	300
41	90	10	300

Peaks were detected by SRM mode. At the end of the daily analyses, the HPLC column was washed with CH_3OH/H_2O (1:1) for 30 min at the flow rate of 0.2 mL/min.

The temperature of the autosampler and the column was 4°C and 30°C, respectively.

3.7.3.5. Mass spectrometric conditions

The MS conditions were the same reported for quantitation of IDN 6140 from plasma samples.

3.7.3.6. Matrix effect and recovery

Besides the post-column infusion described above, the absence of the matrix effect was ensured by comparing the mean area of the analyte peaks obtained from external standards prepared in MPA/MPB 9:1 with those obtained adding the same quantity of the analyte to biological matrix after the entire procedure of extraction.

There were no significant variations (< 15%) for the areas of IDN 6140 indicating the absence of any matrix effect of ion suppression or enhancement.

Percentage extraction recovery of IDN 6140 at the concentration of 0.025 and 0.100 μg/mL in triplicate was determined by comparing peak-area ratios of analyte and IS from extracted samples with those from external standards prepared in MPA/MPB 9:1.

3.7.4. *In vitro* metabolism of IDN 6140 using S9 fraction

IDN 6140 solution was prepared in acetonitrile at the concentration of 500 µg/mL (100X the plasma C_{max} obtained after i.v. treatment) to study the *in vitro* metabolism with liver S9 fraction.

Two mg of 7-ethoxycoumarin were dissolved in 1 mL of methanol and diluted to 2 mL with 100 mM Tris buffer pH 7.4. 1 mL of such solution was further diluted to 10 mL with the same buffer.

Liver S9 requires exogenous cofactors for activity. The cofactors used consist of an NADPH-regenerating system (phase I oxidation), uridine 5'-diphospho-α-D-glucuronic acid (UDPGA; phase II glucuronidation), and 3'-phosphoadenosine-5'-phosphosulphate (PAPS; phase II sulfation). Incubations were conducted in 100 mM Tris buffer pH 7.4.

The NADPH Regenerating System (NRS) was prepared following the procedure reported below:

1.7 mg/mL NADP (170 mg for 100 mL), 7.8 mg/mL glucose-6-phosphate (780 mg for 100 mL) and 6 units/mL glucose-6-phosphate dehydrogenase (600 units for 100 mL) were added to a 2% $NaHCO_3$ solution.

In order to study phase II conjugation, immediately before the incubation, 1.9 mg/mL UDPGA (190 mg for 100 mL) and 100 µg/mL PAPS (10 mg for 100 mL) were added to a portion of NRS.

Samples were prepared by adding 320 µL of 100 mM Tris buffer pH 7.4, 125 µL of NRS (with or without UDPGA and PAPS), 5 µL of IDN 6140 or 7-ethoxycoumarin standard solution. In the samples incubated either without S9 fraction or IDN 6140, an equal volume of 100 mM Tris buffer pH 7.4 buffer was added.

The reaction was started by adding 50 µL of the liver S9 fraction to the samples. IDN 6140 and 7-ethoxycoumarin samples were incubated at 37 °C up to 120 minutes.

The sample scheme comprised a blank sample (without adding IDN 6140), T_0 and T_{2h} (stopped immediately or 2 hours after the adding of S9 fraction, respectively) samples in triplicate and a T_{2h} sample obtained by the addition of boiled S9 fraction to evaluate IDN 6140 stability.

The same scheme was used for incubation of 7-ethoxycoumarin to evaluate the metabolic activity of the microsomes: 7-hydroxycoumarin was identified on the basis of the retention time in comparison with the standard and used as a marker of oxidative metabolism.

The reaction was stopped at selected times by adding 1 mL of methanol. Samples were shaken, centrifuged at 13000 rpm for 10 minutes (4°C) and the supernatants used for LC-MS/MS analysis.

3.7.4.1. Samples analysis

7-ethoxycoumarin and 7-hydroxycoumarin were analysed according to the HPLC method described in Appendix 1. Qualitative analyses of IDN 6140 for the identification of metabolites were done with a HPLC-MS system consisting of a Surveyor autosampler and Surveyor MS pump (Thermo Finnigan) combined with a LCQ Deca XP Plus ion trap mass spectrometer (Thermo Electron, Waltham, MA, USA). Separation was performed using a Zorbax SB-C18 column, 150 x 0.5 mm ID (Agilent, Santa Clara, CA, USA) at a flow rate of 10 µL/min. The elution solvents were: water with 0.1% of formic acid (solvent A) and acetonitrile (solvent B); the elution gradient was from 50 to 100% of solvent B in 20 min, with a 6 min hold of 100% B and a final re-equilibrating step to 50% of B for 12 min.

The LCQ ion trap was used in negative ion mode, with the same conditions used for the analyses of IDN 5738 and IDN 5839.

3.7.4.2. Results evaluation

The chromatograms obtained were compared among the groups to detect the generated metabolites.

3.7.5. IDN 6140 quantitation in faeces and urine

IDN 6140 was assayed by LC-MS/MS in faeces and urine collected before dosing and 24 and 48 hours after the administration of 5.4 mg/kg of the compound.

The extraction method from urine samples was the same developed for IDN 6140 quantitation in plasma. The matrix effect was defined by the post-column infusion of an IDN 6140 solution at the concentration of 50 ng/mL in MPA/MPB 1:1 while a blank extracted sample was injected on the chromatographic column.

As regards faeces, firstly, recovery and matrix effect were evaluated. To assess them, I used control faeces from mice treated with only the vehicle used to dissolve IDN 6140 for animal treatment. A volume of 4% BSA solution in proportion 1:3 w/v and successively, a volume of bidistilled water in proportion 1:3 v/v were added to control faeces. Then, control faeces were homogenized and vortexed and finally, aliquots of 1 mL were collected. The extracted sample was obtained adding 3 mL of 0.1% HCOOH in CH_3CN to the 1 mL aliquot. Then the mixture was vortexed and centrifuged for 10 min at 4000 rpm and at 4°C. The obtained supernatant was dried under nitrogen and the residue was dissolved in 200 µL of MPA/MPB 1:1. The reconstituted sample was then vortexed, centrifuged at 13000 rpm for 10 min at 4°C and transferred to vials for the injection into the HPLC system. The matrix effect was assessed by using the post-

column infusion method. A suppression contribution of the matrix on IDN 6140 signal was evaluated, but it was steady and not so important to prevent the quantitation.

The recovery was evaluated at the concentration of 0.100 µg/mL in triplicate and because of the matrix effect, the percentage extraction recovery was defined by comparing peak-area ratios of analyte/IS from extracted samples with those prepared adding the same quantity of the analyte to a faeces sample after the entire procedure of extraction.

To prepare standards and quality control samples, control faeces were homogenized with a 4% BSA solution and water as previously described. Aliquots of 900 µL of the mixture obtained were spiked with 100 µL of standard solutions or quality control solutions and shaken.

Faeces samples were weighed, added with a BSA solution in the proportion 1:3 (w/v) and homogenized by the means of an ultra turrax. 4 mL were then collected from the mixture and added with 12 mL of bidistilled water. After vigorously shaking of the samples, 1 mL was collected and used to dose IDN 6140. 506 ng of IS and 3 mL of 0.1% HCOOH in CH_3CN were then added to samples, standards and quality controls. The supernatant extraction mixture was vortexed, centrifuged and dried under nitrogen. The residue was rinsed with 200 µL of MPA/MPB 1:1, vortexed and centrifuged again for 10 min at 4000 rpm and 4°C.

Ten µL were injected into the HPLC system. The chromatographic and mass spectrometric conditions were the same set up for plasma samples.

CHAPTER 4

RESULTS

4.1. IDN 5390

When I started my research project with IDN 5390, it had been previously reported that it has at least two mechanisms of action, one related to antimitotic effect causing direct cytotoxicity and the other one related to its antiangiogenic properties. This second one is probably particularly important when the compound is given continuously for a prolonged time. Experimental evidence suggested that IDN 5390 given daily by oral route for a prolonged time had good antitumor activity with very limited toxicity. A pharmacokinetic study conducted in mice in our lab, showed that this compound is rapidly (T_{max} = 0.25 h) absorbed after oral administration of a dose of 60 mg/kg and has a good oral bioavailability, of 43%. This finding could be explained by the fact that IDN 5390, unlike paclitaxel and docetaxel, is a poor substrate for the P-gp or other transporters that pump the drug out of the cells and that are particularly abundant in the gastrointestinal mucosa. The plasma AUC after three oral doses of 60, 90 and 120 mg/kg indicated a dose-dependent increase of this pharmacokinetic parameter, being 9.9, 19.8 and 35.1 μg/mL*h respectively, but not in bioavailability - assessed by dividing the AUC after oral route by the AUC after i.v. route - which decreased from 43% to 27% at the highest dose tested. The reason for this decrease appeared to be related to a dose-dependent kinetics after intravenous administration, the clearance being 2.6, 1.4 and 0.9 L/kg and the half-life 24, 36 and 54 min respectively, after the dose of 60, 90 and 120 mg/kg, respectively. This caused a much greater increase in AUC values after i.v. administration comparing to the oral one. At this point, it was very important to try to understand if the dose-dependent kinetics of IDN 5390 was caused by the saturation of its elimination.

4.1.1. Faecal and urinary excretion

4.1.1.1. Elimination of unchanged IDN 5390

Firstly, I investigated the faecal and urinary excretion of IDN 5390 in CDF1 female mice treated i.v. and orally with 60, 90 and 120 mg/kg. Excretion of the parent drug *per se* was low (Table 7).

Dose/via	Actual dose	0-24 h (% of dose)		24-48 h (% of dose)		Total dose recovered (%)	
(mg/kg)	(mg)	feces	urine	feces	urine	feces	urine
60 p.o. 60 i.v.	4.9 5.4	3.0 2.8	0.27 0.30	0.14 0.06	0.05 0.15	3.1 2.9	0.32 0.45
90 p.o. 90 i.v.	7.0 7.2	3.6 3.2	0.29 1.24	0.12 /	0.19 0.15	3.8 3.2	0.48 1.40
120 p.o. 120 i.v.	9.7 9.7	4.2 2.9	0.17 0.83	0.51 0.14	0.06 0.14	4.7 3.1	0.20 1.00

Table 7. Faecal and urinary excretion of IDN 5390 in female CDF1 mice after different p.o. and i.v. doses

The percentage of IDN 5390 eliminated in faeces after intravenous treatment did not appear to depend on the doses, being in the range of 2.9-3.2% of the dose. After oral treatment the range of excretion was slightly superior ranging between 3.1 and 4.7%. The elimination of the compound in urine was much lower than in faeces, but was higher after i.v. (0.5-1.4%) than after oral doses (0.2-0.5%).

Since IDN 5390 was excreted to a similar extent at all three doses, it was possible to exclude saturation in the elimination process of the compound.

4.1.1.2. Elimination of metabolites

In order to detect even those metabolites formed in a small amount, only samples of mice treated with the highest dose were analysed. Therefore, I performed HPLC-MS/MS analysis in faeces and urine of mice treated with the dose of 120 mg/kg. Figure 21 shows the typical fragmentation pattern of IDN 5390 obtained by LC-MS/MS analysis.

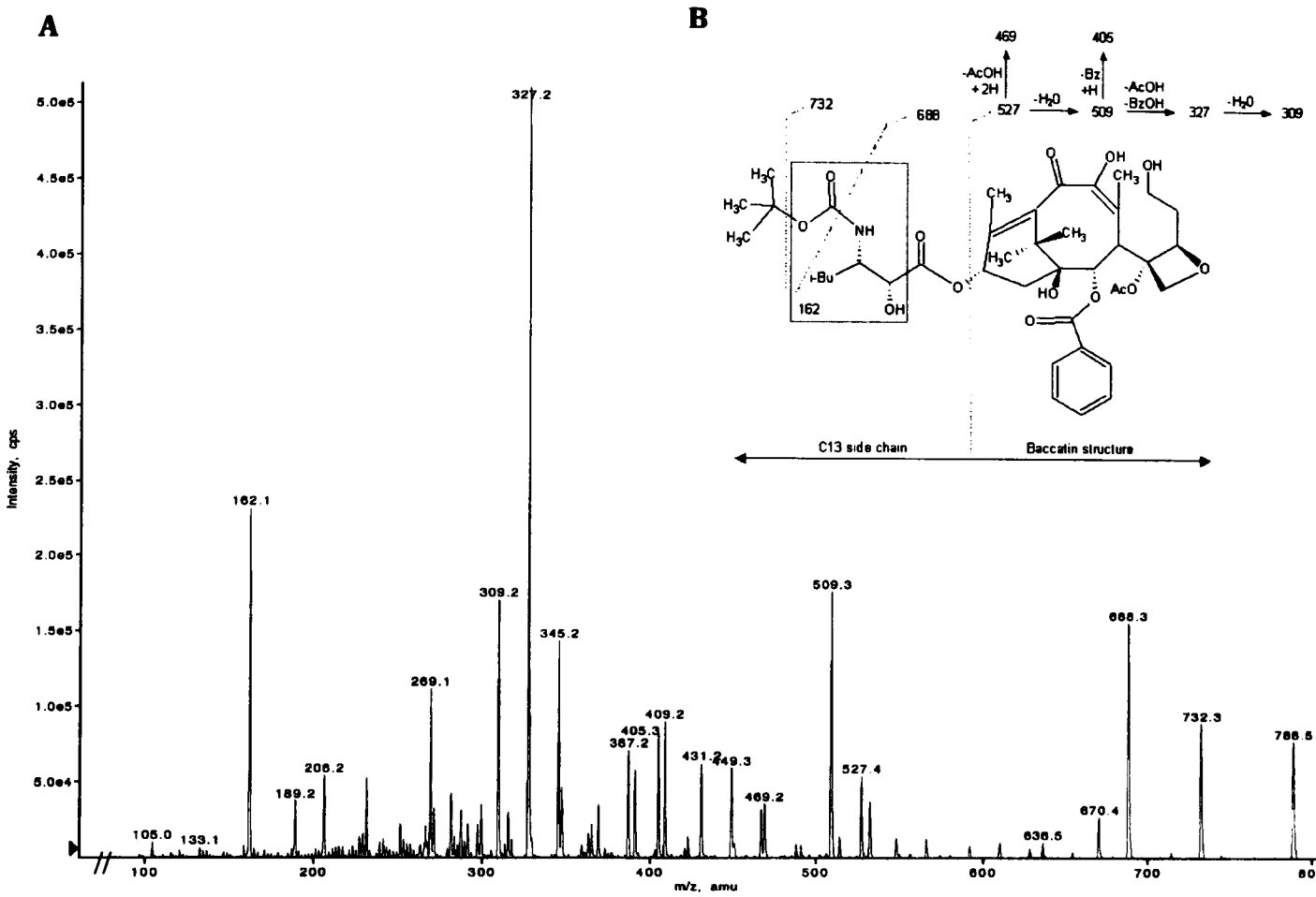

Figure 21. Positive-ion ElectroSpray Ionization-MS/MS spectrum of IDN 5390 (panel A) and scheme of fragmentation pattern (panel B). Amu, atomic mass unit(s) [instrument used: API 4000 mass spectrometer]

Faeces and urine of mice revealed that IDN 5390 was extensively metabolized and after both p.o. and i.v. single doses, several taxane-related structures were found. On the basis of the *m/z* ratio, I hypothesized the formation of metabolites mainly derived from reactions of oxidation, mono- and di-hydroxylation of IDN 5390 and conjugation with sulphate (figure 22).

A

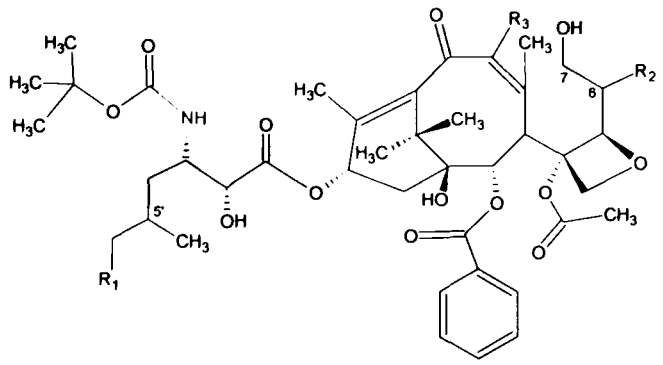

B

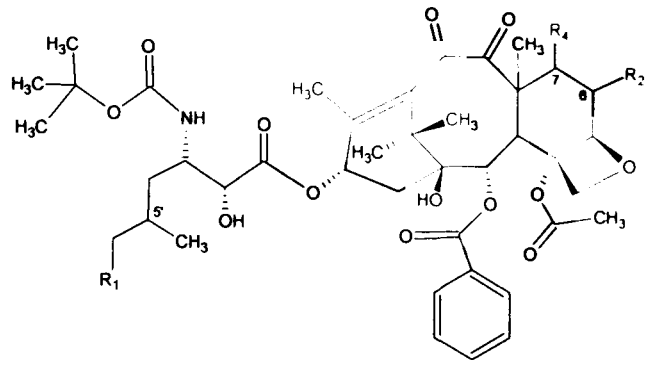

Structure	R_1	R_2	R_3	R_4	$[M+H^+]$	Major fragment ions (m/z)
Series A:						
IDN 5390	H	H	OH	-	788	732, 688, 509, 327
6'-monohydroxy IDN 5390 (M1)*	OH	H	OH	-	804	748, 704, 327, 178
6,6'-dihydroxy IDN 5390 (M3)	OH	OH	OH	-	820	764, 720, 343, 178
9-sulfate IDN 5390 (M4)	H	H	OSO_3H	-	868	812, 768, 389, 162
6'-monohydroxy-9-sulfate IDN 5390 (M5)	OH	H	OSO_3H	-	884	828, 784, 407, 178
Series B:						
7,8-cyclized IDN 5390 (C1)	H	H	-	OH	786	730, 686, 525, 403
6-monohydroxy-7,8-cyclized IDN 5390 (C2)*	H	OH	-	OH	802	746, 702, 541, 341
6,6'-dihydroxy-7,8-cyclized IDN 5390(C4)	OH	OH	-	OH	818	762, 718, 341, 178
7-sulfate-7,8-cyclized IDN 5390 (C5)	H	H	-	OSO_3H	866	810, 766, 644, 483
6'-monohydroxy-7-sulfate-7,8-cyclized IDN 5390 (C6)	OH	H	-	OSO_3H	882	826, 782, 660, 483
6,6'-dihydroxy-7-sulfate-7,8-cyclized IDN 5390 (C7)	OH	OH	-	OSO_3H	898	842, 798, 676, 499

*Two isomers of M1 and C2 (M2 and C3) were also identified

Figure 22. LC-MS/MS fragmentations of IDN 5390 and metabolites derived directly from the parent drug (series A) and from the retrograde cyclization product, 7,8 cyclized IDN 5390 (series B)

On the basis of the fragmentation pattern obtained by the ion trap mass spectrometer, it was not possible to ascertain the exact identity of the products of metabolic modifications of taxane structure. In analogy with information on the murine metabolism of paclitaxel [36, 186], I considered position 6 as a possible target of hydroxylation reaction.

According to figure 22, the hydroxyl function most likely to be conjugated with sulphate is in position 9 for the parent drug (A series) in view of its enolic nature and in 7 for 7,8-cyclized IDN 5390 derivatives (B series). Table 8 tentatively reports the

percentages of faecal and urinary excretion of the main hypothesized metabolites, assuming that the metabolites and the parent compound had similar responses in the mass spectrometer.

Compound	MW	Retention time (min)	oral		intravenous	
			urine (%)	faeces (%)	urine (%)	faeces (%)
IDN 5390	787	23.7	0.17	4.2	0.83	2.9
M1	803	19.9	0.13	9.1	0.94	5.8
M2	803	22.2	0.16	/	0.44	/
M3	819	19.1	0.11	/	0.30	0.5
M4	867	21.5	/	15.0	/	10.8
M5	883	16.5	/	7.9	/	4.4
C1	785	27.3	0.24	/	0.46	/
C2	801	23.6	0.04	1.7	0.09	1.6
C3	801	21.9	0.04	/	0.13	/
C4	817	19.6	0.04	4.8	0.13	6.2
C5	865	27.4	/	0.9	/	0.4
C6	881	21.0	/	1.1	/	0.6
C7	897	17.1	/	0.8	/	/
Total excretion (%)			0.9	45.5	3.3	33.2
			46.4		36.5	

Table 8. Faecal and urinary excretion (percentage of the dose) of the main IDN 5390 metabolites in CDF1 female mice after intravenous or oral treatment with 120 mg/kg of the compound

After oral treatment, the most abundant metabolites in faeces, as a percentage of the dose, were M4 (15.0%), M1 (9.1%) and M5 (7.9%). M4 and M1 are products of sulphate conjugation and hydroxylation of IDN 5390, respectively, while M5 is the sulphate of M1. Modification of IDN 5390 structure involving formation of the typical taxane scaffold and di-hydroxylation gave C4, amounting to 4.8% of the dose. These

metabolites (M1, M4, M5 and C4) were also the most abundant after intravenous treatment. As reported in table 8, several other metabolites were quantified in faeces after both treatments. The total amount of the dose recovered, as IDN 5390 *per se* and metabolites, amounted to respectively 45.5 and 33.2% after oral and intravenous treatment.

In urine, 3.3% of IDN 5390 and metabolites was recovered after intravenous treatment and 0.9% after oral administration. M2 and C3, two isomers of M1 and C2 with different retention times, were found in urine. M2 is probably an epimer of M1 and C3 could be an epimer or a structural isomer of C2. From the fragmentation pattern of these monohydroxylated derivatives (figure 22), it was not possible to establish which stereogenic centre was involved in the epimerization and which part of the ring system in the isomerism. As it is possible to notice in figure 23 (panel A), besides the stereogenic centres already present in IDN 5390 structure, with the cyclization of C ring, two new centres were formed in positions 7 and 8, generating theoretically 4 different isomers as shown in panel B.

A

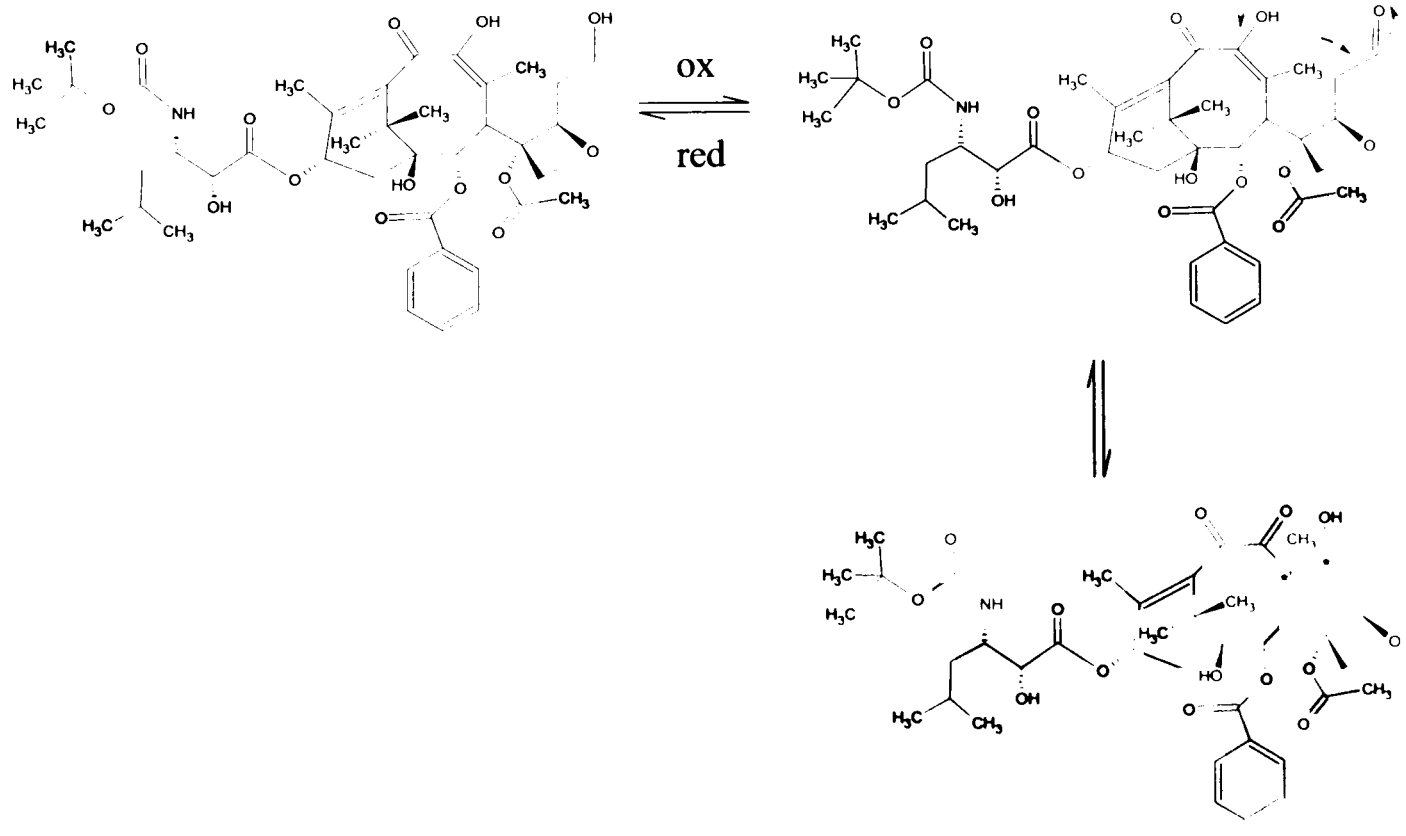

7,8-cyclized IDN 5390

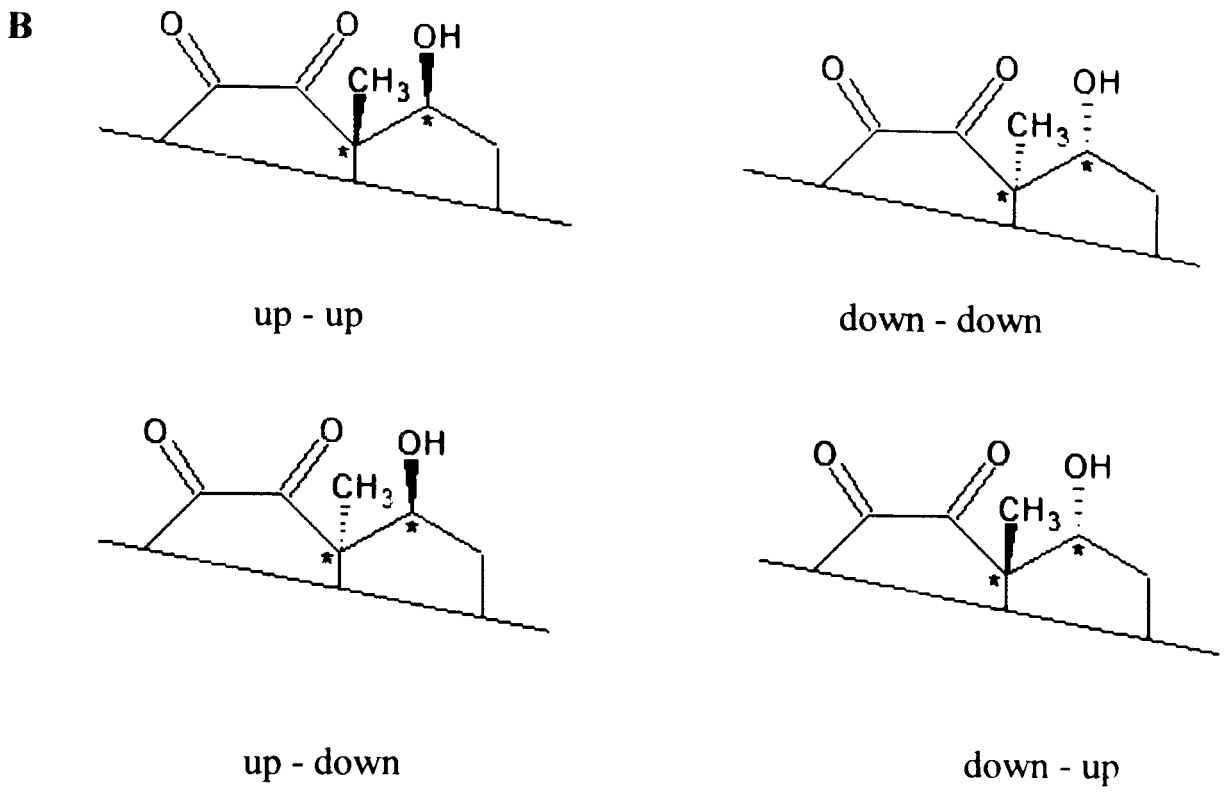

Figure 23. Mechanism of C ring cyclization (panel A) and 4 possible isomers consequent to the formation of the stereogenic centres in positions 7 and 8 (panel B)

The percentage of metabolites excreted was higher after oral (42%) than i.v. treatment (33%), suggesting a relevant contribution of the intestinal metabolism and/or liver first-pass effect. According to this observation, it is important to notice that all the sulphate conjugates (M4, M5, C5, C6, C7) were more abundant in faeces of mice treated orally (in the range of 1.4-2.3 fold higher) than intravenously and that these metabolites were not present in urine.

4.1.2. Identification of metabolites in plasma samples

On the basis of the knowledge about the metabolites found in faeces and urine samples, it was decided to better define the metabolic pathway of IDN 5390 searching for the same compounds in plasma. For analytical reasons, the study of metabolites was conducted in faeces and urine of mice treated with a dose of 120 mg/kg but, with plasma samples, the dose investigated was the one used in the optimal schedule for antitumour activity: 90 mg/kg[161, 162].

LC-MS/MS analysis showed that among the metabolites found in faeces and urine, the most abundant in plasma were C1, M1, C3 and M3.

As shown in figure 24, reporting the plasma profile of formation and elimination of these metabolites in comparison with the one of the parent drug, they were found at levels 4-5 fold lower than IDN 5390.

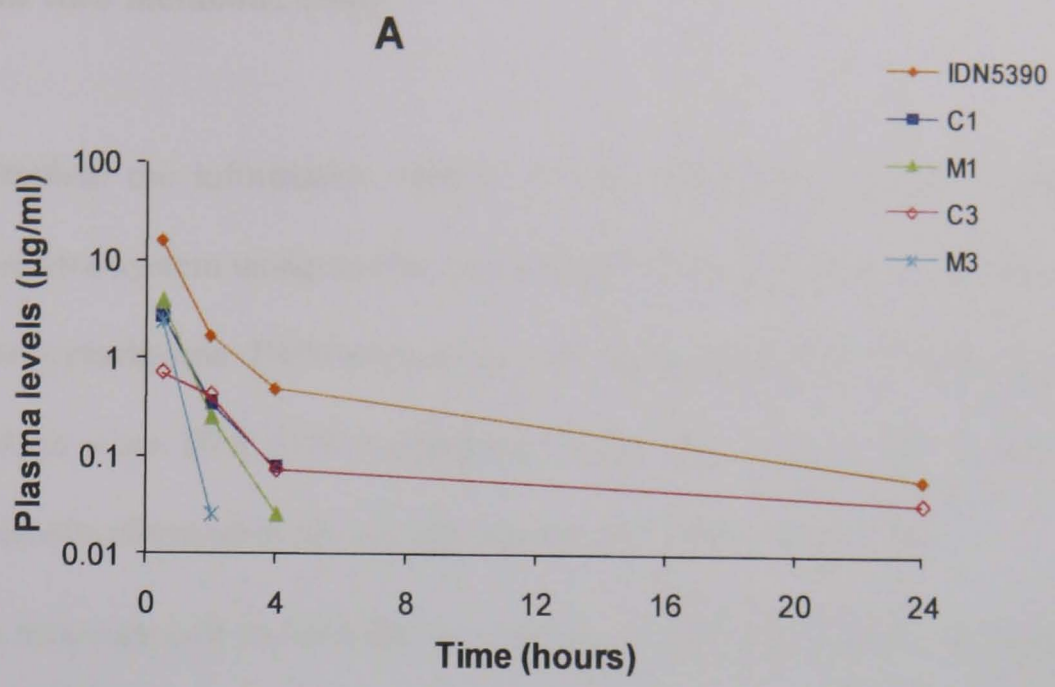

Figure 24. Plasma pharmacokinetic profile in CDF1 mice of the main metabolites of IDN 5390 and the parent drug after intravenous (panel A) and oral administration (panel B). (Plasma levels in logarithmic scale)

4.1.3. *In vitro* metabolic study

In order to complete the information relative to the metabolism, it was decided to investigate an *in vitro* system using murine and human liver microsomes with the aim of determining the cytochrome P450-associated metabolic properties, establishing the extent to which *in vitro* IDN 5390 metabolism fitted the *in vivo* data in mice and comparing the results obtained *in vitro* using microsomes of the two species.

First of all, the recovery and the stability percentage of IDN 5390 were determined in the two microsomal systems using average values of the chromatographic peak area obtained by three different samples. The recovery of IDN 5390 from murine and human microsomes was 111.2 and 106.4%, respectively. The stability of IDN 5390 in the reaction conditions after 4 hours incubation was 83.1 and 85.8% with mouse and human microsomes, respectively.

As reported in table 9, after 4 hours incubation, the formation of 13 and 5 metabolites was observed with mouse and human liver microsomes, respectively. Based on the retention time and the fragmentation pattern, the table reports the name of the detected metabolites only if they were already characterized in urine, faeces or plasma samples.

Compound	MW	Retention time (min)	Microsomes (relative percentage, %)	
			murine	human
IDN 5390	787	23.7	44.0	0.8
M1	803	19.9	20.1	56.6
M3	819	19.1	1.8	10.1
	785	23.5	0.4	/
	785	25.2	1.1	/
	785	26.3	0.4	/
C1	785	27.3	0.2	0.3
	785	28.7	0.6	/
	785	29.6	0.9	/
	801	20.0	3.5	/
C3	801	21.9	4.6	/
	801	22.2	1.2	/
C2	801	23.6	7.1	5.2
C4	817	19.6	3.4	5.4

Table 9. Relative percentage of IDN 5390 and its metabolites formed in murine and human microsome systems

IDN 5390 was extensively metabolized with human microsomes - the percentage of unchanged parent compound was only 0.8% in the end of the reaction - whereas less than 60% was modified with murine microsomal system. The most abundant metabolite in both the systems was the monohydroxylated derivative of IDN 5390 (M1).

The data suggested that the reaction of retrograde C cyclization (figure 23, panel A) is more favoured in the murine system not only for the presence of six peaks with molecular weight of 785 in murine samples vs just one, C1, in human microsomes - but also considering the second metabolite in terms of relative percentage of formation: in

the murine system, it was a derivative of series B (C2, figure 22) whereas with human microsomes, a derivative of series A (M3).

As already mentioned and shown in figure 23, the other 5 metabolites with a molecular weight of 785 were probably isomers of C1. The same explanation can be given to the presence of 4 mono-hydroxylated derivatives of C1. Going on the analysis of the murine samples, I also found one di-hydroxylated metabolite of IDN 5390 and one of C1 amounting to 1.8 and 3.4%, respectively.

No differences were detectable in the concentrations of IDN 5390 and metabolites from the samples incubated with and without UDPGA, indicating that UGTs do not play any role in the metabolism of IDN 5390.

In our lab a decrease of IDN 5390 bioavailability was demonstrated after 1 or 2 weeks of single or double oral daily doses of 90 mg/kg of the compound; i.e. the AUC value after p.o. daily administration on day 14 was 2-fold lower than that on day 1. This phenomenon was not due to the vehicle, polysorbate 80, that was reported to potentially affect the absorption of several drugs, reducing their bioavailability. Mice received polysorbate 80 daily for 1 week, followed by a single dose of IDN 5390 at 90 mg/kg. The AUC in these mice was superimposable with that obtained after a single dose without polysorbate 80 pretreatment [187].

In the light of the knowledge about IDN 5390 metabolism, to explain the decrease of IDN 5390 disposition, it was hypothesized a metabolic auto induction mechanism as already suggested for paclitaxel [188]. An experiment was performed to determine whether liver metabolic induction was responsible for the decrease in IDN 5390 AUC. The pharmacokinetics was studied following an i.v. dose of 90 mg/kg IDN 5390 given after a week of daily oral treatment with 90 mg/kg. IDN 5390 was quantified in these plasma samples and the pharmacokinetic parameters were elaborated: there was no reduction of plasma levels, and the AUC after chronic treatment was 37.9 μg/mL*h, close to the 42.0

μg/mL*h found after a single dose. These data suggest a metabolic auto induction mechanism at the level of the intestinal metabolism of IDN 5390 following prolonged oral treatment.

Among the different metabolites tentatively characterized, C1 appeared to be the most interesting one because, thanks to the formation of the bond between the positions 7 and 8, it showed the same tetracyclic core of paclitaxel. Although IDN 5390 is an active compound, the opening of the convex taxane core has *per se* a detrimental effect on the activity of paclitaxel [159, 189, 190]. Moreover, it would have been relevant to know its exact structure considering that it is the parent compound of series B metabolites (figure 22) and it is a circulating derivative. Indena S.p.A. synthesized and provided us two different products of the cyclization reaction of IDN 5390. They were analysed by the mass spectrometer and one of them, named IDN 5910 and having the structure shown in figure 25, corresponded to C1.

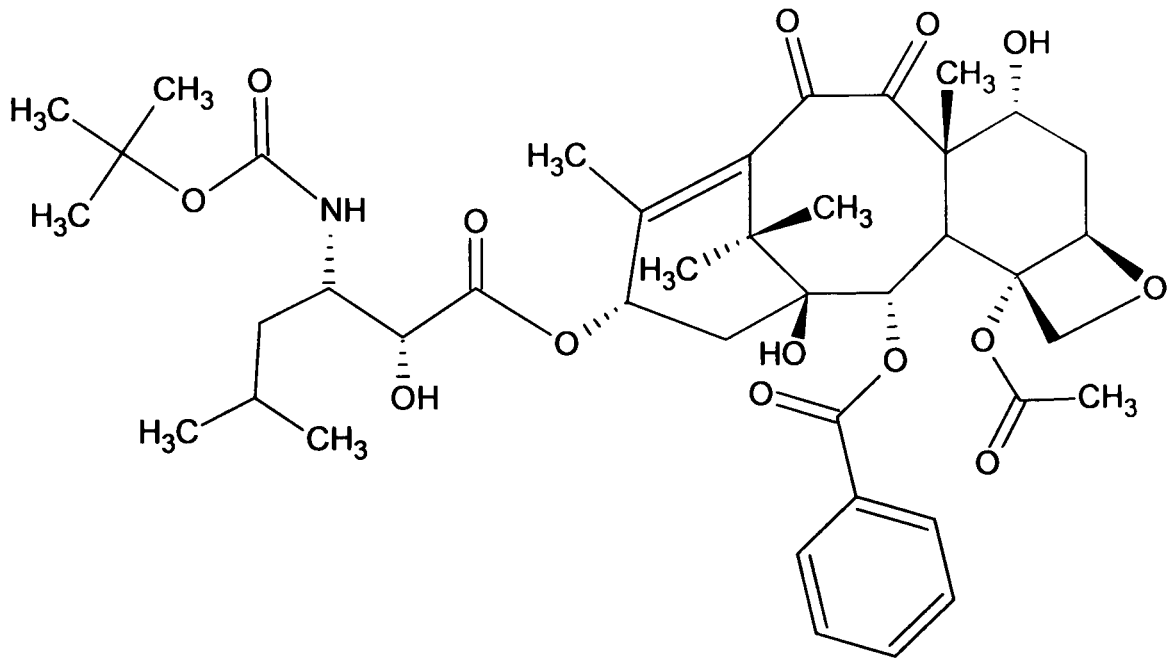

Figure 25. Chemical structure of C1 (IDN 5910)

In summary, IDN 5390 is able to affect endothelial cell motility [160], it has a favourable bioavailability, it is well tolerated without causing any apparent toxicity (i.e. no body weight loss at therapeutically active dose), even upon repeated oral treatment, and

shows significant antineoplastic activity on a panel of different tumour models, including some paclitaxel-resistant tumours [161, 162].

Despite the favourable properties described above, IDN 5390 has a very high metabolic clearance with a short half-life: twelve metabolites were identified in faeces and urine, four of them were found in plasma at detectable levels and seven present the restored taxane scaffold. With human microsomes, the percentage of metabolized IDN 5390 at the end of the incubation time was 99%. For all these reasons, IDN 5390 is difficult to manage and its metabolic-pharmacokinetic profile has to be carefully evaluated - in terms of activity and toxicity of every metabolite - in case of further clinical development, particularly with a prolonged schedule of daily dose.

4.2. IDN 5614

The results obtained, prompted Indena S.p.A. to synthesize an IDN 5390 derivative (IDN 5614, figure 26) having the two positions involved in the cyclization reaction protected by a methyl group in order to preserve the antiangiogenic properties of IDN 5390 - emphasized by its low toxicity - and to diminish the metabolic clearance.

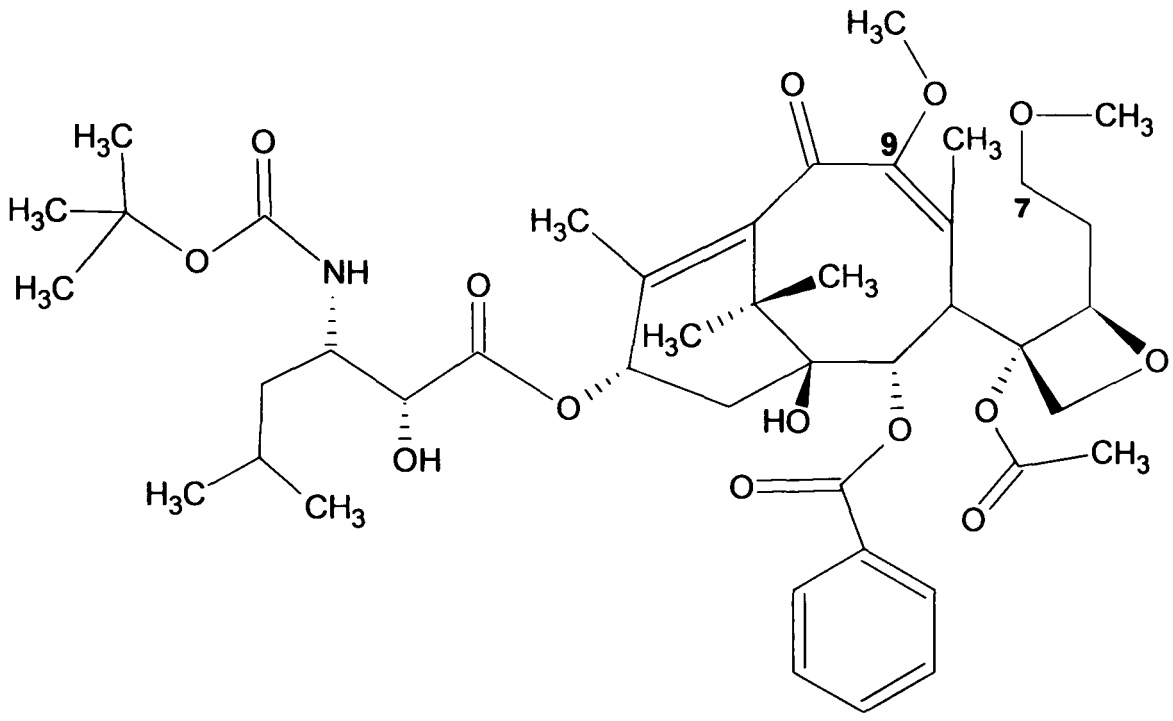

Figure 26. Chemical structure of IDN 5614

To verify the success of the introduced modifications that had led to IDN 5614, it was decided to define first its metabolic profile *in vitro,* using mouse liver microsomes, before further characterizing the *in vivo* pharmacokinetic profile of this new taxane derivative. IDN 5614 is structurally related to IDN 5390. Therefore, in order to compare their metabolic pattern, the incubation of IDN 5390 with mouse liver microsomes was repeated reproducing exactly the same experimental conditions for both taxanes, in particular as regards the chromatography.

Figure 27 shows the Total Ion Chromatogram (TIC) acquired in MS scan of an IDN 5614 sample with incubation time equal to 0, T_0, (panel A) and after 4 hours

microsomal reaction, T_{4h} (panel B). Obviously, by displaying data as a TIC, the mass spectrometer is used as a general detector; there is no selectivity in the data, but it is useful in understanding the overall chromatography and hunting for new peaks.

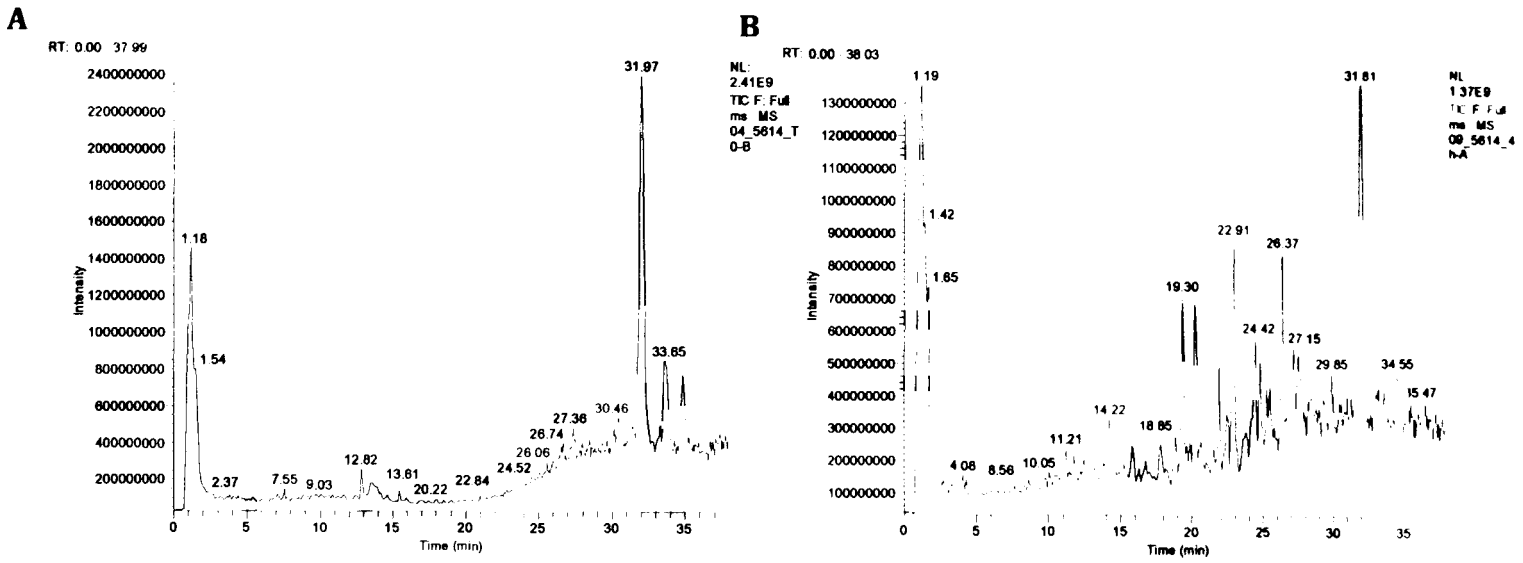

Figure 27. TIC of the incubation sample of IDN 5614 at T_0 (panel A) and after 4 hours of microsomal reaction, T_{4h} (panel B) [instrument used: LCQ Deca XP Plus ion trap mass spectrometer]

Basing on TIC data, in T_{4h} sample IDN 5614 presents, at about 32 minutes, a peak height almost halved in comparison with T_0 sample and the formation of several metabolites. Table 10 reports the quantitative evaluation of the obtained results: more than 50% of IDN 5614 was metabolized within 4 hours (table 10).

IDN 5614 parameter	Amount (%)
metabolization without addition of UDPGA	51.2
stability in the incubation medium	87.5
recovery from microsomes	87.9

Table 10. Quantitative evaluation of the results obtained incubating IDN 5614 with mouse microsomes for 240 minutes

The percentages reported in table 10 were obtained using the average values of IDN 5614 chromatographic peak area, obtained in three different samples. In this experiment, the stability of IDN 5614 in the reaction conditions after 4 hours incubation and its recovery with the extraction followed procedure, were both found to be around 90%.

To make a quantitative estimation of the reaction products, it was assumed that the metabolites and IDN 5614 had similar response in the mass spectrometer. On the basis of the HPLC-MS/MS analysis, IDN 5390 was found among the metabolites of IDN 5614.

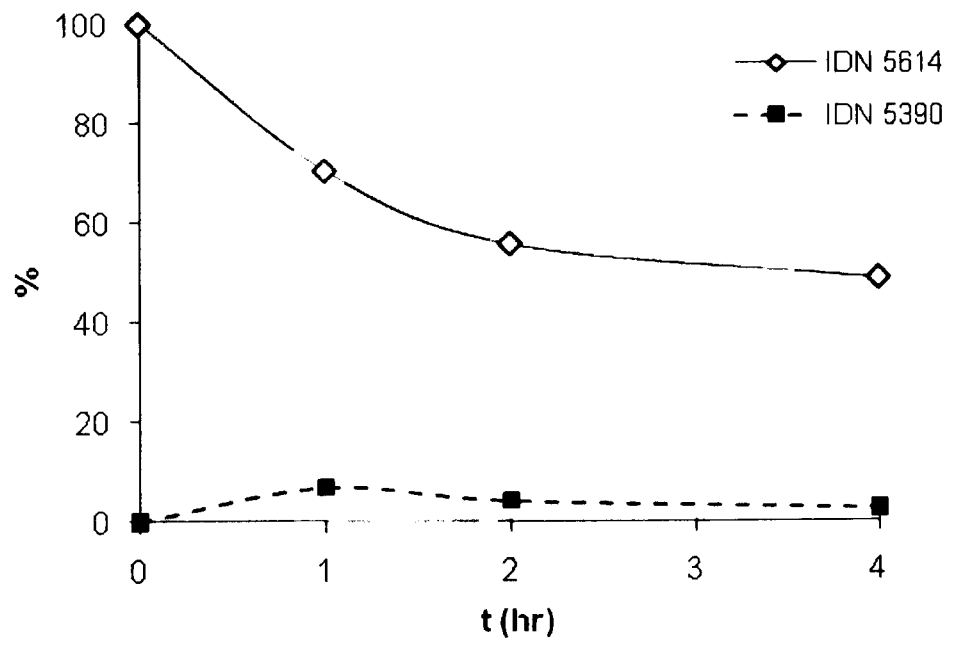

Figure 28. IDN 5614 disappearance and IDN 5390 formation kinetics after microsomal incubation of IDN 5614

As shown in figure 28, after 1 h incubation, the percentage of IDN 5614 decreased from 100% to 70% and IDN 5390 was 6.8% of the total amount of the parent compound. Afterwards, even the percentage of IDN 5390 decreased to 2.4% at 4 h, probably as a consequence of its metabolism.

Having found IDN 5390, as a product of di-demethylation of IDN 5614 in position 7 and 9, it was searched for a metabolite with *m/z* ratio of 802, that is the product of

mono-demethylation. Three peaks, characterized by *m/z* ratio of 802, were identified, but on the basis of their MS^2 obtained with the ion trap mass spectrometer, it was not possible to understand if they were metabolites of IDN 5614 (mono-demethylated derivatives) or of IDN 5390 (monohydroxy-7,8-cyclized IDN 5390 derivatives). However, it is worth noting that the chromatographic trace related to metabolites with *m/z* ratio of 802 generated by microsomal reaction of IDN 5614 (figure 29, panel A) is different from the one of IDN 5390 (figure 29, panel B). Therefore, they may be mono-demethylated derivatives of IDN 5614.

A

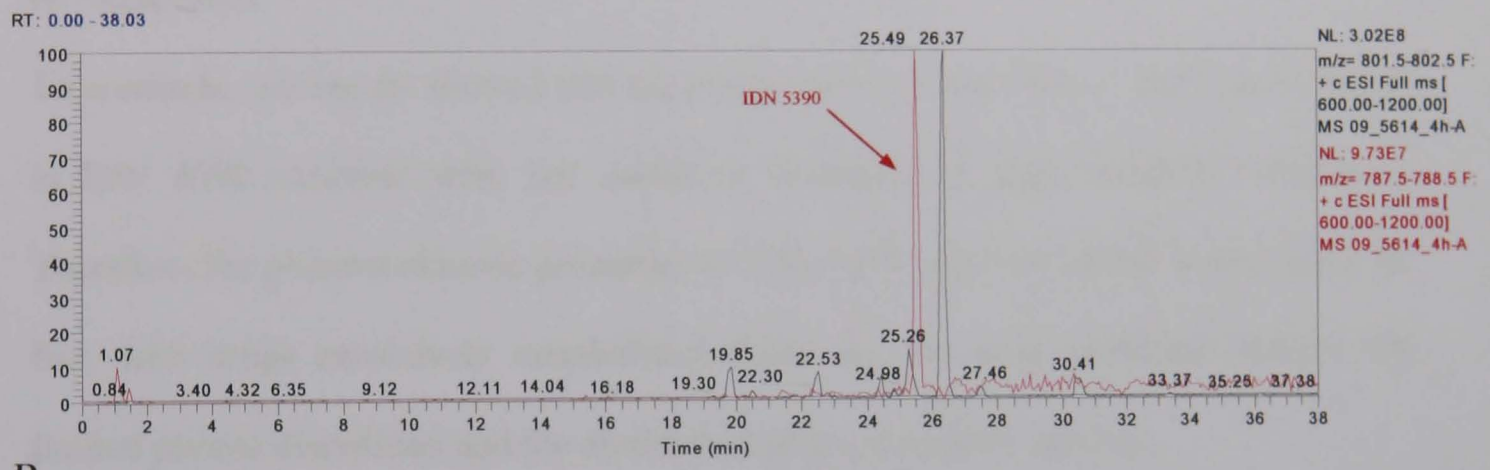

B

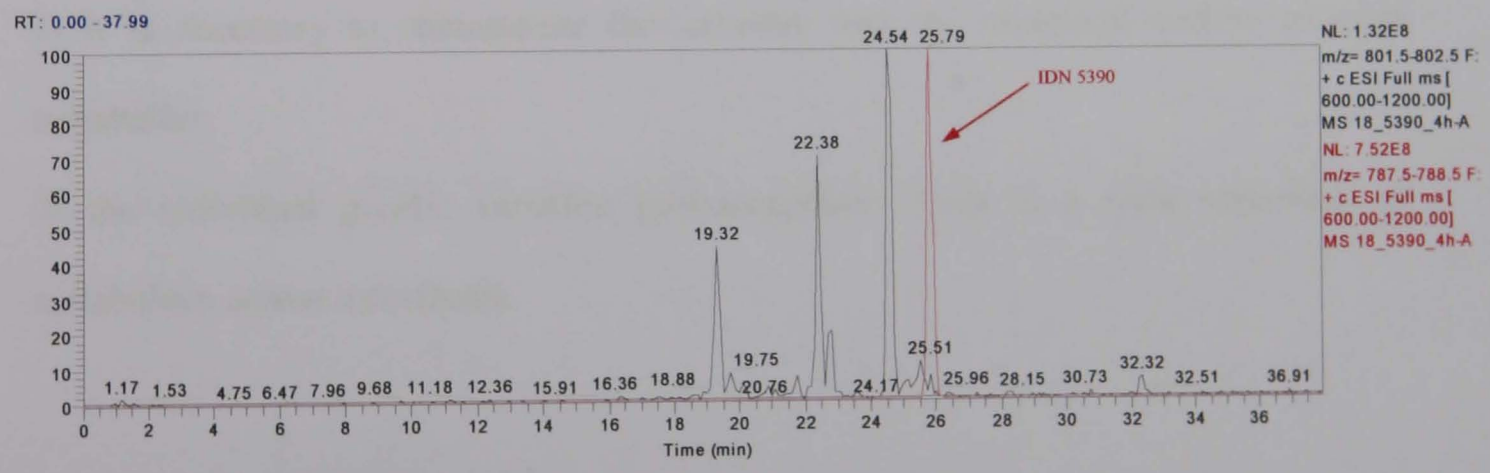

Figure 29. Chromatographic traces of metabolites with *m/z* ratio of 802 obtained after microsomal reaction of IDN 5614 (panel A) and of IDN 5390 (panel B) [instrument used: LCQ Deca XP Plus ion trap mass spectrometer]

Among the metabolites found in the incubation sample of IDN 5614, two with *m/z* ratio of 786 and 800 were probably characterized by the formation of the typical C-ring of

taxanes. In fact, to obtain the closing of C-ring it is sufficient to have demethylation in position 9 (figure 23, panel A).

All the metabolites described after microsomal reaction with IDN 5390 were found also after IDN 5614 incubation, rendering very difficult to understand if they were direct products of IDN 5614 or originated by IDN 5390. For this reason, it was decided not to further characterize IDN 5614 metabolic profile. No differences were observed in the chromatograms obtained from the samples incubated with and without UDPGA, indicating that the UGTs have not a significant role in the metabolism of IDN 5614 and its metabolites.

To conclude, my results showed that the methylations, in positions 7 and 9, introduced in IDN 5390 structure were not useful to minimize its high metabolic clearance. Therefore, the pharmacokinetic properties of IDN 5614 were not further investigated. In fact, with drugs extensively metabolized, there are two main problems besides the limited plasma disposition and the diminished pharmacological activity:

1- it is necessary to characterize the structure and the biological activity of each metabolite;

2- the individual genetic variation (polymorphism) leads to a wide variability of metabolism across individuals.

IDN 5738, IDN 5839 and IDN 6140

The other three taxane derivatives, provided by Indena S.p.A., were IDN 5738, IDN 5839 and IDN 6140 (see structures in figure 30 and 43). All of them were obtained by modifying the ortataxel structure. The first two compounds were obtained at the same moment whereas IDN 6140 was received successively. For this reason, the studies on IDN 5738 and IDN 5839 were conducted in parallel and therefore, the work done on these two taxane derivatives, is reported comparing each other.

The metabolism of ortataxel was previously investigated both *in vitro* and *in vivo*. In the literature, it was reported that the metabolic pathways - characterized in rats and dogs *in vivo* and in rat, dog and human liver microsomes - mainly involve the formation of products of phase I biotransformation reactions. In particular, they are a monohydroxy derivative, the metabolite lacking the side chain in position 13 and the epimers of them and of the parent compound [191, 192].

Accordingly, it was expected ortataxel derivatives would have not presented the problem of an extensive metabolism, therefore it was decided to begin the study of these new taxanes, defining their pharmacokinetic profile in mice.

4.3. IDN 5738 and IDN 5839

4.3.1. Method development

IDN 5738 and IDN 5839 differ from each other in the groups bound to the positions 1 and 14 (figure 30).

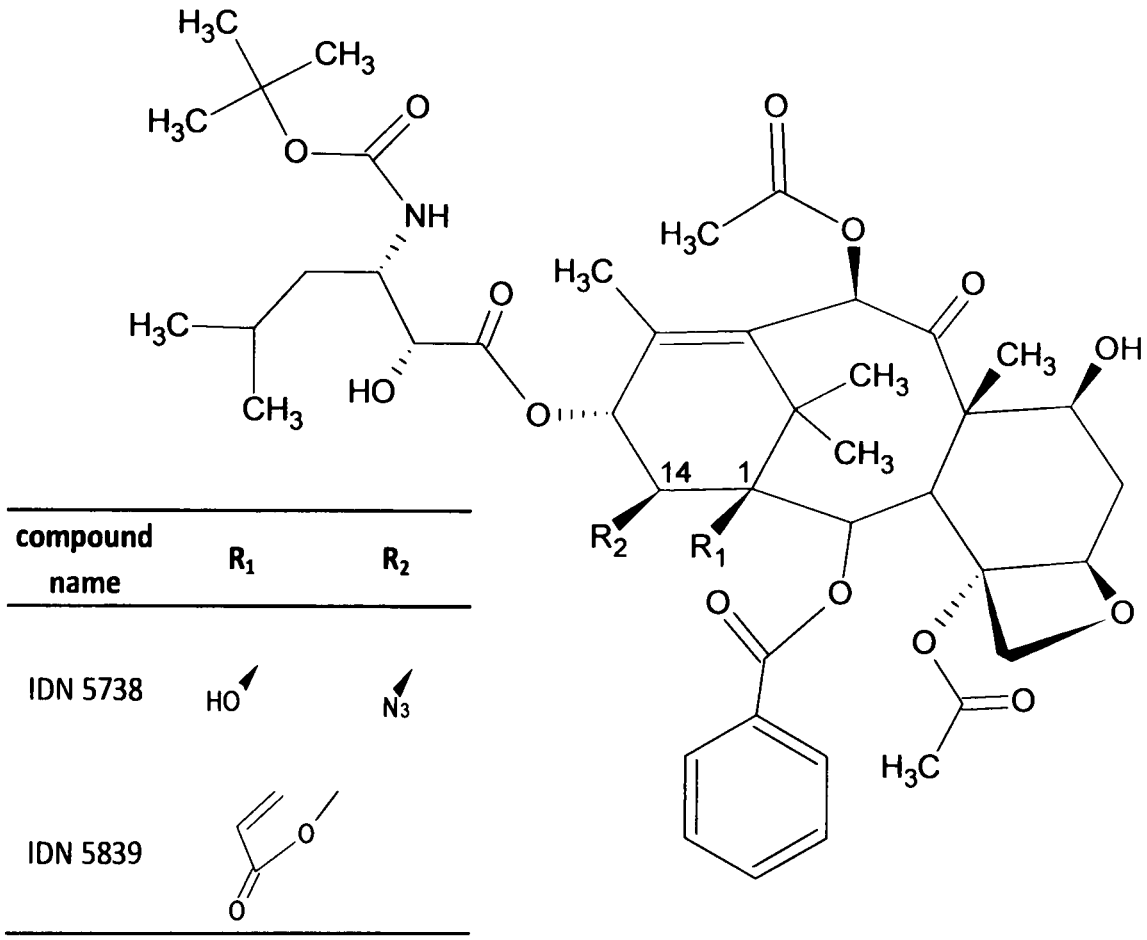

Figure 30. Chemical structure of IDN 5738 and IDN 5839

4.3.1.1. HPLC-MS/MS

In figures 31 and 32 (panel C), are reported the typical SRM chromatograms for IDN 5738 and IDN 5839 respectively, showing the quantifier transition of IDN 5738 and IDN 5839 for an extracted mouse plasma standard sample at LOQ, containing the compounds at the concentration of 25 ng/mL and IS (IDN 5127) at 1 µg/mL in comparison with a chromatogram of a blank plasma sample (panel A) and a blank plasma sample with IS added (panel B).

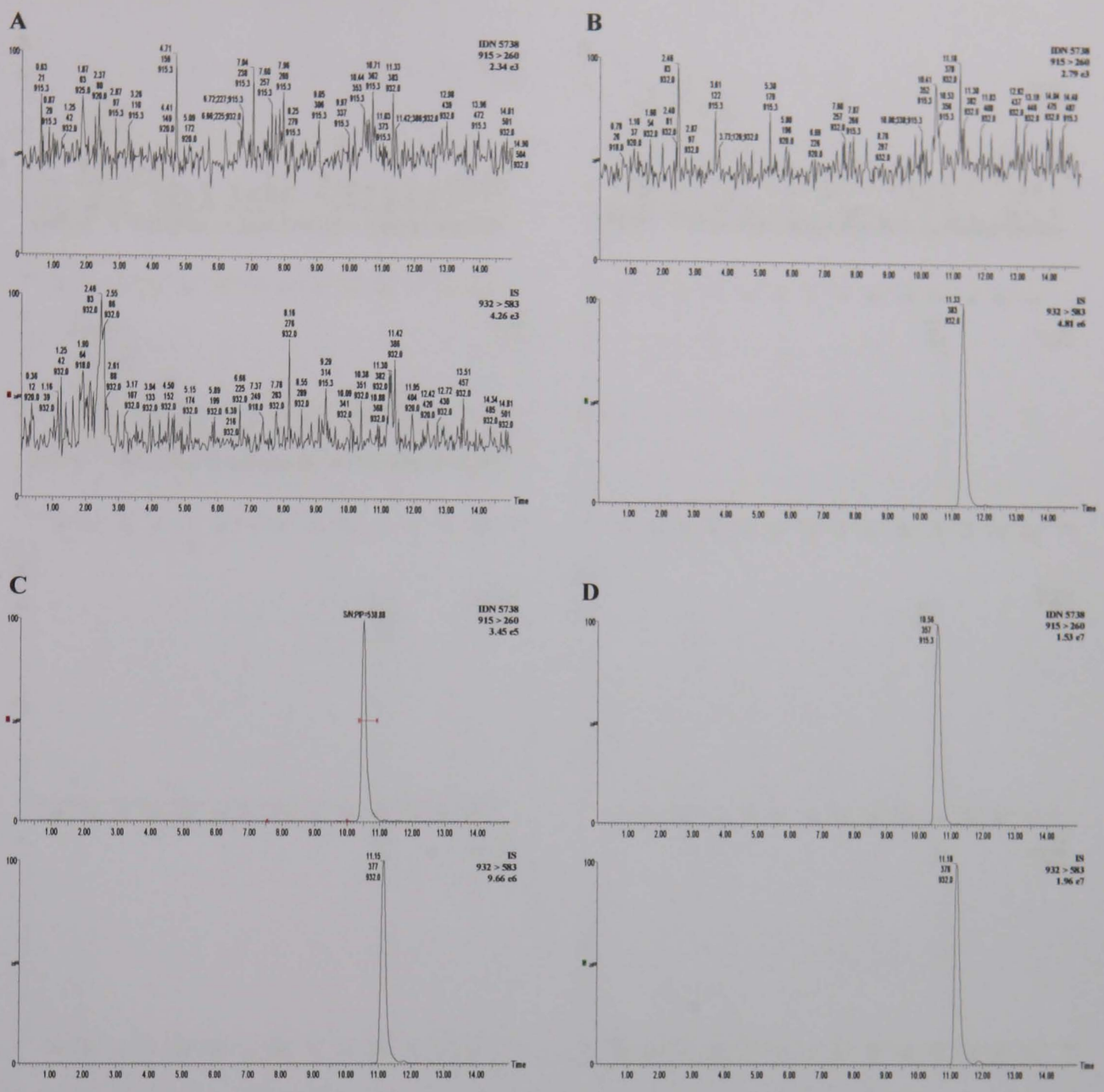

Figure 31. (A) SRM chromatograms of a mouse blank plasma sample; (B) SRM chromatograms of a mouse blank plasma with IS added; (C) Signal-to-noise ratio of IDN 5738 at LOQ concentration (25 ng/mL); (D) SRM chromatograms of an extracted plasma sample of a treated mouse showing IDN 5738 and IS. The measured concentration was 70.7 µg/mL [instrument used: API 4000 mass spectrometer]

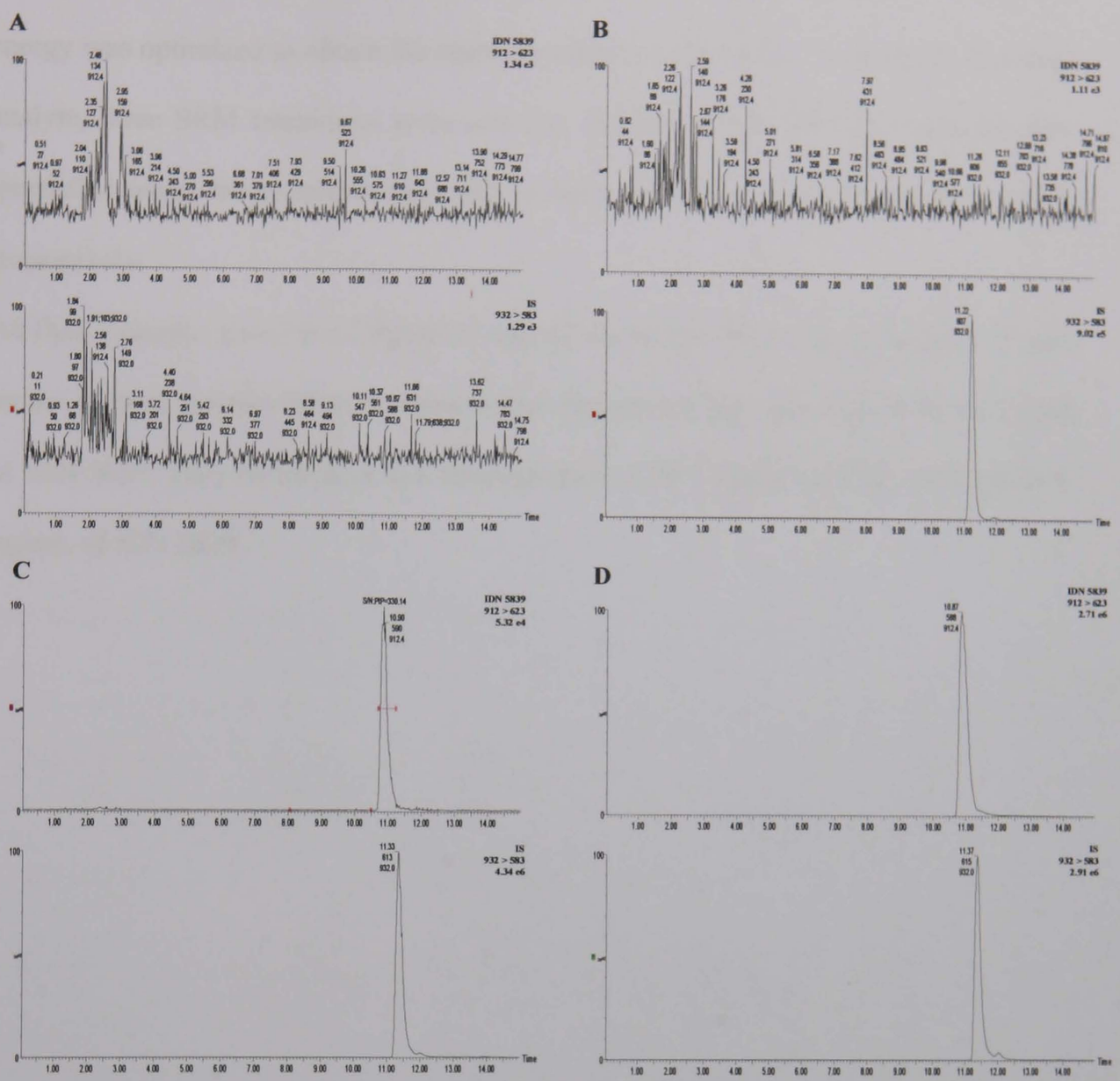

Figure 32. (A) SRM chromatograms of a mouse blank plasma sample; (B) SRM chromatograms of a mouse blank plasma with IS added; (C) Signal-to-noise ratio of IDN 5839 at LOQ concentration (25 ng/mL); (D) SRM chromatograms of an extracted plasma sample of a treated mouse showing IDN 5839 and IS. The measured concentration was 57.8 µg/mL [instrument used: API 4000 mass spectrometer]

The elution of the analytes was selective with a good separation of peaks in about 11 minutes (IDN 5738 at 10.6 min, IDN 5839 at 10.9 and IS at 11.2 min). No interfering peaks were present at these retention times and the peaks of all compounds were completely resolved from the plasma matrix.

The $[M+HCOO]^-$ of each analyte was selected as the precursor ion and the collision energy was optimized to obtain the respective product ions with a high signal. For each analyte, three SRM transitions were selected and IDN 5738, IDN 5839 and IS were quantified using the transition *m/z* 915 > 260, *m/z* 912 > 623 and *m/z* 932 > 583, respectively.

As final example, panel D of figure 31 and 32 shows the SRM chromatograms of two mouse plasma samples taken 5 minutes after the intravenous treatment with IDN 5738 or IDN 5839. They correspond to a concentration of 70.7 µg/mL of IDN 5738 and 57.8 µg/mL of IDN 5839.

4.3.2. Validation study

4.3.2.1. Matrix effect and recovery

According to the method described in section 3.6.6., it was possible to exclude the presence of any matrix effect of ion suppression or enhancement. The recovery was evaluated in triplicate at 2 or 3 different concentrations of IDN 5738 and IDN 5839, respectively. As shown in table 11, the mean extraction recovery for IDN 5738 at 0.100 and 1.000 µg/mL was >96%, with good reproducibility indicated by the CV < 3%. The recovery of IDN 5839 at 0.100, 1.000 and 4.000 µg/mL was higher than 90%, with reproducibility expressed as CV ≤ 14%.

Concentration µg/mL	Recovery ratio (%)	CV%
IDN 5738		
0.100	96.4	2.5
1.000	99.6	0.8
IDN 5839		
0.100	90.1	14.0
1.000	98.4	13.8
4.000	109.5	4.8

Table 11. Recovery of IDN 5738 and IDN 5839 from mouse plasma (N=3)

4.3.2.2. Calibration curves

Table 12 reports the accuracy and precision for each analyte determined at every day of the two validation studies.

Concentration µg/mL			
Spiked	Found (mean ± SD, 3 days)	Precision (%) between runs	Accuracy (%)
IDN 5738			
0.025	0.021 ± 0.002	7.2	85.3
0.050	0.050 ± 0.002	3.0	100.7
0.100	0.112 ± 0.001	1.3	112.0
0.500	0.540 ± 0.023	3.1	107.9
1.000	1.006 ± 0.032	3.2	100.6
1.500	1.450 ± 0.023	1.6	96.6
IDN 5839			
0.025	0.020 ± 0.000	0.0	80.0
0.050	0.052 ± 0.005	9.0	104.7
0.100	0.111 ± 0.003	2.5	111.0
0.500	0.532 ± 0.018	3.5	106.4
1.000	1.025 ± 0.070	6.8	102.5
2.000	2.045 ± 0.087	4.3	102.2
5.000	4.904 ± 0.147	3.0	98.1

Calibration curve parameters	**IDN 5738**	**IDN 5839**
R^2	0.997 ± 0.001	0.998 ± 0.001
X-coefficient	0.811 ± 0.052	0.347 ± 0.035
Y-intercept	0.007 ± 0.004	0.005 ± 0.000

Table 12. Accuracy and precision data for calibration curves of IDN 5738 and IDN 5839

The peak area ratios of analyte/IS versus the nominal concentrations were plotted and a least-squares linear regression, weighted by the reciprocal of the concentration, was applied to generate the calibration curves. The calibration curves, prepared on three different days, showed good linearity (figures 33 and 34) and acceptable data over a wide range of concentrations (0.025-1.500 µg/mL for IDN 5738 and 0.025-5.000

µg/mL for IDN 5839), with the coefficients of determination, R^2, equal to or better than 0.996.

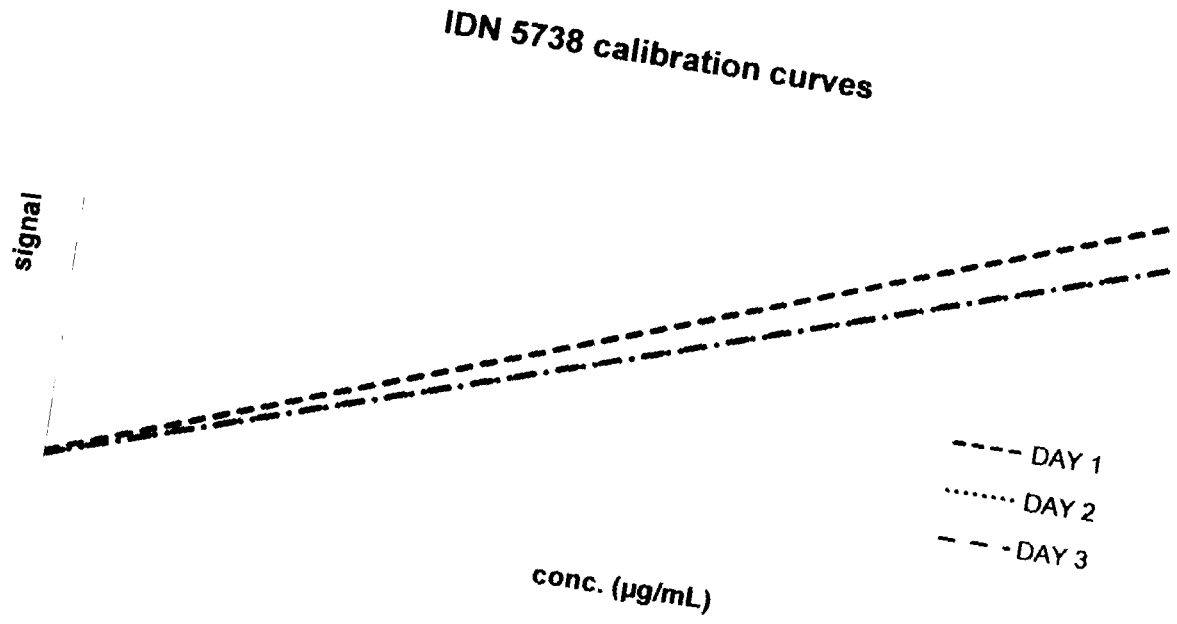

Figure 33. IDN 5738 calibration curves

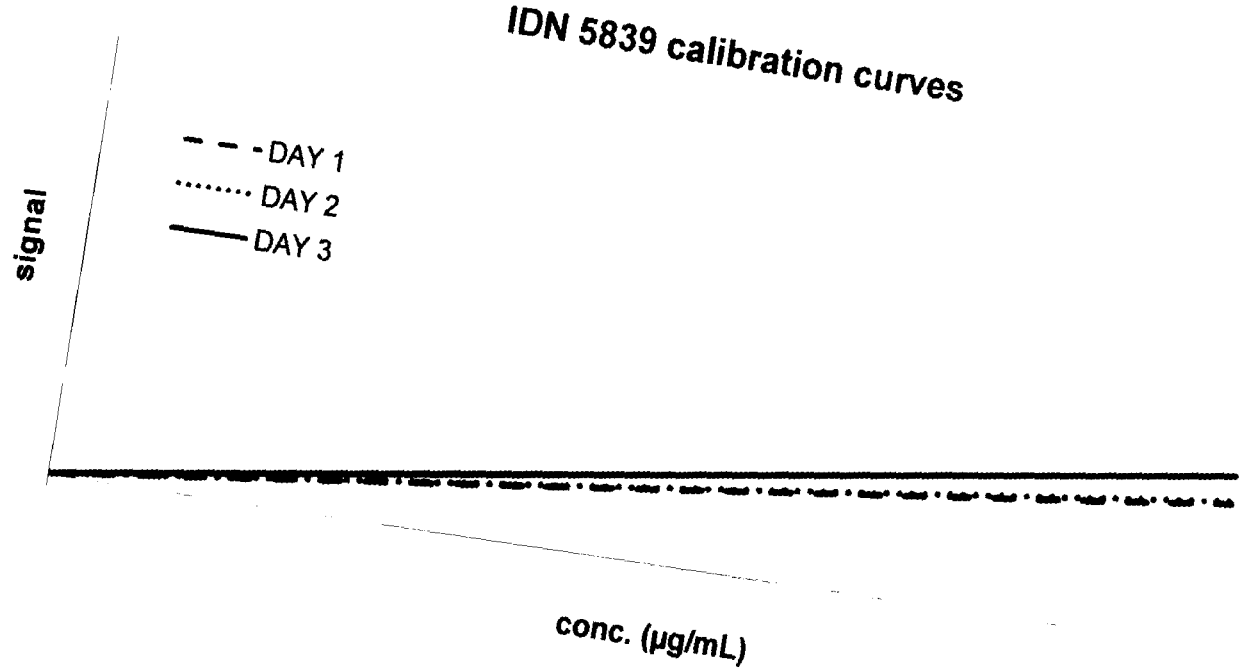

Figure 34. IDN 5839 calibration curves

Mean accuracy was in the range 85.3-112.0% for IDN 5738 and between 80.0 (at LOQ) and 111.0% for IDN 5839. The precision expressed as CV% was in the range 1.3-7.2% for IDN 5738 and 0.0-9.0% for IDN 5839.

4.3.2.3. Precision, accuracy and LOQ

The precision and accuracy of the two methods were evaluated analyzing three replicates of the QC samples at 0.075, 0.600 and 1.500 µg/mL for IDN 5738 and 0.075, 1.500 and 4.000 µg/mL for IDN 5839, within a single-run analysis for intra-day study, and over three consecutive runs for inter-day study. The accuracy and precision (CV%) for the two analytes are shown in table 13.

	IDN 5738 theoretical concentration (µg/mL)			**IDN 5839 theoretical concentration (µg/mL)**		
	0.075	0.600	1.500	0.075	1.500	4.000
Intra-day						
DAY 1						
Mean (N=3)	0.076	0.553	1.117	0.068	1.528	3.505
CV%	5.7	2.3	1.0	3.7	4.0	2.5
Accuracy%	101.3	92.2	93.1	91.1	101.9	87.6
DAY 2						
Mean (N=3)	0.085	0.582	1.183	0.076	1.586	3.527
CV%	2.0	1.8	11.2	3.3	4.6	2.9
Accuracy%	113.3	97.1	98.6	100.9	105.7	88.2
DAY 3						
Mean (N=3)	0.084	0.552	1.252	0.074	1.429	3.436
CV%	2.2	8.2	2.8	3.4	1.8	2.0
Accuracy%	112.0	92.0	104.3	99.1	95.2	85.9
Inter-day						
Mean (N=9)	0.082	0.562	1.184	0.073	1.514	3.489
CV%	5.8	5.5	7.4	5.5	5.6	2.4
Accuracy%	109.2	93.6	99.2	97.0	100.9	87.2

Table 13. Intra- and inter-day validation of the method for quantitative determination of IDN 5738 and IDN 5839

The methods were precise and accurate, with intra- and inter-day CV $\leq$ 12% and accuracy in the range of 92.0-113.3% for IDN 5738 and 85.9-105.7% for IDN 5839.

The LOQ was defined as the lowest concentration that could be measured with a precision within 20% and accuracy between 80 and 120%. Consistent with our aims, the LOQ was set at 25.0 ng/mL for both the analytes and validated through five replicates. At the LOQ, the intra-day CV% and accuracy were respectively 7.9% and 96.8% for IDN 5738 and 9.6% and 103.2% for IDN 5839. It is important to note that, as shown in panel C of figures 31 and 32, because of the high signal-to-noise ratio (> 500 for IDN 5738 and > 300 for IDN 5839), a lower LOQ could have been set for both the analytes, being LODs of 0.14 and 0.25 ng/mL for IDN 5738 and IDN 5839, respectively.

4.3.2.4. Stability in frozen matrix

The stability of the two taxane derivatives was assessed by analyzing QC samples at concentrations of 0.075, 0.600 and 1.500 μg/mL for IDN 5738 and 0.075, 1.500 and 4.000 μg/mL for IDN 5839. The results obtained for the short term stability of the two new taxane derivatives in frozen matrix showed that they are stable over about one month in mice plasma at -20°C. For IDN 5738, the accuracy was in the range 99.1-109.4% and the CV% between 6.1 and 12.2% while for IDN 5839, the accuracy and the CV% were in the range 85.1-100.9% and 0.0-12.8%, respectively.

In summary, the present methods revealed high selectivity, precision and accuracy and they are sensitive enough to allow the determination of the plasma concentrations of the two compounds in mice.

4.3.3. Pharmacokinetic results

The two developed assays for the determination of IDN 5738 and IDN 5839 were employed to measure plasma concentrations of the two compounds in mice and applied to study the preclinical pharmacokinetics of the two taxane derivatives. Figures 35 and 36 report the concentration-time profiles of IDN 5738 and IDN 5839 in plasma of CD1 female mice after i.v. and p.o. administration of 60 mg/kg of the two novel taxanes (the concentration-time data are listed in appendices 3 and 4).

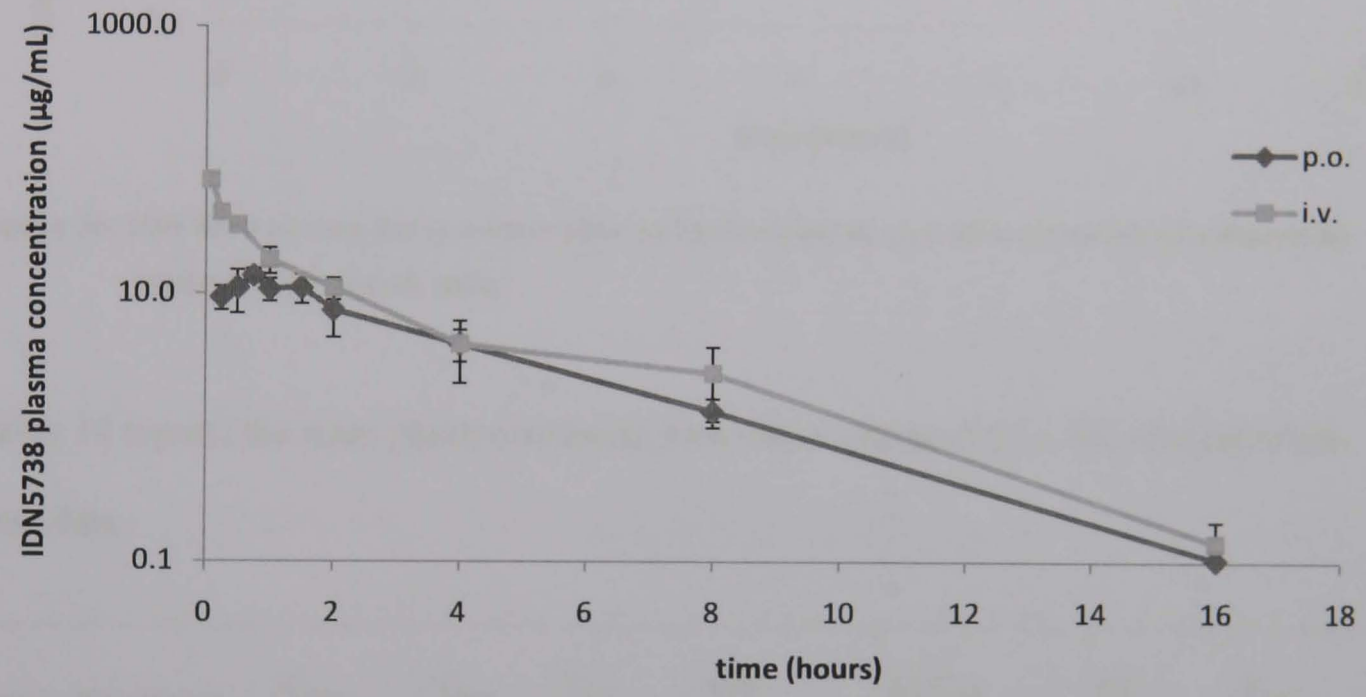

Figure 35. IDN 5738 plasma decay curves after an intravenous or p.o. administration of a dose of 60 mg/kg in CD1 female mice

Plasma samples taken at the first time points after the treatment were diluted with an appropriate quantity of control mouse plasma determined on the basis of ortataxel pharmacokinetics [168]. In spite of that, plasma samples from 5 minutes to 1 hour after the intravenous treatment with IDN 5738 and at 5 minutes after the i.v. administration of IDN 5839, showed concentrations superior to the highest standard point of the calibration curve, therefore they were suitably diluted with control mouse plasma and re-analysed after having assessed the independence of analysis from the dilution. It was

evaluated by adding control mouse plasma to a standard at a ten-fold ULOQ concentration in order to have 1:10 and 1:100 ratios.

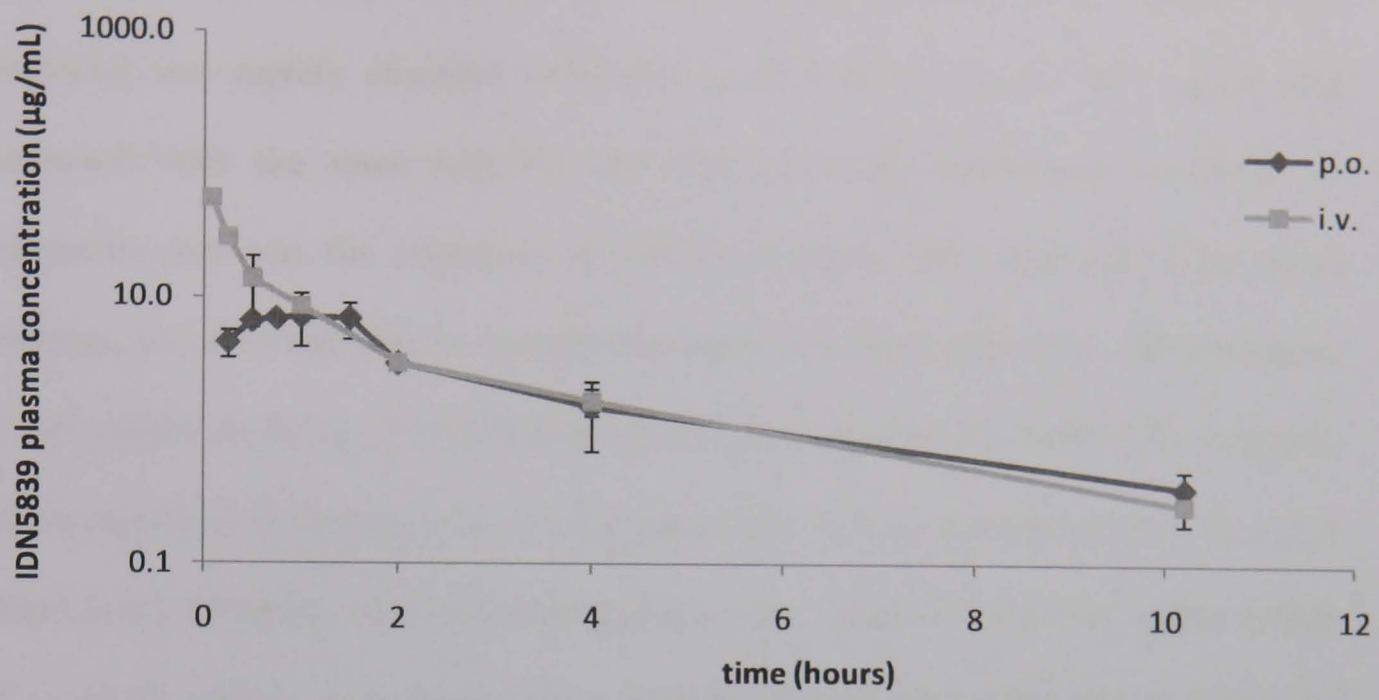

Figure 36. IDN 5839 plasma decay curves after an intravenous or p.o. administration of a dose of 60 mg/kg in CD1 female mice

Table 14 reports the main pharmacokinetic parameters obtained from the concentration-time data.

Compound	Treatment	C_{max} (µg/mL)	T_{max} (h)	$T_{1/2}$ (h)	AUC (µg/mL*h)	AUC_{inf} (µg/mL*h)	Cl (L/h/kg)	V_{bd} (L/kg)	F (%)
IDN 5738	i.v.	71.2	0.08	2.2	92.5	93.0	0.6	2.1	
	p.o.	13.7	0.75	2.3	49.1	49.4	/	/	53.1
IDN 5839	i.v.	55.2	0.08	2.4	40.0	40.9	1.5	5.0	
	p.o.	7.1	1.00	2.8	22.1	23.6	/	/	56.1

Table 14. Main pharmacokinetic parameters of IDN 5738 and IDN 5839 after i.v. and oral administration of a dose of 60 mg/kg in female CD1 mice

Following the intravenous bolus of IDN 5738, a C_{max} of 71.2 μg/mL was achieved and after a rapid distribution phase the compound was eliminated with a terminal half-life ($T_{½}$) of 2.2 hours and a clearance (Cl) 0.6 L/h/kg. After the oral treatment, the compound was rapidly absorbed achieving at 45 min a C_{max} of 13.7 μg/mL and eliminated with the same half-life observed after the intravenous treatment. A comparison between the experimental AUCs obtained after oral and intravenous treatment, revealed that this compound has good absorption after oral administration, the bioavailability being 53.1%. Similar results were obtained for IDN 5839, that after intravenous bolus achieved a C_{max} of 55.2 μg/mL and it was eliminated with a $T_{½}$ of 2.4 h and Cl of 1.5 L/h/kg. After oral administration, the compound achieved within 1 hour a C_{max} of 7.1 μg/mL, then plasma concentration declined with a half-life of 2.8 h; the bioavailability was 56.1%. The high bioavailability of the two taxanes under examination supports the fact that they are not pumped out of the cells by P-gp and this evidence is in line with the cytotoxic data obtained on two human breast cancer cell lines, sensitive (LCC6 and MCF7) and resistant (LCC6-R and MCF7-R) to paclitaxel [144]. That is why, on LCC6-R cell line, characterized by the overexpression of P-gp, IDN 5738 and IDN 5839 were more toxic than paclitaxel and docetaxel with lower resistance index of 8 and 6, respectively in comparison with those of the two parent drugs of 111 and 92. The better cytotoxicity of these new derivatives in comparison with paclitaxel and docetaxel is shown even on MCF7-R cell line with IDN 5738 and IDN 5839 having a resistance index of 8 and 43, respectively compared to 253 and 460 of paclitaxel and docetaxel, respectively.

IDN 5738 and IDN 5839 showed plasma concentrations consistent with those indicated to be cytotoxic against the aforementioned cell lines both sensitive and resistant ones. These concentrations were maintained in plasma of mice up to at least 16 and 10 hours after the administrations of IDN 5738 and IDN 5839, respectively.

4.3.4. Circulating metabolites of IDN 5738 and IDN 5839

The expected lack of extensive metabolism of IDN 5738 and IDN 5839 had to be assessed *in vivo*, thus it was decided to search for metabolites in the same plasma samples analysed for defining the pharmacokinetics of the two new taxanes.

It was not expected to define the metabolic pathway of the two compounds under study, but only to verify or deny the hypothesis made on the basis of structural evaluations. As regards the circulating metabolites, no sulfate or glucuronide derivatives were found in plasma of mice treated with IDN 5738 or IDN 5839.

Among IDN 5738 metabolites, 4 monohydroxylated derivatives (M1-M4) were found. As shown in figure 37, the retention time of these metabolites were 18.49, 18.80, 19.46 and 20.60 minutes against 26.69 of the parent compound (the mass spectra fragmentation patterns and chromatograms to back up identification of IDN 5738 metabolites are listed in appendix 5).

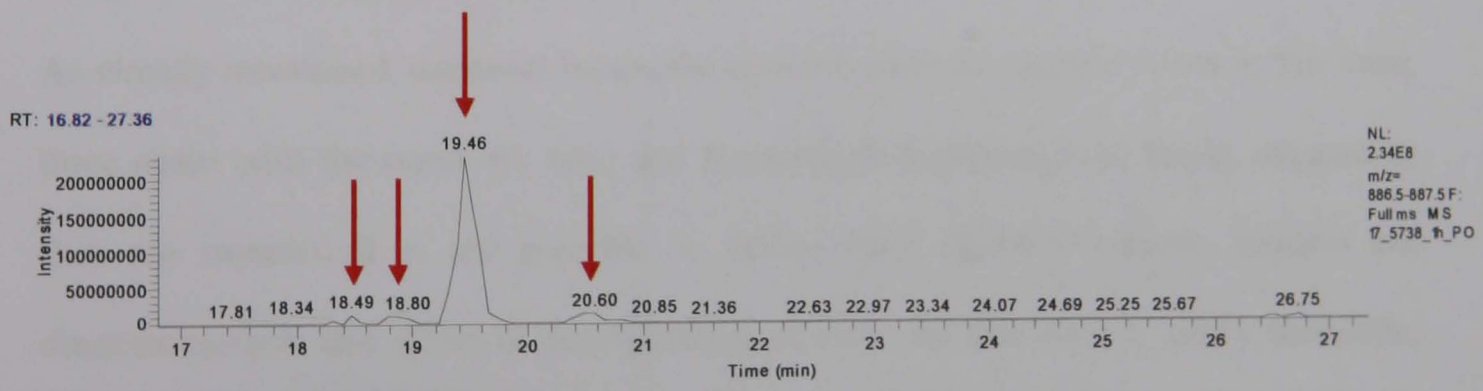

Figure 37. Chromatographic trace relative to monohydroxylated derivatives of IDN 5738

[instrument used: LCQ Deca XP Plus ion trap mass spectrometer]

The first three peaks were referable to derivatives (M1-M3) characterized by the hydroxylation on the benzoyl group in position 2 (figure 38).

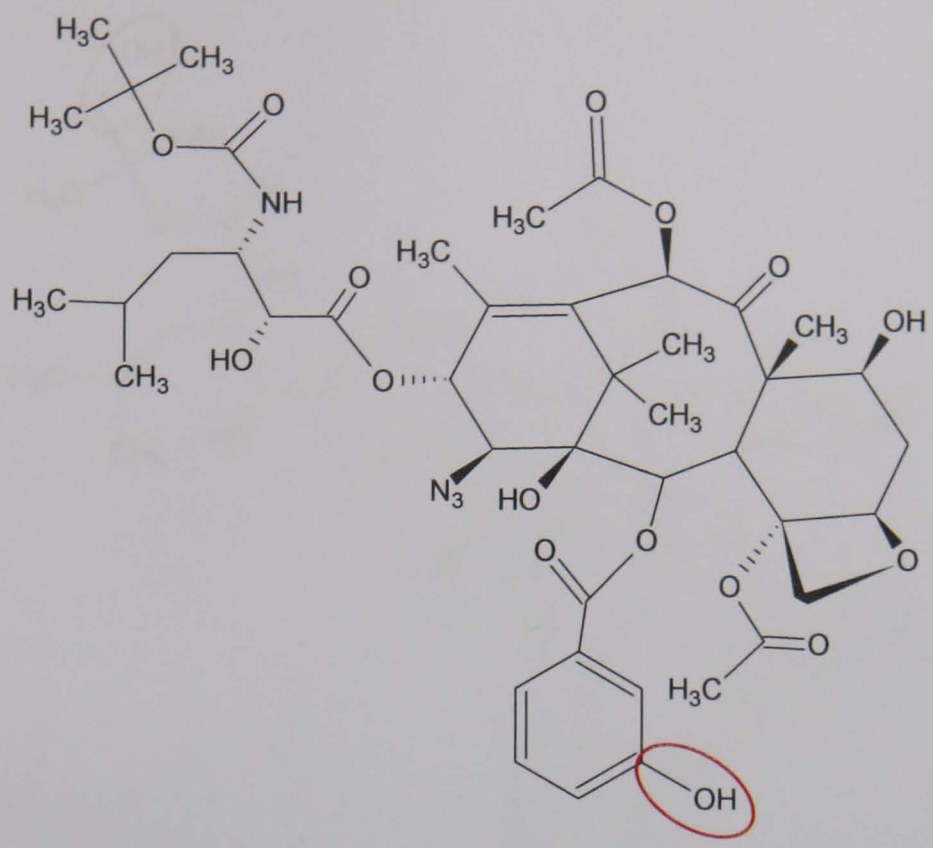

Figure 38. Hypothesized structure for monohydroxylated metabolites of IDN 5738 (M1-M3)

The structure of monohydroxylated derivatives was hypothesized and designed with the hydroxyl group in meta position according to paclitaxel metabolic pattern, but on the basis of the ion trap mass spectrometer spectra, it was not possible to draw definitive conclusions on the structure of these metabolites.

As already mentioned, ortataxel incurs the epimerization in position 7, but in this case, three peaks with the same *m/z* ratio and fragmentation pattern were found, suggesting they are isomers. It is not possible to define them epimers because epimers are diastereoisomers that differ in configuration of only one stereogenic centre therefore, generating just two compounds.

The fourth peak, at retention time of 20.60 min, is believed to be the metabolite (M4) with the hydroxyl group on the t-butyl group of the side chain in position 13 (figure 39).

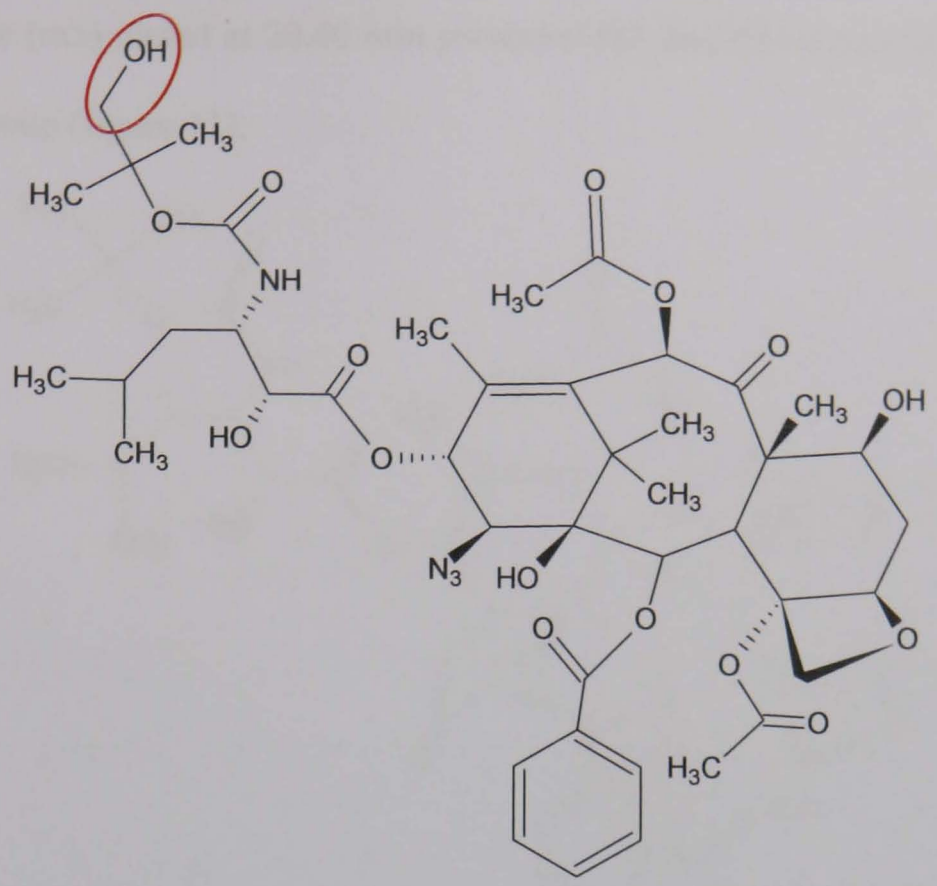

Figure 39. Structure of a monohydroxylated metabolite of IDN 5738 (M4)

No dihydroxylated metabolites either related to 14 substituted baccatin III were present in the analysed samples. The metabolites were present in detectable quantities up to the plasma sample taken after 8 hours since both the oral and intravenous treatments.

As regards IDN 5839 metabolites, only two monohydroxylated derivatives (m1 and m2) were found at the retention time of 20.40 and 21.66 minutes (figure 40) against 27.73 of the parent compound (the mass spectra fragmentation patterns and chromatograms to back up identification of IDN 5839 metabolites are listed in appendix 6).

Figure 40. Chromatographic trace relative to monohydroxylated derivatives of IDN 5839 (m1 and m2) [instrument used: LCQ Deca XP Plus ion trap mass spectrometer]

The metabolite (m1) eluted at 20.40 min presented the modification on the carbonyl of the benzoyl group (figure 41).

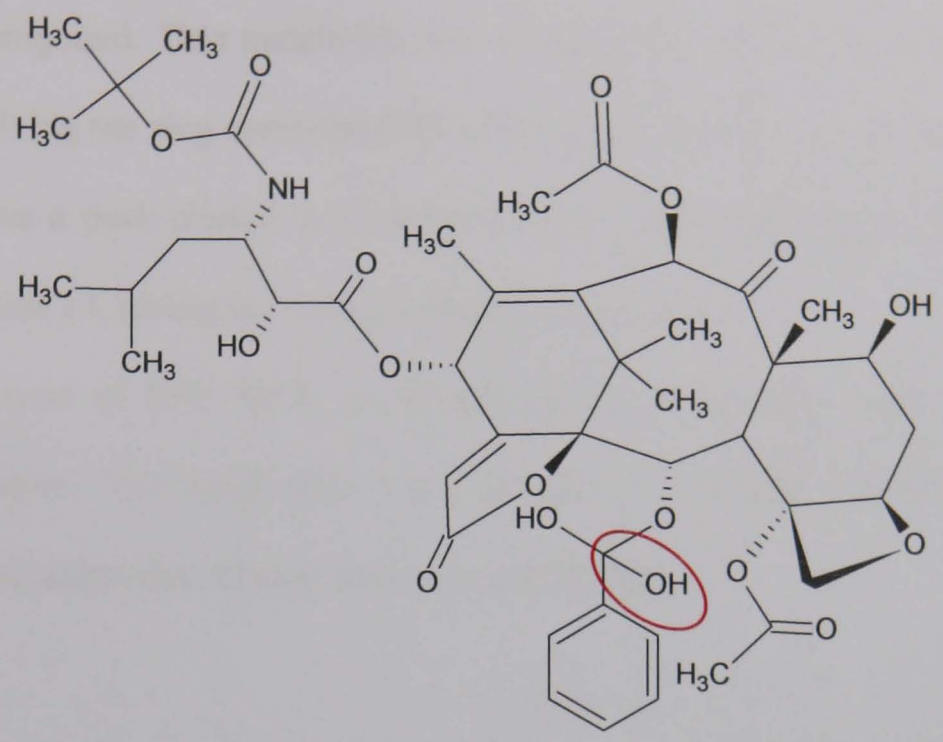

Figure 41. Structure of a monohydroxylated metabolite of IDN 5839 (m1)

The derivative (m2) having retention time of 21.66 min is characterized by the presence of the hydroxyl group on the t-butyl group of the side chain in position 13 (figure 42).

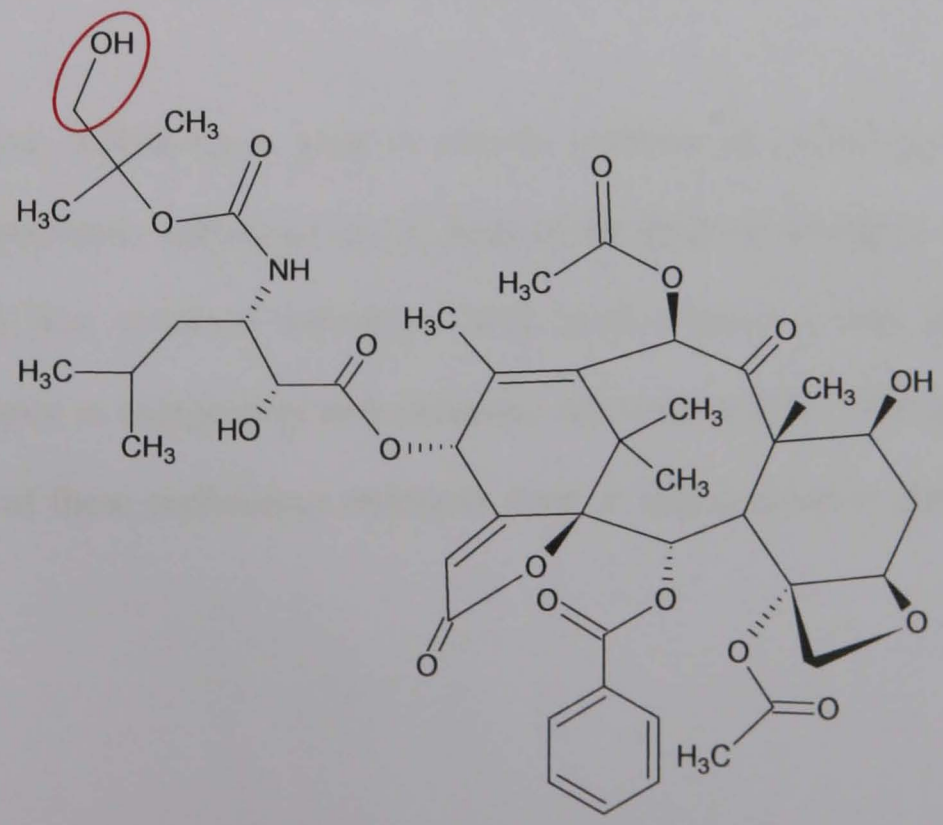

Figure 42. Structure of a monohydroxylated metabolite of IDN 5839 (m2)

At the retention time of 18.40 min, it was found a peak corresponding to a metabolite (m3) characterized by the *m/z* ratio of 824, that is lacking of 44 Da in comparison with the parent compound. This metabolite was probably the product of a decarboxylation reaction involving the ring comprised between the positions 1 and 14. Finally, at 16.36 min, there was a peak related to a metabolite (m4) characterized by the loss of side chain in position 13, giving the 1,14 substituted baccatin III.

Even in the case of IDN 5839, no dihydroxylated metabolites were present in the analysed samples. The metabolites were present in detectable quantities up to the plasma sample taken after 4 hours since the oral treatment.

In summary, my data defined for these compounds an interesting pharmacokinetic profile, nevertheless superimposable with that of ortataxel against a halved half life and a comparable cytotoxic activity on the sensitive and resistant LCC6 and MCF-7 cell lines.

In the meantime, Indena S.p.A. went on with the synthesis and screening of new taxane derivatives structurally optimized on the basis of the findings related to IDN 5738 and IDN 5839. A new ortataxel derivative, IDN 6140, showed a very good cytotoxic activity, not only in comparison with ortataxel, but even to IDN 5738 and IDN 5839. On the basis of these preliminary results *in vitro*, it was decided to draw attention to IDN 6140.

4.4. IDN 6140

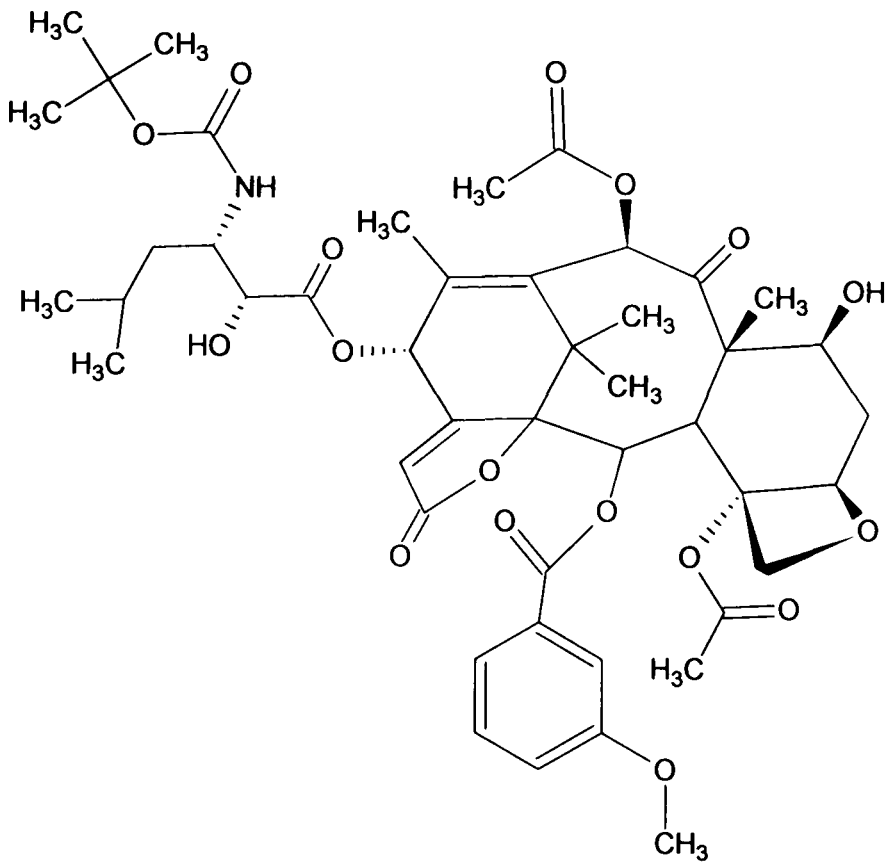

Figure 43. Chemical structure of IDN 6140

4.4.1. Method development

In figure 44 (panel C), it is reported the SRM chromatogram for IDN 6140, showing the quantifier transition for an extracted mouse plasma standard sample at LOQ, containing the compound at the concentration of 10 ng/mL and IS at 0.5 μg/mL in comparison with a chromatogram of a blank plasma sample (panel A) and a blank plasma sample with IS added (panel B).

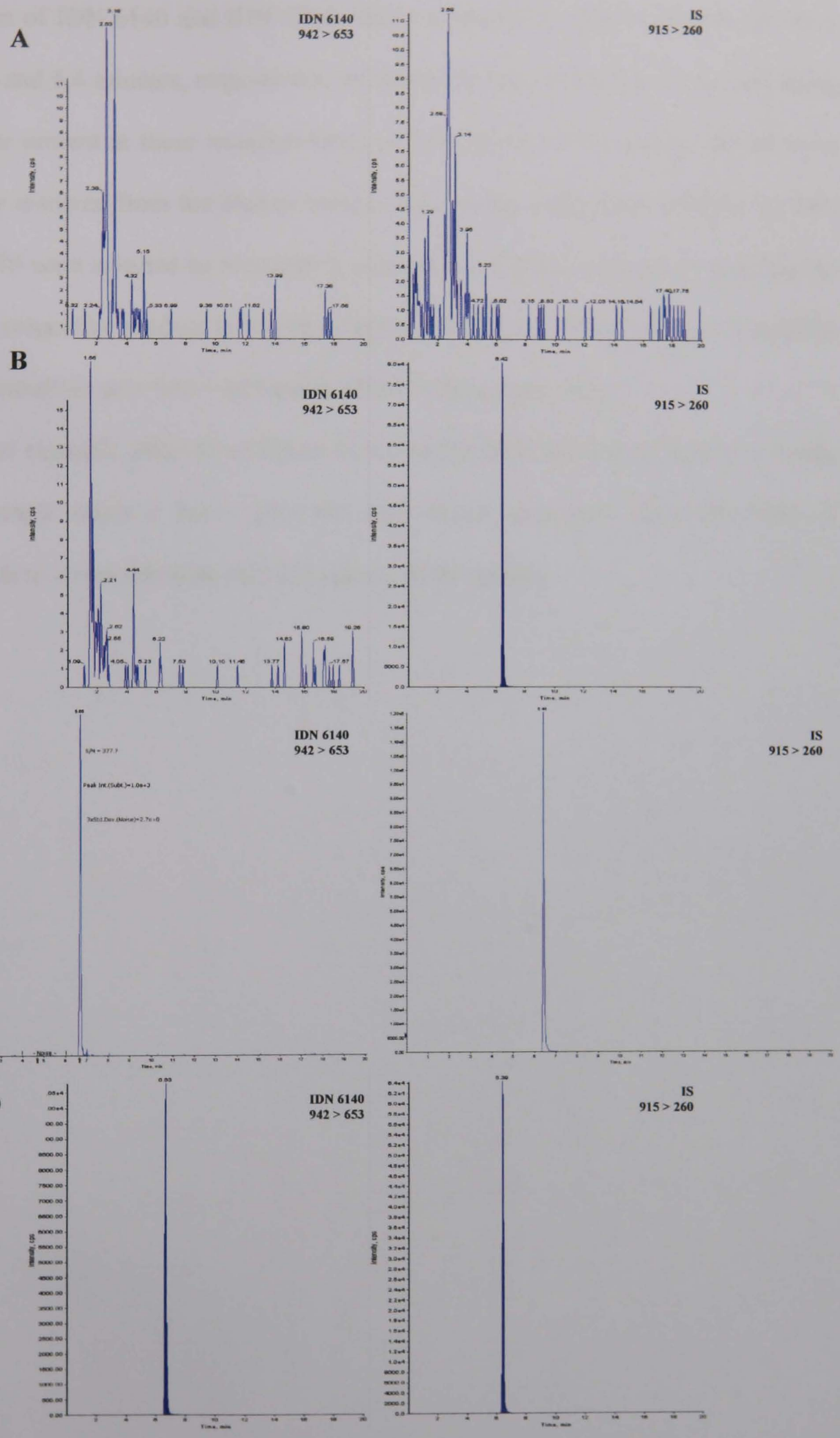

Figure 44. (A) SRM chromatograms of a mouse blank plasma sample; (B) SRM chromatograms of a mouse blank plasma with IS added; (C) Signal-to-noise ratio (377.7) of IDN 6140 at LOQ concentration (10 ng/mL); (D) SRM chromatograms of an extracted mouse plasma sample 2 hours after i.v. treatment. The measured concentration was 0.225 µg/mL

The elution of IDN 6140 and IDN 5738, used as Internal Standard (IS) was selective and at 6.7 and 6.4 minutes, respectively. As shown in figure 44 panel A, no interfering peaks were present at these retention times and the peaks of the analyte and IS were completely resolved from the plasma matrix. The formate adduct $[M+HCOO]^-$ of IDN 6140 and IS were selected as precursor ions and the collision energy was optimized to obtain the respective product ions with a high signal. IDN 6140 and IS were quantified using the transition *m/z* 942 > 653 and *m/z* 915 > 260, respectively.

As the final example, panel D of figure 44 shows the SRM chromatograms of a mouse plasma sample taken 2 hours after the intravenous treatment with IDN 6140. It corresponds to a concentration of 0.225 μg/mL of the analyte.

4.4.2. Validation study

4.4.2.1. Matrix effect and recovery

The matrix effect was assessed by infusing post-column a solution of IDN 6140 at the concentration of 50 ng/mL during the chromatographic run of an extracted plasma matrix sample.

Close to IDN 6140 retention time, there were no variations into the chromatographic profile indicating the absence of any enhancement or suppression effect, thus indicating absence of matrix effect.

Recovery experiments were performed in triplicate at 3 representative concentrations over the calibration range: 0.025, 0.100 and 2.000 µg/mL. As shown in table 15, the mean extraction recovery for IDN 6140 was higher than 85% with a reproducibility expressed as CV≤ 5%.

Concentration µg/mL	Recovery ratio (%)	CV%
0.025	85.5	5.0
0.100	114.0	3.5
2.000	112.7	4.1

Table 15. Recovery of IDN 6140 from mouse plasma (N=3)

4.4.2.2. Calibration curves

Extracted standard curves prepared in the concentration range of 0.010-2.000 μg/mL showed a good linearity, with the coefficient of determination, R^2, always greater than 0.998 (table 16).

Calibration curve accuracy (%)									
Days	**0.010**	**0.025**	**0.050**	**0.100**	**0.500**	**1.000**	**2.000**	**R^2**	**slope**
1	110.0	96.0	100.0	96.0	101.0	103.7	98.2	0.99931	4.07
2	100.0	108.0	88.0	101.0	100.8	103.8	98.1	0.99911	3.98
3	90.0	88.0	114.0	111.0	93.4	100.4	100.7	0.99854	3.34
Mean	100.0	97.3	100.7	102.7	98.4	102.6	99.0	0.99899	3.80
SD	10.0	10.1	13.0	7.6	4.3	1.9	1.5	0.0004	0.40
CV%	10.0	10.3	12.9	7.4	4.4	1.9	1.5		10.5

Table 16. Precision, accuracy and linearity of the calibration curves

The table also reports the results of the accuracy of the calibration curve during the three days of the validation study. Mean accuracy values were between 97.3 and 102.7% and the precision, expressed as CV%, was in the range: 1.5-12.9%.

4.4.2.3. Precision, accuracy and LOQ

The LOD was defined as the concentration at which the signal-to-noise ratio was 3. The calculated LOD was 0.079 ng/mL.

Consistent with the prearranged aims, the LOQ of IDN 6140 was set at 10.0 ng/mL and validated through five replicates. As shown in table 17, the intra-day CV% and accuracy were respectively 4.9% and 92.0%.

Nominal conc. ng/mL	Mean observed conc. (ng/mL)	N	CV (%)	Accuracy (%)
10.0	9.2	5	4.9	92.0

Table 17. Limit of quantitation of IDN 6140 in mouse plasma

The reproducibility of the method was evaluated analyzing three replicates of three QC samples containing IDN 6140 at the nominal concentrations of 0.015 (QCL), 0.075 (QCM) and 1.500 µg/mL (QCH) in three different days using, each day, extracted standard curves made in the range 0.010-2.000 µg/mL. The intra- and inter-day precision and accuracy are reported in table 18.

	Day	QCs	Mean concentration observed (µg/mL)	CV %	% Accuracy
Intra-day	1	L	0.014	7.1	93.3
		M	0.078	9.1	104.0
		H	1.455	6.8	97.0
	2	L	0.014	4.1	93.3
		M	0.083	1.2	110.7
		H	1.440	3.4	96.0
	3	L	0.016	6.2	106.7
		M	0.068	4.5	90.7
		H	1.352	3.5	90.1
Inter-day	overall	L	0.015	8.1	98.5
		M	0.077	9.9	102.1
		H	1.415	5.4	94.4

Table 18. Summary of intra- and inter-assay precision and accuracy of the quantitation method of IDN 6140

The method was found to be precise and accurate, being CV≤ 9.9% and accuracy in the range of 90.1-110.7% for each tested concentration.

4.4.2.4. Stability

4.4.2.4.1. In frozen matrix

The stability of IDN 6140 was assessed by analyzing QC samples of frozen plasma at concentrations of 0.015, 0.075 and 1.500 μg/mL. The results obtained for the short term stability of the new taxane derivative, in frozen matrix, showed that it is stable over about one month in mice plasma at -20°C, the accuracy being in the range: 89.5-100.0% and the CV% between 0.6 and 12.3%.

4.4.2.4.2. Freeze/thaw stability

The freeze/thaw stability was defined by processing and analyzing in triplicate a standard sample - at the concentration of 0.100 μg/mL - fresh, and after the first, the second and the third freeze/thaw cycle. IDN 6140 was stable in mouse plasma over three freeze/thaw cycles as demonstrated by a CV% and the accuracy of 4.4 and 97.2 after the first, 3.5 and 100.3 after the second and 0.9% and 98.0% after the third cycle, respectively.

Considering the satisfactory results obtained during the validation, it was possible to conclude that the developed method for the quantitation of IDN 6140 was suitable to measure plasma concentrations of the new taxane. Therefore it was applied to study the preclinical pharmacokinetics of the compound in examination in mice.

4.4.3. Pharmacokinetic results: definition of the intravenous and oral pharmacokinetics of IDN 6140 and assessment of its bioavailability in CD1 mice

Figure 45 shows the pharmacokinetic profiles of IDN 6140 in plasma of CD1 female mice after i.v. or p.o. administration of 5.4 mg/kg of the taxane derivative (the concentration-time data are listed in appendix 7).

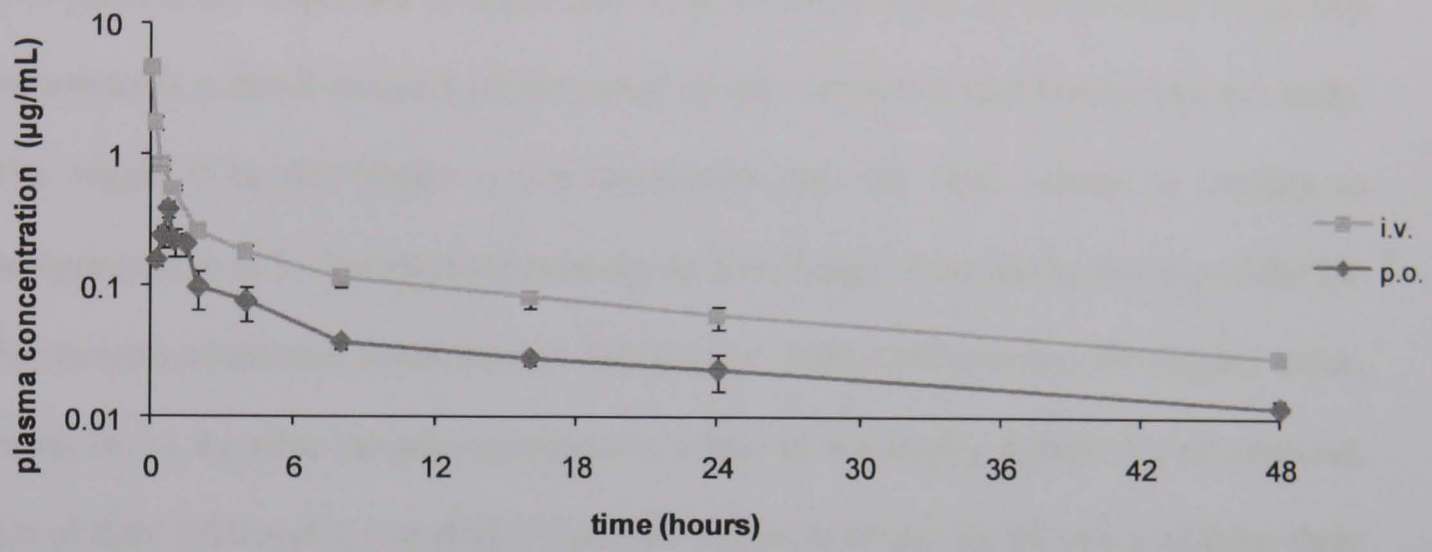

Figure 45. IDN 6140 plasma decay curves after an intravenous or p.o. administration of a dose of 5.4 mg/kg in CD1 female mice

Following the intravenous bolus, IDN 6140 disappeared from plasma according to a two compartment open model with a long terminal half-life of 21.8 h and a clearance of 0.8 L/h/kg (see table 19).

Treatment	C_{max} (µg/mL)	T_{max} (h)	$T_{1/2}$ (h)	AUC (µg/mL*h)	AUC_{inf} (µg/mL*h)	Cl (L/h/kg)	V_{bd} (L/kg)	F (%)
i.v.	4.7	0.08	21.8	5.6	6.5	0.8	26.1	
p.o.	0.4	0.75	26.0	1.7	2.1	/	/	33

Table 19. Main pharmacokinetic parameters of IDN 6140 after i.v. and oral administration of a dose of 5.4 mg/kg in female CD1 mice

After oral administration, the drug achieved a C_{max} of 0.38 μg/mL within 1 hour and then the plasma concentration declined with an elimination half-life of 26.0 h. The bioavailability (F) of the oral administration was 33%. IDN 6140 was still detectable up to 48 h at a concentration of 13.4 nM, 20-fold higher than that necessary to exert cytotoxic activity on human lung tumour cell line H460 (IC_{50}=0.49±0.03 nM, determined after 72 hours exposure).

It is particularly important to notice the value of the volume of distribution (V_{bd}): this parameter is a direct measure of the extent of the compound distribution into the body. The bigger it is, the higher is the distribution into the body, either by binding to components in or by partitioning extensively into tissues. Comparing the V_{bd} of the 14-functionalized taxanes considered in this project, IDN 6140 showed the biggest value, being 26.1 L/kg after the administration of a dose of 5.4 mg/kg, against 5.9 of ortataxel, 5.0 of IDN 5839 and 2.1 of IDN 5738, after a dose of 60 mg/kg for every of these three derivatives. This finding prompted me to investigate the distribution of IDN 6140 into tissues, also considering the good partition of ortataxel into organs [191].

4.4.4. IDN 6140 distribution into tissues

4.4.4.1. Brain

4.4.4.1.1. Method development

In figures 46 (panel C), the SRM chromatogram for IDN 6140 obtained in brain tissue was reported, showing the quantifier transition for an extracted mouse standard sample at LOQ, containing the compound at the concentration of 10 ng/mL and IS at 0.5 μg/mL in comparison with a chromatogram of a blank sample (panel A) and a blank sample with IS added (panel B).

Even from brain tissue, the elution of IDN 6140 and IDN 5738 (IS) was selective and at 6.8 and 6.6 minutes, respectively. As shown in panel A of the same figure, no interfering peaks were present at these retention times and the peaks of the analyte and IS were completely resolved from the brain matrix. With regard to mass spectrometer conditions, the same ones optimized for analysing IDN 6140 in plasma samples were used.

As a final example, panel D shows the SRM chromatograms of a mouse brain sample taken 2 hours after the intravenous treatment with IDN 6140. It corresponds to a concentration of 0.634 μg/sample of the analyte.

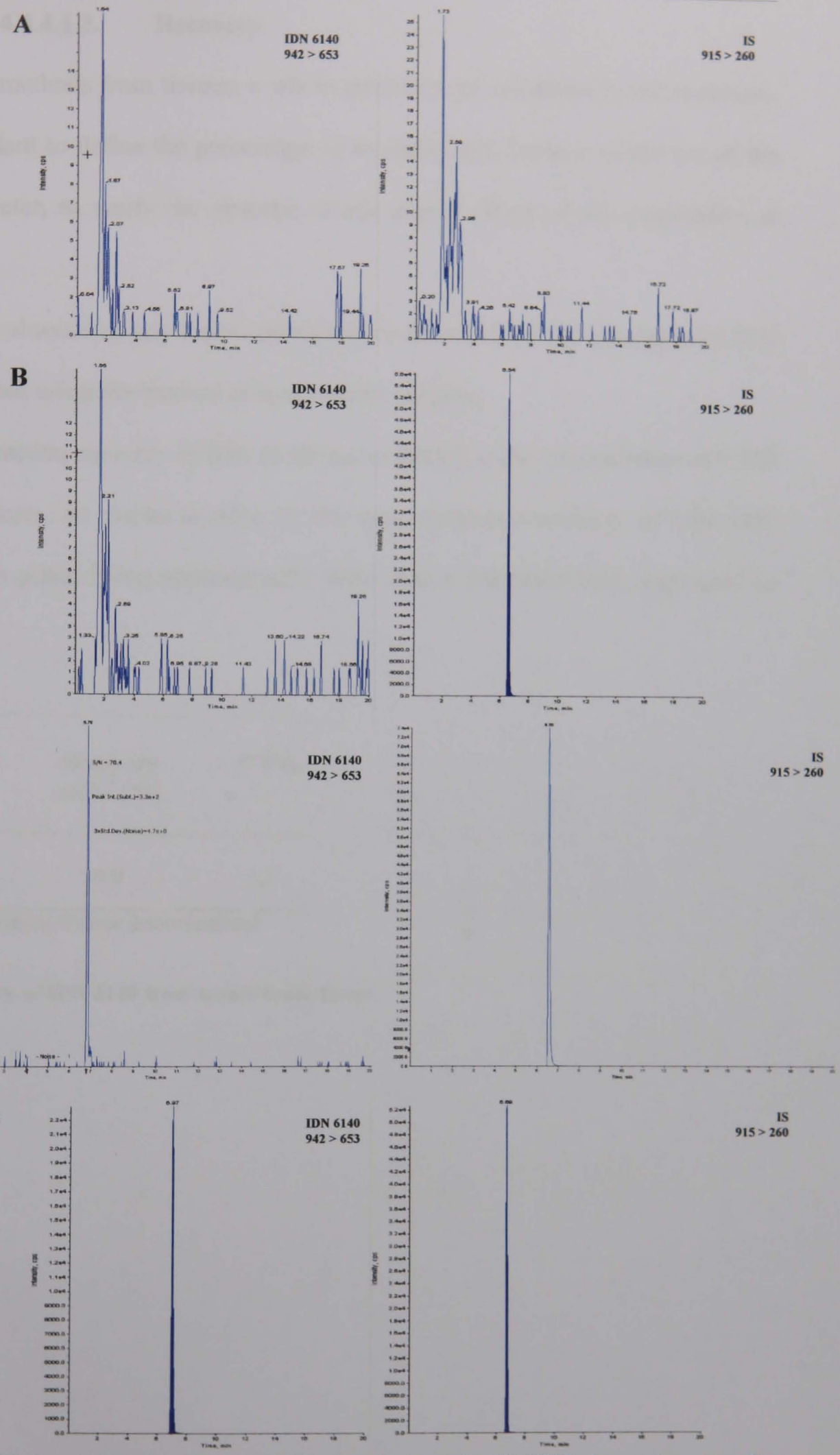

Figure 46. (A) SRM chromatograms of a mouse blank brain sample; (B) SRM chromatograms of a mouse blank sample with IS added; (C) Signal-to-noise ratio (70.4) of IDN 6140 at LOQ concentration (10 ng/mL); (D) SRM chromatograms of an extracted sample of a treated mouse. The measured concentration was 0.634 µg/sample

4.4.4.1.2. Recovery

For extraction methods from tissues, a whole procedure of validation is not necessary, but it is important to define the percentage of recovery and, because of the use of the mass spectrometer, to verify the absence of any matrix effect of ion suppression or enhancement.

First of all, the absence of any matrix effect that could influence the ionization of IDN 6140 was ensured using the method of post-column infusion.

Percentage extraction recovery of IDN 6140 was evaluated at the concentration of 0.100 µg/mL in triplicate. As shown in table 20, the mean extraction recovery of IDN 6140 from brain was good, being approximately 80% with a reproducibility, expressed as CV%, of 5.2.

Concentration (µg/mL)	**Recovery ratio* (%)**	**CV%**
0.100	79.9	5.2

*Each value is the mean of three determinations

Table 20. Recovery of IDN 6140 from mouse brain tissue

4.4.4.1.3. Distribution of IDN 6140 in mouse brain tissue

Figure 47 shows the distribution of IDN 6140 in brain tissue of CD1 female mice after i.v. and p.o. administration of 5.4 mg/kg of the compound (the concentration-time data are listed in appendix 8).

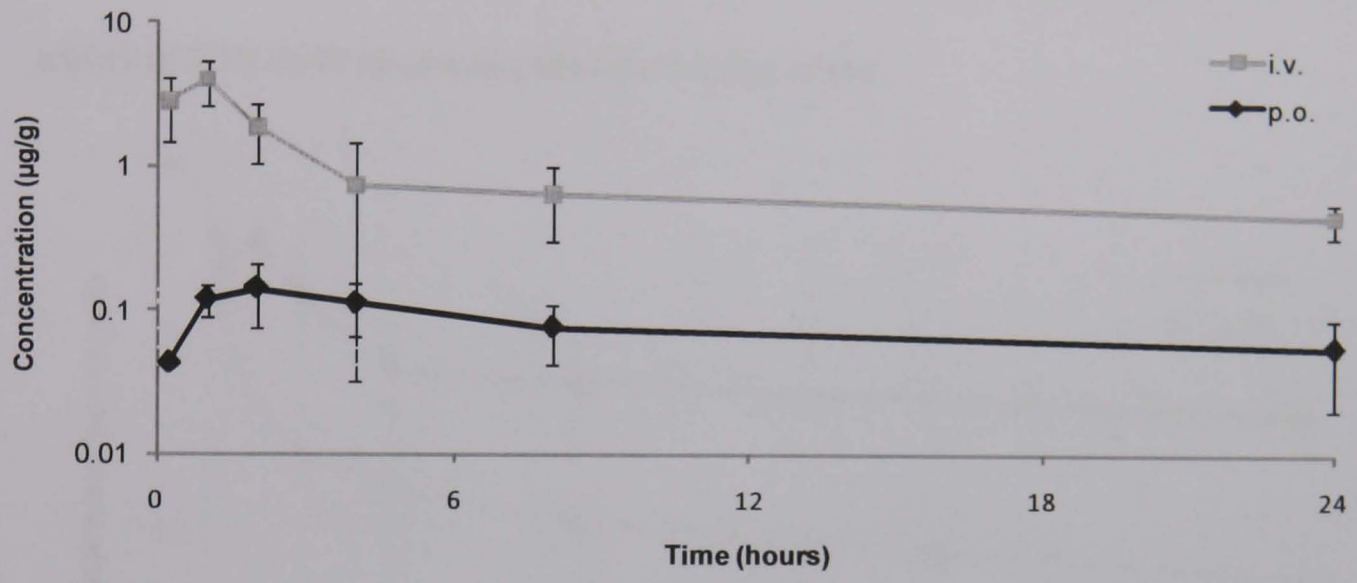

Figure 47. Brain concentration-time curves of IDN 6140 in mice after oral and i.v. administration of 5.4 mg/kg of the compound. Each point represents the mean obtained from four mice

Main pharmacokinetic parameters of IDN 6140 in brain tissue are shown in table 21. After oral and i.v. administration, IDN 6140 was rapidly, the T_{max} being ≤ 2 h, and well distributed in the brains of mice achieving a C_{max} of 0.14 and 4.00 µg/mL, respectively.

Treatment	C_{max} (µg/mL)	T_{max} (h)	$T_{1/2}$ (h)	AUC (µg/mL·h)	*Ratio AUC	*Ratio C_{max}
i.v.	4.00	1	30.3	20.5	3.7	0.8
p.o.	0.14	2	36.3	1.9	1.1	0.4

*brain/plasma

Table 21. Main pharmacokinetic parameters of IDN 6140 in brain tissue, after i.v. and oral administration of a dose of 5.4 mg/kg to female CD1 mice

The compound disappeared from brain with half-lives higher than those determined in the plasma compartment, 30.3 hours after i.v. and 36.3 hours after p.o. against 21.8 hours (after i.v) and 26 hours (after p.o.), indicating accumulation in brain tissue.

The ratio brain AUC/plasma AUC for IDN 6140 was 1.1 after oral and 3.7 after i.v. administration (table 21). This indicates a high distribution of the compound in this tissue in comparison with the plasma compartment (figure 48), reflecting the high ability of IDN 6140 of crossing the blood brain barrier.

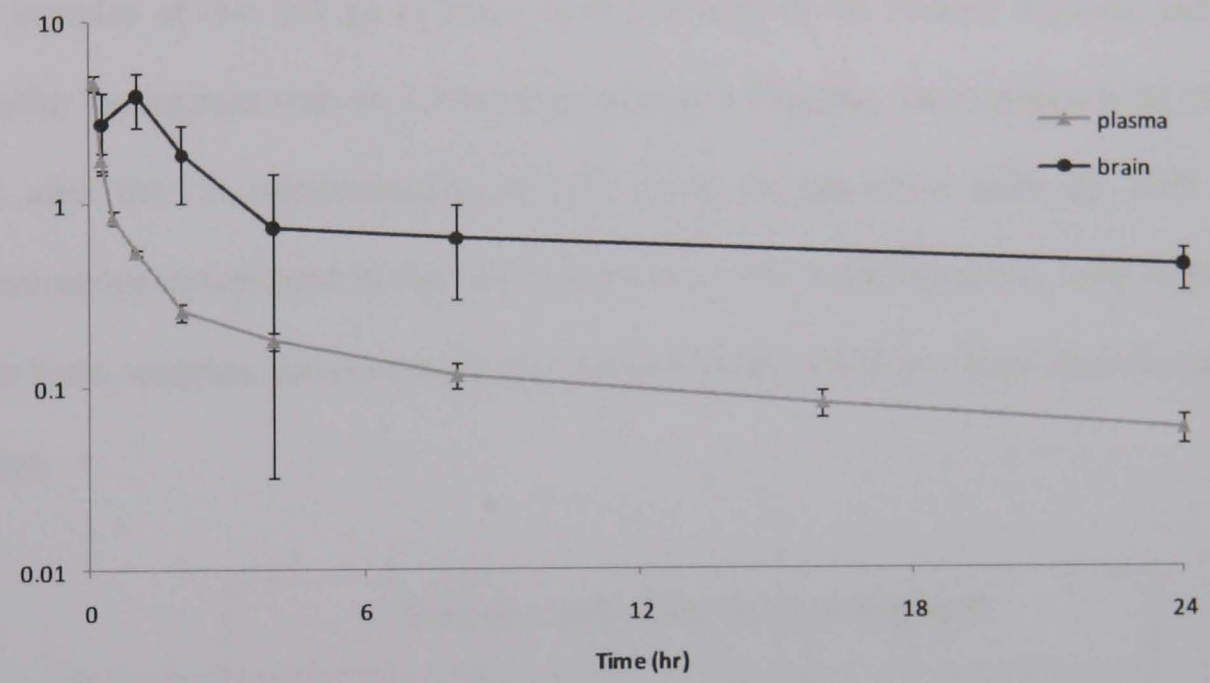

Figure 48. Plasma and brain concentration-time curves of IDN 6140 in mice after i.v. administration of 5.4 mg/kg of the compound. Each point represents the mean obtained from four mice

4.4.4.1.4. Tumour

Considering the encouraging results obtained on normal brain tissue, it was decided to verify the distribution of IDN 6140 in brain tumour tissue. CD1 xenografted nude mice were obtained, by a colleague of mine, inoculating intracranially U-87 MG human glioma cell line. The first step, to ensure a correct quantitation of IDN 6140, was to verify the complete healing up of the blood brain barrier (BBB) consequent to the injection of cells. Therefore, IDN 6140 concentrations were measured in plasma and brain samples of two groups of mice, with and without the tumour implant, treated 2 days after the implant with an intravenous dose of 5.4 mg/kg. The samples were taken 2 hours after the i.v. administration of IDN 6140. As shown in table 22, IDN 6140 concentrations determined in the two conditions were superimposable, both in plasma and in brain samples, demonstrating the integrity of the BBB two days after the tumour implant.

	Two days after the tumour implant					
Tumour implant	**Plasma (µg/mL)**	**mean**	**sd**	**Brain (µg/g)**	**mean**	**sd**
yes	0.095 0.069 0.063	0.076	0.017	1.128 0.860 0.997	0.995	0.134
no	0.080 0.077 0.059	0.072	0.011	1.172 1.146 1.032	1.117	0.074

Table 22. Plasma and brain levels of IDN 6140 in CD1 nude mice, with or without brain tumour implant, after single i.v. bolus of 5.4 mg/kg

To determine IDN 6140 distribution in tumour, two xenografted mice were treated intravenously with a dose of 7.0 mg/kg, 4 weeks after the tumour implant. The tumour was collected 2 hours after the treatment and IDN 6140 was measured both in tumour and in the remainder of the brain tissue. In one sample a concentration of 2.194 µg/g

was achieved in normal tissue against 24.583 in tumour and in the other one 1.510 μg/g in normal brain tissue against 96.000 in tumour. Even though this experiment was conducted just in two mice, there are no doubts about IDN 6140 ability of distributing in tumour achieving a concentration 10-40 fold higher than in the normal brain tissue. It is very important to note that this concentration is 2-9 fold higher than the one necessary to exert cytotoxic activity on U-87 MG *in vitro* (12 nM).

4.4.4.2. Liver

4.4.4.2.1. Method development

In order to understand if the high distribution of IDN 6140 was not limited to brain but also to other tissues, the relative distribution of this taxane derivative was evaluated in liver. The optimization of the extraction procedure from liver tissue was really time consuming because of a very important matrix effect during the MS/MS analysis: an almost complete suppression of IDN 6140 and IS signals was observed. Many organic solvents were tested and a method was developed characterized by the use of methanol/0.1% formic acid in acetonitrile 1:1 as extraction solvent and by a very long chromatographic run (41 minutes). As shown in figure 49, the matrix effect was completely knocked down: no interfering peaks were present on the chromatographic trace of blank sample (panel A) and the signal-to-noise ratio at the concentration of 10 ng/mL (LOQ) was 188.3 (C).

As final example, in panel D is reported the SRM chromatograms of a mouse liver sample taken 2 hours after the intravenous treatment with IDN 6140. It corresponds to a concentration of 1.124 μg/mL of the analyte.

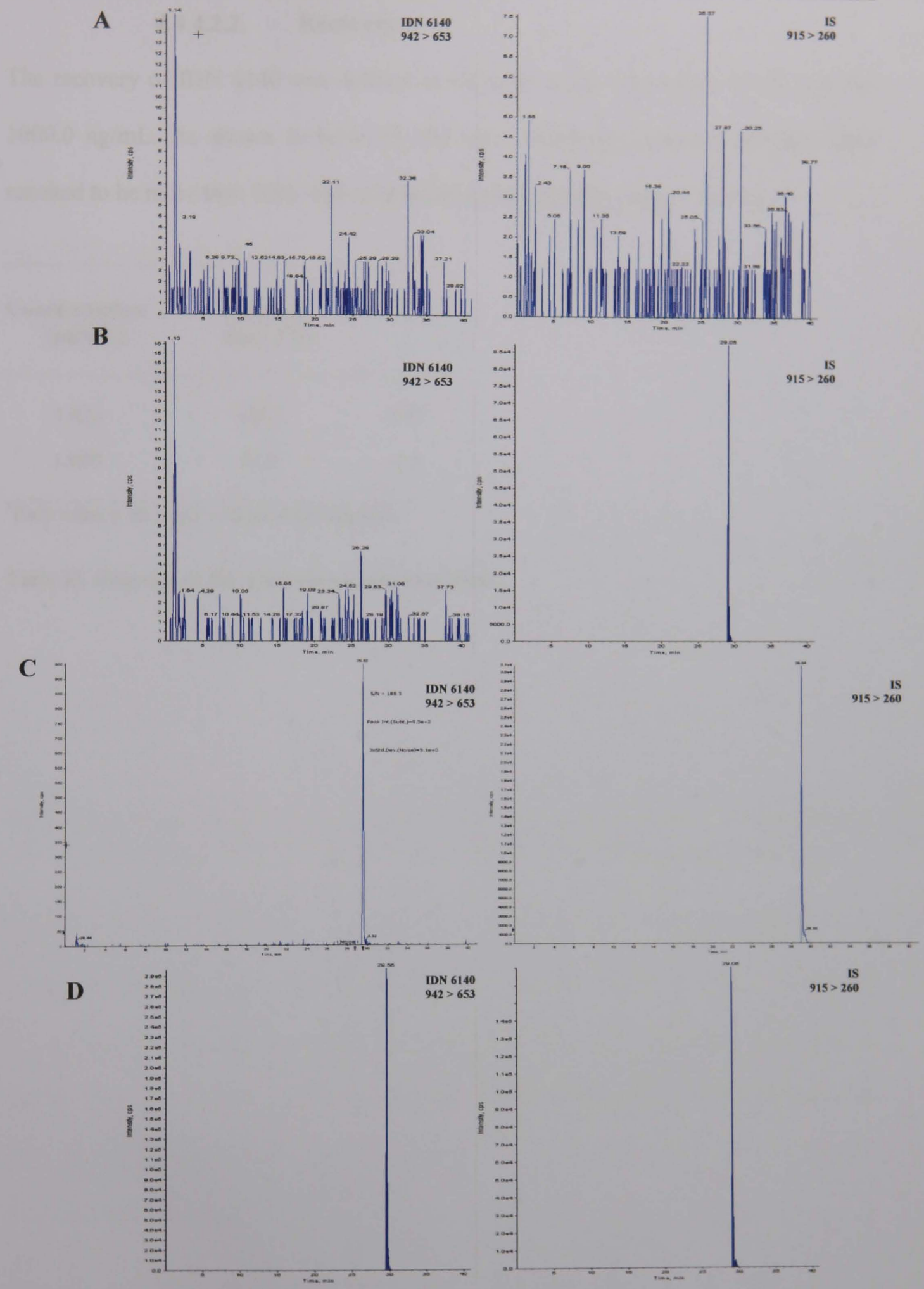

Figure 49. (A) SRM chromatograms of a mouse blank liver sample; (B) SRM chromatograms of a mouse blank sample with IS added; (C) Signal-to-noise ratio (188.3) of IDN 6140 at LOQ concentration (10 ng/mL); (D) SRM chromatograms of an extracted sample of a treated mouse showing IDN 6140 and IS. The measured concentration was 1.124 µg/mL [instrument used: API 4000 mass spectrometer]

4.4.4.2.2. Recovery

The recovery of IDN 6140 was defined in triplicate at the concentrations of 25.0 and 1000.0 ng/mL. As shown in table 23, the mean extraction recovery for IDN 6140 resulted to be more than 80% with acceptable reproducibility, being <15.0%.

Concentration (µg/mL)	Recovery ratio* (%)	CV%
0.025	103.2	14.9
1.000	82.9	4.1

*Each value is the mean of three determinations

Table 23. Recovery of IDN 6140 from mouse liver tissue

4.4.4.2.3. Distribution of IDN 6140 in mouse liver tissue

Figure 50 shows the distribution of IDN 6140 in liver tissue of CD1 female mice after i.v. and p.o. administration of 5.4 mg/kg of the compound (the concentration-time data are listed in appendix 9).

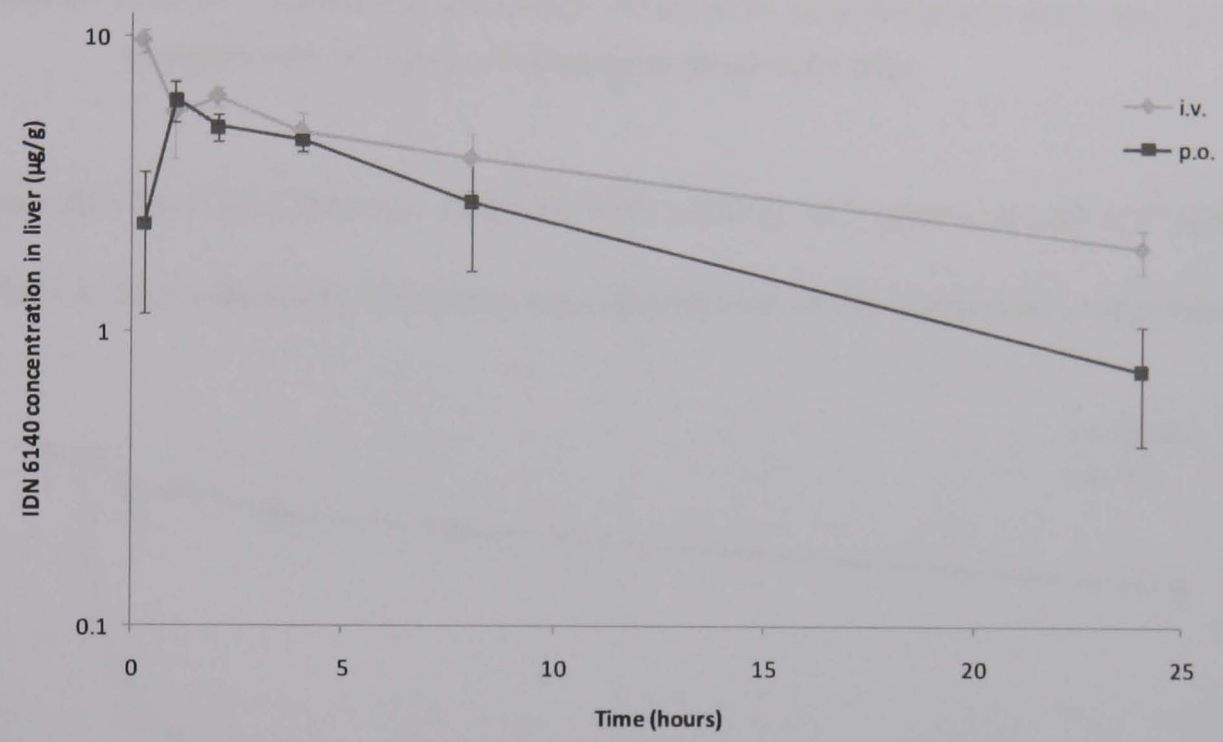

Figure 50. Liver concentration-time curves of IDN 6140 in mice after oral and i.v. administration of 5.4 mg/kg of the compound. Each point represents the mean obtained from four mice

As shown in table 24, after oral and i.v. administration, IDN 6140 was rapidly, the T_{max} being ≤ 1 h, and extensively distributed in the liver of mice achieving a C_{max} of 6.15 and 9.76 µg/mL, respectively. It is worth noticing that differently from plasma compartment and brain, in liver tissue the half life after oral treatment not only is shorter than the one after i.v. administration, but it resulted to be halved. This may be due to the first pass effect through the liver.

Treatment	C_{max} (µg/mL)	T_{max} (hr)	$T_{1/2}$ (hr)	AUC (µg/mL·h)	*Ratio AUC	*Ratio C_{max}
i.v.	9.76	0.25	16.0	89.0	15.9	2.1
p.o.	6.15	1	8.0	61.5	36.2	15.4

*liver/plasma

Table 24. Main pharmacokinetic parameters of IDN 6140, concerning liver tissue, after i.v. and oral administration of a dose of 5.4 mg/kg in female CD1 mice

The ratio liver AUC/plasma AUC for IDN 6140 is 36.2 after oral and 15.9 (figure 51) after i.v. administration, indicating high distribution of the compound in this tissue.

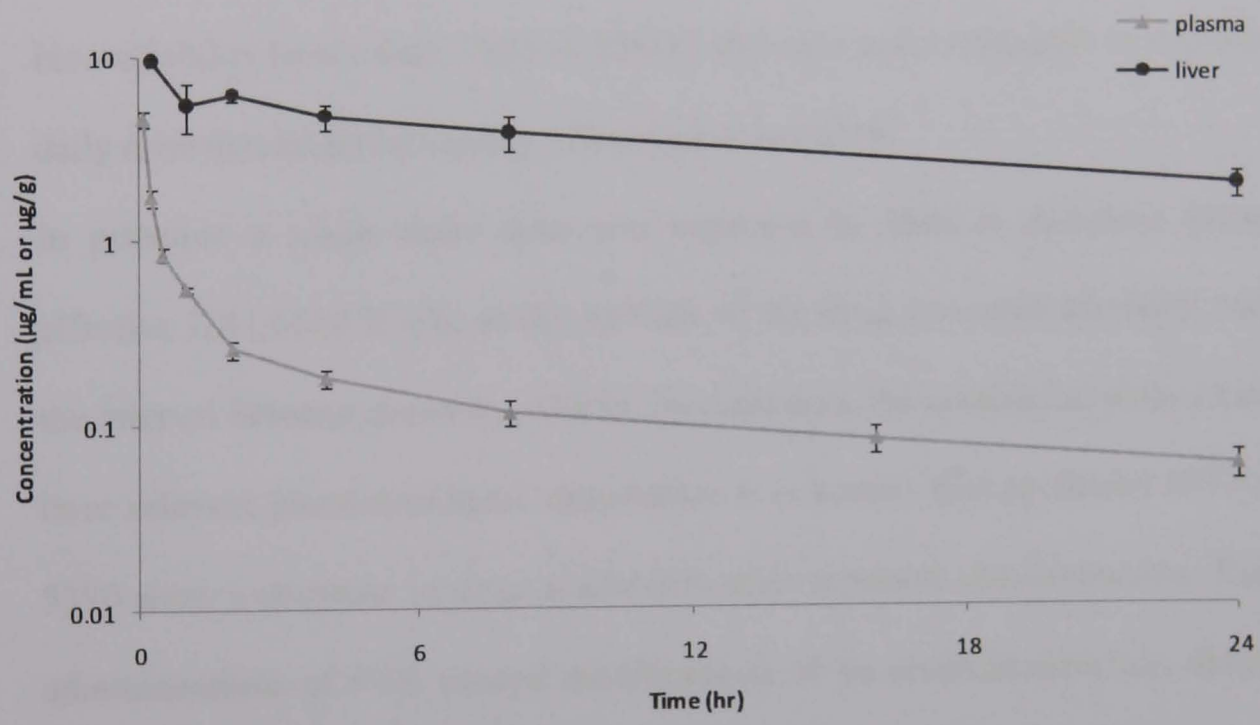

Figure 51. Plasma and liver concentration-time curves of IDN 6140 in mice after i.v. administration of 5.4 mg/kg of the compound. Each point represents the mean obtained from four mice

4.4.5. Pharmacokinetics of IDN 6140 after Oral Repeated Treatment

On the basis of the good distribution of IDN 6140 in brain tissue, obtained after both i.v. and p.o. administrations, it has been decided to define its activity in U-87 MG glioma tumour model.

A colleague of mine performed an intravenous treatment with a dose of 7 mg/kg administered once a week for three consecutive weeks. A significant reduction of the tumour mass was achieved increasing the life span of mice. Nevertheless, this schedule was associated with a high degree of toxicity (only three administrations were given instead of four because of the body weight loss of 20%). It was reasoned that the good bioavailability (more than 30%) of IDN 6140 could make it feasible to test repeated low daily dose that might be equally effective but less toxic.

In principle a single daily dose was expected be ideal to maintain therapeutically effective IDN 6140 levels, as the half-life of the drug was approximately equivalent to the interval between doses ($t_{1/2}$=26 h). Nevertheless, the continuous daily treatment may have relevant pharmacokinetic drawbacks: it is known that paclitaxel (PTX) and IDN 5390 show a decrease in drug availability after repeated administrations. Repeated i.v. administrations of PTX caused modifications of its pharmacokinetics, diminishing its plasma levels up to 96 hours after the last administration [188]. As regards IDN 5390, after prolonged daily oral doses given for two weeks, a decrease in drug bioavailability was found [187]. These literature data, reported for other taxanes, prompted an evaluation of whether prolonged oral daily treatment with IDN 6140 did not induce relevant pharmacokinetic changes. Mice were treated p.o. with a daily dose of 5.4 mg/kg for 10 days and on day 10, another group of mice was treated with a single oral dose of 5.4 mg/kg in order to compare the concentration plasma level after chronic and acute treatment. For both treatments, plasma was collected at 30 and 45 minutes and at 1, 2, 6

and 24 hours after the administration of IDN 6140 and this taxane derivative was determined by LC-MS/MS.

IDN 6140 C_{max} at 45 minutes was 91.3 ng/mL after a 10 days chronic treatment compared to 602.8 ng/mL after the acute one. The AUC value after the chronic treatment, 420.4 ng/mL*hr, was much lower than that found following the single dose administration, 1318.1 ng/mL*hr. These results clearly indicated that IDN 6140 exposure was decreased after repeated administrations. We can make two hypotheses to explain these findings after repeated oral treatment:

1- there could be a reduction of absorption of IDN 6140 or

2- an induction of IDN 6140 metabolism

In any case, the relevant observed pharmacokinetic changes prevented undertaking an evaluation of the antitumour activity of IDN 6140 given orally for a prolonged time.

4.4.6. Metabolism

4.4.6.1. *In vitro* metabolic profile

The *in vitro* metabolism of IDN 6140 was assessed using liver S9 fraction. Liver S9 fractions are subcellular fractions that contain drug-metabolizing enzymes including the cytochromes P450 and flavin monooxygenases. With this system, it is possible to evaluate even two phase II reactions, the conjugation with glucuronic acid and the sulfation.

After 2 hours incubation, only 10% of IDN 6140 was metabolized with the formation of 6 detectable metabolites (M1-M6). Two of them (M1 and M2), probably epimers, were related to the loss of the side chain in position 13, giving a derivative of baccatin III (figure 52) and four (M3-M6) were products of mono-hydroxylation reaction.

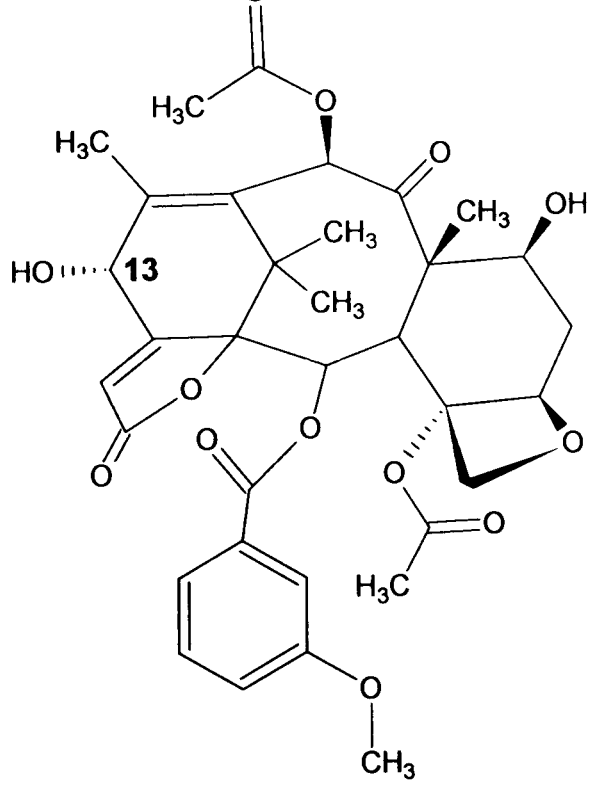

Figure 52. Hypothesized structure of IDN 6140 metabolites showing baccatin III related scaffold (M1 and M2)

Among the mono-hydroxylated metabolites, three (M3-M5) showed the modification in the side chain in position 13 and one (M6) on the benzoyl group in position 2. The hypothesized structure of M6 is reported in figure 53.

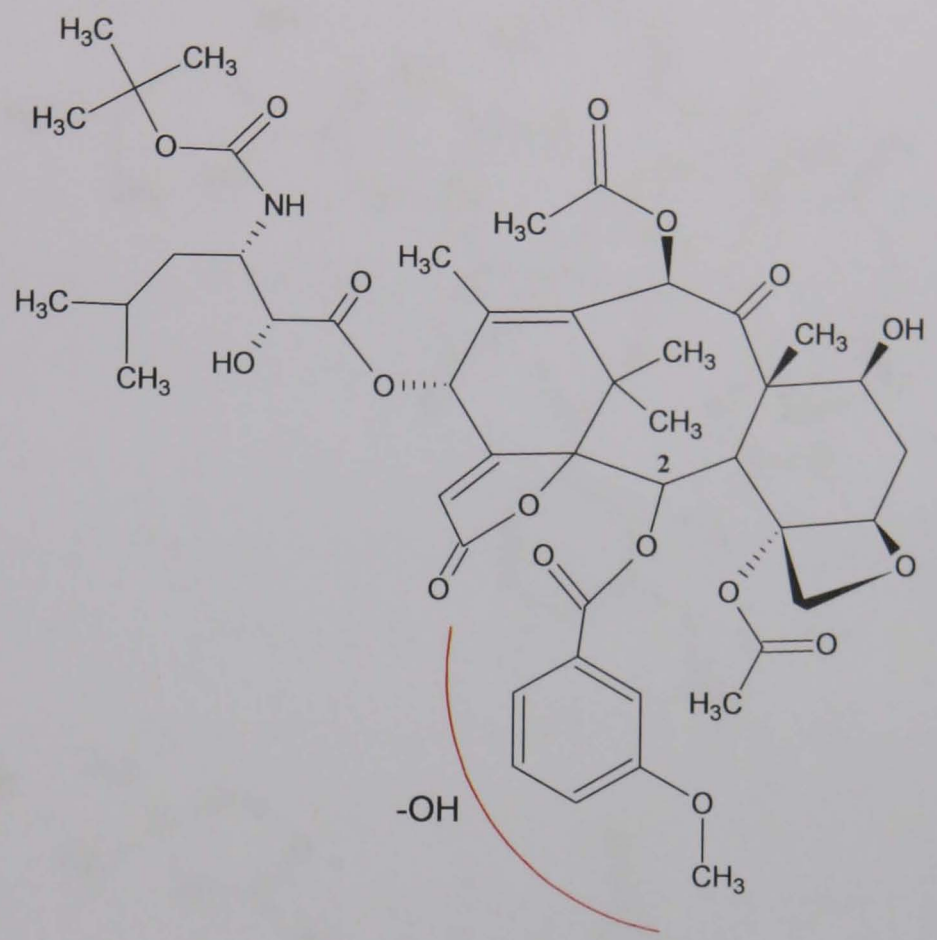

Figure 53. Hypothesized structure for the mono-hydroxylated metabolite of IDN 6140 (M6) on the benzoyl group in position 2

It was not provided the structure of M6 with the hydroxyl group in a specific position on the benzoyl group because, on the basis of ion trap mass spectrometer spectra, it was not possible to affirm it for a certainty and it was difficult to speculate on the favoured reaction site.

As regards the mono-hydroxylated derivatives on the side chain in position 13 (M3-M5), one of them (M3) may present the modification on the t-butyl group (figure 54, panel A) and the others (M4 and M5) on the isopropyl group (figure 54, panel B). Even in this case, probably the two peaks, characterized by the same *m/z* ratio and fragmentation pattern, are related to two epimers.

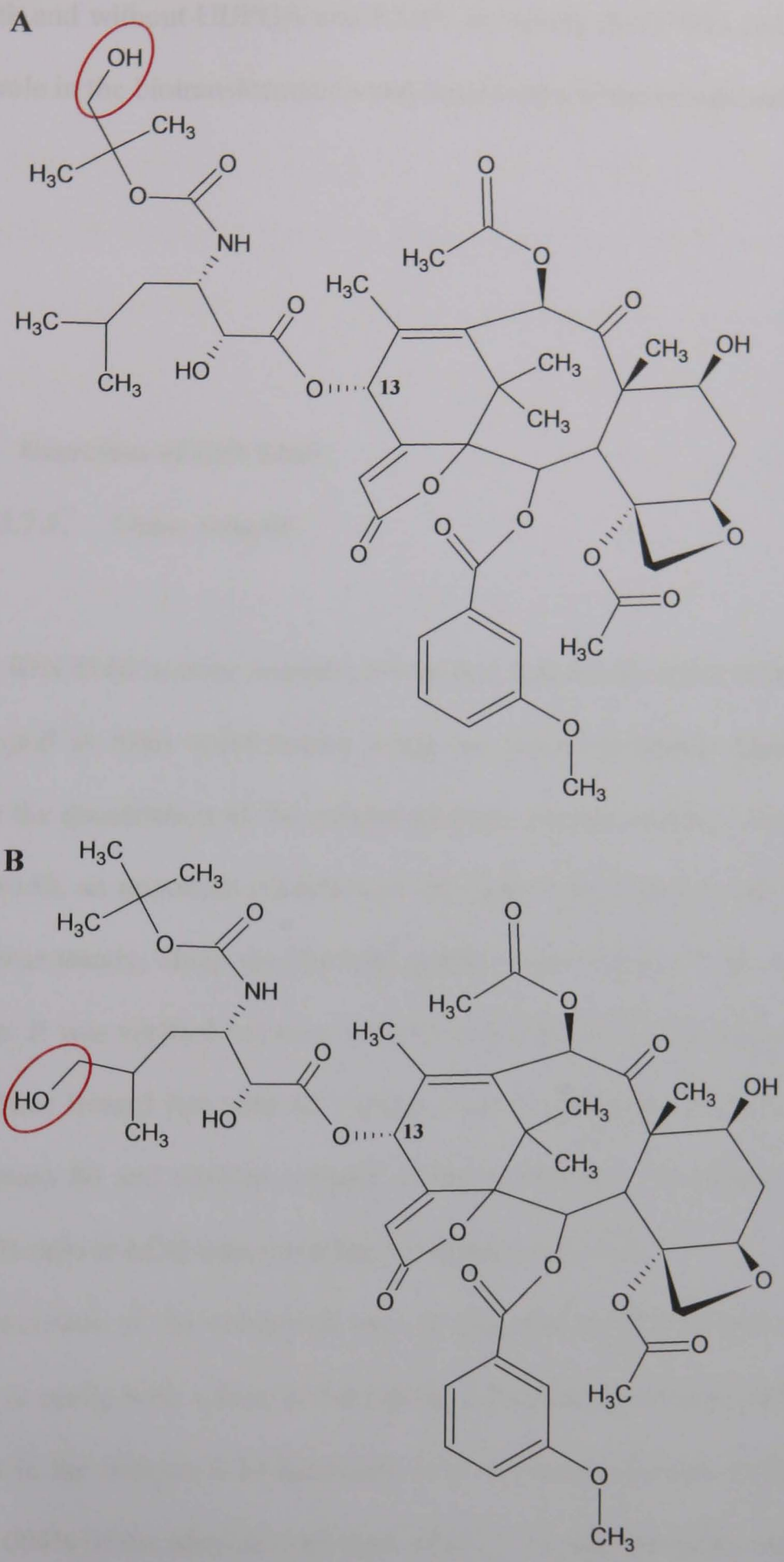

Figure 54. Hypothesized structure for monohydroxylated metabolites of IDN 6140 (M3-M5) on the side chain in position 13: M3 is shown in panel A and M4 and M5 in panel B

No dihydroxylated metabolites were present in the analysed samples. No differences were detectable in the concentrations of IDN 6140 and metabolites from the samples

incubated with and without UDPGA and PAPS, indicating that UGTs and sulfation do not play any role in the biotransformation and inactivation of the compound.

4.4.7. Excretion of IDN 6140

4.4.7.1. Urine samples

To determine IDN 6140 in urine samples, it was first defined the effect of this matrix on IDN 6140 signal at mass spectrometer using the same chromatographic conditions optimized for the quantitation of the compound from plasma samples. At the retention time of IDN 6140, an important reduction of the signal was observed, but the effect of urine matrix was steady, along the chromatographic trace, from 6.3 minutes up to the end of the run. It was verified not only the effect of a blank sample, but even of urine collected by mice treated just with the vehicle used to administer IDN 6140, that is a solution of tween 80 and absolute ethanol in the proportion 1:1 further diluted with saline. The S/N ratio at LOQ concentration (10 ng/mL) was 92.8.

The urinary excretion of the compound was investigated in CD1 female mice treated intravenously or orally with a dose of 5.4 mg/kg. After both treatments, IDN 6140 was detectable just in the fraction 0-24 hours and in a very small amount, corresponding to 0.009% and 0.006% of the administered dose, after i.v. or oral treatment, respectively.

4.4.7.2. Faeces samples

Even with this matrix, it was firstly defined its effect on IDN 6140 signal for the mass spectrometer using the same chromatographic conditions optimized for the quantitation of the compound in plasma samples. At the retention time of IDN 6140, a strong suppression of the signal was observed, but the effect of faeces matrix was constant, along the chromatographic trace, from 5 up to 7 minutes. It was verified the effect of faeces collected up to 24 hours, from mice treated just with the vehicle used to administer IDN 6140. The S/N ratio at LOQ concentration (10 ng/mL) was 10.1.

Because of the matrix effect, the recovery of IDN 6140 was defined comparing the peak area ratio of analyte/IS obtained from extracted faeces samples and faeces in which the same quantity of IDN 6140 was added after the entire procedure of extraction. The percentage extraction recovery of IDN 6140 was evaluated at the concentration of 0.100 μg/mL in triplicate. As shown in table 25, the mean recovery of IDN 6140 from faeces was good, being approximately 90% with a reproducibility, expressed as CV%, of 2.1.

Concentration (μg/mL)	Recovery ratio* (%)	CV%
0.100	90.6	2.1

*Each value is the mean of three determinations

Table 25. Recovery of IDN 6140 from mouse faeces

The faecal excretion of the compound was investigated in CD1 female mice treated intravenously or orally with a dose of 5.4 mg/kg. After both treatments, IDN 6140 was detectable both in the fractions 0-24 and 24-48 hours. As shown in table 26, the percentage excretion of IDN 6140 was very different between the two routes of administration, being 6.4 and 70.8% of the administered dose, after i.v. or oral treatment, respectively.

Dose/via (mg/kg)	Actual dose (mg)	0-24 h (% of dose)	24-48 h (% of dose)	Total dose recovered (%)
5.4 i.v.	0.523	4.14	2.23	6.37
5.4 p.o.	0.518	68.96	1.87	70.83

Table 26. Faecal excretion of IDN 6140 in female CD1 mice after i.v. and p.o. administration of a dose of 5.4 mg/kg

The very large excretion after oral treatment could be explained considering the bioavailability of IDN 6140, amounting to 33%. As IDN 6140 does not incur an extensive metabolism, it is possible to hypothesize that the amount not absorbed after oral administration, may be excreted in faeces as IDN 6140 *per se*.

The low excretion percentage obtained after the intravenous treatment, together with the high volume of body distribution determined (26.1 L/kg) and the long half-life, clearly suggests a wide partition of IDN 6140 into tissues in agreement with what observed in brain and liver.

CHAPTER 5

DISCUSSION

Taxol went into Phase I clinical trials in 1984 and already in 1982, Kingston's group had started to try to modify paclitaxel functional groups one at a time, to see whether they were individually necessary for the *in vitro* activity of the compound [193]. Many different changes have been made on taxane structure in order to try to improve cytotoxicity and chemical properties of paclitaxel. Kingston et al. summarized only some of chemical modifications introduced on paclitaxel structure (figure 55).

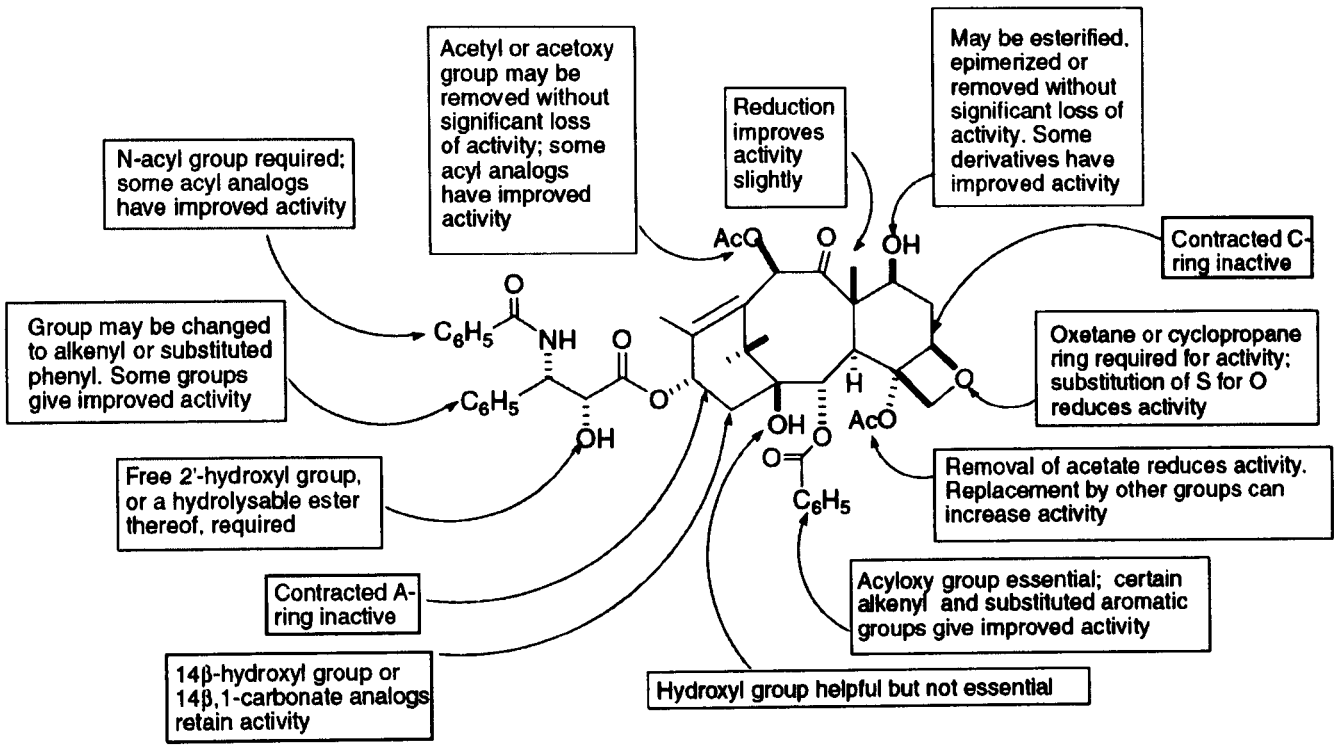

Figure 55. Structure-activity relationships of paclitaxel [Kingston 2007]

Among all the investigated changes, two of them - the C-ring opening through the cleavage of bond 7-8 and the introduction of a functional group in position 14 - led to the compounds studied in this thesis: IDN 5390, IDN 5614, IDN 5738, IDN 5839 and IDN 6140. The opening of C-ring led to C-seco paclitaxel analogues, IDN 5390 and IDN 5614, while IDN 5738, IDN 5839 and IDN 6140 have an introduction of a functional group in position 14.

As regards the considered C-seco derivatives, I demonstrated that both of them were characterized by extensive metabolism. Data collected after the reaction of IDN 5390 with human and murine microsomes suggested that there is a variation, both

quantitative and qualitative, in the metabolic profile across the two studied species. In the Safety Testing of Drug Metabolites issued in February 2008, FDA suggests the identification of differences in drug metabolism, between animals used in nonclinical safety assessments and humans, as early as possible, during the drug development process, because the discovery of disproportionate drug metabolites late in drug development can potentially cause development and marketing delays. In fact generally, metabolites identified only in human plasma or metabolites present at disproportionately higher levels in humans than in any of the animal test species should be considered for safety assessment. FDA recommends a safety concern for human metabolites, that are formed at greater than 10 percent of parent drug systemic exposure at steady state, because of the metabolites themselves may be toxic or pharmacologically active. In the case of IDN 5390 *in vitro* metabolism with human microsomes, it was found a monohydroxylated derivative of the compound amounted to 57% while it was only 20% after reaction with murine microsomes. Even if the system used did not refer to the steady state, it clearly indicated that IDN 5390 metabolic profile had to be carefully evaluated in case of further clinical development.

In order to evaluate metabolites safety, two approaches could be followed:

1- To identify an animal species that forms the metabolite at adequate exposure levels (equivalent or greater than the human exposure) and then investigate the drug toxicity in that species or

2- To synthesize the drug metabolite and directly administer it to the animal for further safety evaluation.

To assess the safety of the disproportionate drug metabolite, the studies that may need to be performed comprise: *general toxicity studies* - in which the toxicity of the drug metabolite should be investigated at multiples of the human exposure or at least at levels comparable to those measured in humans -; *genotoxicity studies*, *embryo-fetal*

development toxicity studies (when a drug is intended for use in a population that includes women of childbearing potential) and *carcinogenicity studies* (for drugs that are administered continuously for at least 6 months, or that are used intermittently in the treatment of chronic or recurrent conditions).

As concerned the toxicities possibly correlated to the administration of IDN 5390, besides the very important differences both qualitative and quantitative between the metabolic pattern obtained after human or mouse microsomes reaction, another point deserves to be considered. *In vivo* data concerning the fecal excretion of IDN 5390 in mouse showed that three metabolites amounted each to 8-15% of the total dose administered due to the biliary elimination as the predominant route of excretion, as already known for taxanes. Further characterization of these metabolites should be done because they may reflect potential localized bile duct toxicity and gastro-intestinal mucositis.

Besides the limited plasma disposition and the diminished pharmacological activity, another problem correlated to the extensive metabolism of this compound is referable to the individual genetic variation (polymorphism) that leads to a wide variability of metabolism across individuals [73, 97].

For all the reasons listed before, a careful characterization of the main IDN 5390 metabolites in terms of *in vitro* biological activity and toxicity would be advisable.

Considering the large extent of IDN 5390 metabolites and the difficulties in synthesizing them due to the presence of some stereogenic centres on the parent compound, the introduction of some modifications on IDN 5390 structure, in order to obtain a new derivative potentially less subject to the metabolism, seemed to be the best way to follow. Considering that many IDN 5390 metabolites were derived from the retro-cyclization reaction, forming C-ring, the protection of the involved positions, 7 and 9, seemed to be sufficient to assure the decrease of the metabolism. Following this

address, IDN 5614 was synthesized by the methylation of positions 7 and 9 of IDN 5390 structure. The followed line seemed to lead to a compound that potentially showed two advantages: the decrease of metabolic clearance and the preservation of the antioangiogenic properties of IDN 5390.

All taxanes show antiangiogenic properties through their ability in inhibiting of endothelial cell motility. In fact, the motility of endothelial cells is a crucial event in the process of angiogenesis, the complex formation of a new, functional vascular network, necessary for tumour and metastasis growth [194]. In this view, IDN 5390 appeared to be a particular taxane because of its antiangiogenic properties compared to a weak cytotoxicity, rendering this taxane a cytostatic compound rather than a cytotoxic one [195]. Comparing IDN 5390 structure to that of paclitaxel and docetaxel, the main difference is in the C-ring and for this reason, it may be that the integrity of C-ring is fundamental to maximize the cytotoxic activity but not to exert the antiangiogenic one.

In fact, it is already known that the ability of paclitaxel to inhibit cell motility occurs at low concentrations and is unrelated to its anti-proliferative activity [196]. This is consistent with an antiangiogenic activity of taxanes at subcytotoxic concentrations.

Unfortunately, the *in vitro* definition of IDN 5614 metabolism, showed that the chemical modifications introduced on IDN 5390 structure were not able to prevent the formation of the C-ring - having found IDN 5390 as an IDN 5614 metabolite - convincing me of not studying further the pharmacokinetic profile of IDN 5614.

Consequently on my results, it was decided to tentatively define the cytotoxicity of IDN 5390 metabolites formed after the incubation with liver microsomes. Therefore, a colleague of mine compared the cytotoxicity of IDN 5390, before and after incubation with mouse microsomes, on human ovarian cancer cell line (A2780) [187]. Many different IDN 5390 concentrations, in the range 0 to 800 nM, were incubated with microsomes and, after 4 hours, a small amount of the incubation mixtures was added to the cells

obtaining final theoretical IDN 5390 concentrations in the range 0 to 80 nM. After 72 hours of exposure, the cytotoxicity of the incubation mixture was approximately 10-fold higher than IDN 5390 *per se* demonstrating the high activity of the metabolites formed during the reaction with mouse liver microsomes.

Among the different metabolites tentatively characterized, the one obtained just from the formation of the bond between the positions 7 and 8 appeared to be the most interesting one, as a cytotoxic agent, because it showed the same tetracyclic core of paclitaxel. Indena S.p.A. synthesized this metabolite, obtaining IDN 5910. They successively compared the cytotoxicity of this new derivative to IDN 5390 one on a human mammary carcinoma, sensitive and resistant cell line (MCF-7 and MCF-7/R) and on a human lung tumour cell line (H460) (table 27).

compound	cell line			
	MCF-7	MCF-7/R	RI	H460
	IC_{50} (nM ± SE)			IC_{50} (nM ± SE)
IDN 5390	11.2 ± 0.8	1044 ± 93	93	29 ± 7
IDN 5910	1.1 ± 0.1	97 ± 11	88	1.7 ± 0.5

Cell lines: MCF-7/R, subline with acquired resistance to doxorubicin and collateral resistance to paclitaxel and docetaxel
RI: IC_{50} resistant cell line/IC_{50} sensitive line

Table 27. Cytotoxic potency of IDN 5910 compared to IDN 5390

After 72 hours of exposure, IDN 5910 cytotoxicity was at least 10-fold higher than IDN 5390 one on all the tested cell lines. These results confirmed once more the connection between the integrity of C-ring and the cytotoxic activity of taxane derivatives.

The importance of this metabolite is highlighted by the fact that I found it as one of the major circulating metabolites in plasma of mice treated with IDN 5390. In fact, it was demonstrated by LC-MS/MS analysis, that the metabolite obtained by the retro-cyclization of C-ring and formed *in vitro* showed the same structure of that one found *in*

vivo. Therefore, it probably plays an important role in the pharmacological effect of IDN 5390.

With regard to the 14-functionalized derivatives, three different compounds - IDN 5738, IDN 5839 and IDN 6140 - were considered. The last one was obtained by a further structural modification on IDN 5839 structure.

I firstly characterized the pharmacokinetic profile of IDN 5738 and IDN 5839. On the basis of both *in vitro* and *in vivo* experiments, even though the considered compounds were only two, some structural-activity considerations could be tentatively drawn. The high bioavailability of the two taxanes supports the fact that they are not pumped out of the cells by P-gp and this evidence is in line with the cytotoxic data obtained on human breast tumour cell lines sensitive (LCC6) and resistant cell sub-lines (LCC6-MDR) [178]. In fact, on LCC6-MDR lines, characterized by the overexpression of P-gp, IDN 5738 and IDN 5839 were more toxic than paclitaxel and docetaxel with lower resistance index of 8 and 6 respectively, in comparison with those of the two parent drugs of 111 and 92, confirming the ability of the 14-modified taxanes to overcome multi-drug resistance effect, as was demonstrated for ortataxel [180]. However, a 1,14 carbonyl bridge may be essential for a good cytotoxicity against multi-drug resistant cell lines as ortataxel and IDN 5839 are more cytotoxic than IDN 5738 that lacks this group [179]. The replacement of 14-oxygen with a methylidene group seems to be not significant for the cytotoxicity and the oral absorption being 48.0% and 56.1%, the bioavailability of ortataxel and IDN 5839, respectively. In contrast, as seen for IDN 5738, the introduction of an azido group in 14 seems to negatively modulate the potency of the product, whilst acquiring a very interesting resistance index and maintaining a very good oral absorption (F = 53%).

These findings suggested that the further modification in the positions 1,14 of the baccatin ring gave rise to a series of new compounds which maintain the relevant features of the parent compound: ortataxel.

Taking the pharmacokinetic profile of these new derivatives into consideration, it is possible to observe that they were rapidly absorbed (within 1 h) with bioavailability higher than 50% and plasma concentrations that are consistent with those shown to be active in cytotoxic studies on two human breast cancer cell lines sensitive (MCF7 and LCC6) and resistant (cell sub-lines: MCF7-R and LCC6-MDR) to paclitaxel. These concentrations were maintained in plasma of mice up to at least 16 and 10 hours after the administrations of IDN 5738 and IDN 5839, respectively.

In summary, my data defined for these compounds a favourable pharmacokinetic profile, nevertheless superimposable with that of ortataxel against a halved half-life and a comparable cytotoxic activity on the sensitive and resistant LCC6 and MCF-7 cell lines, rendering IDN 5738 and IDN 5839 little interesting for further development.

Successively, Indena S.p.A. went on with the synthesis and screening of new taxane derivatives structurally optimized on the basis of the findings related to IDN 5738 and IDN 5839 and they succeeded in getting IDN 6140. This new taxane derivative was obtained by the introduction of a methoxy meta-substituent on the 2-benzoate of taxane scaffold of IDN 5839 structure. The interest for IDN 6140 was based on a well known and reported characteristic of paclitaxel chemistry. The meta derivatives, and in particular methoxy derivatives, were much more cytotoxic than paclitaxel, thanks to the "*meta*-effect" that is the enhanced interaction between the C-2 ring and asp224 in the β-tubulin binding pocket [181, 182].

This new ortataxel derivative showed a very good cytotoxic activity on a human lung cancer cell line (H460), superior not only to paclitaxel and ortataxel, but even to IDN 5738 and IDN 5839.

The defined pharmacokinetic profile of IDN 6140 was very different from that of the other derivatives. In fact it showed, besides a sufficiently good bioavailability (33%), at 48 hours after the administration, concentrations 20-fold higher than the IC_{50} determined on H460 cell line as the outcome of a very long elimination half-life (22 and 26 hours after i.v. and p.o. treatment, respectively). Nevertheless, the most interesting feature of this new derivative consisted in its large volume of distribution. This parameter is a direct measure of the extent of drug distribution into the body and being at least 4-fold higher for IDN 6140 than one of the other 14-functionalized derivatives, it was decided to investigate the distribution of IDN 6140 into tissues. Knowing the feature of ortataxel to cross the Blood Brain Barrier (BBB) [174], IDN 6140 distribution was defined in brain tissue. Table 28 summarizes the pharmacokinetic parameters related to the brain distribution of IDN 6140 in comparison with the ones of paclitaxel and ortataxel [174]. The ratio between brain and plasma AUC of IDN 6140 was 20 and 292-fold higher than ortataxel and paclitaxel one respectively, indicating the very good ability of IDN 6140 to cross the BBB.

Parameter	**paclitaxel**	**ortataxel**	**IDN 6140**
i.v. dose (mg/kg)	54	90	5.4
Plasma AUC 0-6 hours (μg/mL * h)	116.6	36	*3.2
Brain AUC 0-6 hours (μg/mL * h)	1.4	6.3	*11.2
R	**0.012**	**0.175**	**3.5**
T/2 α (min)	35	8	5
T/2 β (hr)	1.0	2.1	21.8

*AUC 0-8 hours

R: ratio between brain and plasma AUC

T/2 α: plasma distribution half-life

T/2 β: plasma elimination half-life

Table 28. Comparison between the brain distribution of paclitaxel, ortataxel and IDN 6140

At Mario Negri Institute and at National Tumor Institute the cytotoxicity of IDN 6140 on two human glioma cell lines, U-87 MG and GBM (data not shown) was tested. On both the cell lines, IDN 6140 was as potent as ortataxel and slightly more potent than paclitaxel against both the cell lines [174].

As already mentioned, it may be inferred from the presence of P-gp in brain capillaries that this drug efflux pump is a factor in limiting the penetration of certain agents into brain tumours. However, by contrast with normal brain capillaries which constitute the BBB, brain tumour capillaries are compromised or "leaky", and the extent to which P-gp expression in brain tumours neovasculature retains its capacity to limit drug penetration had seemed to be reduced. Gallo et al. demonstrated that even in the neovasculature of brain tumours, P-gp has the facility to limit paclitaxel penetration, although somewhat less so than in normal brain [137]. That renders particularly important the distribution of IDN 6140 in normal brain tissue but even more in tumour brain tissue. The tumour brain distribution of IDN 6140 was defined in CD1 xenografted nude mice - obtained inoculating intracranially U-87 MG cell line - treated intravenously with the taxane derivative. Even though this experiment was conducted just in two mice, there are no doubts about the ability of distributing in tumour and the potentially activity of IDN 6140. In fact, in comparison with its concentration in normal brain tissue, it achieved a concentration 10-40 fold higher in tumour and this concentration was 2-9 fold higher than the one necessary to exert cytotoxic activity on U-87 MG *in vitro* (12 nM).

In parallel, IDN 6140 concentrations were determined also in a glioblastoma cell line (GBM), in order to define the uptake in this cells showing an IC_{50} around 17 nM. Knowing that a mean diameter of a GBM cell is around 24 μm, we found an IDN 6140 intracellular concentration of 1.2 mM after one hour treatment with a 10 μM solution of the compound. This information suggests that there is a high cellular uptake of IDN

6140. Taking all these results together, they prompted us to define IDN 6140 *in vivo* activity to verify if its ability to cross the BBB could be translated into efficacy against brain tumours. A colleague of mine performed an evaluation of IDN 6140 antitumour activity against two orthotopically growing human glioma, U-87 MG and GBM, in nude mice. On U-87 MG tumour model, paclitaxel (PTX), used as reference drug, was given intravenously at the dose of 54 mg/kg four times every fourth day and IDN 6140 was administered i.v. according to two different schedules: 5.4 mg/kg four times every fourth day and 7 mg/kg four times every seven days [197]. To define the ability of IDN 6140 to affect the growth of intracranial tumours, the following parameters were considered: the *efficacy* expressed as increment of life span (ILS%) - calculated as: (T-C)/C where T and C were the median survival time of treated and control groups, respectively -, the *tumour growth* monitored by Magnetic Resonance Imaging and the mouse *body weight* recorded to evaluate the compound toxicity. The schedule of treatment with the dose of 7 mg/kg was interrupted (three administrations were given instead of four) due to the observed toxicity in mice (body weight loss of 20%). As shown in figure 56, even if IDN 6140 was effective in increasing the survival of mice ($P < 0.015$ and 0.0001) bearing U-87 MG tumour, the ILS (35%) did not reach the conventional limit defining the antitumour activity (40%).

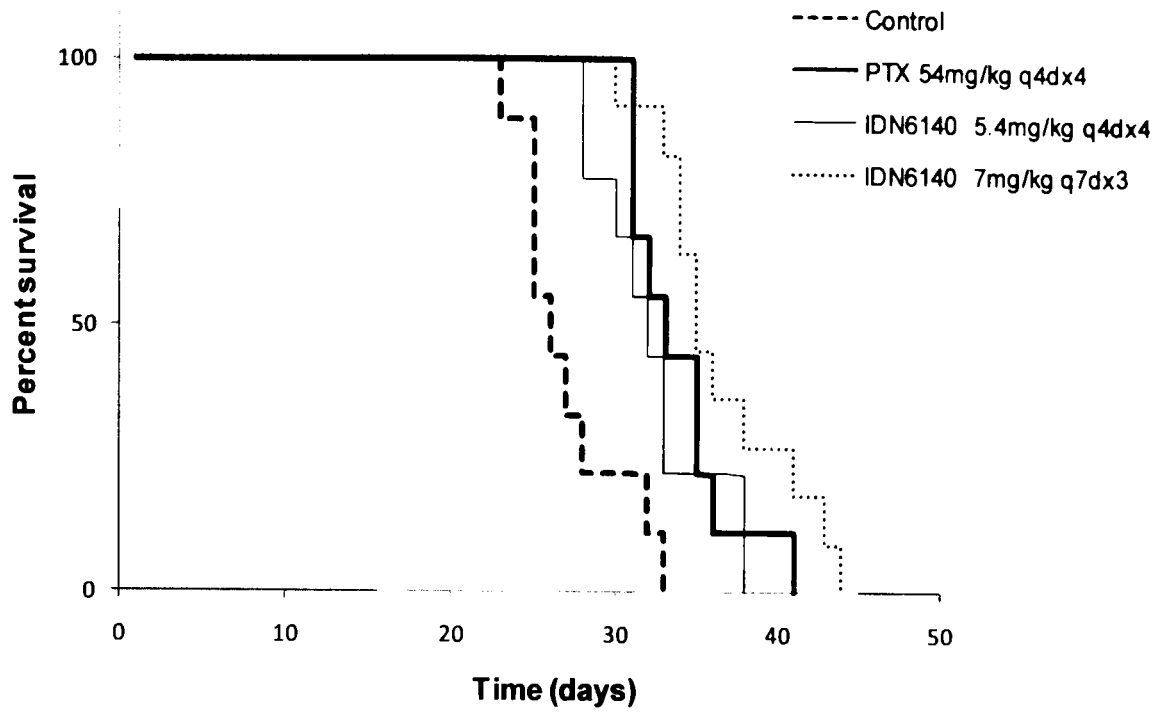

- ILS%: 27 for PTX, 23 and 35 for IDN 6140 after the doses of 5.4 and 7.0 mg/Kg respectively;
- P<0.002 for PTX vs control, 0.015 and <0.0001 for IDN 6140 (vs control) and 0.036 for IDN 6140 at 7.0 mg/Kg vs IDN6140 at 5.4 mg/Kg

Figure 56. Survival curves obtained testing different schedules in mice transplanted with U-87 MG tumour cells

In figure 57, images obtained by magnetic resonance are reported and they clearly indicate a significant reduction of the tumour mass in mice treated with IDN 6140.

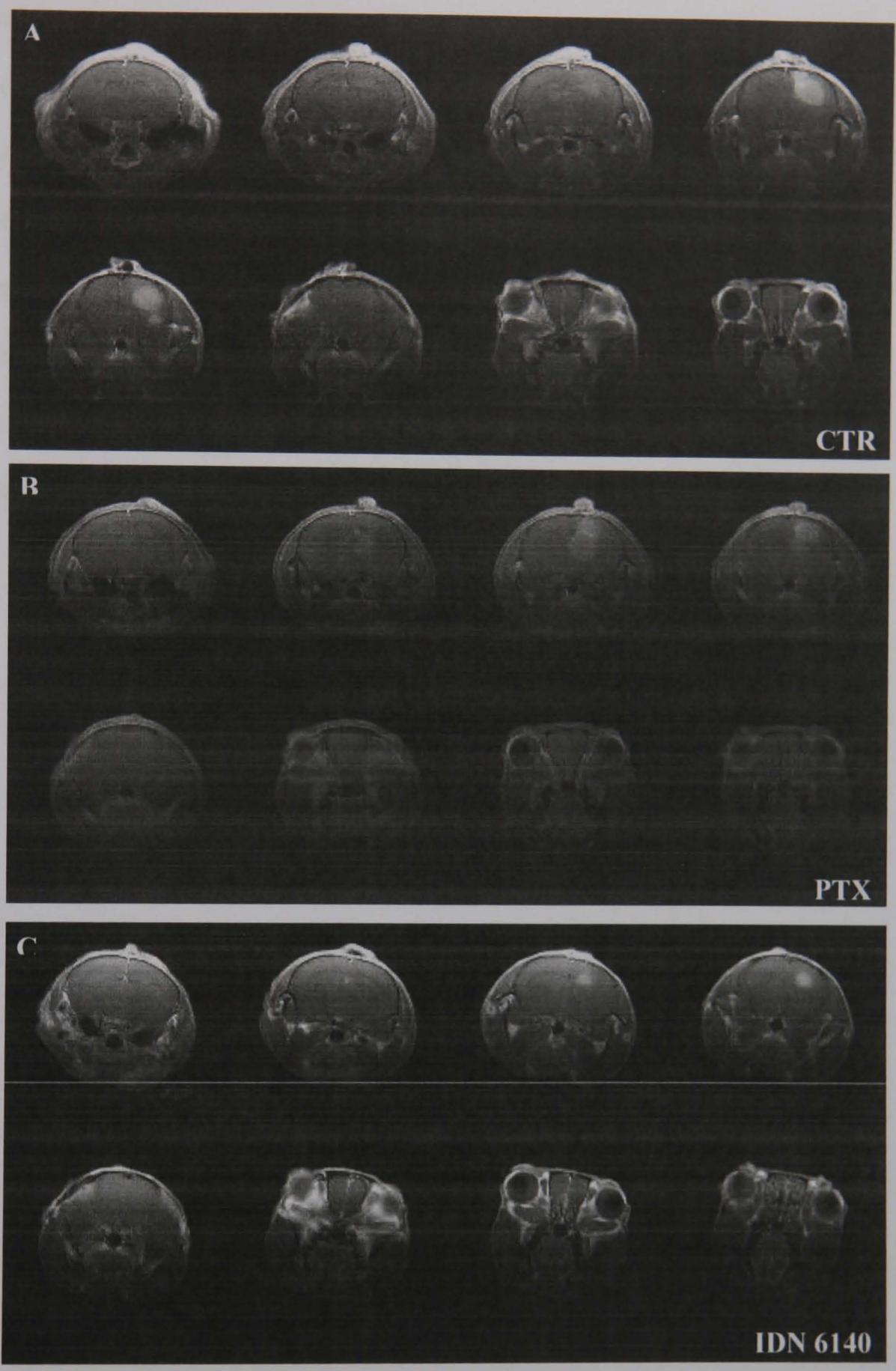

Different coronal RARE T1w images after Gd-DTPA contrast agent i.p. injection; bright areas show the tumor region. The three different panels refer respectively to a control mouse, PTX treated mouse and IDN 6140 treated mouse. Images have been acquired by a 7T Bruker Biospec 70/30 with the following parameters: repetition time, 700 ms; echo time, 9.2 ms; FOV 2x2 cm^2; slice thickness, 1 mm; 256x256 data matrix.

Figure 57. Magnetic resonance images of brain of human glioma (U-87 MG) bearing mice untreated (panel A), treated with paclitaxel (panel B) and with IDN 6140 (panel C)

A similar experiment was performed in human glioma tumour (GBM) bearing mice treated with IDN 6140 at the dose of 4 mg/kg given every week for six times. This different schedule was chosen in order to diminish the dose of administration, avoiding toxicities, and to treat the animals for a longer period. In this experiment, the chosen reference was ortataxel. Even in this orthotopic tumour model, characterized by a slower rate of growth, the increment of survival time (ILS=30%) was not sufficient to gain antitumour activity of IDN 6140 (figure 58), but the reduction of tumour volume was appreciable 69 days post inoculum (figure 59).

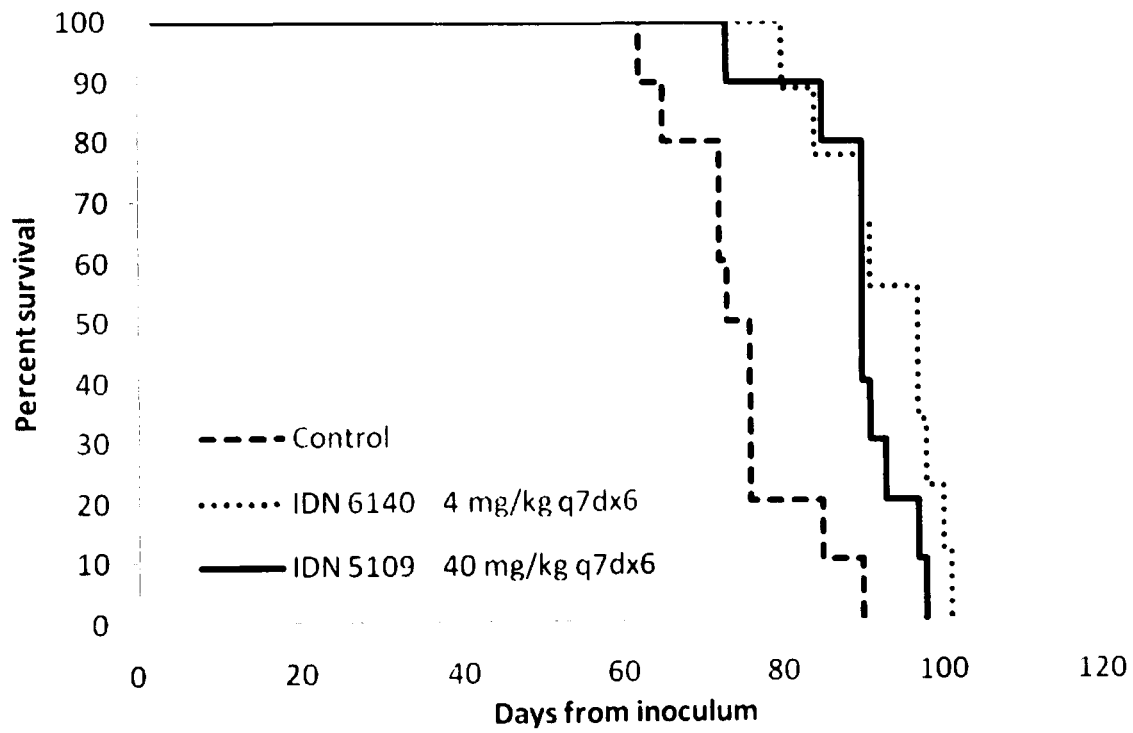

- ILS%: 21 for ortataxel (IDN 5109) and 30 for IDN 6140;
- P<0.0006 for ortataxel (IDN 5109) vs control, 0.0003 for IDN 6140 vs control

Figure 58. Survival curves obtained testing different schedules in mice transplanted with GBM tumour cells

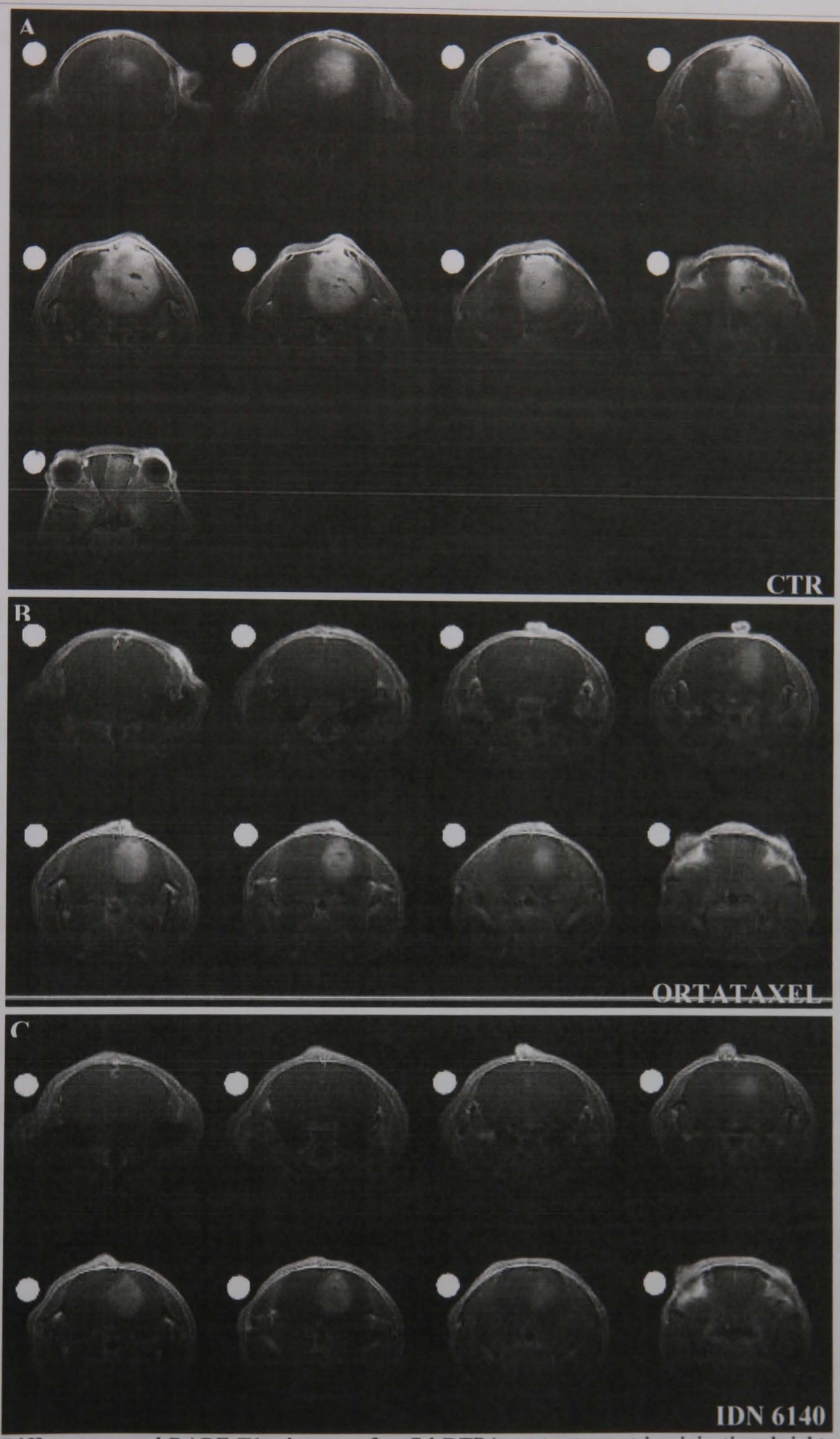

Different coronal RARE T1w images after Gd-DTPA contrast agent i.v. injection; bright areas show the tumor region. The three different panels refer respectively to a control mouse, ortataxel treated mouse and IDN 6140 treated mouse. Images have been acquired by a 7T Bruker Biospec 70/30 with the following parameters: repetition time, 700 ms; echo time, 9.2 ms; FOV 2x2 cm^2; slice thickness, 1 mm; 256x256 data matrix.

Figure 59. Magnetic resonance images of brain of human glioma (GBM) bearing mice untreated (panel A), treated with ortataxel (panel B) and with IDN 6140 (panel C)

Summarizing all the data concerning IDN 6140, it was found:

- kinetics characterized by a very long half-life;
- good distribution both in normal and tumour brain tissue;
- good cytotoxic activity on human glioma cell lines, U-87 MG and GBM;
- considerable reduction in tumour volume;
- increasing in life span of treated mice not too far from the limit established for defining antitumour activity;
- toxicity observed in mice with all the doses and schedules tested, even if with lower doses it was possible to treat the animals for a longer period;

it is possible to conclude that probably the tested schedules were not optimal for this compound. The good reduction in tumour volume is not in accordance with the marginal antitumour activity observed, probably due to the restarting of cancer growth at the end of the treatment. For this reason, considering the different growth rate of the two tumour models, the optimal schedule, on the slower one (GBM), for a compound with such a long half-life and associated to toxicity when administered more frequently than once a week, may be made up in repeated cycles. For example, cycles of four weekly administrations could be suspended with a break to allow the animal recovery from toxicity and then re-started obtaining in this way, the extension of the treatment.

Translating the half-life obtained in mice to humans, it may be of some days and taking together with the quite good bioavailability of IDN 6140 and the related toxicity, this compound might be administered to patients weekly by oral route. This would be in line with what has been highlighted for docetaxel and paclitaxel: the adoption of weekly schedule seems well tolerated and more effective than 3-weekly regimen [56]. The potential efficacy of IDN 6140 could be employed for the therapy of Central Nervous System (CNS) tumours and metastasis - the latter originated from advanced breast cancer - according to the known *in vitro* activity of taxanes on human glioblastoma and

breast cancer cells and taking into consideration that about 30% of advanced breast cancer patients shows relapses on CNS.

As final consideration of this thesis work, I would like to highlight the importance of pharmacokinetic studies during preclinical evaluations of new compounds. The preclinical development of new anticancer agents towards initial phases of clinical investigation is very expensive and time-consuming. In many cases, the pharmacokinetics of new anticancer agents is investigated when the toxicological evaluations are performed.

The data shown in the present thesis indicate that it is important to undertake pharmacokinetic and metabolism studies early on during the initial process of preclinical development. Knowledge of metabolism and pharmacokinetics can in fact help to take rational go/no-go decisions, providing indications on structural changes required to improve the pharmacological properties and thus the effectiveness of the new molecule.

CHAPTER 6

REFERENCES

1. Price RA. The genera of *Taxaceae* in the southeastern United States. *Journal of the Arnold Arboretum* 1990;**71**:69.

2. Bugala W. Systematics and variability. In: Bialobok S, editor. The yew: *Taxus Baccata* L. . Warsaw, Poland; 1978. p. 149.

3. Lewington A, Parker E. In: Ancient trees: trees that live for 1000 years. London: Collins and Brown; 1999. p. 66-76.

4. Tekol Y. The medieval physician Avicenna used an herbal calcium channel blocker, Taxus baccata L. *Phytother Res* 2007;**21**:701-2.

5. Wani MC, Taylor HL, Wall ME, Coggon P, McPhail AT. Plant antitumor agents. VI. The isolation and structure of taxol, a novel antileukemic and antitumor agent from Taxus brevifolia. *J Am Chem Soc* 1971;**93**:2325-7.

6. Wall ME, Wani MC. Camptothecin and taxol: discovery to clinic--thirteenth Bruce F. Cain Memorial Award Lecture. *Cancer Res* 1995;**55**:753-60.

7. Stephenson F. *A Tale of Taxol.* Florida State University Office of Research http://www.research.fsu.edu/researchr/fail2002/taxol.html.

8. Pellegrini F, Budman DR. Review: tubulin function, action of antitubulin drugs, and new drug development. *Cancer Invest* 2005;**23**:264-73.

9. Bhalla KN. Microtubule-targeted anticancer agents and apoptosis. *Oncogene* 2003;**22**:9075-86.

10. Schiff PB, Horwitz SB. Taxol stabilizes microtubules in mouse fibroblast cells. *Proc Natl Acad Sci U S A* 1980;**77**:1561-5.

11. Schiff PB, Horwitz SB. Taxol assembles tubulin in the absence of exogenous guanosine 5'-triphosphate or microtubule-associated proteins. *Biochemistry* 1981;**20**:3247-52.

12. Herbst RS, Khuri FR. Mode of action of docetaxel - a basis for combination with novel anticancer agents. *Cancer Treat Rev* 2003;**29**:407-15.

13. National Comprehensive Cancer Network, Clinical Practice Guidelines in Oncology: Breast Cancer v2 http://www.nccn.org/professionals/physician_gls/default.asp. 2008.

14. Wiernik PH, Schwartz EL, Strauman JJ, Dutcher JP, Lipton RB, Paietta E. Phase I clinical and pharmacokinetic study of taxol. *Cancer Res* 1987;**47**:2486-93.

15. McGuire WP, Hoskins WJ, Brady MF, et al. Cyclophosphamide and cisplatin versus paclitaxel and cisplatin: a phase III randomized trial in patients with suboptimal stage III/IV ovarian cancer (from the Gynecologic Oncology Group). *Semin Oncol* 1996;**23**:40-7.

16. Neijt JP, Engelholm SA, Tuxen MK, et al. Exploratory phase III study of paclitaxel and cisplatin versus paclitaxel and carboplatin in advanced ovarian cancer. *J Clin Oncol* 2000;**18**:3084-92.

17. Ettinger DS, Finkelstein DM, Sarma RP, Johnson DH. Phase II study of paclitaxel in patients with extensive-disease small-cell lung cancer: an Eastern Cooperative Oncology Group study. *J Clin Oncol* 1995;**13**:1430-5.

18. Forastiere AA, Shank D, Neuberg D, Taylor SGt, DeConti RC, Adams G. Final report of a phase II evaluation of paclitaxel in patients with advanced squamous cell

carcinoma of the head and neck: an Eastern Cooperative Oncology Group trial (PA390). *Cancer* 1998;**82**:2270-4.

19. Holmes FA, Walters RS, Theriault RL, et al. Phase II trial of taxol, an active drug in the treatment of metastatic breast cancer. *J Natl Cancer Inst* 1991;**83**:1797-805.

20. Schiller JH, Harrington D, Belani CP, et al. Comparison of four chemotherapy regimens for advanced non-small-cell lung cancer. *N Engl J Med* 2002;**346**:92-8.

21. Gill PS, Tulpule A, Espina BM, et al. Paclitaxel is safe and effective in the treatment of advanced AIDS-related Kaposi's sarcoma. *J Clin Oncol* 1999;**17**:1876-83.

22. Hainsworth JD, Erland JB, Kalman LA, Schreeder MT, Greco FA. Carcinoma of unknown primary site: treatment with 1-hour paclitaxel, carboplatin, and extended-schedule etoposide. *J Clin Oncol* 1997;**15**:2385-93.

23. Lissoni A, Zanetta G, Losa G, Gabriele A, Parma G, Mangioni C. Phase II study of paclitaxel as salvage treatment in advanced endometrial cancer. *Ann Oncol* 1996;7:861-3.

24. Eisenhauer EA, Vermorken JB. The taxoids. Comparative clinical pharmacology and therapeutic potential. *Drugs* 1998;**55**:5-30.

25. Trudeau ME, Eisenhauer EA, Higgins BP, et al. Docetaxel in patients with metastatic breast cancer: a phase II study of the National Cancer Institute of Canada-Clinical Trials Group. *J Clin Oncol* 1996;**14**:422-8.

26. Martin M, Pienkowski T, Mackey J, et al. Adjuvant docetaxel for node-positive breast cancer. *N Engl J Med* 2005;**352**:2302-13.

27. Gligorov J, Lotz JP. Preclinical pharmacology of the taxanes: implications of the differences. *Oncologist* 2004;**9 Suppl 2**:3-8.

28. Haldar S, Basu A, Croce CM. Bcl2 is the guardian of microtubule integrity. *Cancer Res* 1997;**57**:229-33.

29. Riou JF, Naudin A, Lavelle F. Effects of Taxotere on murine and human tumor cell lines. *Biochem Biophys Res Commun* 1992;**187**:164-70.

30. Pradier O, Rave-Frank M, Lehmann J, et al. Effects of docetaxel in combination with radiation on human head and neck cancer cells (ZMK-1) and cervical squamous cell carcinoma cells (CaSki). *Int J Cancer* 2001;**91**:840-5.

31. Jones SE, Erban J, Overmoyer B, et al. Randomized phase III study of docetaxel compared with paclitaxel in metastatic breast cancer. *J Clin Oncol* 2005;**23**:5542-51.

32. Eiseman JL, Eddington ND, Leslie J, et al. Plasma pharmacokinetics and tissue distribution of paclitaxel in CD2F1 mice. *Cancer Chemother Pharmacol* 1994;**34**:465-71.

33. Monsarrat B, Alvinerie P, Wright M, et al. Hepatic metabolism and biliary excretion of Taxol in rats and humans. *J Natl Cancer Inst Monogr* 1993:39-46.

34. Monsarrat B, Mariel E, Cros S, et al. Taxol metabolism. Isolation and identification of three major metabolites of taxol in rat bile. *Drug Metab Dispos* 1990;**18**:895-901.

35. Klecker RW, Jamis-Dow CA, Egorin MJ, et al. Effect of cimetidine, probenecid, and ketoconazole on the distribution, biliary secretion, and metabolism of [3H]taxol in the Sprague-Dawley rat. *Drug Metab Dispos* 1994;**22**:254-8.

36. Bardelmeijer HA, Oomen IA, Hillebrand MJ, Beijnen JH, Schellens JH, van Tellingen O. Metabolism of paclitaxel in mice. *Anticancer Drugs* 2003;**14**:203-9.

37. Gelderblom H, Verweij J, Nooter K, Sparreboom A. Cremophor EL: the drawbacks and advantages of vehicle selection for drug formulation. *Eur J Cancer* 2001;**37**:1590-8.

38. Hamel E, Lin CM, Johns DG. Tubulin-dependent biochemical assay for the antineoplastic agent taxol and application to measurement of the drug in serum. *Cancer Treat Rep* 1982;**66**:1381-6.

39. Brown T, Havlin K, Weiss G, et al. A phase I trial of taxol given by a 6-hour intravenous infusion. *J Clin Oncol* 1991;**9**:1261-7.

40. Grem JL, Tutsch KD, Simon KJ, et al. Phase I study of taxol administered as a short i.v. infusion daily for 5 days. *Cancer Treat Rep* 1987;**71**:1179-84.

41. Longnecker SM, Donehower RC, Cates AE, et al. High-performance liquid chromatographic assay for taxol in human plasma and urine and pharmacokinetics in a phase I trial. *Cancer Treat Rep* 1987;**71**:53-9.

42. Rowinsky EK, Burke PJ, Karp JE, Tucker RW, Ettinger DS, Donehower RC. Phase I and pharmacodynamic study of taxol in refractory acute leukemias. *Cancer Res* 1989;**49**:4640-7.

43. Horikoshi N, Inoue K, Aiba K, et al. [Phase I study of paclitaxel]. *Gan To Kagaku Ryoho* 1994;**21**:2407-14.

44. Tamura T, Sasaki Y, Eguchi K, et al. Phase I and pharmacokinetic study of paclitaxel by 24-hour intravenous infusion. *Jpn J Cancer Res* 1994;**85**:1057-62.

45. Huizing MT, Giaccone G, van Warmerdam LJ, et al. Pharmacokinetics of paclitaxel and carboplatin in a dose-escalating and dose-sequencing study in patients with non-small-cell lung cancer. The European Cancer Centre. *J Clin Oncol* 1997;**15**:317-29.

46. Sparreboom A, van Tellingen O, Nooijen WJ, Beijnen JH. Nonlinear pharmacokinetics of paclitaxel in mice results from the pharmaceutical vehicle Cremophor EL. *Cancer Res* 1996;**56**:2112-5.

47. Henningsson A, Karlsson MO, Vigano L, Gianni L, Verweij J, Sparreboom A. Mechanism-based pharmacokinetic model for paclitaxel. *J Clin Oncol* 2001;**19**:4065-73.

48. Mross K, Hollander N, Hauns B, Schumacher M, Maier-Lenz H. The pharmacokinetics of a 1-h paclitaxel infusion. *Cancer Chemother Pharmacol* 2000;**45**:463-70.

49. Ohtsu T, Sasaki Y, Tamura T, et al. Clinical pharmacokinetics and pharmacodynamics of paclitaxel: a 3-hour infusion versus a 24-hour infusion. *Clin Cancer Res* 1995;**1**:599-606.

50. Panday VR, Huizing MT, van Warmerdam LJ, et al. Pharmacologic study of 3-hour 135 mg M-2 paclitaxel in platinum pretreated patients with advanced ovarian cancer. *Pharmacol Res* 1998;**38**:231-6.

51. Gianni L, Kearns CM, Giani A, et al. Nonlinear pharmacokinetics and metabolism of paclitaxel and its pharmacokinetic/pharmacodynamic relationships in humans. *J Clin Oncol* 1995;**13**:180-90.

52. Ye M, Zhu Z, Fu Q, Shen K, Li DK. Nonlinear pharmacokinetics of paclitaxel in ovarian cancer patients. *Acta Pharmacol Sin* 2000;**21**:596-9.

53. Sonnichsen DS, Hurwitz CA, Pratt CB, Shuster JJ, Relling MV. Saturable pharmacokinetics and paclitaxel pharmacodynamics in children with solid tumors. *J Clin Oncol* 1994;**12**:532-8.

54. Baker SD, Verweij J, Rowinsky EK, et al. Role of body surface area in dosing of investigational anticancer agents in adults, 1991-2001. *J Natl Cancer Inst* 2002;**94**:1883-8.

55. Mielke S, Sparreboom A, Behringer D, Mross K. Paclitaxel pharmacokinetics and response to chemotherapy in patients with advanced cancer treated with a weekly regimen. *Anticancer Res* 2005;**25**:4423-7.

56. Gonzalez-Angulo AM, Hortobagyi GN. Optimal schedule of paclitaxel: weekly is better. *J Clin Oncol* 2008;**26**:1585-7.

57. Kumar GN, Walle UK, Bhalla KN, Walle T. Binding of taxol to human plasma, albumin and alpha 1-acid glycoprotein. *Res Commun Chem Pathol Pharmacol* 1993;**80**:337-44.

58. Glantz MJ, Choy H, Kearns CM, et al. Paclitaxel disposition in plasma and central nervous systems of humans and rats with brain tumors. *J Natl Cancer Inst* 1995;**87**:1077-81.

59. Fujita H, Okamoto M, Takao A, Mase H, Kojima H. [Pharmacokinetics of paclitaxel in experimental animals. Part 2. Tissue distribution]. *Gan To Kagaku Ryoho* 1994;**21**:659-64.

60. Lesser GJ, Grossman SA, Eller S, Rowinsky EK. The distribution of systemically administered [3H]-paclitaxel in rats: a quantitative autoradiographic study. *Cancer Chemother Pharmacol* 1995;**37**:173-8.

61. Walle T, Walle UK, Kumar GN, Bhalla KN. Taxol metabolism and disposition in cancer patients. *Drug Metab Dispos* 1995;**23**:506-12.

62. Dowling TC, Briglia AE, Fink JC, et al. Characterization of hepatic cytochrome p4503A activity in patients with end-stage renal disease. *Clin Pharmacol Ther* 2003;**73**:427-34.

63. Michaud J, Dube P, Naud J, et al. Effects of serum from patients with chronic renal failure on rat hepatic cytochrome P450. *Br J Pharmacol* 2005;**144**:1067-77.

64. Pichette V, Leblond FA. Drug metabolism in chronic renal failure. *Curr Drug Metab* 2003;**4**:91-103.

65. Fennelly D. The role of high-dose chemotherapy in the management of advanced ovarian cancer. *Curr Opin Oncol* 1996;**8**:415-25.

66. Fennelly D, Aghajanian C, Shapiro F, et al. Phase I and pharmacologic study of paclitaxel administered weekly in patients with relapsed ovarian cancer. *J Clin Oncol* 1997;**15**:187-92.

67. Panday VR, Huizing MT, Willemse PH, et al. Hepatic metabolism of paclitaxel and its impact in patients with altered hepatic function. *Semin Oncol* 1997;**24**:S11-34-S11-38.

68. Venook AP, Egorin MJ, Rosner GL, et al. Phase I and pharmacokinetic trial of paclitaxel in patients with hepatic dysfunction: Cancer and Leukemia Group B 9264. *J Clin Oncol* 1998;**16**:1811-9.

69. Harris JW, Katki A, Anderson LW, Chmurny GN, Paukstelis JV, Collins JM. Isolation, structural determination, and biological activity of 6 alpha-hydroxytaxol, the principal human metabolite of taxol. *J Med Chem* 1994;**37**:706-9.

70. Huizing MT, Keung AC, Rosing H, et al. Pharmacokinetics of paclitaxel and metabolites in a randomized comparative study in platinum-pretreated ovarian cancer patients. *J Clin Oncol* 1993;**11**:2127-35.

71. Sparreboom A, Huizing MT, Boesen JJ, Nooijen WJ, van Tellingen O, Beijnen JH. Isolation, purification, and biological activity of mono- and dihydroxylated paclitaxel metabolites from human feces. *Cancer Chemother Pharmacol* 1995;**36**:299-304.

72. Cresteil T, Monsarrat B, Alvinerie P, Treluyer JM, Vieira I, Wright M. Taxol metabolism by human liver microsomes: identification of cytochrome P450 isozymes involved in its biotransformation. *Cancer Res* 1994;**54**:386-92.

73. Henningsson A, Marsh S, Loos WJ, et al. Association of CYP2C8, CYP3A4, CYP3A5, and ABCB1 polymorphisms with the pharmacokinetics of paclitaxel. *Clin Cancer Res* 2005;**11**:8097-104.

74. Rahman A, Korzekwa KR, Grogan J, Gonzalez FJ, Harris JW. Selective biotransformation of taxol to 6 alpha-hydroxytaxol by human cytochrome P450 2C8. *Cancer Res* 1994;**54**:5543-6.

75. Harris JW, Rahman A, Kim BR, Guengerich FP, Collins JM. Metabolism of taxol by human hepatic microsomes and liver slices: participation of cytochrome P450 3A4 and an unknown P450 enzyme. *Cancer Res* 1994;**54**:4026-35.

76. Henningsson A, Sparreboom A, Sandstrom M, et al. Population pharmacokinetic modelling of unbound and total plasma concentrations of paclitaxel in cancer patients. *Eur J Cancer* 2003;**39**:1105-14.

77. Rowinsky EK, Jiroutek M, Bonomi P, Johnson D, Baker SD. Paclitaxel steady-state plasma concentration as a determinant of disease outcome and toxicity in lung cancer patients treated with paclitaxel and cisplatin. *Clin Cancer Res* 1999;**5**:767-74.

78. Bissery MC, Nohynek G, Sanderink GJ, Lavelle F. Docetaxel (Taxotere): a review of preclinical and clinical experience. Part I: Preclinical experience. *Anticancer Drugs* 1995;**6**:339-55, 363-8.

79. Clarke SJ, Rivory LP. Clinical pharmacokinetics of docetaxel. *Clin Pharmacokinet* 1999;**36**:99-114.

80. Sparreboom A, van Tellingen O, Nooijen WJ, Beijnen JH. Preclinical pharmacokinetics of paclitaxel and docetaxel. *Anticancer Drugs* 1998;**9**:1-17.

81. Bissery MC. Preclinical pharmacology of docetaxel. *Eur J Cancer* 1995;**31A Suppl 4**:S1-6.

82. Gaillard C, Monsarrat B, Vuilhorgne M, et al. Docetaxel (Taxotere) metabolism in the rat *in vivo* and *in vitro*. *Proc. Am. Assoc. Cancer. Res.* 1994;**35**:(abs n.2553).

83. Lavelle F, Bissery MC, Combeau C, Riou JF, Vrignaud P, Andre S. Preclinical evaluation of docetaxel (Taxotere). *Semin Oncol* 1995;**22**:3-16.

84. Marlard M, Gaillard C, Sanderink GJ, et al. Kinetics, distribution, metabolism and excretion of radiolabelled taxotere (14C-RP56976) in mice and dogs. *Proc. Am. Assoc. Cancer Res.* 1993;**34**:Abs n°2343.

85. Sparreboom A, van Asperen J, Mayer U, et al. Limited oral bioavailability and active epithelial excretion of paclitaxel (Taxol) caused by P-glycoprotein in the intestine. *Proc Natl Acad Sci U S A* 1997;**94**:2031-5.

86. Van Asperen J, Van Tellingen O, Beijnen JH. The pharmacological role of P-glycoprotein in the intestinal epithelium. *Pharmacol Res* 1998;**37**:429-35.

87. Malingre MM, Richel DJ, Beijnen JH, et al. Coadministration of cyclosporine strongly enhances the oral bioavailability of docetaxel. *J Clin Oncol* 2001;**19**:1160-6.

88. Bruno R, Hille D, Riva A, et al. Population pharmacokinetics/pharmacodynamics of docetaxel in phase II studies in patients with cancer. *J Clin Oncol* 1998;**16**:187-96.

89. Bruno R, Vivier N, Veyrat-Follet C, Montay G, Rhodes GR. Population pharmacokinetics and pharmacokinetic-pharmacodynamic relationships for docetaxel. *Invest New Drugs* 2001;**19**:163-9.

90. Rosing H, Lustig V, van Warmerdam LJ, et al. Pharmacokinetics and metabolism of docetaxel administered as a 1-h intravenous infusion. *Cancer Chemother Pharmacol* 2000;**45**:213-8.

91. Slaviero KA, Clarke SJ, McLachlan AJ, Blair EY, Rivory LP. Population pharmacokinetics of weekly docetaxel in patients with advanced cancer. *Br J Clin Pharmacol* 2004;**57**:44-53.

92. Baker SD, Sparreboom A, Verweij J. Clinical pharmacokinetics of docetaxel : recent developments. *Clin Pharmacokinet* 2006;**45**:235-52.

93. Urien S, Barre J, Morin C, Paccaly A, Montay G, Tillement JP. Docetaxel serum protein binding with high affinity to alpha 1-acid glycoprotein. *Invest New Drugs* 1996;**14**:147-51.

94. Bruno R, Olivares R, Berille J, et al. Alpha-1-acid glycoprotein as an independent predictor for treatment effects and a prognostic factor of survival in patients with non-small cell lung cancer treated with docetaxel. *Clin Cancer Res* 2003;**9**:1077-82.

95. Minami H, Kawada K, Sasaki Y, et al. Population pharmacokinetics of docetaxel in patients with hepatic dysfunction treated in an oncology practice. *Cancer Sci* 2009;**100**:144-9.

96. Sparreboom A, Van Tellingen O, Scherrenburg EJ, et al. Isolation, purification and biological activity of major docetaxel metabolites from human feces. *Drug Metab Dispos* 1996;**24**:655-8.

97. Baker SD, Verweij J, Cusatis GA, et al. Pharmacogenetic pathway analysis of docetaxel elimination. *Clin Pharmacol Ther* 2009;**85**:155-63.

98. Shou M, Martinet M, Korzekwa KR, Krausz KW, Gonzalez FJ, Gelboin HV. Role of human cytochrome P450 3A4 and 3A5 in the metabolism of taxotere and its derivatives: enzyme specificity, interindividual distribution and metabolic contribution in human liver. *Pharmacogenetics* 1998;**8**:391-401.

99. Monsarrat B, Royer I, Wright M, Cresteil T. Biotransformation of taxoids by human cytochromes P450: structure-activity relationship. *Bull Cancer* 1997;**84**:125-33.

100. Commercon A, Bourzat JD, Bézard D, Vuilhorgne M. Partial synthesis of major human metabolites of docetaxel. *Tetrahedron* 1994;**50**:10289-98.

101. Monegier B, Gaillard C, Sablè S, Vuilhorgne M. Structures of the major human metabolites of docetaxel (RP 56976 - Taxotere®). *Tetrahedron lett* 1994;**35**:3715-8.

102. Royer I, Monsarrat B, Sonnier M, Wright M, Cresteil T. Metabolism of docetaxel by human cytochromes P450: interactions with paclitaxel and other antineoplastic drugs. *Cancer Res* 1996;**56**:58-65.

103. Marre F, Sanderink GJ, de Sousa G, Gaillard C, Martinet M, Rahmani R. Hepatic biotransformation of docetaxel (Taxotere) in vitro: involvement of the CYP3A subfamily in humans. *Cancer Res* 1996;**56**:1296-302.

104. Veyrat-Follet C, Bruno R, Olivares R, Rhodes GR, Chaikin P. Clinical trial simulation of docetaxel in patients with cancer as a tool for dosage optimization. *Clin Pharmacol Ther* 2000;**68**:677-87.

105. Baker SD, Li J, ten Tije AJ, et al. Relationship of systemic exposure to unbound docetaxel and neutropenia. *Clin Pharmacol Ther* 2005;**77**:43-53.

106. Charles KA, Rivory LP, Stockler MR, et al. Predicting the toxicity of weekly docetaxel in advanced cancer. *Clin Pharmacokinet* 2006;**45**:611-22.

107. Bartels CL, Wilson AF. Drug Formulation Developments: Paclitaxel. *US Pharmacist* 2004;**29**:HS 18-23.

108. Piccart MJ, Klijn J, Paridaens R, et al. Corticosteroids significantly delay the onset of docetaxel-induced fluid retention: final results of a randomized study of the European Organization for Research and Treatment of Cancer Investigational Drug Branch for Breast Cancer. *J Clin Oncol* 1997;**15**:3149-55.

109. Bardelmeijer HA, Ouwehand M, Malingre MM, Schellens JH, Beijnen JH, van Tellingen O. Entrapment by Cremophor EL decreases the absorption of paclitaxel from the gut. *Cancer Chemother Pharmacol* 2002;**49**:119-25.

110. Malingre MM, Schellens JH, Van Tellingen O, et al. The co-solvent Cremophor EL limits absorption of orally administered paclitaxel in cancer patients. *Br J Cancer* 2001;**85**:1472-7.

111. Gelderblom H, Mross K, ten Tije AJ, et al. Comparative pharmacokinetics of unbound paclitaxel during 1- and 3-hour infusions. *J Clin Oncol* 2002;**20**:574-81.

112. Khan A, McNally D, Tutschka PJ, Bilgrami S. Paclitaxel-induced acute bilateral pneumonitis. *Ann Pharmacother* 1997;**31**:1471-4.

113. Weiss RB, Donehower RC, Wiernik PH, et al. Hypersensitivity reactions from taxol. *J Clin Oncol* 1990;**8**:1263-8.

114. Verweij J, Clavel M, Chevalier B. Paclitaxel (Taxol) and docetaxel (Taxotere): not simply two of a kind. *Ann Oncol* 1994;**5**:495-505.

115. Miele E, Spinelli GP, Tomao F, Tomao S. Albumin-bound formulation of paclitaxel (Abraxane ABI-007) in the treatment of breast cancer. *Int J Nanomedicine* 2009;**4**:99-105.

116. Morris PG, Fornier MN. Microtubule active agents: beyond the taxane frontier. *Clin Cancer Res* 2008;**14**:7167-72.

117. Sparreboom A, Baker SD, Verweij J. Paclitaxel repackaged in an albumin-stabilized nanoparticle: handy or just a dandy? *J Clin Oncol* 2005;**23**:7765-7.

118. Gradishar WJ, Tjulandin S, Davidson N, et al. Phase III trial of nanoparticle albumin-bound paclitaxel compared with polyethylated castor oil-based paclitaxel in women with breast cancer. *J Clin Oncol* 2005;**23**:7794-803.

119. Sparreboom A, Scripture CD, Trieu V, et al. Comparative preclinical and clinical pharmacokinetics of a cremophor-free, nanoparticle albumin-bound paclitaxel (ABI-007) and paclitaxel formulated in Cremophor (Taxol). *Clin Cancer Res* 2005;**11**:4136-43.

120. Nyman DW, Campbell KJ, Hersh E, et al. Phase I and pharmacokinetics trial of ABI-007, a novel nanoparticle formulation of paclitaxel in patients with advanced nonhematologic malignancies. *J Clin Oncol* 2005;**23**:7785-93.

121. Kim SC, Kim DW, Shim YH, et al. In vivo evaluation of polymeric micellar paclitaxel formulation: toxicity and efficacy. *J Control Release* 2001;**72**:191-202.

122. Kim TY, Kim DW, Chung JY, et al. Phase I and pharmacokinetic study of Genexol-PM, a cremophor-free, polymeric micelle-formulated paclitaxel, in patients with advanced malignancies. *Clin Cancer Res* 2004;**10**:3708-16.

123. Lim WT, Tan EH, Toh CK, et al. Phase I pharmacokinetic study of a weekly liposomal paclitaxel formulation (Genexol(R)-PM) in patients with solid tumors. *Ann Oncol* 2009.

124. Eichhorn ME, Becker S, Strieth S, et al. Paclitaxel encapsulated in cationic lipid complexes (MBT-0206) impairs functional tumor vascular properties as detected by dynamic contrast enhanced magnetic resonance imaging. *Cancer Biol Ther* 2006;**5**:89-96.

125. Bartelheim K, Ognerubov NA, Semiglazov VF, Vtoraya OM, Kaletta C, Reichenberger I, Michaelis U, Naujoks K, M. Clemens Russian breast cancer study group. Phase Ib study of the anti-neovascular agent MBT-0206 to evaluate safety and efficacy in patients with metastatic breast cancer. *J Clin Oncol* 2004;**22**:Abs n° 3079.

126. Casazza AM, Fairchild CR. Paclitaxel (Taxol): mechanisms of Resistance. *Cancer Treat Res* 1996;**87**:149-71.

127. Horwitz SB, Cohen D, Rao S, Ringel I, Shen HJ, Yang CP. Taxol: mechanisms of action and resistance. *J Natl Cancer Inst Monogr* 1993:55-61.

128. Cordon-Cardo C, O'Brien JP, Boccia J, Casals D, Bertino JR, Melamed MR. Expression of the multidrug resistance gene product (P-glycoprotein) in human normal and tumor tissues. *J Histochem Cytochem* 1990;**38**:1277-87.

129. Thiebaut F, Tsuruo T, Hamada H, Gottesman MM, Pastan I, Willingham MC. Cellular localization of the multidrug-resistance gene product P-glycoprotein in normal human tissues. *Proc Natl Acad Sci U S A* 1987;**84**:7735-8.

130. Helgason HH, Kruijtzer CM, Huitema AD, et al. Phase II and pharmacological study of oral paclitaxel (Paxoral) plus ciclosporin in anthracycline-pretreated metastatic breast cancer. *Br J Cancer* 2006;**95**:794-800.

131. Woo JS, Lee CH, Shim CK, Hwang SJ. Enhanced oral bioavailability of paclitaxel by coadministration of the P-glycoprotein inhibitor KR30031. *Pharm Res* 2003;**20**:24-30.

132. Abbott NJ, Romero IA. Transporting therapeutics across the blood-brain barrier. *Mol Med Today* 1996;**2**:106-13.

133. Abbott N. Astrocyte-endothelial interactions and blood-brain barrier permeability. *J Anat* 2002;**200**:527.

134. Beaulieu E, Demeule M, Ghitescu L, Beliveau R. P-glycoprotein is strongly expressed in the luminal membranes of the endothelium of blood vessels in the brain. *Biochem J* 1997;**326 (Pt 2)**:539-44.

135. Kemper EM, van Zandbergen AE, Cleypool C, et al. Increased penetration of paclitaxel into the brain by inhibition of P-Glycoprotein. *Clin Cancer Res* 2003;**9**:2849-55.

136. Fellner S, Bauer B, Miller DS, et al. Transport of paclitaxel (Taxol) across the blood-brain barrier in vitro and in vivo. *J Clin Invest* 2002;**110**:1309-18.

137. Gallo JM, Li S, Guo P, Reed K, Ma J. The effect of P-glycoprotein on paclitaxel brain and brain tumor distribution in mice. *Cancer Res* 2003;**63**:5114-7.

138. Giannakakou P, Sackett DL, Kang YK, et al. Paclitaxel-resistant human ovarian cancer cells have mutant beta-tubulins that exhibit impaired paclitaxel-driven polymerization. *J Biol Chem* 1997;**272**:17118-25.

139. Kavallaris M, Kuo DY, Burkhart CA, et al. Taxol-resistant epithelial ovarian tumors are associated with altered expression of specific beta-tubulin isotypes. *J Clin Invest* 1997;**100**:1282-93.

140. Hanahan D, Bergers G, Bergsland E. Less is more, regularly: metronomic dosing of cytotoxic drugs can target tumor angiogenesis in mice. *J Clin Invest* 2000;**105**:1045-7.

141. Kerbel RS, Kamen BA. The anti-angiogenic basis of metronomic chemotherapy. *Nat Rev Cancer* 2004;**4**:423-36.

142. Miller KD, Sweeney CJ, Sledge GW, Jr. Redefining the target: chemotherapeutics as antiangiogenics. *J Clin Oncol* 2001;**19**:1195-206.

143. Beer M, Lenaz L, Amadori D and Ortataxel Study Group. Phase II study of ortataxel in taxane-resistant breast cancer. *J Clin Oncol* 2008;**26**:Abs n° 1066.

144. Ramnath N, Hamm J, Schwartz G, et al. A phase I and pharmacokinetic study of BAY59: a novel taxane. *Oncology* 2004;**67**:123-9.

145. Broker LE, de Vos FY, van Groeningen CJ, et al. Phase I trial with BMS-275183, a novel oral taxane with promising antitumor activity. *Clin Cancer Res* 2006;**12**:1760-7.

146. Broker LE, Veltkamp SA, Heath EI, et al. A phase I safety and pharmacologic study of a twice weekly dosing regimen of the oral taxane BMS-275183. *Clin Cancer Res* 2007;**13**:3906-12.

147. Advani R, Fisher GA, Lum BL, et al. Phase I and pharmacokinetic study of BMS-188797, a new taxane analog, administered on a weekly schedule in patients with advanced malignancies. *Clin Cancer Res* 2003;**9**:5187-94.

148. Fishman MN, Garrett CR, Simon GR, et al. Phase I study of the taxane BMS-188797 in combination with carboplatin administered every 3 weeks in patients with solid malignancies. *Clin Cancer Res* 2006;**12**:523-8.

149. Yamamoto N, Boku N, Minami H. Phase I study of larotaxel administered as a 1-h intravenous infusion every 3 weeks to Japanese patients with advanced solid tumours. *Cancer Chemother Pharmacol* 2009;**65**:129-36.

150. Mita AC, Denis LJ, Rowinsky EK, et al. Phase I and pharmacokinetic study of XRP6258 (RPR 116258A), a novel taxane, administered as a 1-hour infusion every 3 weeks in patients with advanced solid tumors. *Clin Cancer Res* 2009;**15**:723-30.

151. Lockhart AC, Bukowski R, Rothenberg ML, et al. Phase I trial of oral MAC-321 in subjects with advanced malignant solid tumors. *Cancer Chemother Pharmacol* 2007;**60**:203-9.

152. Baas P, Szczesna A, Albert I, et al. Phase I/II study of a 3 weekly oral taxane (DJ-927) in patients with recurrent, advanced non-small cell lung cancer. *J Thorac Oncol* 2008;**3**:745-50.

153. Glasspool RM, Boddy AV, Evans TR, Griffin MJ, Anthoney A, Barker A, Longley RE, Twelves CJ, Edwards CJ and Wilcox HE. A phase I study of a novel taxane, TL310, orally administered every week in patients (pts) with advanced solid tumors. *J Clin Oncol* 2007;**25**:Abs n° 2544.

154. Eckstein JW. Drug evaluation: Bay-59-8862. *IDrugs* 2004;**7**:575-81.

155. Spratlin J, Sawyer MB. Pharmacogenetics of paclitaxel metabolism. *Crit Rev Oncol Hematol* 2007;**61**:222-9.

156. Taniguchi R, Kumai T, Matsumoto N, et al. Utilization of human liver microsomes to explain individual differences in paclitaxel metabolism by CYP2C8 and CYP3A4. *J Pharmacol Sci* 2005;**97**:83-90.

157. Ojima I, Borella CP, Wu X, et al. Design, synthesis and structure-activity relationships of novel taxane-based multidrug resistance reversal agents. *J Med Chem* 2005;**48**:2218-28.

158. Kingston DGI. Studies on the chemistry of Taxol. *Pure & Appl. Chem.* 1998;**70**:331-4.

159. Appendino G, Danieli B, J. J, Belloro E, Scambia G, Bombardelli E. Synthesis and evaluation C-*seco* paclitaxel analogues. *Tetrahedron lett* 1997;**16**:4273-4276.

160. Taraboletti G, Micheletti G, Rieppi M, et al. Antiangiogenic and antitumor activity of IDN 5390, a new taxane derivative. *Clin Cancer Res* 2002;**8**:1182-8.

161. Petrangolini G, Cassinelli G, Pratesi G, et al. Antitumour and antiangiogenic effects of IDN 5390, a novel C-seco taxane, in a paclitaxel-resistant human ovarian tumour xenograft. *Br J Cancer* 2004;**90**:1464-8.

162. Pratesi G, Laccabue D, Lanzi C, et al. IDN 5390: an oral taxane candidate for protracted treatment schedules. *Br J Cancer* 2003;**88**:965-72.

163. Ferlini C, Raspaglio G, Mozzetti S, et al. The seco-taxane IDN5390 is able to target class III beta-tubulin and to overcome paclitaxel resistance. *Cancer Res* 2005;**65**:2397-405.

164. Kingston DG. The shape of things to come: structural and synthetic studies of taxol and related compounds. *Phytochemistry* 2007;**68**:1844-54.

165. Geney R, Chen J, Ojima I. Recent advances in the new generation taxane anticancer agents. *Med Chem* 2005;**1**:125-39.

166. Baldelli E, Battaglia A, Bombardelli E, et al. Diastereoselective 14beta-hydroxylation of baccatin III derivatives. *J Org Chem* 2003;**68**:9773-9.

167. Barboni L, Ballini R, Giarlo G, Appendino G, Fontana G, Bombardelli E. Synthesis and biological evaluation of methoxylated analogs of the newer generation taxoids IDN5109 and IDN5390. *Bioorg Med Chem Lett* 2005;**15**:5182-6.

168. Nicoletti MI, Colombo T, Rossi C, et al. IDN5109, a taxane with oral bioavailability and potent antitumor activity. *Cancer Res* 2000;**60**:842-6.

169. Polizzi D, Pratesi G, Tortoreto M, et al. A novel taxane with improved tolerability and therapeutic activity in a panel of human tumor xenografts. *Cancer Res* 1999;**59**:1036-40.

170. Sano D, Matsuda H, Ishiguro Y, Nishimura G, Kawakami M, Tsukuda M. Antitumor effects of IDN5109 on head and neck squamous cell carcinoma. *Oncol Rep* 2006;**15**:329-34.

171. Silbergeld DL, Chicoine MR, Madsen CL. In vitro assessment of Taxol for human glioblastoma: chemosensitivity and cellular locomotion. *Anticancer Drugs* 1995;**6**:270-6.

172. Terzis AJ, Thorsen F, Heese O, et al. Proliferation, migration and invasion of human glioma cells exposed to paclitaxel (Taxol) in vitro. *Br J Cancer* 1997;**75**:1744-52.

173. Joo KM, Park K, Kong DS, et al. Oral paclitaxel chemotherapy for brain tumors: ideal combination treatment of paclitaxel and P-glycoprotein inhibitor. *Oncol Rep* 2008;**19**:17-23.

174. Laccabue D, Tortoreto M, Veneroni S, et al. A novel taxane active against an orthotopically growing human glioma xenograft. *Cancer* 2001;**92**:3085-92.

175. Gurtler J, Von Pawel J, Spiridonidis CH, Grossi F, Larriba JL, Moscovici M, Markovitz E, Voliotis D, Gottfried M. An uncontrolled phase II study evaluating anti-tumor efficacy and safety of ortataxel (BAY 59-8862) in patients with taxane-resistant non-small cell lung cancer. *J Clin Oncol* 2004;**22**:Abs n° 7136.

176. Baldelli E, Battaglia A, Bombardelli E, et al. New taxane derivatives: synthesis of baccatin[14,1-d]furan-2-one nucleus and its condensation with the norstatine side chain. *J Org Chem* 2004;**69**:6610-6.

177. Battaglia A, Baldelli E, Bombardelli E, Carenzi G, Fontana G, Gelmi ML, Guerrini A, Pocar D. Selective synthesis of 14 β-amino taxanes. *Tetrahedron* 2005;**61**:7727.

178. Bombardelli E, Manzotti C, Fontana G, Riva A, Battaglia A, Gelmi ML, Pera P, Bernacki RJ, Morazzoni P. *In vitro* cytotoxicity profile of 14-functionalized taxanes. *Proc Amer Assoc Cancer Res* 2004;**45**:Abs n° 2484.

179. Fontana G, Battaglia A, Gelmi ML, Baldelli E, Carenzi G, Contini A, Bombardelli E, Manzotti C, Bernacki RJ, Zucchetti M. SAR of 14-substituted taxanes. *Proc Amer Chem Soc* 2004:Abs n° 99.

180. Vredenburg MR, Ojima I, Veith J, et al. Effects of orally active taxanes on P-glycoprotein modulation and colon and breast carcinoma drug resistance. *J Natl Cancer Inst* 2001;**93**:1234-45.

181. Chaudhary AG, Gharpure MM, Rimoldi JM, Chordia MD, Gunatilaka AAL, Kingston DGI. Unexpectedly Facile Hydrolysis of the 2-Benzoate Group of Taxol and Syntheses of Analogs with Increased Activities. *J. Am. Chem. Soc.* 1994;**116**:4097-8.

182. Ganesh T, Guza RC, Bane S, et al. The bioactive Taxol conformation on beta-tubulin: experimental evidence from highly active constrained analogs. *Proc Natl Acad Sci U S A* 2004;**101**:10006-11.

183. Marangon E, Sala F, Manzotti C, et al. IDN 6140: A new taxane derivative exhibiting a different and favorable pharmacokinetic profile from paclitaxel. *AACR-NCI-EORTC International Conference: Molecular targets and cancer therapeutics, San Francisco, CA* 2007:Abs n°c146.

184. Matuszewski BK, Constanzer ML, Chavez-Eng CM. Strategies for the assessment of matrix effect in quantitative bioanalytical methods based on HPLC-MS/MS. *Anal Chem* 2003;**75**:3019-30.

185. Mallet CR, Lu Z, Mazzeo JR. A study of ion suppression effects in electrospray ionization from mobile phase additives and solid-phase extracts. *Rapid Commun Mass Spectrom* 2004;**18**:49-58.

186. Sparreboom A, van Tellingen O, Nooijen WJ, Beijnen JH. Tissue distribution, metabolism and excretion of paclitaxel in mice. *Anticancer Drugs* 1996;**7**:78-86.

187. Frapolli R, Marangon E, Zaffaroni M, et al. Pharmacokinetics and metabolism in mice of IDN 5390 (13-(N-Boc-3-i-butylisoserinoyl)-C-7,8-seco-10-deacetylbaccatin III), a new oral c-seco-taxane derivative with antiangiogenic property effective on paclitaxel-resistant tumors. *Drug Metab Dispos* 2006;**34**:2028-35.

188. Gustafson DL, Long ME, Bradshaw EL, Merz AL, Kerzic PJ. P450 induction alters paclitaxel pharmacokinetics and tissue distribution with multiple dosing. *Cancer Chemother Pharmacol* 2005;**56**:248-54.

189. Bouchard H, Pulicani JP, Vuilhorgne M, Bourzat JD, Commercon A. Improved access to 19-nor-7β, 8β-methylene-taxoids and formation of a 7-membered C-ring analog of docetaxel by electrochemistry. *Tetrahedron lett* 1994;**35**:9713-6.

190. Liang X, Kingston DGI, Long BH, Fairchild CA, Johnston KA. Synthesis, Structure Elucidation and Biological Evaluation of C-Norpaclitaxel. *Tetrahedron lett.* 1995;**36**:7795-8.

191. Pratesi G, Laccabue D. BAY 59-8862. *Drugs of the Future* 2001;**26**:533-44.

192. BAY 59-8862:Investigator's Brochure. *Bayer health care Pharmaceuticals, West Haven, CT, US* 2004.

193. Kingston DG. Taxol, a molecule for all seasons. *Chem. Commun:* 2001:867-880.

194. Carmeliet P. Mechanisms of angiogenesis and arteriogenesis. *Nat Med* 2000;**6**:389-95.

195. Taraboletti G, Micheletti G, Giavazzi R, Riva A. IDN 5390: a new concept in taxane development. *Anticancer Drugs* 2003;**14**:255-8.

196. Vacca A, Ribatti D, Iurlaro M, et al. Docetaxel versus paclitaxel for antiangiogenesis. *J Hematother Stem Cell Res* 2002;**11**:103-18.

197. Marangon E, Sala F, Frapolli R, Manzotti C, Morazzoni P, Pratesi G, Petrangolini G, Tortoreto M, D'Incalci M, Zucchetti M. The novel taxane derivative, IDN 6140, crosses the blood brain barrier and has a promising activity in CNS tumors. *Eur J Cancer* 2008;**6**:Abs n° 180.

CHAPTER 7

APPENDIX

Appendix 1. Analytical method for 7-ethoxycoumarin and its metabolite

Analytical standards

7-ethoxycoumarin	batch 054K3687	Sigma
7-hydroxycoumarin	batch 1123370	Fluka

Preparation of mobile phase solution

0.5 % (v/v) acetic acid

5 mL of acetic acid were diluted to 1000 mL with deionized water

HPLC conditions

HPLC	Alliance series 2695 HPLC system (Waters Associates, Milford, MA, USA)
Detector	W2487 at variable-wavelenght UV/VIS (Waters Associates); λ 320 nm
Column	Symmetry C18, 150 x 4.60 mm, 5 µm; with Symmetry C18 precolumn (Waters Associates)
Mobile phase A:	0.5 % acetic acid (v/v)
Mobile phase B:	acetonitrile
Injection volume	10 µL
Flow rate	0.8 mL/min
Run time:	25 minutes

Gradient elution program:

Time (min.)	% A	% B
0	93	7
5	80	20
13	40	60
18	40	60
19	93	7
24	93	7

7-ethoxycoumarin retention time: 16 minutes

7-hydroxycoumarin retention time: 10.8 minutes

Acquisition system: Empower Software Chromatography Manager (Waters Associates)

Appendix 2. Analytical method for IDN 5614 and its metabolites

Analytical standards

IDN 5614	lot # PGB646	Indena S.p.A.

Preparation of mobile phase solution

- 0.1 % (v/v) formic acid in water

  1 mL of formic acid was diluted to 1000 mL with deionized water

- 0.1 % (v/v) formic acid in acetonitrile

  1 mL of formic acid was diluted to 1000 mL with acetonitrile

HPLC-MS/MS conditions

HPLC-MS/MS system consisting of a Surveyor autosampler and Surveyor MS pump were obtained from Thermo Finnigan, combined with LCQ Deca XP Plus ion trap mass spectrometer (Thermo Electron, Waltham, MA, USA). The analysis was performed in positive ion mode.

Column	Omnispher 3 C18, 100 x 2 mm, 3 μm; (Varian)
Mobile phase A:	0.1 % formic acid (v/v) in water
Mobile phase B:	0.1% formic acid (v/v) in acetonitrile
Injection volume	10 μL
Flow rate	0.2 mL/min
Run time:	46 minutes

Gradient elution program:

Time (min.)	% A	% B
0	60	40
24	0	100
36	0	100
38	60	40
46	60	40

IDN 5614 retention time: about 32 minutes

Appendix 3. Raw data of IDN 5738 plasma concentrations in mice

IDN 5738 plasma concentrations in mice after oral or i.v. administration of 60 mg/Kg of the drug					
Schedule	Mouse N°	Timepoints (h)	conc.(µg/ml)	mean	standard deviation
P.O.	1	0.25	9.56	9.48	1.91
	2		7.53		
	3		11.34		
	4	0.5	13.93	11.14	3.99
	5		12.91		
	6		6.57		
	7	0.75	12.79	13.67	1.69
	8		15.62		
	9		12.60		
	10	1	12.64	10.91	2.10
	11		8.58		
	12		11.51		
	13	1.5	13.38	11.23	2.76
	14		8.12		
	15		12.19		
	16	2	10.76	7.65	2.91
	17		7.20		
	18		4.99		
	19	4	5.26	4.28	1.15
	20		3.02		
	21		4.55		
	22	8	1.12	1.33	0.33
	23		1.18		
	24		1.71		
	25	16	0.17	0.10	0.10
	26		0.04		
	27		blq		
	28	24	blq	/	/
	29		blq		
	30		0.03		
I.V.	31	0.08	67.92	71.16	3.47
	32		74.82		
	33		70.74		
	34	0.25	40.68	40.73	1.52
	35		42.28		
	36		39.24		
	37	0.5	31.80	32.74	1.75
	38		31.66		
	39		34.76		
	40	1	14.43	18.12	4.02
	41		17.54		
	42		22.40		
	43	2	13.51	11.12	2.07
	44		9.81		
	45		10.04		
	46	4	2.56	4.25	2.09
	47		6.59		
	48		3.61		
	49	8	4.12	2.59	1.46
	50		1.20		
	51		2.44		
	52	16	0.14	0.14	0.00
	53		0.14		
	54		0.05		
	55	24	blq	/	/
	56		blq		
	57		0.02		

loq = 0.025 µg/ml

Appendix 4. Raw data of IDN 5839 plasma concentrations in mice

IDN 5839 plasma concentrations in mice after oral or i.v. administration of 60 mg/Kg of the drug					
Schedule	Mouse N°	Timepoints (h)	conc.(µg/ml)	mean	standard deviation
P.O.	1	0.25	5.24	4.57	1.05
	2		5.10		
	3		3.36		
	4	0.5	7.30	6.65	0.68
	5		6.70		
	6		5.94		
	7	0.75	6.90	6.93	0.33
	8		6.62		
	9		7.28		
	10	1	6.86	7.13	2.85
	11		4.42		
	12		10.10		
	13	1.5	4.62	6.96	2.11
	14		8.72		
	15		7.54		
	16	2	3.21	3.21	0.21
	17		3.41		
	18		3.00		
	19	4	1.54	1.52	0.82
	20		0.69		
	21		2.33		
	22	10.2	0.52	0.38	0.13
	23		0.33		
	24		0.28		
I.V.	31	0.08	57.82	55.15	2.35
	32		54.26		
	33		53.38		
	34	0.25	28.20	28.03	0.24
	35		27.86		
	36		/		
	37	0.5	18.94	13.80	6.77
	38		16.34		
	39		6.13		
	40	1	6.26	8.64	2.06
	41		9.90		
	42		9.75		
	43	2	3.32	3.20	0.26
	44		3.38		
	45		2.91		
	46	4	2.11	1.67	0.38
	47		1.40		
	48		1.50		
	49	10.2	0.21	0.28	0.08
	50		0.36		
	51		0.28		

loq = 0.025 µg/ml

Appendix 5. Mass spectra fragmentation patterns and chromatograms to back up identification of IDN 5738 metabolites

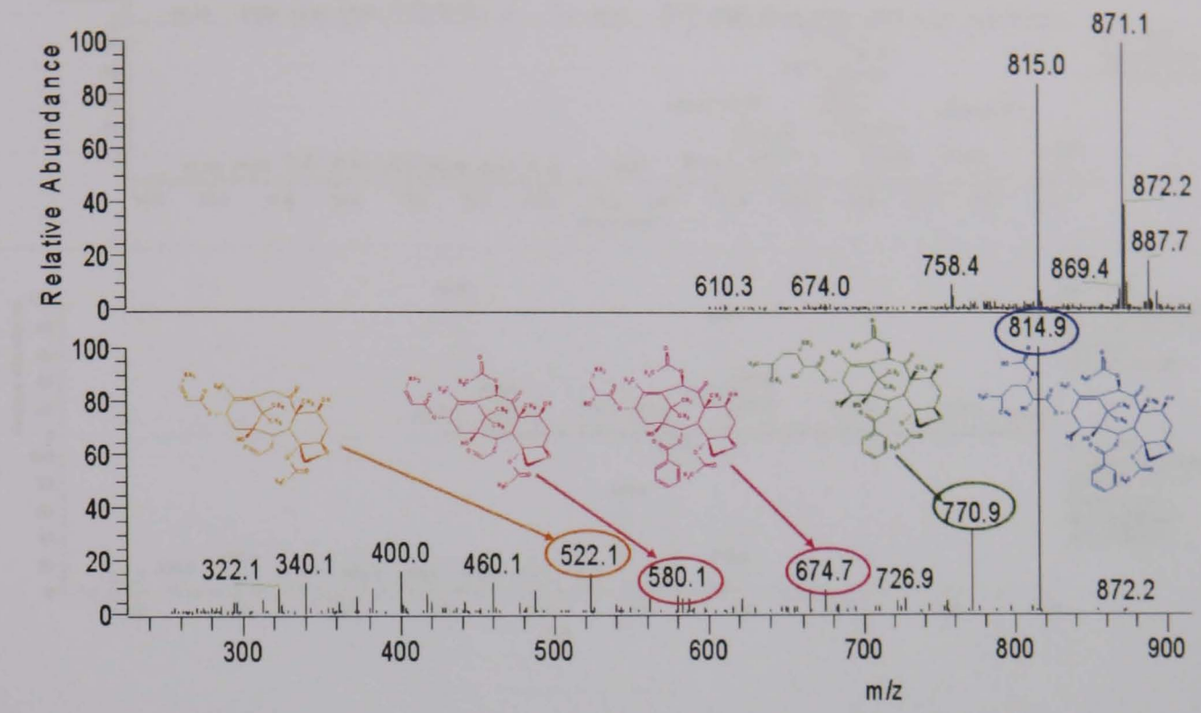

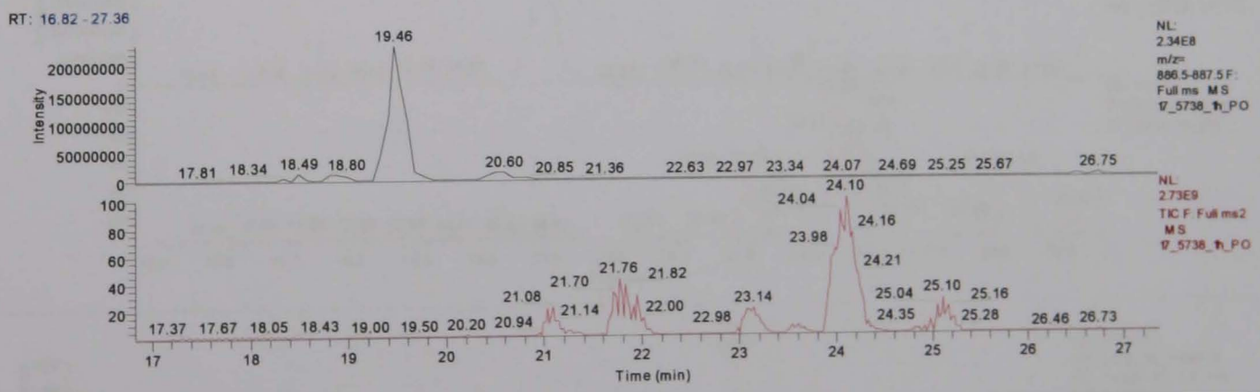

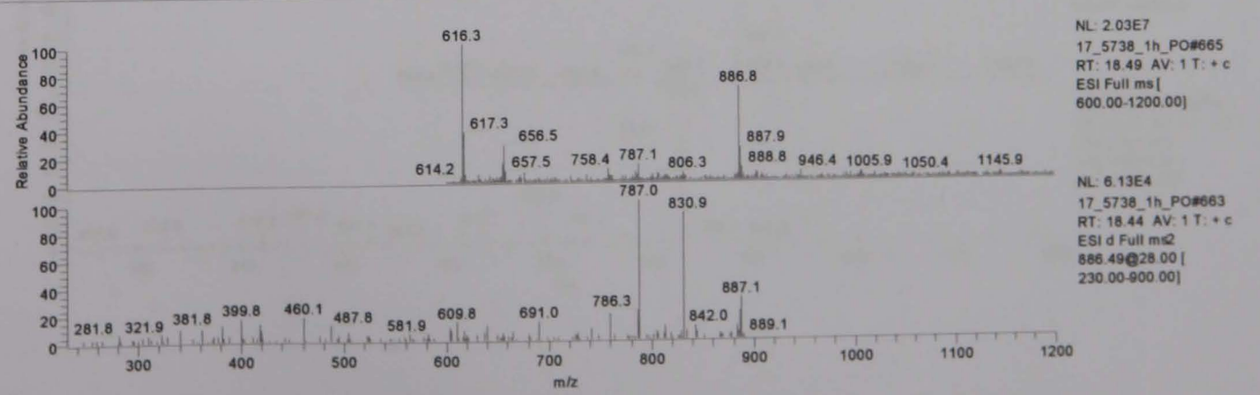

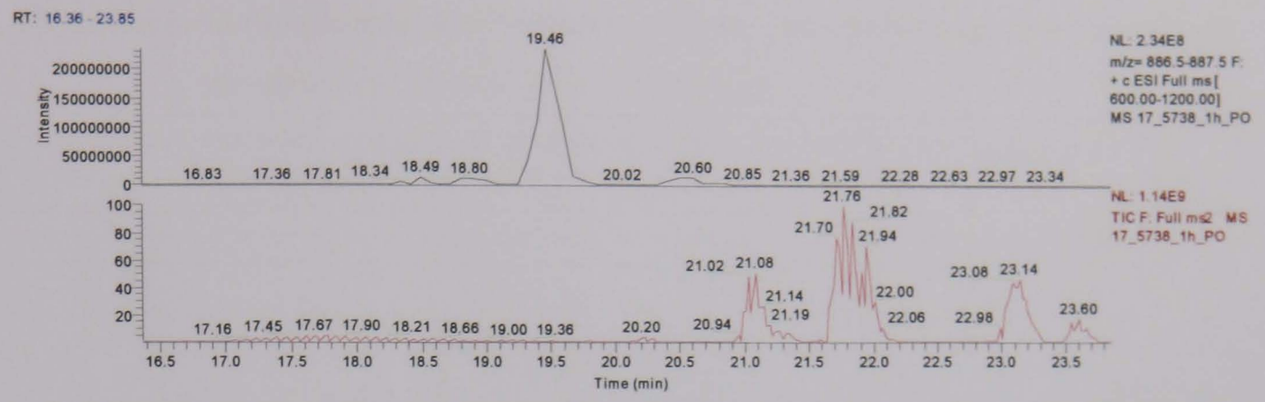
RT: 16.36 - 23.85
Intensity
Time (min)
NL: 2.34E8
m/z= 886.5-887.5 F:
+ c ESI Full ms [
600.00-1200.00]
MS 17_5738_1h_PO
NL: 1.14E9
TIC F: Full ms2 MS
17_5738_1h_PO

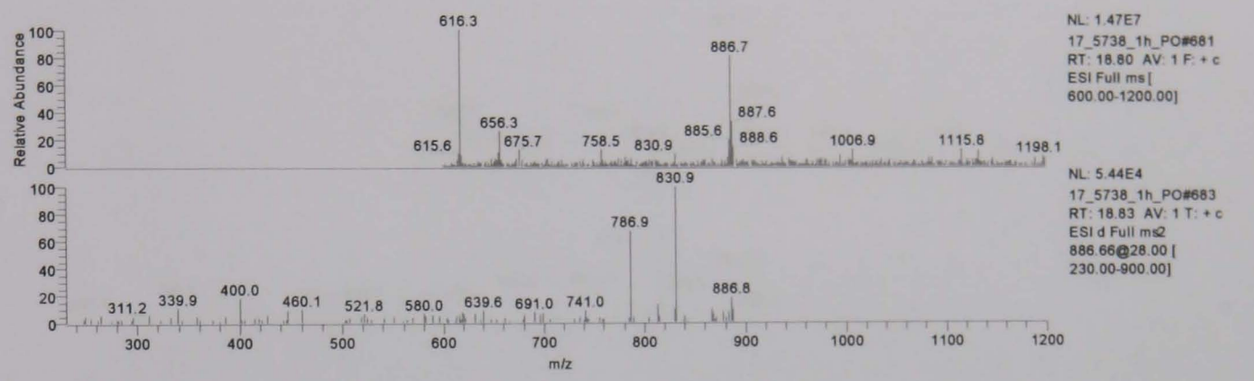
Relative Abundance
m/z
NL: 1.47E7
17_5738_1h_PO#681
RT: 18.80 AV: 1 F: + c
ESI Full ms [
600.00-1200.00]
NL: 5.44E4
17_5738_1h_PO#683
RT: 18.83 AV: 1 T: + c
ESI d Full ms2
886.66@28.00 [
230.00-900.00]

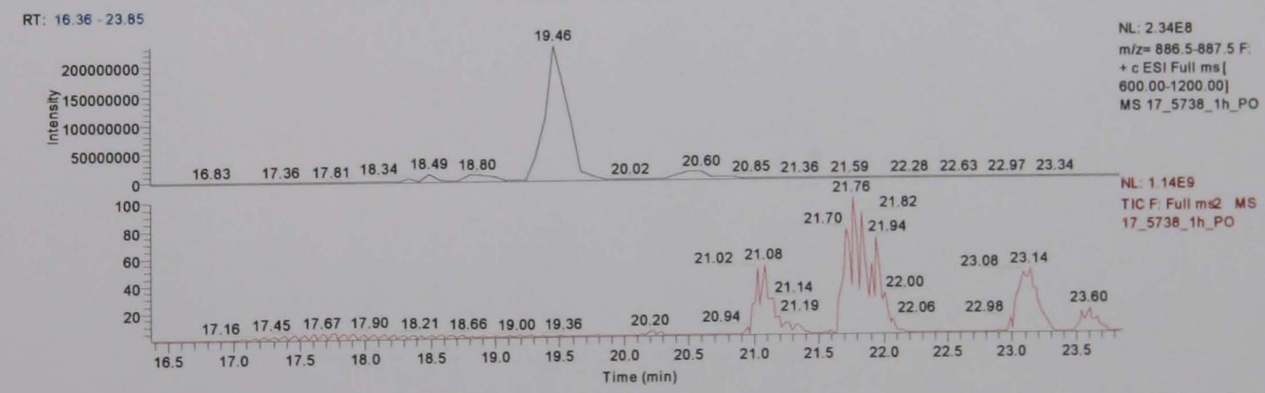
RT: 16.36 - 23.85
Intensity
Time (min)
NL: 2.34E8
m/z= 886.5-887.5 F:
+ c ESI Full ms [
600.00-1200.00]
MS 17_5738_1h_PO
NL: 1.14E9
TIC F: Full ms2 MS
17_5738_1h_PO

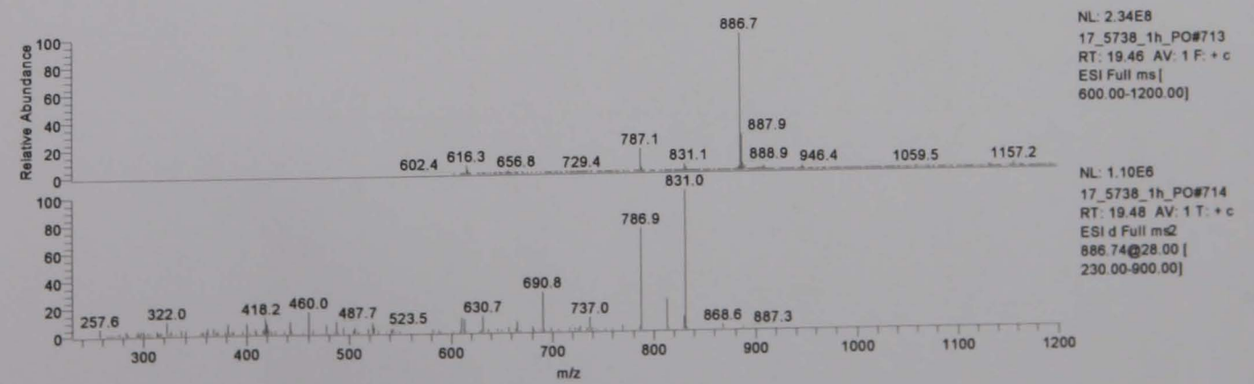
Relative Abundance
m/z
NL: 2.34E8
17_5738_1h_PO#713
RT: 19.46 AV: 1 F: + c
ESI Full ms [
600.00-1200.00]
NL: 1.10E6
17_5738_1h_PO#714
RT: 19.48 AV: 1 T: + c
ESI d Full ms2
886.74@28.00 [
230.00-900.00]

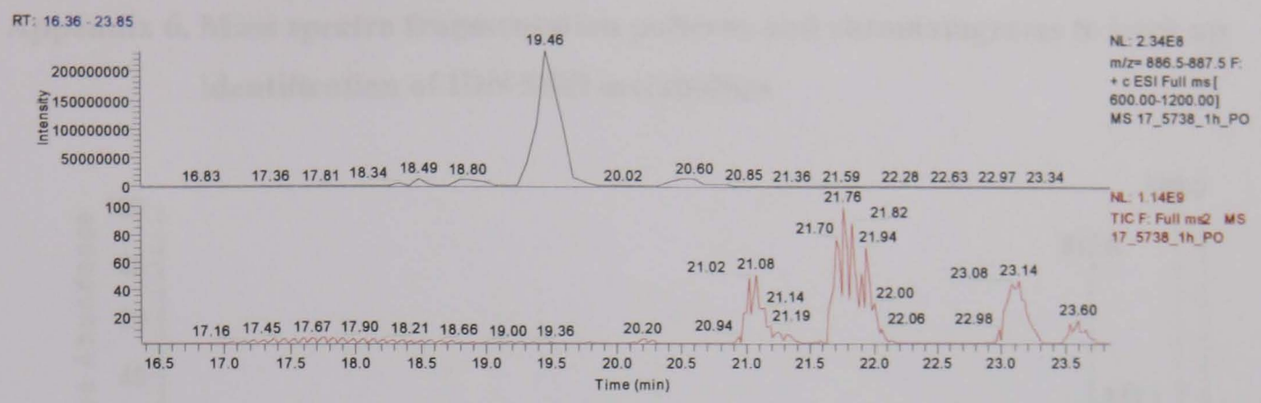
RT: 16.36 - 23.85
NL: 2.34E8
m/z= 886.5-887.5 F:
+ c ESI Full ms [
600.00-1200.00]
MS 17_5738_1h_PO
NL: 1.14E9
TIC F: Full ms2 MS
17_5738_1h_PO
Intensity
Time (min)

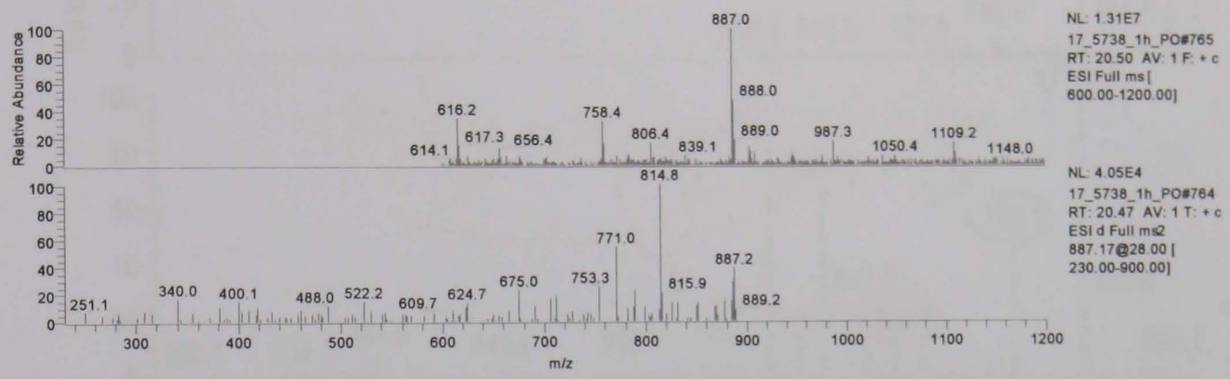
NL: 1.31E7
17_5738_1h_PO#765
RT: 20.50 AV: 1 F: + c
ESI Full ms [
600.00-1200.00]
NL: 4.05E4
17_5738_1h_PO#764
RT: 20.47 AV: 1 T: + c
ESI d Full ms2
887.17@28.00 [
230.00-900.00]
Relative Abundance
m/z

Appendix 6. Mass spectra fragmentation patterns and chromatograms to back up identification of IDN 5839 metabolites

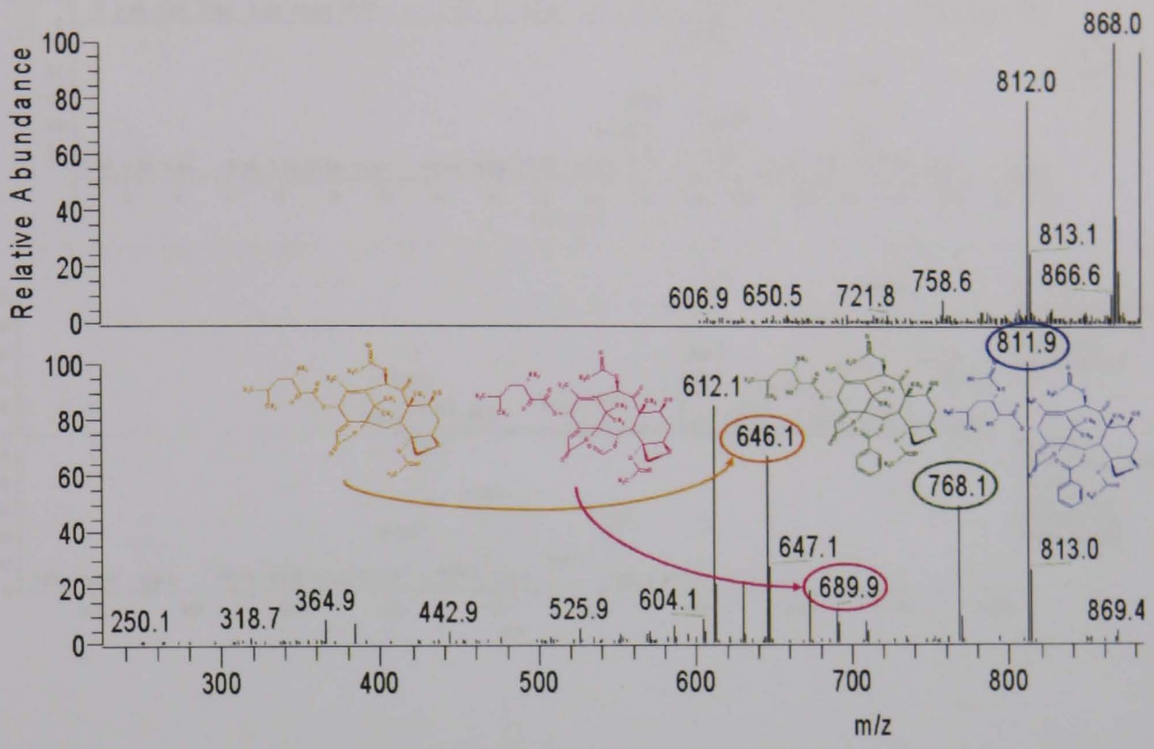

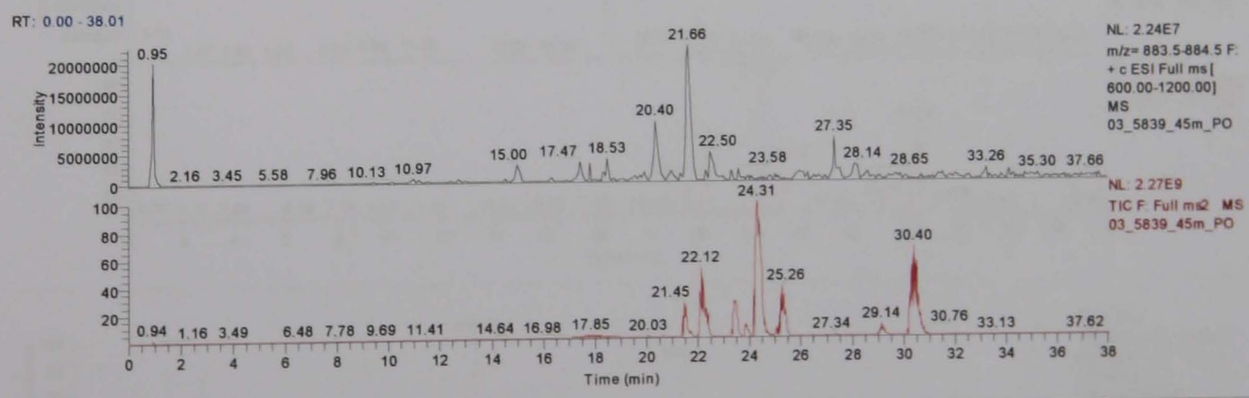

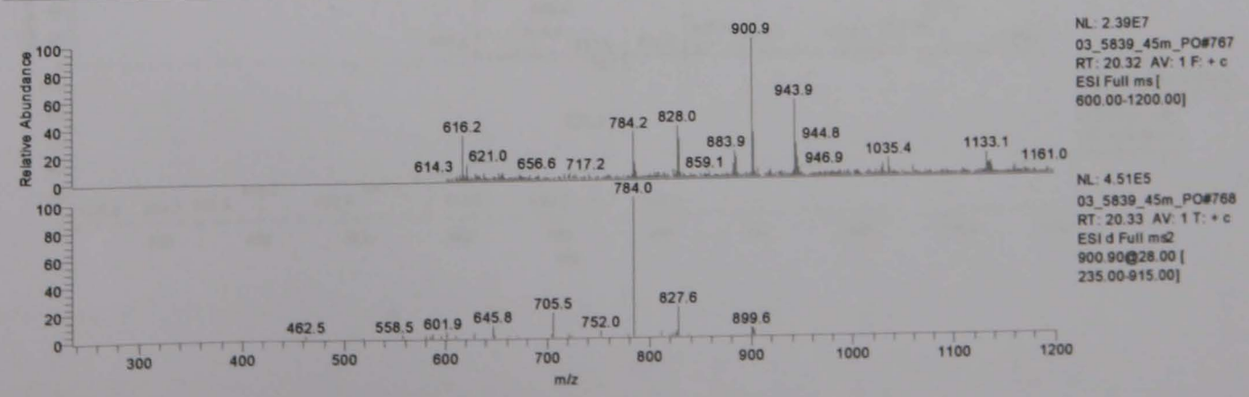

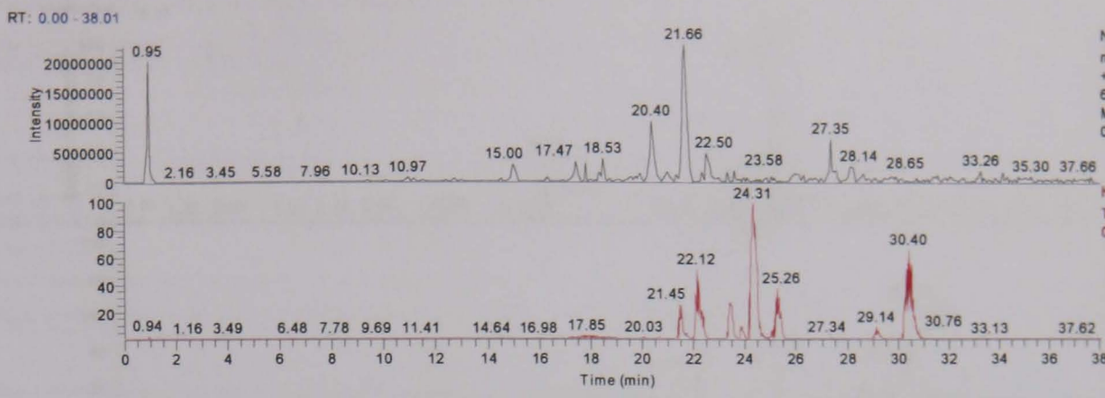
RT: 0.00 - 38.01
Intensity
Time (min)
NL: 2.24E7
m/z= 883.5-884.5 F:
+ c ESI Full ms [
600.00-1200.00]
MS
03_5839_45m_PO
NL: 2.27E9
TIC F: Full ms2 MS
03_5839_45m_PO

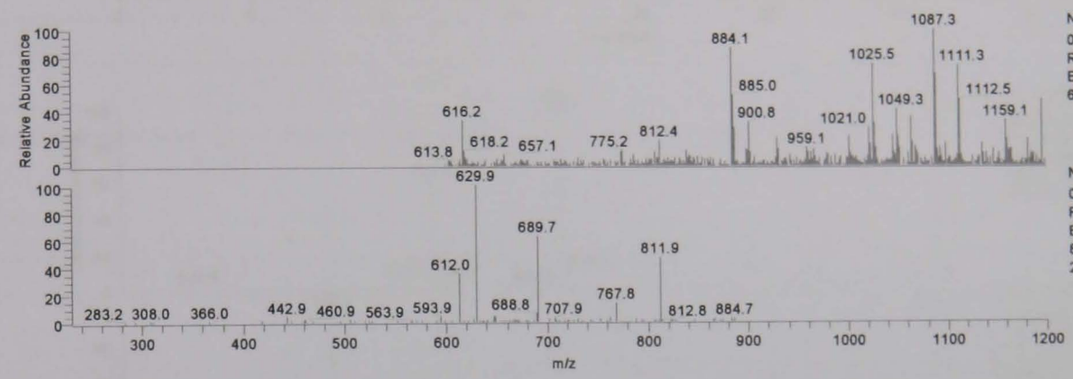
Relative Abundance
m/z
NL: 1.25E7
03_5839_45m_PO#843
RT: 21.79 AV: 1 F: + c
ESI Full ms [
600.00-1200.00]
NL: 8.02E5
03_5839_45m_PO#845
RT: 21.83 AV: 1 T: + c
ESI d Full ms2
884.07@28.00 [
230.00-895.00]

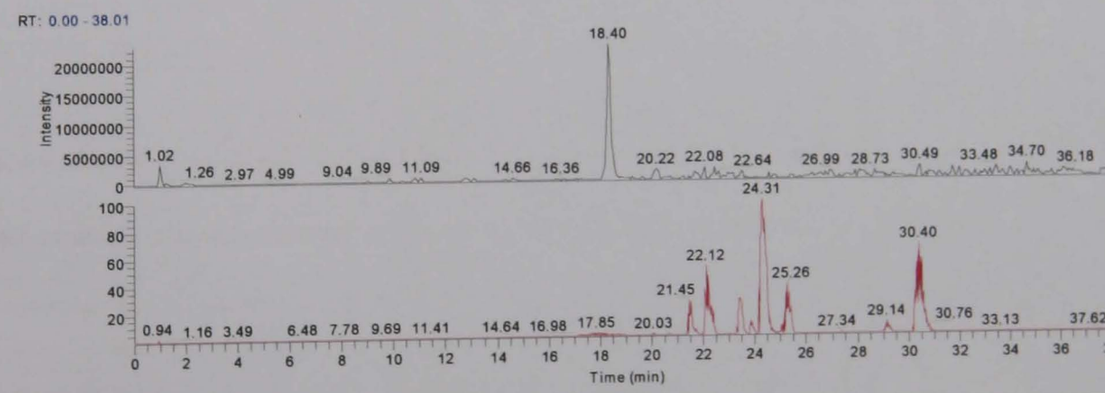
RT: 0.00 - 38.01
Intensity
Time (min)
NL: 2.27E7
m/z= 823.5-824.5 F:
+ c ESI Full ms [
600.00-1200.00]
MS
03_5839_45m_PO
NL: 2.27E9
TIC F: Full ms2 MS
03_5839_45m_PO

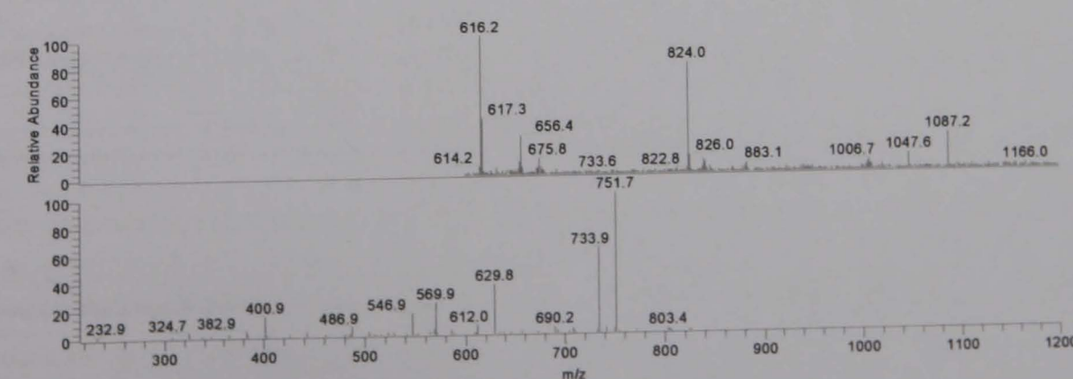
Relative Abundance
m/z
NL: 2.41E7
03_5839_45m_PO#671
RT: 18.47 AV: 1 F: + c
ESI Full ms [
600.00-1200.00]
NL: 1.40E6
03_5839_45m_PO#665
RT: 18.37 AV: 1 T: + c
ESI d Full ms2
823.92@28.00 [
215.00-835.00]

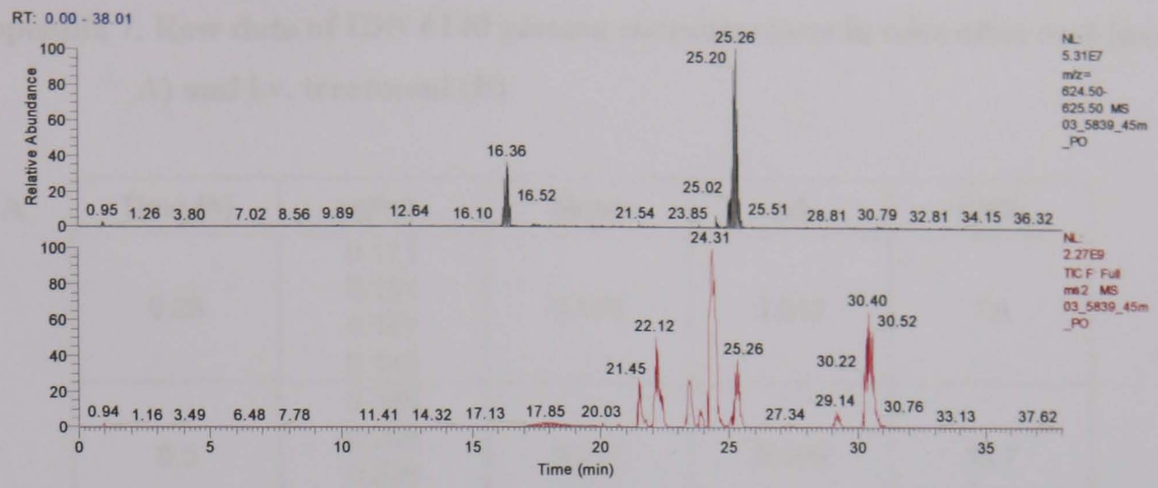
RT: 0.00 - 38.01
Relative Abundance
Time (min)
NL: 5.31E7 m/z= 624.50-625.50 MS 03_5839_45m_PO
NL: 2.27E9 TIC F Full ms2 MS 03_5839_45m_PO

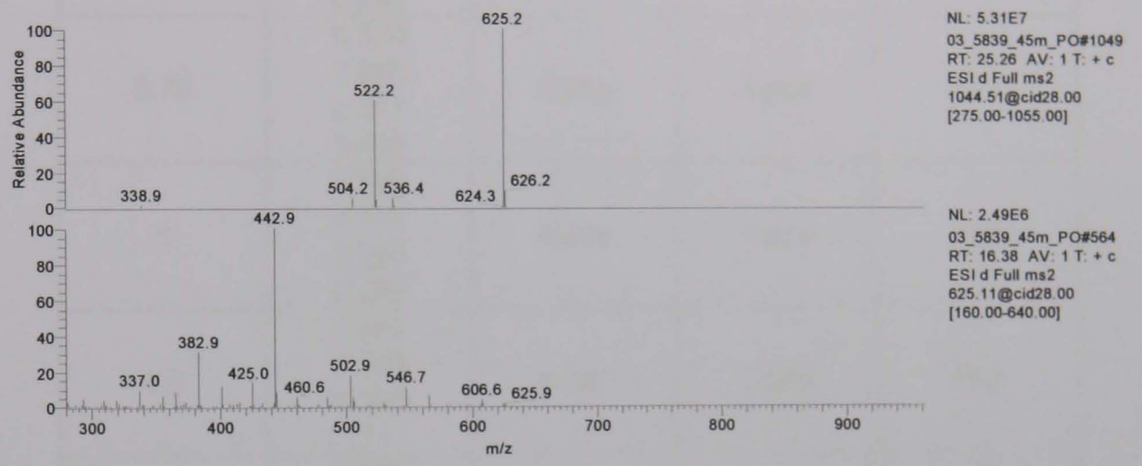
Relative Abundance
m/z
NL: 5.31E7
03_5839_45m_PO#1049
RT: 25.26 AV: 1 T: + c
ESI d Full ms2
1044.51@cid28.00
[275.00-1055.00]
NL: 2.49E6
03_5839_45m_PO#564
RT: 16.38 AV: 1 T: + c
ESI d Full ms2
625.11@cid28.00
[160.00-640.00]

Appendix 7. Raw data of IDN 6140 plasma concentrations in mice after oral (panel A) and i.v. treatment (B)

A

Time (h)	µg/mL	Mean	sd	CV%
0.25	0.171 0.151 0.157 0.143	0.156	0.012	7.6
0.5	0.186 0.268 0.226 0.269	0.237	0.040	16.7
0.75	0.374 0.350 0.347 0.462	0.383	0.054	14.1
1	0.192 0.161 0.286 0.239	0.220	0.055	24.9
1.5	0.253 0.179 0.188 /	0.207	0.040	19.5
2	0.135 0.099 0.097 0.056	0.097	0.032	33.4
4	0.089 0.100 0.064 0.050	0.076	0.023	30.1
8	0.041 0.039 0.036 0.032	0.037	0.004	10.6
16	0.028 0.024 0.029 0.031	0.028	0.003	10.5
24	0.029 0.016 0.028 0.017	0.023	0.007	30.9
48	0.011 0.012 0.015 0.011	0.012	0.002	15.5

B

Time (h)	µg/mL	Mean	sd	CV%
0.083	4.264 4.456 4.628 5.376	4.681	0.487	10.4
0.25	1.802 1.942 1.484 1.802	1.758	0.194	11.0
0.5	0.757 0.840 0.938 0.860	0.849	0.074	8.8
1	0.532 0.579 0.538 0.560	0.552	0.022	3.9
2	0.260 0.274 0.262 0.246	0.261	0.030	11.5
4	0.197 0.192 0.180 0.150	0.180	0.021	11.7
8	0.096 0.130 0.105 0.133	0.116	0.018	15.8
16	0.094 0.093 0.064 0.077	0.082	0.014	17.4
24	0.046 0.056 0.065 0.070	0.059	0.011	17.8
48	0.026 0.027 0.031 0.032	0.029	0.003	10.2

Appendix 8. Raw data of IDN 6140 concentrations in mice brain tissue after oral (A) or intravenous (B) administration of the compound

A

oral treatment

IDN 6140							
brain	weight	concentration (ng/sample)	concentration (ng/g)	mean	s.d.	time	s.d.*100/ mean
1	0.42	16.8	40.0	42.0	1.5	15 min	3.7
2	0.4	17.5	43.8				
3	0.44	18.6	42.3				
4	0.42	17.6	41.9				
13	0.42	45.5	108.3	118.8	29.0	1 h	24.4
14	0.4	33.7	84.3				
15	0.37	56.0	151.4				
16	0.35	46.0	131.4				
21	0.42	101.7	242.1	142.4	66.6	2 h	46.8
22	0.41	43.7	106.6				
23	0.43	49.7	115.6				
24	0.42	44.3	105.5				
25	0.4	47.9	119.8	112.5	45.1	4 h	40.1
26	0.49	82.1	167.6				
27	0.36	37.6	104.4				
28	0.43	25.0	58.1				
29	0.39	44.0	112.8	75.6	33.8	8 h	44.7
30	0.43	20.1	46.7				
31	0.4	26.9	67.3				
32	0.41	5.4	13.2				
37	0.42	39.3	93.6	56.1	35.3	24 h	63.0
38	0.37	9.8	26.5				
39	0.3	23.7	79.0				
40	0.35	8.9	25.4				

-value outside of the considered range

B

i.v. treatment

IDN 6140							
brain	weight	concentration (ng/sample)	concentration (ng/g)	mean	s.d.	time	s.d.*100/ mean
45	0.37	343.8	929.2	2785.1	1322.4	15 min	47.5
46	0.41	1147.4	2798.5				
47	0.34	1182.4	3477.6				
48	0.41	1613.3	3934.9				
53	0.43	2484.2	5777.2	3988.9	1331.9	1 h	33.4
54	0.45	1876.8	4170.7				
55	0.37	1010.0	2729.7				
56	0.4	1311.2	3278.0				
57	0.41	413.0	1007.3	1878.2	841.1	2 h	44.8
58	0.33	631.5	1913.6				
59	0.4	633.6	1584.0				
60	0.28	842.2	3007.9				
61	0.41	58.2	142.0	747.7	716.5	4 h	95.8
62	0.44	92.2	209.5				
63	0.38	372.8	981.1				
64	0.45	746.2	1658.2				
65	0.41	310.5	757.3	650.9	347.6	8 h	53.4
66	0.44	59.2	134.5				
67	0.41	344.3	839.8				
68	0.43	374.9	871.9				
73	0.45	270.0	600.0	466.3	123.8	24 h	26.6
74	0.43	190.7	443.5				
75	0.4	142.2	355.5				
76	0.42	25.2	60.0				

-value not included in the mean calculation

- value outside of the considered range

Appendix 9. Raw data of IDN 6140 concentrations in mice liver tissue after oral (A) or intravenous (B) administration of the compound

A

oral treatment

IDN 6140									
liver number	time (hr)	weight (g)	vol (mL)	total vol (mL)	concentration (ng/ 1 mL)	concentration (ng/tot mL)	concentration (ng/g)	mean (ng/g)	sd (ng/g)
1	0.25	1.42	7.10	8.52	156.3	1331.4	937.6	2323.3	1171.5
2		1.54	7.70	9.24	295.3	2728.3	1771.6		
3		1.32	6.60	7.92	533.5	4225.6	3201.2		
4		1.18	5.90	7.08	563.8	3991.5	3382.6		
13	1	1.05	5.25	6.3	1125.0	7087.5	6750.0	6154.7	955.7
14		1.11	5.55	6.66	922.6	6144.5	5535.6		
15		0.85	4.25	5.1	1194.5	6092.0	7167.0		
16		1.12	5.60	6.72	861.0	5785.9	5166.0		
21	2	1.22	6.10	7.32	960.5	7030.9	5763.0	4965.8	535.4
22		1.39	6.95	8.34	787.2	6565.2	4723.2		
23		1.16	5.80	6.96	794.2	5527.6	4765.2		
24		1.39	6.95	8.34	768.6	6410.1	4611.6		
25	4	0.97	4.85	5.82	834.8	4858.5	5008.8	4514.0	409.8
26		1.37	6.85	8.22	676.4	5560.0	4058.4		
27		1.13	5.65	6.78	775.6	5258.6	4653.6		
28		1.19	5.95	7.14	722.5	5158.7	4335.0		
29	8	1.04	5.20	6.24	550.0	3432.0	3300.0	2795.3	1171.5
30		1.13	5.65	6.78	180.1	1221.1	1080.6		
31		1.14	5.70	6.84	618.1	4227.8	3708.6		
32		1.08	5.40	6.48	515.3	3339.1	3091.8		
37	24	1.14	5.70	6.84	190.2	1301.0	1141.2	756.6	333.0
38		1.33	6.65	7.98	78.8	628.8	472.8		
39		1.42	7.10	8.52	154.8	1318.9	928.8		
40		0.99	4.95	5.94	80.6	478.8	483.6		

B

i.v. treatment

IDN 6140									
liver number	time (hr)	weight (g)	vol (mL)	total vol (mL)	concentration (ng/ 1 mL)	concentration (ng/tot mL)	concentration (ng/g)	mean (ng/g)	sd (ng/g)
45	0.25	1.39	6.95	8.34	1795.3	14972.8	10771.8	9757.7	836.2
46		1.23	6.15	7.38	1588.5	11723.1	9531.0		
47		1.19	5.95	7.14	1659.8	11851.0	9958.8		
48		1.17	5.85	7.02	1461.5	10259.7	8769.0		
53	1	1.00	5.00	6.00	922.2	5533.2	5533.2	5546.1	1635.4
54		1.25	6.25	7.50	583.0	4372.5	3498.0		
55		1.27	6.35	7.62	1250.0	9525.0	7500.0		
56		1.15	5.75	6.90	942.2	6501.2	5653.2		
57	2	1.51	7.55	9.06	946.6	8576.2	5679.6	6303.3	485.6
58		1.27	6.35	7.62	1104.3	8414.8	6625.8		
59		1.27	6.35	7.62	1124.1	8565.6	6744.6		
60		1.27	6.35	7.62	1027.2	7827.3	6163.2		
61	4	1.14	5.70	6.84	846.1	5787.3	5076.6	4820.1	782.7
62		1.13	5.65	6.78	895.9	6074.2	5375.4		
63		1.01	5.05	6.06	861.2	5218.9	5167.2		
64		0.97	4.85	5.82	610.2	3551.4	3661.2		
65	8	0.94	4.70	5.64	580.5	3274.0	3483.0	3925.7	875.4
66		1.00	5.00	6.00	541.8	3250.8	3250.8		
67		1.21	6.05	7.26	866.6	6291.5	5199.6		
68		1.00	5.00	6.00	628.2	3769.2	3769.2		
73	24	1.19	5.95	7.14	305.4	2180.6	1832.4	2007.6	344.8
74		1.25	6.25	7.50	269.0	2017.5	1614.0		
75		1.18	5.90	7.08	370.6	2623.8	2223.6		
76		0.97	4.85	5.82	393.4	2289.6	2360.4		

7.1. List of abbreviations

amu	atomic mass unit
APCI	Atmospheric Pressure Chemical Ionization
CE	Collision Energy
CXP	Collision cell exit potential
DA	Dalton
DC	Direct Current
DDA	Data Dependent Acquisition
DP	Declustering Potential
EP	Entrance Potential
ESI	Electro Spray Ionization
HPLC	High Performance Liquid Chromatography
HPLC-UV/VIS	High Performance Liquid Chromatography-UltraViolet Visible Spectroscopy
IS	Internal Standard
LC-MS	Liquid Chromatography-Mass Spectrometry
LC-MS/MS	Liquid Chromatography Tandem Mass Spectrometry
MP	Mobile Phase
MS	Mass Spectrometry
MW	Molecular Weight
RF	Radio Frequency
rpm	rotation per minute
SRM	Selected Reaction Monitoring
TIC	Total Ion Chromatogram

CV	Coefficient of Variation
LOQ	Limit of Quantification
LOD	Limit of Detection
QC	Quality Control
SD	Standard Deviation
SE	Standard Error
ULOQ	Upper Limit of Quantification

AUC	Area Under the Curve
AUC_{inf}	Area Under the Curve extrapolated to infinite
Cl	plasma clearance
C_{max}	maximum plasma concentration
E	extraction ratio
F	bioavailability
i.p.	intraperitoneal
i.v.	intravenous
Ke	costant of elimination
M1	metabolite 1
p.o.	per os
R_{Cmax}	accumulation factor for Cmax values
R_{AUC}	accumulation factor for AUC values
s.c.	subcutaneous
T_{max}	maximum time
$T_{1/2}$	half-life
V_{bd}	volume of distribution

ABCB1	ATP-Binding Cassette Sub-Family B Member 1
BBB	Blood Brain Barrier
Bcl-2	B-cell leukemia 2
BSA	Bovine Serum Albumin
CNS	Central Nervous System
CYP	Cytocrome P
DCC	Dicyclohexylcarbodiimide
DMAP	Dimethylaminopyridine
DMPU	Dimethylpropyleneurea
DMSO	Dimethyl sulfoxide
FDA	Food and Drug Administration
GLP	Good Laboratory Practice
GDP	Guanosyl diphosphate
GTP	Guanosyl triphosphate
HSRs	Hyper Sensitivity Reactions
IC_{50}	Inhibitory concentration 50%
MBT	Metastatic Breast Cancer
MDR	Multi Drug Resistance
MTD	Maximum Tolerated Dose
NCI	National Cancer Institute
NCCN	National Comprehensive Cancer Network
NSCLC	Non Small Cell Lung Cancer
PAPS	Phosphoadenyl phosphosulfate
P-gp	P-glycoprotein
R.I.	Resistant Index
THF	TetraHydroFuran

UGTs	Uridinediphosphoglucuronosyltransferases
UDPGA	Uridinediphosphateglucuronic Acid
ULN	Upper Limit of Normal

7.2. List of publications

1. Marangon E, Falcioni C, Manzotti C, Fontana G, D'Incalci M and Zucchetti M (under review). Development and validation of a LC-MS/MS method for the determination of the novel oral 1,14 substituted taxane derivatives, IDN 5738 and IDN 5839, in mouse plasma and its application to the pharmacokinetic study. *J Chromatogr B Analyt Technol Biomed Life Sci* 2009;**877**:4147-53.

2. Sala F, Zucchetti M, Bagnati R, et al. Development and validation of a liquid chromatography-tandem mass spectrometry method for the determination of ST1926, a novel oral antitumor agent, adamantyl retinoid derivative, in plasma of patients in a Phase I study. *J Chromatogr B Analyt Technol Biomed Life Sci* 2009;**877**:3118-26.

3. Marangon E, Citterio M, Sala F, et al. Pharmacokinetic profile of imatinib mesylate and N-desmethyl-imatinib (CGP 74588) in children with newly diagnosed Ph+ acute leukemias. *Cancer Chemother Pharmacol* 2009;**63**:563-6.

4. Marangon E, Sala F, Caffo O, Galligioni E, D'Incalci M, Zucchetti M. Simultaneous determination of gemcitabine and its main metabolite, dFdU, in plasma of patients with advanced non-small-cell lung cancer by high-performance liquid chromatography-tandem mass spectrometry. *J Mass Spectrom* 2008;**43**:216-23.

5. Gambacorti-Passerini CB, Tornaghi L, Marangon E, et al. Imatinib concentrations in human milk. *Blood* 2007;**109**:1790.

6. D'Incalci M, Brunelli D, Marangon E, et al. Modulation of gene transcription by natural products--a viable anticancer strategy. *Curr Pharm Des* 2007;**13**:2744-50.

7. Bagnati R, Bianchi G, Marangon E, Zuccato E, Fanelli R, Davoli E. Direct analysis of isopropylthioxanthone (ITX) in milk by high-performance liquid chromatography/tandem mass spectrometry. *Rapid Commun Mass Spectrom* 2007;**21**:1998-2002.

8. Frapolli R, Marangon E, Zaffaroni M, et al. Pharmacokinetics and metabolism in mice of IDN 5390 (13-(N-Boc-3-i-butylisoserinoyl)-C-7,8-seco-10-deacetylbaccatin III), a new oral c-seco-taxane derivative with antiangiogenic property effective on paclitaxel-resistant tumors. *Drug Metab Dispos* 2006;**34**:2028-35.

9. Sissi C, Marangon E, Chemello A, Noble CG, Maxwell A, Palumbo M. The effects of metal ions on the structure and stability of the DNA gyrase B protein. *J Mol Biol* 2005;**353**:1152-60.

10. Fleming I, Marangon E, Roni C, Russell MG, Chamudis ST. Reactions of phenyldimethylsilyllithium with β-N,N-dimethylaminoenones: A convenient synthesis of β-dimethyl(phenyl)silylacrylic acid and its derivatives. *Can J Chem* 2004;**82**:325-332.

11. Fleming I, Marangon E, Roni C, Russell MG, Chamudis ST. Reactions of phenyldimethylsilyllithium with beta-N,N-dimethylaminoenones. *Chem Commun (Camb)* 2003:200-1.